

QC
869.4
.U6
G46
1995/6

W/OH
3
m

GEOPHYSICAL FLUID DYNAMICS LABORATORY

RECEIVED

JAN 16 1996

Executive Affairs
NWS-NOAA

G
F
D
L



U.S. DEPARTMENT OF COMMERCE
National Oceanic and Atmospheric Administration
Environmental Research Laboratories



GEOPHYSICAL FLUID DYNAMICS LABORATORY

ACTIVITIES - FY95

PLANS - FY96

OCTOBER 1995

GEOPHYSICAL FLUID DYNAMICS LABORATORY
PRINCETON, NEW JERSEY

QC
869.4
.46
G46
1995/6



UNITED STATES
DEPARTMENT OF COMMERCE

RONALD H. BROWN
SECRETARY OF COMMERCE

NATIONAL OCEANIC AND
ATMOSPHERIC ADMINISTRATION

D. JAMES BAKER
UNDERSECRETARY FOR OCEANS
AND ATMOSPHERE

ENVIRONMENTAL
RESEARCH
LABORATORIES

ALAN R. THOMAS
DIRECTOR

NOTICE

Mention of a commercial company or product does not constitute an endorsement by NOAA Environmental Research Laboratories. Use for publicity or advertising purposes of information from this publication concerning proprietary products or the tests of such products is not authorized.

PREFACE

This document is intended to serve as a summary of the work accomplished at the Geophysical Fluid Dynamics Laboratory (GFDL) and to present a glimpse of the near future direction of its research plans.

It has been prepared within GFDL and its distribution is primarily limited to GFDL members, to Princeton University affiliates, to interested offices of the National Oceanic and Atmospheric Administration (NOAA), to other relevant government agencies and national organizations, and to interested individuals.

The organization of the document encompasses an overview, project activities and plans for the current and next fiscal year, and appendices. The overview covers highlights of the three major research areas that correspond to Strategic Plan Elements in NOAA's Environmental Assessment and Prediction Portfolio: Advance Short-Term Forecasts and Warnings; Seasonal to Interannual Climate Forecasts; and Predict and Assess Decadal to Centennial Changes. The body of the text describes goals, specific recent achievements and future plans for the following major research categories: Climate Dynamics; Middle Atmosphere Dynamics and Chemistry; Experimental Prediction; Oceanic Circulation; Planetary Circulations; Observational Studies; Hurricane Dynamics; and Mesoscale Dynamics. These categories, which correspond to the GFDL organization of research groups, are different from the NOAA categories and are far from being mutually exclusive. Interaction occurs among the various groups and is strongly encouraged.

The appendices contain the following: a list of GFDL staff members and affiliates during Fiscal Year 1995; a bibliography of relatively recent research papers published by staff members and affiliates during their tenure with GFDL (these are referred to in the main body according to the appropriate reference number or letter); a description of the Laboratory's computational support and its plans for Fiscal Year 1996; a listing of seminars presented at GFDL during Fiscal Year 1995; a list of seminars and talks presented during Fiscal Year 1995 by GFDL staff members and affiliates at other locations.

Although the specific names of individuals are not generally given in the overview, an entire listing of project participants can be found in Appendix A. Research staff personnel can normally be identified by consulting the cited Appendix B references or the names listed in the body of the text.

The Scientific Editor for this year's report was John Sheldon, with Wendy Marshall serving as Technical Editor. This report is the culmination of a team effort involving a large majority of the GFDL staff and their Princeton University collaborators. Special thanks are extended to all who contributed to this substantial effort.

September 1995



TABLE OF CONTENTS

A. AN OVERVIEW	1
SCOPE OF THE LABORATORY'S WORK	3
HIGHLIGHTS OF FY95 AND IMMEDIATE OBJECTIVES	5
ADVANCE SHORT-TERM FORECASTS AND WARMINGS	9
SEASONAL TO INTERANNUAL CLIMATE FORECASTS	12
PREDICT AND ASSESS DECADAL TO CENTENNIAL CHANGES	15
B. PROJECT ACTIVITIES FY95, PROJECT PLANS FY96	23
1. CLIMATE DYNAMICS	25
1.1 OCEAN-ATMOSPHERE INTERACTION	25
1.1.1 Transient Response to CO ₂	25
1.1.1.1 Tropical Response	25
1.1.1.2 Sea Level Rise	28
1.1.2 Climate Variability	30
1.1.2.1 SST Variability in Greenland Sea	30
1.1.2.2 Simulated and Observed SST Variability	32
1.1.2.3 Interannual Pacific Variability	34
1.1.3 Paleoclimate	36
1.1.3.1 Abrupt Climate Change	36
1.1.3.2 Paleoclimate Model Intercomparison Project	37
1.1.4 Model Development	39
1.1.4.1 Coupled Model with Higher Resolution	39
1.1.4.2 Sea Ice Model	40
1.2 CONTINENTAL HYDROLOGY AND CLIMATE	41
1.2.1 Simulation of Runoff and River Discharge	41
1.2.2 Intercomparison of Land-Surface Parameterization Schemes	43
1.2.3 Water and Heat Fluxes in Desert Soils	44
1.3 PLANETARY WAVE DYNAMICS	44

1.3.1	Baroclinic Instability, Geostrophic Turbulence, and Extratropical Dynamics	44
1.3.1.1	Quasi-Geostrophic Turbulence and Eddy Flux Parameterization	44
1.3.1.2	The Effects of Latent Heating on Eddy Statistics	46
1.3.1.3	Storm Tracks	46
1.3.2	Generation of Tropical Transient Waves	48
1.3.3	NOAA/University Joint Study of the Maintenance of Regional Climates and Low Frequency Variability in GCMs	49
1.4	PLANETARY ATMOSPHERES	51
1.4.1	Stability and Genesis of Vortex Sets	51
1.4.2	Stability and Genesis of Jet Sets	52
1.4.3	Model Development	52
2.	RADIATION AND CLOUDS	53
2.1	SOLAR SPECTRUM	53
2.1.1	Multiple-Scattering Approximation	53
2.1.2	Parameterizations	54
2.1.3	H ₂ O and CO ₂ Effects in the Stratosphere	57
2.1.4	Benchmark Computations	57
2.2	LONGWAVE SPECTRUM	59
2.2.1	Parameterization	59
2.2.2	Comparison of Line-by-Line Calculations with Observations	59
2.3	CONVECTION-CLOUDS-RADIATION-CLIMATE INTERACTIONS	61
2.3.1	Cumulus Parameterization	61
2.3.2	Limited-Area Nonhydrostatic Model Development	62
2.3.3	Radiative-Convective Equilibria with Explicit Moist Convection	64
2.3.4	Atmospheric Ice Clouds	65
2.3.5	Interactions Between Water Vapor, Radiation, and Circulation	66

2.3.6 GCM Studies of Cloud Radiative Effects	67
2.4 DIAGNOSTIC ANALYSES USING SATELLITE OBSERVATIONS	68
2.4.1 Tropospheric Water Vapor and the Infrared Radiation Budget	68
2.4.2 Deep Convection and Upper Tropospheric Humidity	69
2.4.3 Moisture Transport Diagnostics from Satellite Imagery	69
2.5 EFFECT OF CHANGES IN ATMOSPHERIC COMPOSITION	73
2.5.1 Simulation with Additional Trace Gases	73
2.5.2 Temperature Changes Due to the Observed 1979-1990 Ozone Loss	73
2.5.3 Intercomparison of Radiative Forcing Due to Ozone Losses	76
2.5.4 Ozone-Temperature Relation in the Stratosphere	77
3. MIDDLE ATMOSPHERE DYNAMICS AND CHEMISTRY	79
3.1 ATMOSPHERIC TRACE CONSTITUENT STUDIES	79
3.1.1 ZODIAC Global Chemical Tracer Model Development	79
3.1.2 SKYHI Chemical Model Development	81
3.1.2.1 Stratosphere	81
3.1.2.2 Troposphere	84
3.1.2.3 Analysis Code Development	85
3.1.3 Tropospheric Reactive Nitrogen in the ZODIAC GCTM	85
3.1.4 Tropospheric Ozone in the GCTM	86
3.1.5 Transport Studies	88
3.1.6 Atmospheric Sulfur Chemistry and Transport in the GCTM	90
3.2 ATMOSPHERIC DYNAMICS AND CIRCULATION	92
3.2.1 SKYHI Model Development	92
3.2.2 SKYHI Control Integrations and Basic Model Climatology	93
3.2.3 Studies of Diurnal Variability	93
3.2.4 High Horizontal Resolution Integration with SKYHI	93
3.2.5 Resolved Gravity Waves in the SKYHI Model	93

3.2.6	Sensitivity of the Middle Atmospheric Gravity Wave Field to Changes in the Moist Convection Parameterization	94
3.2.7	Experiments with Simple Models of Wave Propagation	96
3.2.8	GCM Simulation with an Imposed Tropical Quasi-biennial Oscillation	97
3.2.9	Observations and GCM Simulation of the Ozone Quasi-biennial Oscillation	98
3.2.10	Tropical Waves Observed in High-Resolution Radiosonde Data	98
3.2.11	SKYHI Simulations with an Imposed Kelvin Wave Forcing	99
3.2.12	Dynamics of the Martian Atmosphere	101
4.	EXPERIMENTAL PREDICTION	103
4.1	STOCHASTIC DYNAMIC PREDICTION	103
4.1.1	Selection of Initial Conditions for Ensembles	103
4.1.2	Methods for Interpretation and Validation of Ensemble Forecasts	104
4.1.3	Theoretical Limits of Predictability	104
4.1.4	Norms for Dynamical Systems	104
4.2	DEVELOPMENT OF MONTHLY TO SEASONAL FORECAST MODELS	105
4.2.1	Atmospheric Models	105
4.2.1.1	Global Grid Point Model	105
4.2.1.2	Spectral Model Improvements	106
4.2.1.3	Development of Subgrid Scale Parameterizations	106
4.2.1.4	Modular Physics Packages	106
4.2.1.5	Modular Spectral Dynamical Core	106
4.2.2	Ocean Model	107
4.2.2.1	Maintenance of Equatorial Thermocline	107
4.2.2.2	Sensitivity to Subgrid Scale Parameterizations	107
4.2.3	Land Surface Model	107
4.2.4	Coupled Atmosphere-Ocean-Land Models	107

4.3 ATMOSPHERIC AND OCEANIC PREDICTION AND PREDICTABILITY	108
4.3.1 Coupled Model Prediction	108
4.3.1.1 ENSO (El Niño Southern Oscillation) Forecasts	108
4.3.1.2 Improvement of Seasonal Cycle	109
4.3.2 Atmospheric Predictability	109
4.3.2.1 Impacts of Clouds and Radiation	109
4.3.2.2 Intraseasonal Variability	110
4.3.2.3 Interannual Variability	111
4.3.2.4 Feasibility of Seasonal Forecasts	111
4.3.3 Ocean Predictability	112
4.4 OCEAN DATA ASSIMILATION	113
5. OCEANIC CIRCULATION	115
5.1 OCEAN-ATMOSPHERE INTERACTIONS	115
5.1.1 The Seasonal Cycle Simulated with Coupled GCMs	116
5.1.2 Studies of Decadal Variability	116
5.1.3 Development of Nested Models	117
5.2 WORLD OCEAN STUDIES	118
5.2.1 Nutrient Dynamics in the Equatorial Zone	118
5.2.2 Water Masses and Thermohaline Circulation	120
5.2.3 Using CFCs as Ocean Tracers	122
5.2.4 High-Resolution North Atlantic Studies	124
5.2.5 Thermohaline Circulation Stability	125
5.2.6 North Atlantic Thermohaline Circulation Predictability	126
5.2.7 Modeling Mesoscale Eddies in the Ocean	128
5.3 MODEL DEVELOPMENT	128
5.4 COASTAL OCEAN MODELING AND DATA ASSIMILATION	129
5.4.1 Data Assimilation and Model Evaluation Experiments	129

5.4.2 The East Coastal Forecast System	130
5.4.3 North Atlantic and Arctic Climate Studies	131
5.4.4 Modeling the Mediterranean Outflow	131
5.5 CARBON SYSTEM	132
5.5.1 Ocean Carbon Cycle	132
5.5.2 Ocean Carbon Cycle	134
5.5.3 Measurements	135
5.6 NITROUS OXIDE	136
5.7 OCEAN CIRCULATION TRACERS	137
6. OBSERVATIONAL STUDIES	138
6.1 ATMOSPHERIC DATA PROCESSING	138
6.1.1 Processing of Daily Upper-Air Data	138
6.1.2 Comparison of Daily Radiosonde and Satellite Measures of Upper Tropospheric Humidity	139
6.1.3 Processing and Distribution of Monthly Mean Rawinsonde Data	139
6.2 CLIMATE OF THE ATMOSPHERE	141
6.2.1 Radiosonde and Satellite Observations of Upper Tropospheric Water Vapor and Its Trends	141
6.2.2 15-Year Global Climatology of Relative Humidity	143
6.2.3 Long-Term Variability in the Hadley Circulation and Its Connection to ENSO	144
6.2.4 Simulation of Atmospheric Variability in Very Long GCM Integrations	144
6.2.5 Hydrological Cycle Over Deserts	146
6.3 AIR-SEA INTERACTIONS	147
6.3.1 Lag Relationships Involving Tropical SSTs	147
6.3.2 Role of the Atmospheric Bridge in Linking Tropical Pacific ENSO Events to Extratropical SST Anomalies	148

6.3.3 Ensemble GCM Experiments Subjected to SST Anomalies for Specific ENSO Events	150
6.4 SATELLITE DATA	151
6.4.1 Relationships Between the Formation of Stratiform Clouds and the Ambient Circulation	151
6.4.2 Circulation Features Associated With Propagating Deep Convective Clouds in Subtropical Frontal Zones	151
6.4.3 Patterns of Cloud Cover in Midlatitude Cyclones	152
7. HURRICANE DYNAMICS	153
7.1 HURRICANE PREDICTION SYSTEM	153
7.1.1 The 1994 Hurricane Season	153
7.1.2 The 1995 Hurricane Season	154
7.2 OBSERVING SYSTEM	156
7.3 BEHAVIOR OF TROPICAL CYCLONES	157
7.3.1 Evolution of Tropical Cyclones	157
7.3.2 Scale Interaction	157
7.3.3 Tropical Cyclone - Ocean Interaction	159
7.4 STRUCTURE OF TROPICAL CYCLONES	159
7.5 MODEL IMPROVEMENT	160
8. MESOSCALE DYNAMICS	161
8.1 THE LIFE CYCLE OF MIDLATITUDE CYCLONES	161
8.1.1 Cyclone Evolution Along Storm Tracks	161
8.1.2 Wavelet Analysis for Detection of Baroclinic Packets in Storm Tracks	162
8.1.3 Energy Flux and Group Velocity in Baroclinic Waves	162
8.1.4 Stages in the Energetics of Baroclinic Systems	163
8.2 SENSITIVITY STUDIES OF MIDLATITUDE CYCLONES	164
8.2.1 The Blizzard of '93	164

8.2.2 Nonlinear Baroclinic Wave Equilibration	165
8.3 TOPOGRAPHIC INFLUENCES IN ATMOSPHERIC FLOWS	166
8.3.1 Blocking and Frontogenesis Due to Topography	166
8.3.2 Resolved Topographic Drag in Global Models	167
8.4 MODEL DEVELOPMENT	167
8.4.1 Improvements to the Hydrostatic Zeta Model	167
8.4.2 The Nonhydrostatic Compressible Zeta Model	168
8.4.3 Model Intercomparisons	168
9. COMPUTATIONAL SERVICES	170
9.1 COMPUTER SYSTEMS	170
9.2 DATA MANAGEMENT AND VISUALIZATION	173
APPENDIX A GFDL STAFF MEMBERS AND AFFILIATED PERSONNEL DURING FISCAL YEAR 1995	A-1
APPENDIX B GFDL BIBLIOGRAPHY	B-1
APPENDIX C SEMINARS GIVEN AT GFDL DURING FISCAL YEAR 1995	C-1
APPENDIX D TALKS, SEMINARS, AND PAPERS PRESENTED OUTSIDE GFDL DURING FISCAL YEAR 1995	D-1
APPENDIX E ACRONYMS	E-1

AN OVERVIEW



SCOPE OF THE LABORATORY'S WORK

The Geophysical Fluid Dynamics Laboratory is engaged in comprehensive long lead-time research fundamental to NOAA's mission.

The goal of this research is to expand the scientific understanding of the physical processes that govern the behavior of the atmosphere and the oceans as complex fluid systems. These systems can then be modeled mathematically and their phenomenology can be studied by computer simulation methods. In particular, GFDL research concerns the following:

- the predictability of weather on large and small scales;
- the structure, variability, predictability, stability and sensitivity of global and regional climate;
- the structure, variability and dynamics of the ocean over its many space and time scales;
- the interaction of the atmosphere and oceans, and how the atmosphere and oceans influence and are influenced by various trace constituents;
- the Earth's atmospheric general circulation within the context of the family of planetary atmospheric circulations.

The scientific work of the Laboratory encompasses a variety of disciplines including meteorology, oceanography, hydrology, classical physics, fluid dynamics, chemistry, applied mathematics, and numerical analysis. Research is also facilitated by the Atmospheric and Oceanic Sciences Program (AOSP), which is a collaborative program at GFDL with Princeton University. Under this program, regular Princeton faculty, research scientists, and graduate students participate in theoretical studies, both analytical and numerical, and in observational experiments in the laboratory and in the field. The program is supported in part by NOAA funds. AOSP scientists may also be involved in GFDL research through institutional or international agreements.

The following sections describe the GFDL contributions to three major research areas that correspond to Strategic Plan Elements in NOAA's Environmental Assessment and Prediction Portfolio.



HIGHLIGHTS OF FY95

and

IMMEDIATE OBJECTIVES

In this section, some research highlights are listed that may be of interest to those persons less concerned with the details of GFDL research. Selected are items that may be of special significance or interest to a wider audience.

Items in this section are placed in the NOAA Strategic Plan Elements:

Advance Short-Term Forecasts and Warnings

Seasonal to Interannual Climate Forecasts

Predict and Assess Decadal to Centennial Changes

These categories are organized rather differently than the GFDL research project areas presented in the main body of the report. The parentheses refer to references in GFDL Activities, FY95; Plans, FY96.



ADVANCE SHORT-TERM FORECASTS AND WARNINGS

The need for short-term warning and forecast products covers a broad spectrum of environmental events which have lifetimes ranging from several minutes up to a month or so. Some examples of these events are tornadoes, hurricanes, tsunamis, and coastal storms, as well as "spells" of unusual weather (warm, cold, wet, or dry). Benefits of these products can be measured in terms of lives saved, injuries averted, and expenses spared. NOAA's vision for improvement in this area involves operational modernization and restructuring, strengthening of observing and prediction systems, and improved applications and dissemination of products and services.

Efforts at GFDL are centered around the development of numerical models which may be used in the prediction of "short-term" atmospheric and oceanic phenomena. Simulations from these models are studied and compared with observed data to aid in the understanding of the processes which govern the behavior of the various phenomena.

With regard to tropical weather systems, efforts are aimed at the genesis, growth, and decay of tropical storms and hurricanes. In extratropical regions, interest includes the development of severe weather systems, the interaction of medium-scale atmospheric flow with that on larger scales, and the influence of the underlying topographic features. Experimental prediction of regional-scale weather parameters weeks to months in advance is being pursued; included in this context is the study of "ensemble forecasting." With regard to the marine environment, forecasts of coastal conditions on a day-to-day basis can be made by coupling of ocean and atmosphere models. Ocean models are also used to simulate coastal bays and estuaries, the response of coastal zones to transient atmospheric storms, and Gulf Stream meanders and rings.

ACCOMPLISHMENTS FY95

Numerical experiments and theoretical studies indicate that tropical intraseasonal oscillations are generated through an evaporation-wind feedback mechanism, while other tropical transient waves appear to be generated by a newly proposed "saturation-triggering mechanism" (1.3.2).

An investigation of ensemble forecasts in simple dynamical systems has given insight into shortcomings of operational ensemble forecasts. New methods for selecting initial conditions have been developed in simple models and are being extended to models of intermediate complexity (4.1).

An efficient data assimilation method that combines the assimilation of satellite-derived data sets is being used for nowcasting the Gulf Stream and the North Atlantic meso-scale variability (5.4.1).

An experimental operational coastal forecast system is making 24-hour forecasts of coastal sea level and storm surges. These predictions are available to the public in real-time through the Internet (5.4.2).

The GFDL Hurricane Prediction System was run at the National Center for Environmental Prediction (NCEP) in test mode for the 1994 hurricane season. Based on an evaluation of its track prediction skill for tropical disturbances (60 cases in the Atlantic and 148 cases in the eastern/central Pacific), the NCEP operationally implemented the GFDL system for the 1995 hurricane season, replacing the previously used hurricane model (7.1.1, 7.1.2).

Investigation of the benefits of dropwindsonde observations for hurricane prediction continued, and an improvement was again noted in the track predictions for new cases. In addition, a small benefit in the intensity forecasts was suggested. In a potential vorticity diagnostics study, the feedback mechanism of hurricane-environment interaction, as well as the mechanism to create a potential vorticity sink at upper levels of storms, were illuminated. Both of these studies illustrate the potential benefits of improved observations and need for better model physics (7.2, 7.3.2).

Asymmetric structures in the interior of tropical cyclones were analyzed and a strong relationship was found between the pattern of accumulated precipitation in the moving storm and the winds near the vortex center relative to the storm motion. An hypothesis that the relative wind could induce an asymmetric divergence field was used to explain the simulated quasi-steady asymmetry (7.4).

The results from several idealized and case studies have been drawn together to form a comprehensive picture of "downstream baroclinic evolution" using local energetics. This picture offers a complementary alternative to the conventional descriptions of cyclone development by reducing cyclogenesis to three basic stages in which energy centers grow initially via energy flux convergence and then by baroclinic conversion (8.1.4).

An idealized study of nonlinear baroclinic wave equilibration in different initial environments and geometries reveals a stark difference between equilibrations in spherical and Cartesian models, with spherical simulations producing much more anticyclonic zonal-mean wind shear and shorter-lived eddies. The main dynamical difference lies in the strength of the positive feedback between the barotropic decay of the eddy and the acceleration of the zonal-mean wind (8.2.2).

A three-dimensional, nonhydrostatic, fully compressible version of the GFDL hydrostatic Zeta model has been constructed and verified against the hydrostatic model by means of idealized simulations of large-scale barotropic and baroclinic instability. Although the hydrostatic and nonhydrostatic simulations are nearly identical, growth rates in the compressible model are smaller because the work done against elasticity during compression represents a source of eddy internal energy and a sink of eddy kinetic energy (8.4.3).

PLANS FY96

- Development and implementation of an operational data assimilation system will be made part of the eastern coastal forecasting system.
- Formulation of a new scheme for hurricane model initialization will be initiated. In this new scheme, vortex specification will be considered in a three-dimensional framework instead of the present axisymmetric approach.
- Studies of the diurnal variation of tropical convection and its effect on the behavior of tropical cyclones and hurricane-ocean interaction will continue. Sensitivity of tropical cyclone development to environmental conditions will be investigated for various time scales, from one day to a month or longer.
- Explosive cyclone development will be evaluated to better understand the role of geopotential fluxes and baroclinic conversion in the evolution of these storms, and whether baroclinic generation alone is sufficient to initiate cyclone development.
- The role of surface heat and momentum fluxes in atmospheric preconditioning and the intensification of extratropical cyclones will continue, and new case studies will be performed to assess the impact of these processes on the development of cyclones of varying intensity in storm tracks.
- Investigation of topographic influences on cyclones and mesoscale systems will continue, and mountain drag estimates will be extended to include more realistic mesoscale circulations. The role of gravity waves in mesoscale circulations will be evaluated.
- Development of limited area models will emphasize improvement of surface flux parameterizations and accuracy of the numerical schemes, as well as incorporation of moist physics and boundary layer physics into the new, higher resolution hydrostatic and non-hydrostatic models.

SEASONAL TO INTERANNUAL CLIMATE FORECASTS

Seasonal to interannual climate fluctuations have far-reaching consequences for agriculture, fishing, water resources, transportation, energy consumption, and commerce, among others. Short-term climate anomalies which persist from a season to several years affect rainfall distributions, surface temperatures, and atmospheric and oceanic circulation patterns. Reliable climate forecasts may be used to reduce the disruption, economic losses, and human suffering that occur in connection with these anomalies. NOAA's vision for improvement in this area is based on better predictive capability, enhanced observations, greater understanding of climate fluctuations, and assessment of impacts.

The study of seasonal to interannual climate fluctuations at GFDL is based on both theoretical and observational studies. Available observations are analyzed to determine the physical processes governing the behavior of the oceans and atmosphere. Mathematical models are constructed to study, simulate, and predict the coupled ocean-atmosphere, land-surface, sea-ice system.

Simulations based on the numerical models maintained at GFDL, in conjunction with observations, are used to study climate variations on seasonal and longer time scales. Processes under study include large-scale wave disturbances and their role in the general circulation, the effects of boundary conditions such as sea surface temperature and soil moisture, influence of clouds, radiation, and atmospheric convection, and the "teleconnection" of atmospheric anomalies across the global atmosphere. Furthermore, experimental model forecasts are used to evaluate atmospheric predictability and to assess skill in forecasting atmospheric and oceanic climate anomalies, both in general and in connection with the El Niño-Southern Oscillation phenomenon. Also, a more accurate representation of the state of the global ocean is being studied through data assimilation for better initialization of seasonal-interannual forecasts.

ACCOMPLISHMENTS FY95

A parameterization of ice content in cirrus clouds has been incorporated into the SKYHI GCM using simple representations of the interactions among ice-mass, ice-particle size, thermodynamics, water cycle, and radiative effects. The principal features of observed cirrus distributions are captured by the model (2.3.4).

Analysis of ensembles of atmospheric model simulations has focused on identifying when and where useful long lead forecasts can be made. A particularly noteworthy result is that a 40-year atmospheric simulation has shown significant correlations between the tropical Southern Oscillation Index and monthly mean precipitation over the southeastern United States. These correlations suggest that

useful monthly mean precipitation forecasts at long leads may be possible for this region. The potential to produce long range forecasts of phenomena such as the tropical intraseasonal oscillation and tropical storm frequency is also being investigated with the same set of tools (4.1, 4.3).

Initial versions of a modular spectral dynamical core and modular grid-point physics modules have been completed. The physics modules have been used in a B-grid model while the spectral core is being tested in an existing general circulation model. The physics modules have proven to be flexible and extremely easy to use (4.2).

The impact of clouds on the seasonal cycle of the coupled model has been studied through a large number of integrations. Substituting prescribed low-level climatological clouds for model predicted low clouds has greatly improved the model's seasonal cycle in sea surface temperature over the eastern tropical Pacific Ocean. The improved seasonal cycle has in turn led to some additional improvements in the coupled model simulations and forecasts (4.3).

Improvements to the ocean data assimilation system have led to the construction of more accurate analyses of the state of the ocean. When used as initial conditions for the ocean component of the coupled model, these improved analyses lead to better forecasts of the tropical Pacific Ocean (4.4).

A new version of the GFDL Modular Ocean Model, MOM 2, has been released to the general public. The release includes complete documentation, a user's guide, and a reference manual. The new version has a flexible memory window in which the model equations can be solved for an arbitrary number of latitude rows at the same time. This allows MOM 2 to run efficiently on all kinds of computer architectures, from workstations to traditional supercomputers and massively parallel systems (5.3).

A 15-year radiosonde dataset has been used to create a first-ever global climatology of relative humidity and its spatial and temporal variability. The results are reliable in the lower and middle troposphere but become more uncertain in the upper troposphere (~ above 400 mb) (6.2.2).

Clear evidence has been found that the tropical Hadley cells tend to strengthen during El Niño conditions, while they tend to weaken during cold La Niña conditions. The anomalies in the strength of the Hadley cells are found to be strongly and inversely correlated with the anomalies in the strength of the Walker Oscillation (6.2.3).

Output from an 100,000-day GCM integration reveals the existence in the model atmosphere of well-defined spatial modes of variability, including a zonally

symmetric mode with a highly skewed probability distribution function, and a westward propagating mode at high latitudes (6.2.4).

A series of GCM experiments was completed using anomalous sea surface temperature (SST) forcing in the tropical Pacific and allowing for air-sea coupling in the extratropics. The results illustrate the importance of the atmospheric circulation as a bridge linking tropical ENSO events and SST variations in the midlatitude oceans (6.3.2).

PLANS FY96

- The interannual variability of runoff implied by a climate model will be evaluated in a comparison with measured river discharges. This study will provide a context for interpretation of runoff-change predictions derived from climate-change experiments.
- Further experiments will be conducted using both idealized and realistic models to examine the effects of condensation, evaporation, and advection on the generation mechanisms of tropical transient waves.
- Quantitative differences between model-computed and observed radiative fluxes, as obtained from satellite and field experiments, will continue to be analyzed. This will include investigations of the atmospheric hydrologic cycle (water vapor and clouds) and its effect on the global radiation budget on various spatial and temporal scales. The satellite-derived products will be used to evaluate the accuracy of the outputs and to improve the quality of simulation of the Laboratory's numerical models.
- A new cumulus parameterization will be incorporated into the SKYHI GCM. This parameterization includes both mass fluxes and vertical velocities and can be used for chemical transport calculations and radiative characteristics.
- The development of a modular atmospheric modeling system will continue. A new modular spectral atmospheric general circulation model will be created by combining the spectral dynamical model core and the B-grid model modular physics packages. This new modular system will permit sharing of physics between a set of flexible, easily understandable atmospheric models which will initially include the eta and sigma vertical coordinate versions of the B-grid and spectral models. The flexibility of the new system should greatly facilitate forecast and simulation comparisons which are essential to improving our ability to make useful forecasts at long leads.
- A large suite of atmosphere-only, ocean-only, and coupled-model runs using frozen versions of a spectral atmospheric GCM will be produced with the goal of

gaining a better understanding of the predictability of coupled model systems. In conjunction with these experiments, additional model runs with only a single parameter change will be used to continue the development of improved forecast models. Particular attention will be given to the effects of convective parameterizations and clouds.

- The ocean data assimilation system will be significantly enhanced by the use of an improved ocean model and enhanced error statistics. A 10-year data set will be produced by the new system and used as both initial conditions and verifications for the ocean component of coupled model forecasts.
- Studies of ensembles of atmosphere-only simulations and coupled-model forecasts will focus on interannual variability. Newly developed tools will be applied to help determine when and where useful long lead forecasts can be produced. Phenomena such as tropical intraseasonal oscillations, tropical storms, and El Niño-Southern Oscillation (ENSO) will be examined to determine the degree to which they can be predicted.
- A data assimilation methodology previously developed for regional models will be tested for the entire North Atlantic Ocean.
- The statistical and dynamical characteristics of the dominant modes of atmospheric variability in the wintertime extratropics will be examined using both observational data records and output from very long GCM integrations. The role of midlatitude air-sea interaction in the sustenance of atmospheric anomalies will be investigated using simulations which incorporate various degrees of coupling between the atmospheric circulation and simple mixed-layer models.
- The origin of inter-sample and inter-event variability in model responses to observed tropical Pacific SST anomalies will be identified by analyzing multiple GCM integrations subjected to SST forcing associated with selected ENSO episodes.

PREDICT AND ASSESS DECADAL TO CENTENNIAL CHANGES

Events such as the Sahel drought, the dust bowls in the Midwest, the Little Ice Age, stratospheric ozone depletion, and global warming may define eras in history. Events such as these have lifetimes of decades to centuries and their causes may be either natural or anthropogenic. An ability to predict such changes and to assess the causes is essential in long-range policy making. Adaptation to the changes and reduction of the effects of human induced changes require enhanced predictive capability. NOAA's vision for improvement in this area is based on a commitment to

research in climate and air quality, as well as to insure long-term climate and chemical records.

The related research efforts at GFDL require judicious combinations of theoretical models and specialized observations. The modeling efforts draw on principles from the atmospheric, oceanic, chemical, and biological sciences. One area of focus is long-term climate variability and secular change associated with the atmosphere and oceans. This area encompasses a number of topics, including the effects of changes in the concentration of atmospheric gases such as carbon dioxide, the simulation of past climates, and the variability of the oceanic thermohaline circulation. Another area of focus is the formation, transport, and chemistry of atmospheric trace constituents. This area addresses problems such as: the transport of quasi-conservative trace gases; the biogeochemistry of climatically significant long-lived trace gases; the transport, sources, and sinks of aerosols; the chemistry of ozone and its regulative trace species; the effects of clouds and aerosols on chemically important trace gases; and the impact of anthropogenic chlorofluorocarbons on stratospheric ozone amounts. Yet another area of focus relates to the modeling of the marine environment. It includes the dispersion of geochemical tracers in the world oceans, the oceanic carbon cycle and trace metal geochemistry, and ecosystem structures.

ACCOMPLISHMENTS FY95

The amplitude of the El Niño/Southern Oscillation (ENSO) appears to fluctuate on a time scale of roughly 50 years, based on analyses of a 350-year proxy record of eastern Pacific SST. This interpretation is also consistent with the observational record of SST for the past century. A similar amplitude modulation occurs for the ENSO-like phenomenon in a control run of the GFDL R15 coupled model. Given that the model ENSO's response to a quadrupling of CO₂ is of comparable magnitude to this internally generated variation in the control ENSO, it will likely be very difficult to unambiguously detect any CO₂-induced change in the real ENSO--at least for the next several decades (1.1.1.1).

Results from a coupled ocean-atmosphere model show that sea level has a very long response time when the atmospheric CO₂ concentration is doubled and then held fixed, with only a small fraction of the equilibrium sea level rise being realized by the time of doubling. The equilibrium sea level response to CO₂ doubling was found to be surprisingly large, 1.7 m, even though only the expansion of sea water was considered. Any additional melting by land ice could make this increase even larger (1.1.1.2).

One prominent signal of interdecadal variability of surface air temperature in a coupled ocean-atmosphere model occurs over Greenland and the Greenland Sea.

These atmospheric variations are associated with oceanic fluctuations in temperature, salinity, and sea ice with a time scale of approximately 50 years (1.1.2.1).

Analysis of a 1,000-year integration of a coupled ocean-atmosphere model revealed that the spatial patterns of interannual to interdecadal variability in the modeled North Pacific bear a distinct resemblance to observations (1.1.2.3).

Sea ice dynamics was incorporated into both the atmosphere-mixed layer ocean model and the coupled atmosphere-ocean model. The addition of this model component will allow for a more realistic treatment of sea ice in a variety of simulation and sensitivity experiments (1.1.3).

Abrupt climate change, similar to that which frequently occurred during the last glacial and postglacial periods, was induced by a massive input of fresh water into the northern North Atlantic of a coupled ocean-atmosphere model (1.1.3.1).

It has been shown that the eddy diffusivity for potential vorticity predicted by a model of homogeneous turbulence can predict the eddy fluxes due to baroclinic instability generated by an unstable zonal jet, if the jet is not too narrow. This work justifies an approach to designing mesoscale eddy flux closure schemes for ocean models in which homogeneous models are used to "measure" the diffusivity in various large-scale environments (1.3.1).

Models of Jupiter's atmosphere now generate the multiple jets that in turn produce multiple vortex sets in low and midlatitudes. The models also isolate the vertical structure of the atmosphere, showing that the motions extend over a 30-50 km deep layer bounded by a 500-1000 km deep abyss. The Galileo spacecraft probe may test this prediction in December 1995 (1.4.2).

A new shortwave radiation parameterization has been developed that involves dividing the spectrum into a number of distinct bands. This strategy will enable a more accurate treatment of the interactions in the different spectral regions in scattering-absorbing atmospheres (2.1.2).

For the first time, the line-by-line longwave radiative computations have been compared with spectral radiances measured under clear-sky conditions during the Spectral Radiation Experiment. The comparisons reveal that a new continuum formulation agrees very well with the measurements, with the exception of some discrepancies at the lowest infrared frequencies (2.2.2).

Satellite measurements of the upwelling 6.7 μm radiance and cloud property information from ISCCP indicate that enhanced convection in the tropics is associated with increased upper tropospheric relative humidity. This positive interrelationship

between deep convection, upper tropospheric humidity and greenhouse effect is consistent with expectations from model simulations and is observed over a wide range of space and time scales (2.4.2).

Satellite radiances in the 6.7 μm spectral region and the total outgoing longwave flux measurements indicate that, in the tropics, increases in the atmospheric radiative trapping (greenhouse effect) are strongly correlated with increased middle and upper tropospheric relative humidity. In the midlatitudes, the atmospheric trapping is only weakly related to variations in tropospheric relative humidity, and more strongly to variations in lapse rate (2.4.2).

SKYHI GCM simulations indicate that the addition of the present-day concentrations of the non- CO_2 trace gases (methane, nitrous oxide and the halocarbons) tends to warm the tropical tropopause, thus alleviating some of the "cold" bias of the model in this region (2.5.1).

A SKYHI GCM simulation indicates that the cooling of the lower stratosphere and the upper troposphere due to the ozone loss over the past decade exceeds considerably that due to any other known causes. The cooling signature due to ozone very likely plays a role in changes in the vertical temperature profile over the past quarter century (2.5.2).

A study of the impact of peroxyacetyl nitrate (PAN) on tropospheric reactive nitrogen (NO_x) has been completed. This revealed that the unique temperature sensitivity of PAN's lifetime produces large winter-spring mixing ratios; however, the maximum global tropospheric mass of NO_x sequestered as PAN never exceeds two days worth of tropospheric NO_x emissions. Nevertheless, the transport of PAN away from NO_x source regions, together with subsequent downstream subsidence, produces a significant redistribution of NO_x due to PAN's thermal decay in the remote oceanic boundary layer (3.1.5).

The 1° SKYHI model was shown to produce an explicit simulation of the middle atmospheric gravity wave field with some quite realistic features. Direct comparisons with lidar and rocket observations show in particular that the overall kinetic energy levels in the field of vertically-propagating gravity waves is well captured in the high-resolution SKYHI simulation (3.2.5).

The detailed stratospheric photochemistry scheme developed over the past few years for use in the SKYHI GCM has now been integrated for several years in the 3° -latitude version of the GCM. Analysis of this model run indicates that the photochemical simulation seems to be producing reasonable seasonal and spatial representations of stratospheric photochemical processes. However, some calculated concentrations of trace species may be significantly affected by the

model's cold polar bias. In addition, the low simulated concentrations of water vapor may have pronounced effects on stratospheric hydrogen chemistry (3.1.2.1).

A new theoretical framework for explaining the ocean's thermohaline circulation has been developed. This view emphasizes the role of the Antarctic Circumpolar Current, as opposed to deep-water formation in high latitudes, for providing the energy which maintains the ocean's global overturning circulation (5.2.2).

A new Carbon Modeling Consortium (CMC) has been initiated with support from the NOAA Office of Global Programs. The CMC has the long term goal of developing an integrated carbon system model capable of providing assessments of future oceanic and terrestrial sinks for anthropogenic carbon (5.5.1).

The oceanic uptake of anthropogenic CO₂ has been estimated with an improved ocean GCM that includes full carbon chemistry and the effect of biological processes. Inclusion of carbon chemistry increases the uptake of anthropogenic CO₂ by 9% compared to the previous perturbation model. Inclusion of biological processes reduces CO₂ uptake by 5% (5.5.1).

Comparison of radiosonde and satellite climatologies of upper tropospheric water vapor for the period 1979-1991 has clearly revealed a 15-20% bias in the relative humidity which was traced to differences in the type of sensors used in eastern Europe and most of Asia (more moist) and those used elsewhere (less moist) (6.2.1).

PLANS FY96

- The study of the transient response of climate to increasing greenhouse gases and atmospheric aerosols will be repeated by use of a more realistic, coupled ocean-atmosphere model with higher computational resolution.
- The natural, internally generated variability of climate will be explored further by repeating the 1,000-year integration using a more realistic coupled ocean-atmosphere model with higher computational resolution.
- CO₂-induced changes in, and interdecadal variability of, tropical climate features, such as tropical storms and ENSO, will be analyzed using data from the latest higher-resolution coupled model experiments and other specialized climate model integrations.
- The transient responses of the thermohaline circulation to increasing greenhouse gases and fresh water input will be investigated by performing a set of numerical experiments with a low-resolution coupled ocean-atmosphere model.

- Participation in the Paleoclimate Model Intercomparison Project (PMIP) will continue in the form of detailed analysis of the recently completed glacial climate simulation and a planned simulation of the so-called “climatic optimum” that occurred 6,000 years ago.

- Studies of the homogeneous turbulence generated by baroclinic instability will be extended to multi-level models with environmental shears and static stabilities of relevance to the ocean, in order to shed light on the factors that control the vertical structure of the eddy fluxes.

- The sensitivity of climate to changes in the concentrations of greenhouse gases, ozone and aerosols, and to changes in the physical properties of clouds will continue to be investigated using GCMs. The explicit simulation of the liquid and the solid phases of H₂O in GCMs and the associated cloud-radiative interactions will be studied.

- Utilizing empirical parameterizations of ozone production in the polluted boundary layer, pre-calculated net ozone chemistry as a function of ozone and reactive nitrogen, and the natural source of tropospheric ozone due to downward transport from the stratosphere, a model simulation of the distribution of ozone throughout the troposphere will be initiated. As part of this study, the natural and anthropogenic contributions to the tropospheric global budget of ozone will be examined.

- Analysis of the new SKYHI integration with 0.6 °x 0.72° latitude horizontal resolution will be performed, focusing on how the mean flow, gravity wave fields, and effect of subgrid-scale parameterizations differ from those in lower resolution versions of the model.

- The influence of SKYHI's cold bias at winter high latitudes and the impact of the low calculated concentrations of stratospheric water vapor on the photochemical simulation will be studied in further detail and improvements will be proposed and evaluated.

- Halogen chemistry will be added to SKYHI and a model run simulating the industrial stratosphere will be initiated to investigate the degree to which today's chlorine levels influence ozone amounts.

- The transport of CO₂ within the atmosphere will be evaluated with respect to oceanic and terrestrial sources and sinks using the GFDL SKYHI model.

- A biogeochemical model of organic matter production will be coupled to an eddy-resolving ocean GCM for the North Atlantic driven by synoptic wind forcing.

- Calculations will continue with the 2-D radiative-convective equilibrium model with very idealized microphysics. The focus will be on the extent to which the moist adiabat constrains the temperature profile, or equivalently, on how the conditional potential energy of the model is maintained. Preliminary 3-D calculations of radiative-convective equilibrium in a small domain will be attempted.
- New diagnostics will be developed for the GFDL ocean model to determine the distribution and sources/sinks of available potential energy.
- An investigation into mixing processes in the Labrador Sea is planned, beginning with a phenomenological study of the Great Salinity Anomaly, a multi-year freshening which propagated into the Labrador Sea through the Denmark Straits during the 1970s.
- Research on the trends in upper tropospheric humidity based on radiosonde and satellite observations will be pursued further.

PROJECT ACTIVITIES FY95

PROJECT PLANS FY96



1. CLIMATE DYNAMICS

GOALS

To construct mathematical models of the atmosphere and of the coupled ocean-atmosphere system which simulate the global large-scale features of climate.

To study the dynamical interaction between large-scale wave disturbances and the general circulation of the atmosphere.

To identify and elucidate the physical and dynamical mechanisms which maintain climate and cause its variation, and to examine their generality in the context of paleoclimate and the atmospheres of other planets.

To evaluate the impact of human activities on climate.

1.1 OCEAN-ATMOSPHERE INTERACTION

1.1.1 Transient Response to CO₂

1.1.1.1 Tropical Response

*D. Gu
T. Knutson*

S. Manabe

ACTIVITIES FY95

The impact of increasing atmospheric CO₂ on several aspects of the tropical climate is being investigated. Specifically, possible CO₂ induced changes in the time-mean tropical Pacific climate and in the amplitude and frequency of El Niño-Southern Oscillation (ENSO) are being examined using extended integrations of a GFDL coupled ocean-atmosphere general circulation model (GCM).

ENSO Response

An important problem with regard to CO₂-induced warming is the impact such a warming would have on ENSO. For example, would the magnitude or frequency of ENSO events increase or decrease? Could the climate enter a permanent El Niño state? How would the anticipated CO₂-induced change compare with the changes in

ENSO due to natural variability alone (*i.e.*, the variation in the absence of anthropogenic climate forcing)?

During the past century, ENSO has exhibited pronounced variability in amplitude (1293), with relatively low amplitudes in the years 1915-1950 and relatively high amplitudes from 1885-1915 and from 1960-present. What has caused this pronounced variation in amplitude? What is its implication for CO₂-induced climate change? These issues are being examined using 1000-year simulations of a GFDL low-resolution coupled ocean-atmosphere GCM (1201, *yk*) and a 350+ year proxy record of eastern tropical Pacific sea surface temperature (SST) from coral $\delta^{18}\text{O}$ measurements (Dunbar, et al., 1994)¹. The 1000-year climate model simulations of ENSO-like activity represent a unique resource for examining these issues. Despite the coarse resolution of the R15 coupled model, the ENSO life cycle in the model resembles the “delayed oscillator” ENSO life cycle obtained using a much higher-resolution ocean component, although the amplitude of the SST fluctuations is about 40% smaller.

A wavelet analysis of the coral data (Fig. 1.1) suggests that the pronounced variations in ENSO amplitude during the past century are not unusual; in fact, the coral-derived SST data show a similar amplitude variation occurring over the past 350 years on a time scale of about one-half century. Moreover, a similar interdecadal-scale variation of amplitude occurs for the ENSO-like phenomenon in the low-resolution coupled climate model (Fig. 1.1). This result suggests that much of the observed variation in ENSO amplitude over the past century (and inferred from coral records for the past 350 years) could have been due to internal variations in the climate system, rather than external forcing (such as solar changes or anthropogenic climate forcing).

Analysis of CO₂ perturbation experiments with the low-resolution model indicate that the amplitude of ENSO-like fluctuations in the model decreases by about 20% with a quadrupling of CO₂ (1268). However, since changes of at least this magnitude occur on a multi-decadal time scale in the control simulation (and in the coral-derived records of the real ENSO), the implication is that it will be very difficult to unambiguously detect a CO₂-induced change in ENSO, at least for the next several decades. This is due to the apparently large natural variability of ENSO’s amplitude which represents a large “noise” component in the system. An important caveat to this result is that it assumes that the relative sensitivity of the real ENSO to CO₂-induced warming is roughly comparable to that obtained using the low-resolution coupled model.

1. Dunbar, R.B., G.M. Wellington, M.W. Colgan, and P.W. Glynn, Eastern Pacific sea surface temperature since 1600 A.D.: The $\delta^{18}\text{O}$ record of climate variability in Galápagos corals, *Paleoceanography*, 9(2), 291-315, 1994.

Normalized Amplitude of 2-7.5 Year Variability

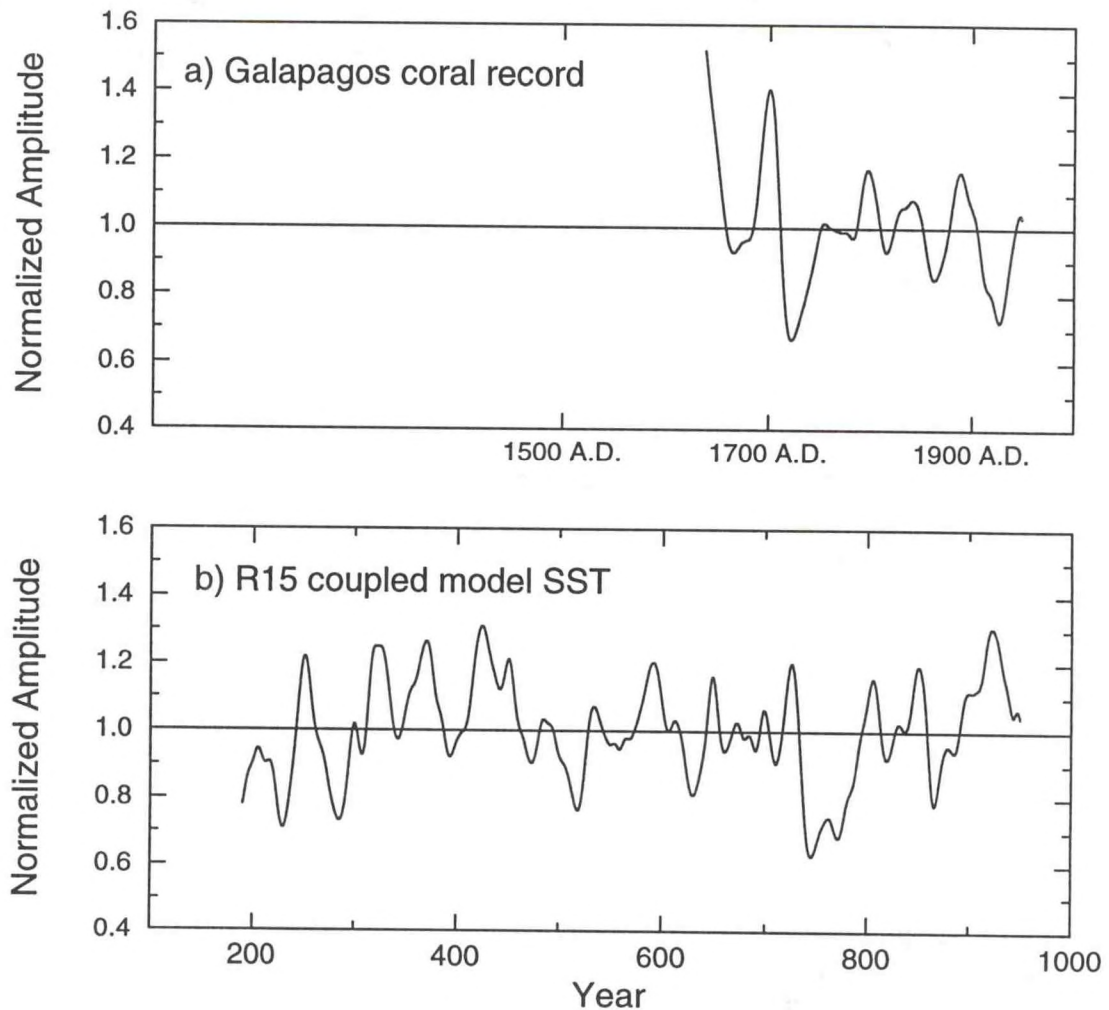


Fig. 1.1 The amplitude of interannual (2-7.5 year) variability, normalized by its standard deviation, for: (a) the $\delta^{18}\text{O}$ coral record of Dunbar et al. (1994)¹ and (b) SST from an 820-year segment of a control run (with no external forcing changes) of a GFDL R15 coupled ocean-atmosphere GCM. The amplitude series were obtained using a wavelet analysis of the 2-7.5 year band as described in (1293). The interdecadal-scale variations of normalized amplitude in (a) and (b) are similar, which suggests that much of the observed variation in ENSO amplitude could be due to internal variations in the climate system, rather than external forcing.

Time-Mean Response

An important element of CO_2 -induced climate changes is the impact on the time-mean zonal SST gradient in the tropical Pacific. For example, if even a 2°C decrease in the east-west contrast in SST occurred with increased CO_2 , it would imply conditions similar to a “permanent El Niño” of moderate intensity. In the R15 coupled

model experiments, the east-west contrast in SST decreases by about 0.8°C with a quadrupling of CO_2 despite an overall warming of the tropical Pacific of $4\text{-}5^{\circ}\text{C}$ (xl). The SST gradient reduction is not clearly identifiable in the model until about 100 years of model integration with CO_2 increasing at $1\%\text{/yr}$ (compounded). This delayed response (in comparison to the overall tropical Pacific SST warming) is due to the slow build-up of CO_2 , internal variability in the model, and the long response time of the coupled ocean-atmosphere system. The GFDL simulation is one of the few simulations indicating such a climate response, and it is also unique in that it has been integrated long enough (>100 years) for the signal to be clearly identified. The importance of the result is that the model *does not* appear to enter a permanent El Niño state, even with a quadrupling of CO_2 .

PLANS FY96

The plan for FY96 is to complete the analysis of the impact of increased CO_2 on ENSO-like phenomena in the R15 coupled model and continue to investigate these phenomena using higher resolution (R30) coupled model experiments. Two additional areas of investigation will be tropical storm frequencies in the GCM experiments and longer-term (>10 year time scale) fluctuations in the tropical and subtropical Pacific in the coupled GCM experiments.

1.1.1.2 Sea Level Rise

S. Manabe *R.J. Stouffer*

ACTIVITIES FY95

An investigation was conducted regarding the response of the coupled ocean-atmosphere system to the rate of increase in the atmospheric carbon dioxide. The model used here is described in (1042). Five integrations of the coupled model have been completed in which atmospheric CO_2 increases at the rates of 0.25, 0.5, 1.0, 2.0 and 4.0% per year (compounded) until it is doubled. The corresponding time required for the doubling of atmospheric CO_2 is 280, 140, 70, 35, 17.5 years, respectively. A control integration was also performed holding the atmospheric carbon dioxide concentration constant.

Table 1.1 indicates that the largest increases in sea level at the time of CO_2 doubling are for the cases with the slowest rates of increase of atmospheric CO_2 concentration, a behavior similar to that noted for surface air temperature. The reason for this response is that the penetration of the temperature anomaly into the model ocean is much deeper and is much larger in the integrations with slow rates of increase of atmospheric CO_2 . Since the expansion of ocean water is mainly related to temperature changes especially at depth, the integrations with the slowest rates of

increase have the largest rise in sea level at the time of doubling. At infinite time to doubling, equilibrium sea level is achieved at the time of doubling. This table also shows that only a small fraction (less than 25%) of the total sea level rise is realized by the time of doubling even in the experiments where CO₂ increased at only 0.25% per year and takes 280 years to reach doubling.

Note from Table 1.1 that, for the integration in which the coupled system is in equilibrium with the doubled atmospheric CO₂ concentration, the sea level rise is very large, 1.7 m. The rise in sea level was calculated based on the warming obtained from a very long term (several thousand year) integration of the coupled model, and accounting only for the thermal expansion of the seawater. Any reduction in land ice volume would be an addition to this amount. Fig. 1.2 shows the increase in sea level in an experiment where the atmospheric CO₂ concentration rose at a rate of 1% per year to doubling (year 70) and then was held fixed. Note that sea level continues to rise for hundreds of years after the CO₂ concentration is stabilized.

Table 1.1. Sea level rise at doubling for the various integrations

Exp. Name	1/4%	1/2%	1%	2%	4%	Equilibrium
Sea level rise (cm)	42	27	15	9	5	171
FRAC	0.245	0.158	0.088	0.053	0.029	1.0

Sea level rise given as the difference between the given integration and the control integration for the given time period. Here sea level rise is only the component of the expansion of the water due to the density changes caused by temperature and salinity changes. FRAC is the fraction of the total sea level rise response, computed by dividing the sea level rise from the given scenario integration by the sea level rise of the equilibrium integration.

PLANS FY96

In-depth analysis of the experiments will continue. Special emphasis of the analysis will be placed upon the comparison between the transient response of the coupled system and its equilibrium response to CO₂-doubling.

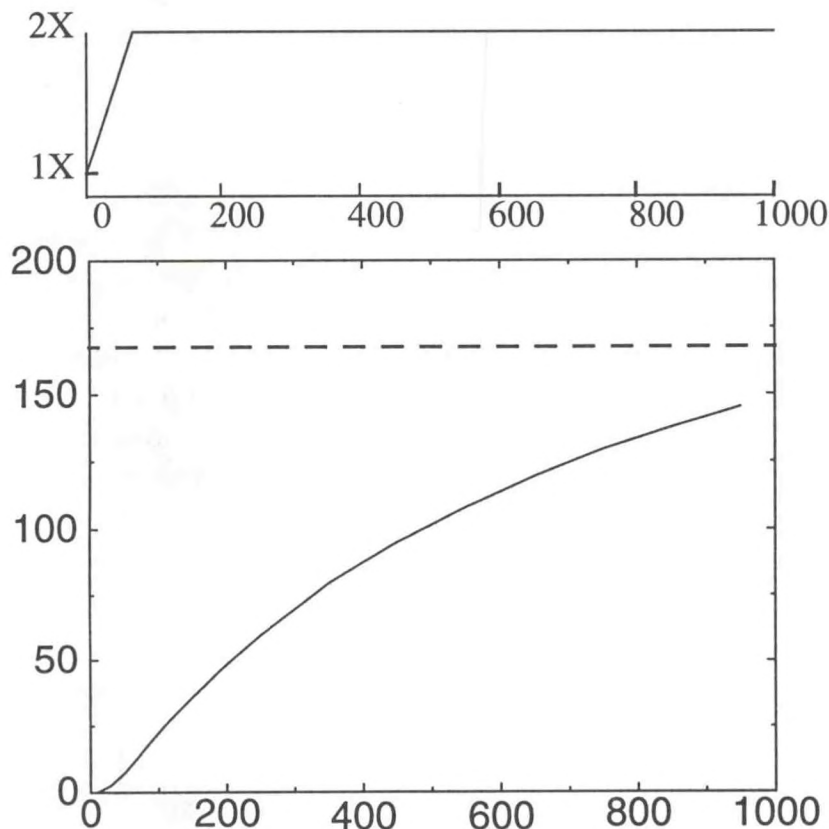


Fig. 1.2 Top: Schematic of prescribed concentration of CO_2 in the atmosphere of the coupled model. The vertical coordinate is the logarithm of the CO_2 concentration which is proportional to the radiative forcing. Bottom: The sea level rise due to expansion only during the first 1000 years of equilibrium integration. The horizontal dashed line indicates the equilibrium sea level rise (1.7 m), obtained from a very long term integration of a coupled model. The units are cm. Both horizontal coordinates are model years. The sea level continues to rise for hundreds of years after the CO_2 concentration is stabilized.

1.1.2 Climate Variability

1.1.2.1 SST Variability in Greenland Sea

*T. Delworth R.J. Stouffer
 S. Manabe*

ACTIVITIES FY95

The variability of oceanic and atmospheric temperature in the coupled model at decadal and longer time scales is characterized, in part, by large, persistent anomalies in the western Greenland Sea, as summarized in Fig. 1.3. An inspection of

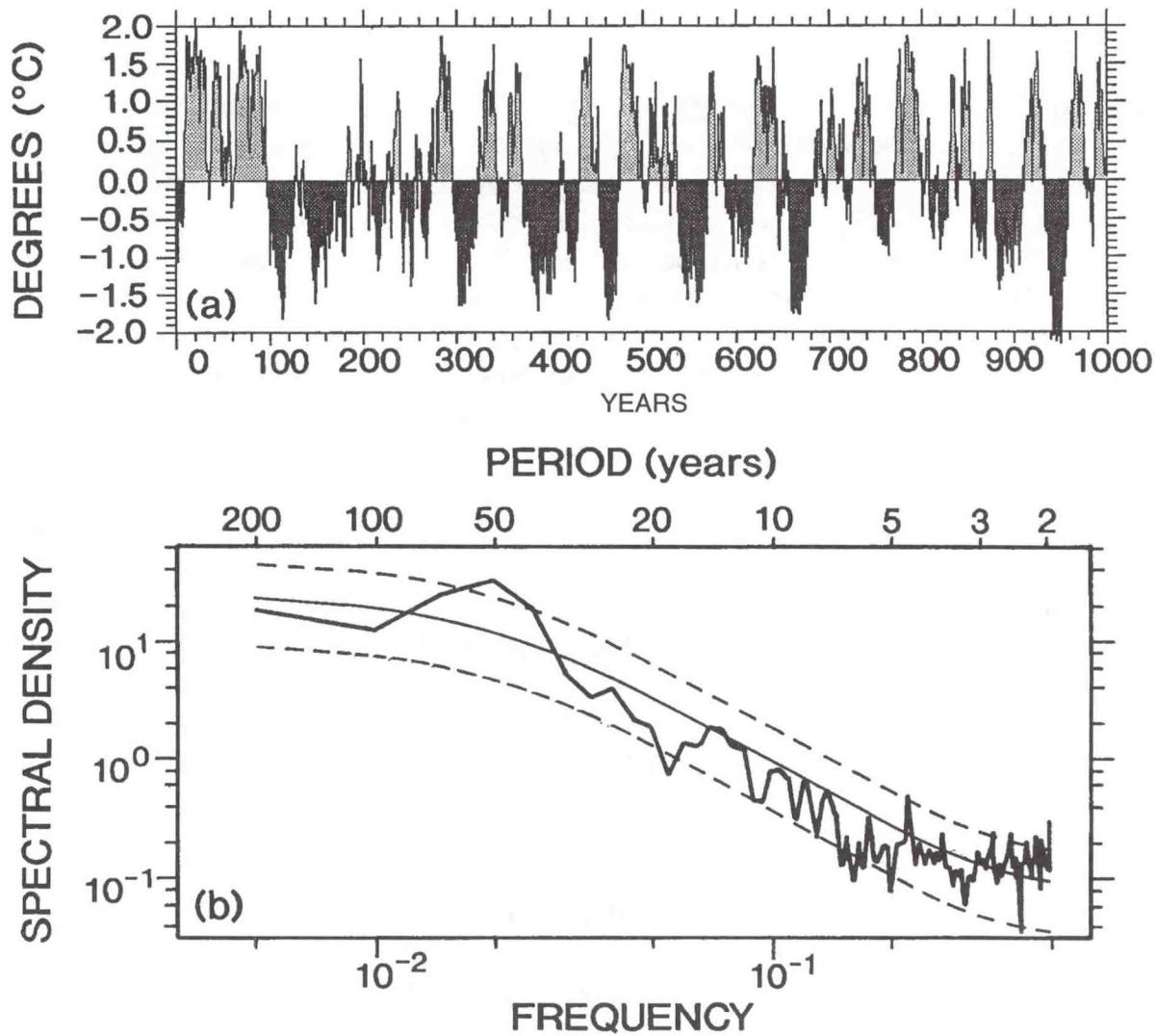


Fig. 1.3 (a) Time series of annual mean model sea surface temperature averaged over the longitude range 15°W to 26°W at 70°N . The values are anomalies from a long term mean. Units are $^{\circ}\text{C}$.

(b) Spectrum of the time series shown in (a). The logarithm of the spectral estimates (thick, solid line) is plotted versus the logarithm of frequency. The thin, solid line denotes the spectrum of a background first order Markov process, and the dashed lines denote the 95% confidence interval about that background spectrum. The period is listed along the top axis in years. The spectrum was estimated by taking the Fourier transform of the autocovariance function using a Tukey window with a maximum lag of 200 years.

the time series of model sea surface temperature (Fig. 1.3a) and its spectrum (Fig. 1.3b) reveal that this variability is characterized by a time scale of approximately 50 years. This is similar to the time scale of the previously identified (1182) fluctuations of the model thermohaline circulation (THC) in the North Atlantic. The possible

relationship between the temperature variability in the western Greenland Sea and the THC was investigated.

Analyses have shown that the surface air temperature variations in the Greenland Sea region are closely linked with changes in oceanic temperature and salinity that extend quite deep in the model ocean (1-2 Km). In the region of the East Greenland current of the model, cold, fresh water overlies warm, saline water. A reduction in the intensity of the East Greenland current (a precursor of an intensifying THC in the North Atlantic) is associated with increased near-surface salinity and enhanced vertical mixing, thereby mixing the warm, deeper water with the cold, near-surface water. This leads to a substantial warming of the surface waters and a reduction of sea ice. The latter enhances the ocean-to-atmosphere heat flux, consequently warming the near-surface atmosphere. These changes appear to lead the changes in the intensity of the THC by approximately 1/4 cycle.

PLANS FY96

The mechanisms responsible for this large signature of interdecadal surface air temperature variability in the coupled ocean-atmosphere model will be further explored.

1.1.2.2 Simulated and Observed SST Variability

A. Hall

S. Manabe

ACTIVITES FY95

Identifying the causes of natural variability in the climate system is a key challenge of present-day research. One theory attempts to explain the mechanism of variability by dividing the climate system into fast and slow components². In this scheme, the atmosphere makes up the fast component, while the slow components include the ocean, cryosphere, and land surface. This "stochastic theory" then explains the variability of any one of the slow components as a "red-noise" response to random, "white-noise" forcing from the atmosphere. The appropriateness of stochastic theory for the mixed-layer ocean may be evaluated by analyzing the variability of sea surface temperature (SST) and sea surface salinity (SSS). This intercomparison of SST and SSS proves useful, since stochastic theory predicts that the spectrum of SSS variability ought to be "redder" than its SST counterpart, owing to the damping of SST anomalies through exchange of heat across the atmosphere-ocean interface.

2. Hasselmann, K., Stochastic climate models, Part I: theory, *Tellus*, 28, 473-485, 1976.

With this prediction in mind, SST and SSS time series were analyzed at four ocean weather stations, along with SST and SSS data from the 1000 year run of the GFDL coupled ocean-atmosphere model. Differences between the model and observations can be used to infer the absence of a particular physical process in the simulation. The data at weather station Papa, in the northeast Pacific, is consistent with the stochastic picture. In this case, it was found that stochastic theory can be applied to salinity as well as temperature, explaining the relative redness of the SSS spectrum as illustrated in Fig. 1.4. Similar results hold for the model grid point nearest Papa. However, at the other weather stations, the stochastic mechanism cannot be the only significant source of SST and SSS variability. At station Panulirus (near Bermuda) mesoscale eddies, which are not resolved by the model, enhance the variability at high frequencies. This is evidenced by a larger signal at time scales less than one year in the observational record relative to the model grid point nearest Panulirus. In addition, unlike the model, observational SST and SSS exhibit significant

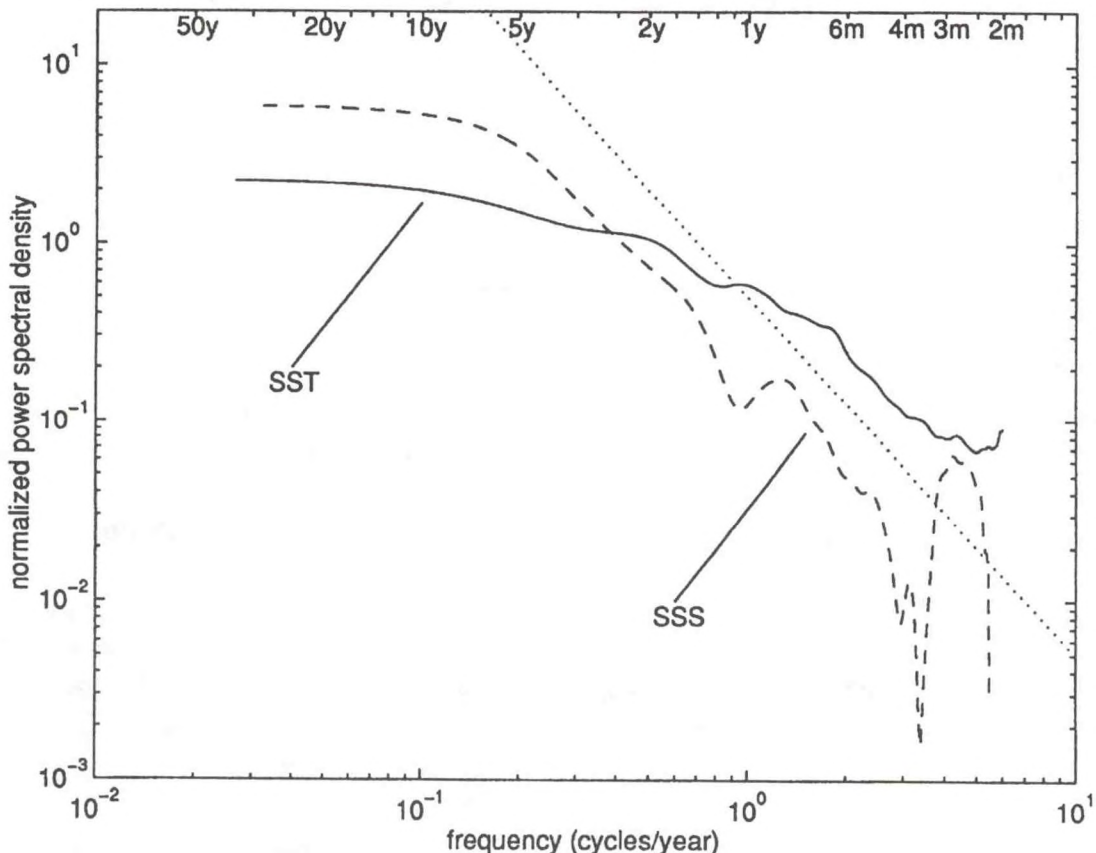


Fig. 1.4 The normalized spectra of SSS (dashed) and SST (solid) at weather station Papa. The spectra were calculated by taking the Fourier transform of the autocorrelation function using a Parzen window with a maximum lag of 6 years. They were then smoothed by equal weighted averaging over a base 10 logarithmic frequency interval of 0.15. The dotted line shows the characteristic predicted ω^{-2} slope². Time scales are shown on the upper edge of the plot. For the data at this station, the simple stochastic model can be applied to salinity as well as temperature.

coherence on these same time scales, indicating the passage of saline, warm-core or fresh, cold-core eddies. At stations India and Mike (North Atlantic), large scale variations of the ocean circulation are responsible for much of the low frequency variability, as evidenced by the high degree of coherence between SST and SSS on long time scales in both the model and observations. These variations in the ocean circulation may be related to changes in the thermohaline circulation of the north Atlantic. Moreover, spectral analysis showed that there is little difference in the redness of the SST and SSS spectra at both of these weather stations and their nearest model grid points, contradicting the prediction of stochastic theory. Thus in the regions of the surface ocean where either mesoscale eddies or large-scale heat and salt transport dominate, stochastic theory cannot adequately explain the variability of the mixed layer.

PLANS FY96

The mechanisms of natural variability will be further explored using a coupled ocean-atmosphere model.

1.1.2.3 Interannual Pacific Variability

T. Delworth *R.J. Stouffer*
S. Manabe

ACTIVITIES FY95

Interannual to interdecadal variability in the North Pacific Ocean has been studied in a coupled ocean-atmosphere model. The objectives of the project are to compare the variability of the model North Pacific to observed climate variability and to elucidate some of the mechanisms involved. The output from the 1000-year integration of the coupled model (1201, yk) formed the dataset for analysis.

Analyses have focused on the Northern Hemisphere winter season, defined as December through February. Prior to analysis, the model SST data were filtered such that time scales longer than 30 years were removed. The first EOF (empirical orthogonal function) of model SST is shown in Fig. 1.5a. This mode is characterized by an anomaly of one sign in the central North Pacific, with a crescent shaped pattern of opposite sign in the eastern portion of the basin. The model EOF may be compared to the first EOF of observed SST, shown in Fig. 1.5b (adapted from Wallace et. al., 1990³). While the model pattern is shifted to the west, the model reproduces many of the features of the observed variability. Spectral analysis of the model EOF time series reveals substantial variability on interannual to interdecadal time scales.

3. Wallace, J.M., C. Smith, and Q. Jiang, Spatial patterns of atmosphere-ocean interaction in the northern winter, *J. Climate*, 3, 990-998, 1990.

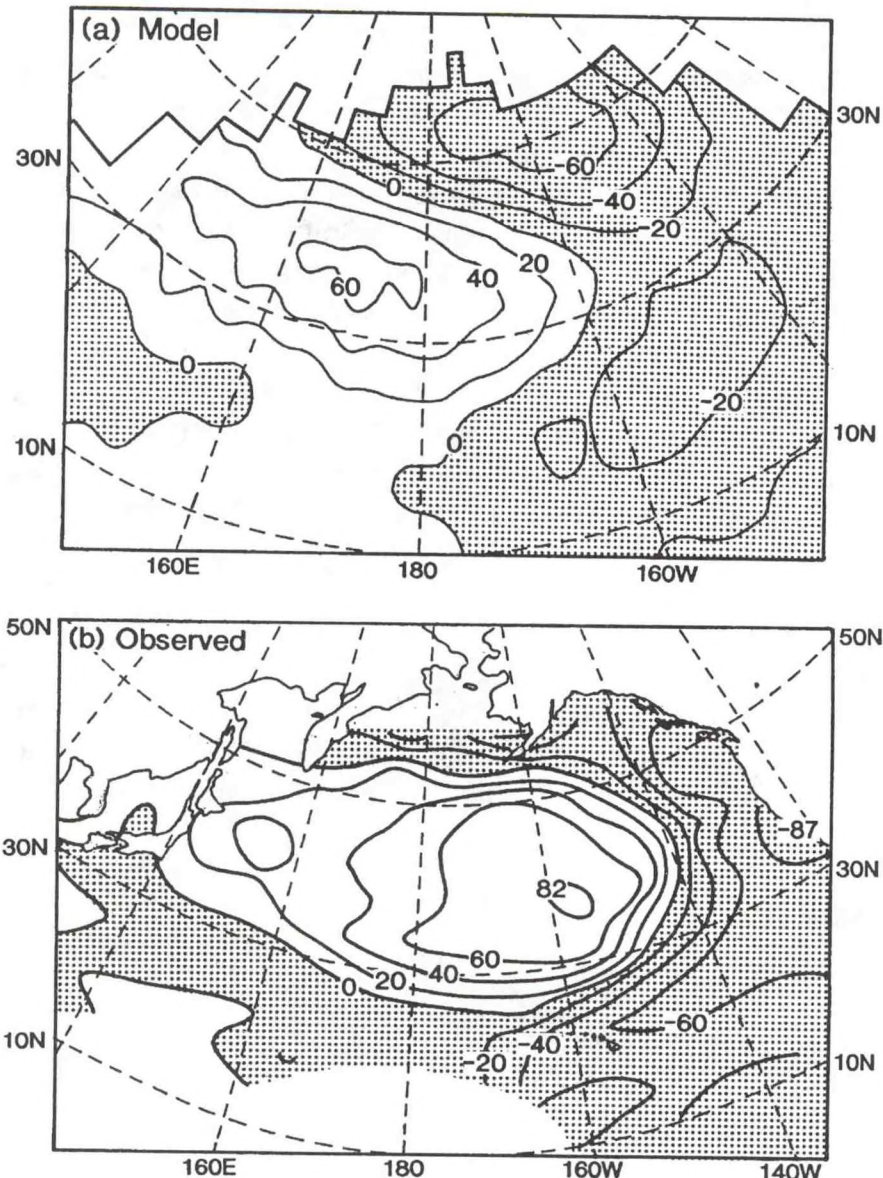


Fig. 1.5 Spatial patterns of the first EOF of seasonal mean (December-February) SST. The value at each grid point denotes the correlation coefficient (multiplied by 100) between the time series of the first EOF and the time series of SST at that point. The EOF analysis used the covariance matrix, and encompassed a domain in the North Pacific north of 20°N. SST values were multiplied by the square root of the cosine of the latitude in order to weight the grid boxes by their respective area.

(a) Model SST, explaining 13.5% of the spatially integrated variance. Values less than zero are stippled. Prior to the EOF analysis, the model SST data were filtered such that timescales longer than 30 years were removed from the data in order to focus on the interannual variability. The analysis period encompassed 800 years of model data.

(b) Observed SST, explaining 24% of the variance (adapted from Wallace et al.³). The analysis period was 1946-1984 using the Comprehensive Ocean-Atmosphere Data Set (COADS).

Diagnostic analyses have shown that the model SST pattern in Fig. 1.5a is primarily attributable to atmospheric forcing through both anomalous surface heat fluxes (dominant around the periphery of the basin) and Ekman pumping (playing a major role in the center of the basin). The oceanic variability may be roughly viewed as the red noise response to the white noise time series of atmospheric forcing. Atmospheric variations have a large characteristic spatial scale, but have little persistence in time (hence, their characterization as "white noise"). The large thermal inertia of the ocean dictates a slow adjustment to this high frequency forcing. The characteristic atmospheric variability associated with this mode of oceanic variability resembles the well-known PNA (Pacific-North American) pattern. Additional analyses of the same atmospheric model coupled to a mixed-layer ocean support the above results.

The success of this model in simulating some of the characteristics of North Pacific SST variability is encouraging. The role of surface fluxes in forcing North Pacific variability is consistent with studies using ocean-only models.

PLANS FY96

Analysis of low frequency variability in the coupled model of the atmosphere-ocean system will be continued, comparing the output of the coupled model to that from extended integrations of an atmospheric model coupled to a mixed-layer ocean, as well as to the output from an atmospheric model with prescribed sea surface temperatures.

1.1.3 Paleoclimate

1.1.3.1 Abrupt Climate Change

S. Manabe *R.J. Stouffer*

ACTIVITIES FY95

The records of isotopic temperature from Greenland ice cores suggest that large and abrupt changes of North Atlantic climate occurred frequently during glacial and postglacial periods in association with the Younger Dryas event and the so-called Dansgaard-Öschger (D-O) oscillation. It has been speculated that these changes result from the rapid changes in the THC of the Atlantic Ocean caused by the release of a large amount of meltwater from continental ice sheets. An attempt has been made to simulate an abrupt climate change by use of a coupled ocean-atmosphere model. In response to a massive surface water flux (e.g., 1 Sv during the first 10 years) into the 50°N-70°N latitude belt in the North Atlantic of the model, the coupled model undergoes an abrupt change similar to that indicated by ice and deep sea

cores. The associated change of surface air temperature is particularly large in the northern North Atlantic, but is relatively small in the rest of the world.

The sudden drop in sea surface temperature which occurs during the first decades of the experiment as indicated in Fig. 1.6a, results partly from the reduction of convective activity which mixes the cold surface water with the warmer subsurface water of the ocean. The SST drop is also attributable to the rapid weakening of the THC (Fig. 1.6b) which advects warm surface water towards the northern North Atlantic. The large initial weakening and subsequent reintensification of the THC appear to be induced by the massive, initial infusion of fresh water and its abrupt termination, respectively. After the initial fluctuation, the THC reintensifies gradually (Fig. 1.6b), increasing both SST and SSS during the next few hundred years.

Recent studies (1146, 1192) have indicated that the CO₂-induced warming of the model atmosphere is accompanied by an increase in the poleward transport of water vapor, leading to a marked increase in precipitation and, accordingly, fresh water supply in the high latitudes. The simulated multi-century response of the THC to a doubling of atmospheric CO₂ resembles the response to the fresh water input described here. Thus, substantial changes in the intensity and distribution of the THC could also occur in response to future increases of greenhouse gases in the atmosphere.

PLANS FY96

The experiment described above will be repeated, but with an alteration of the intensity and duration of fresh water flux. In-depth analysis of the dynamical mechanisms involved will continue.

1.1.3.2 Paleoclimate Model Intercomparison Project

A.J. Broccoli

S. Manabe

C.F. Ip

ACTIVITIES FY95

A new series of paleoclimate modeling experiments was initiated to extend previous research that explored the mechanisms maintaining the ice age climate (630, 707, 769). An updated version of the atmosphere mixed-layer ocean model, designed for paleoclimate experiments, was used to simulate the climate of the last glacial maximum, which occurred approximately 21,000 years ago. The model employs considerably higher horizontal and vertical resolution than had been used in previous GFDL paleoclimate simulations, and includes the effects of sea ice dynamics. To simulate the glacial climate, the ice sheet distribution and continental boundaries were altered to comply with recent geophysical reconstructions, the atmospheric

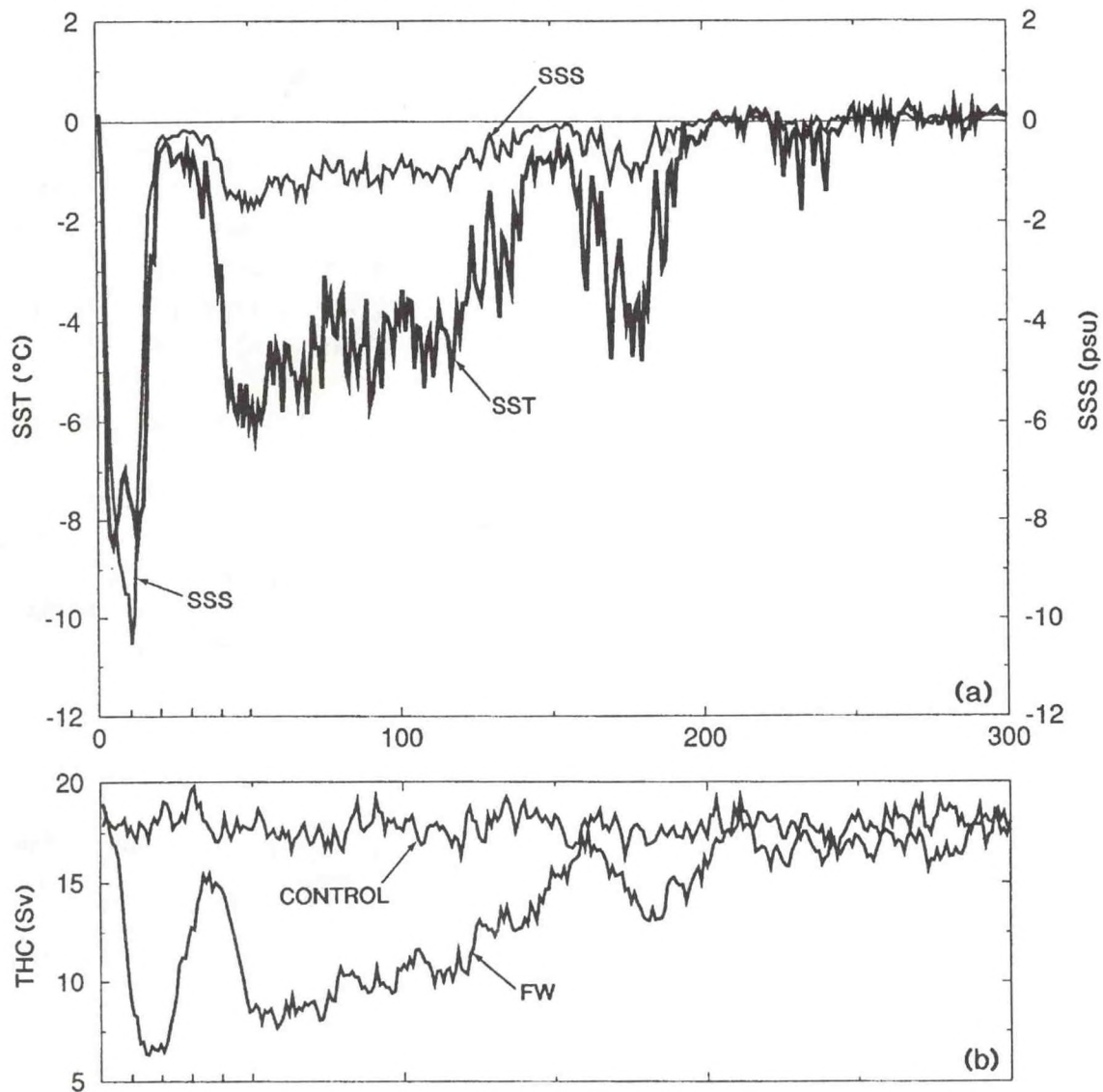


Fig. 1.6 (a) Time series of the deviations of sea surface temperature ($^{\circ}\text{C}$) and sea surface salinity (psu) from their initial values (i.e., 7°C and 35 psu, respectively) at a grid point in the Denmark Strait (60.75°N , 37.50°W) obtained from the present fresh water (FW) experiment. (b) Temporal variations of the rate of thermohaline overturning (Sv , i.e., $10^6 \text{ m}^3/\text{sec}$) in the North Atlantic obtained from the control and perturbed (FW) experiments. Here, the rate of thermohaline overturning is defined as the maximum value of the stream function of meridional circulation in the North Atlantic. The sudden drop in SST during the first decades results from a reduction of convective activity and a weakening of the thermohaline circulation.

greenhouse gas content was reduced to levels measured in ice core bubbles, and the earth orbital parameters were prescribed to be those calculated for 21,000 years ago based on orbital mechanics. By comparing the results of this integration with an analogous simulation of the modern climate, the processes that maintain the glacial climate will be investigated. A preliminary analysis indicates a globally-averaged glacial cooling quite comparable to previous estimates, but with some changes in geographical distribution.

This experiment is one of the cornerstones of the Paleoclimate Model Intercomparison Project (PMIP), which has been designated as a core project of the International Geosphere-Biosphere Project/Past Global Changes (IGBP-PAGES). Over a dozen groups are participating in PMIP, with each group contributing up to three sets of paleoclimate experiments. PMIP seeks to understand the consistencies and inconsistencies among the participating models, to identify geographical regions for intensified effort in paleoclimate reconstruction, and to explore the range of uncertainty in current estimates of climate sensitivity.

PLANS FY96

Analysis of the glacial climate simulation will continue in considerable detail. Of special interest are the simulated mass balance of the continental ice sheets and the evaluation of the sensitivity of tropical temperature using paleoclimatic reconstructions. In addition, a simulation of the so-called "climatic optimum" 6,000 years ago, when summer solar radiation was stronger in the Northern Hemisphere, will be conducted as an additional contribution to the PMIP effort.

1.1.4 Model Development

1.1.4.1 Coupled Model with Higher Resolution

<i>K. Dixon</i>	<i>M. Spelman</i>
<i>S. Manabe</i>	<i>R.J. Stouffer</i>

ACTIVITIES FY95

An experiment using the coupled ocean-atmosphere model with increased computational grid resolution has been completed. The atmospheric component of the coupled model has a grid spacing of 3.8° longitude and 2.2° latitude with 14 vertical levels. In the oceanic component, the grid resolution is 1.9° longitude, 2.2° latitude, and 18 levels. To prevent a systematic drift of the model climate during the integration of the coupled model, a technique called flux adjustment is employed (1042).

In preparation for constructing the coupled model, the time integration of the atmospheric model for 20 years was completed to generate surface boundary data for

the ocean component of the coupled model. The time integration of the ocean model for 2,500 years was completed to generate the initial condition for the coupled model. The surface flux adjustments are computed as the difference between the two sets of fluxes obtained from the integrations of the atmospheric and oceanic models.

The initial conditions for the time integration of the coupled model have realistic seasonal and geographical distributions of surface temperature, surface salinity, and sea ice for which both the atmospheric and oceanic model states are nearly in equilibrium. Starting from the near-equilibrium conditions, the coupled model was integrated over the period of 80 years. Despite the flux adjustments, a rapid drift of the climate away from the initial conditions occurred, especially in the high latitudes of the Southern Hemisphere. This drift appeared to result from a computational instability which developed during the initial integration of the oceanic model. This instability results from the use of the technique for accelerating the approach of the deep layers of the oceanic model toward the equilibrium state. When a new equilibrium state of the oceanic model was computed without the acceleration, the rapid climate drift did not occur. The solution of this instability problem has removed a major obstacle for the successful time integration of the coupled model.

PLANS FY96

Improved versions of the atmospheric and oceanic components of the coupled model will be constructed in an effort to correct deficiencies in the simulations using the model. The improvements include more realistic distributions of temperature, salinity, and sea ice at the ocean surface, and revisions to the diffusion parameters of the oceanic model. Time integrations of the coupled ocean-atmosphere model with higher computational resolution will then be initiated to investigate the climatic impact of increased CO₂ in the atmosphere.

1.1.4.2 Sea Ice Model

<i>A.J. Broccoli</i>	<i>S. Manabe</i>
<i>K. Dixon</i>	<i>M.J. Spelman</i>
<i>C.F. Ip</i>	<i>R.J. Stouffer</i>

ACTIVITIES FY95

A major activity during this year was the incorporation of sea ice dynamics into both the atmosphere-mixed layer ocean model and the coupled ocean-atmosphere model. For this purpose, the cavitating fluid model of Flato and Hibler⁴ was used because of its limited computational cost and suitability for simulating sea ice motion

4. Flato, G. M., and W. D. Hibler III, Modeling pack ice as a cavitating fluid, *J. Phys. Oceanogr.*, 22, 626-651, 1992.

on longer time scales. The implementation of the cavitating fluid sea ice model in these two climate models required extensive coding, and conducting a number of low resolution test integrations. The paleoclimate integrations discussed in section 1.1.3.2 are the first set of sensitivity experiments to employ this sea ice dynamics submodel.

PLANS FY96

Improved boundary layer physics and diurnal variation are other areas of model development that will receive attention in FY96. In addition, efforts to logically restructure the climate model code will continue.

1.2 CONTINENTAL HYDROLOGY AND CLIMATE

1.2.1 Simulation of Runoff and River Discharge

*K.A. Dunne** *R.T. Wetherald*
*P.C.D. Milly**

**U.S. Geological Survey*

ACTIVITIES FY95

A project to evaluate the simulation of runoff by the Climate Dynamics coupled air-sea GCMs was initiated during the past year, focusing on comparisons between model output and observations of annual runoff and its controlling variables, with attention to variability on the annual to decadal time scales. This study should provide a context for interpretation of runoff change predictions derived from climate-change experiments, and may yield insights leading to improved realism in the parameterization of continental water processes.

Observations of river discharge have been used to infer river-basin mean values of runoff for 24 major river basins of the world. Observational time series range in length from 4 to 112 years (half of them having a length of about 50 years or more). Outputs from the R30 and R15 models span 80 and 1000 years, respectively.

Some simple quantitative comparisons between modeled and observed means and variabilities of runoff have been conducted. Basin-mean runoff rates are illustrated in Fig. 1.7. The largest model errors are found in low-runoff basins (Murray, Colorado, Nile, etc.), where the bias is positive, and, for the R15 model only, in the high-runoff Amazon and Orinoco basins, where the bias is negative. These cases aside, the models generally reproduce the geographic variability of river discharge, but err by a factor of 2 or more in many basins. Preliminary analysis suggests that, in many cases, errors in model precipitation contribute significantly to errors in mean runoff.

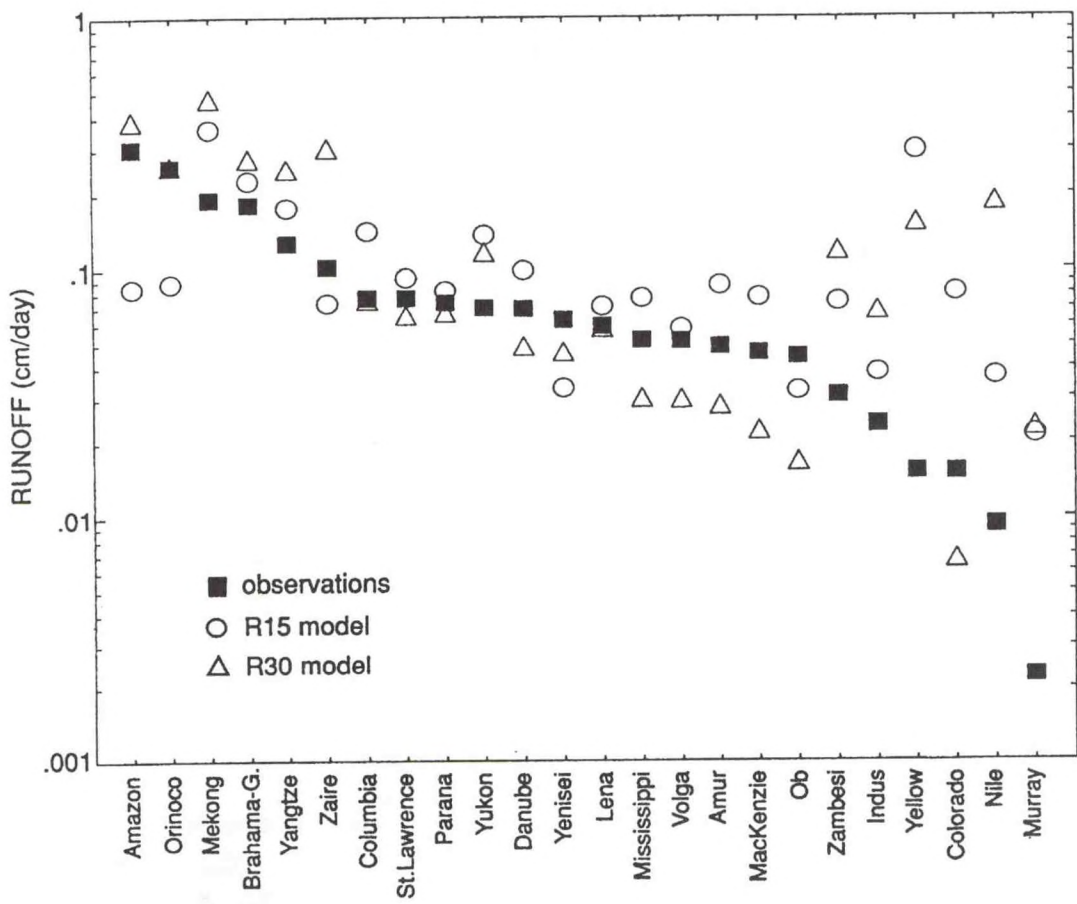


Fig. 1.7 River-basin mean rates of runoff from the GCMs and observations. The basins are arranged in descending order, from left to right, according to the magnitude of the observed basin runoff.

PLANS FY96

Underlying causes for errors in modeled runoff will be sought. Controls on runoff (precipitation, surface net radiation) will be investigated in order to explain model performance with respect to geographic and interannual variability of runoff.

1.2.2 Intercomparison of Land-Surface Parameterization Schemes

K.A. Dunne P.C.D. Milly**

**U.S. Geological Survey*

ACTIVITIES FY95

The Project for Intercomparison of Land-Surface Parameterization Schemes (PILPS) is an international project with the objective of identifying the essential differences among the many parameterizations used to characterize water and energy exchange at land surface in GCMs. In "Phase 1," participants simulate the equilibrium response of land surfaces with specified characteristics to prescribed (synthetic) time series of forcing data. GFDL and USGS are participating by assisting in experimental design and analysis and by providing simulation results for one scheme.

Continuing efforts have been directed at quality control of results submitted for analysis by the 14 schemes now participating in Phase 1, because it has been shown that errors in the execution of the numerical experiments are a major factor contributing to spread among the results. Results from a subset of 8 schemes that satisfy all checks on internal consistency have been analyzed in detail. The analysis suggests that the neglect of stomatal resistance is the modeling assumption having the greatest impact on annual and monthly water and energy balances. Among schemes that include such a resistance, during seasons of little or no water stress, deviations (across schemes) of evaporation appear to be caused primarily by differences in parametrization of bulk stomatal resistance and by the neglect or inclusion of precipitation interception by the plant canopy. However, deviations of monthly fluxes are greatest during seasons of water shortage, and are correlated mainly with the differing propensities of schemes to deplete root-zone soil water. It has also been noted that individual schemes differ markedly and systematically in the partitioning of runoff between surface and subsurface.

One outcome of this analysis has been the recognition that PILPS to date has concentrated on systems with little water stress through most of the year, minimizing the apparent importance of soil-water processes. As a result of this project, the need for attention to more arid environments is now clearly recognized within PILPS.

PLANS FY96

Quality-control work will continue in collaboration with individual participants in an attempt to expand the number of schemes producing usable results. At the same time, the current analysis will be continued. Phase-1 work is expected to near completion in FY96.

1.2.3 Water and Heat Fluxes in Desert Soils

*P.C.D. Milly**

**U.S. Geological Survey*

ACTIVITIES FY95

An understanding of water and heat movement in desert soils is needed for the formulation of models of land-atmosphere interactions and for the interpretation of climatic signals appearing in the soil profiles of water and heat storage. An earlier collaborative study with the University of Texas used a detailed numerical model of soil water and heat flow to interpret an extensive set of data collected in the Chihuahuan Desert of western Texas (1254). That analysis led to the formulation of a hypothesis regarding the character of vertical water flow in arid environments, *i.e.*, that, in a sufficiently arid environment, there exist equal and opposite annual-mean water fluxes driven by gradients of temperature and water potential. This hypothesis has been used to formulate a mathematical model using the theory of non-isothermal water transport in porous media (yn). The model was tested against field observations of moisture potential. Calculated annual-mean profiles and seasonal changes of moisture potential were consistent with observations. The fitted water-transport coefficient was consistent with independent laboratory values. Observed profiles of bomb-fallout isotopic (^{36}Cl and ^3H) concentrations were qualitatively consistent with the liquid and vapor transports of water predicted by the model.

1.3 PLANETARY WAVE DYNAMICS

1.3.1 Baroclinic Instability, Geostrophic Turbulence, and Extratropical Dynamics

<i>J. Anderson</i>	<i>P. Phillipps</i>
<i>S. Chen</i>	<i>A.-M. Treguier</i>
<i>I. Held</i>	<i>J. Zhang</i>
<i>V. Larichev</i>	<i>Q. Zhang</i>
<i>V. Pavan</i>	

ACTIVITIES FY95

1.3.1.1 Quasi-Geostrophic Turbulence and Eddy Flux Parameterization

Work on developing theories for eddy fluxes generated by baroclinic instabilities has progressed on several fronts. The problem has been split into two parts: 1) computing, and developing a theory for, eddy fluxes in horizontally homogeneous flows; and 2) studying the relationship between the fluxes in these homogeneous flows and the fluxes in inhomogeneous flows of interest.

Current research on homogeneous turbulence driven by baroclinic instability has produced a scaling theory for eddy amplitudes, length scales, and potential vorticity fluxes in the “oceanic” parameter regime where the eddy energy level is larger than the mean kinetic energy (w_u, y_w). The key to understanding this turbulent regime is the determination of the eddy length scale, which can be much larger than the radius of deformation because of the existence of an inverse energy cascade. The theory predicts eddy statistics that are very sensitive to the mean temperature gradients. In particular, the eddy heat flux is proportional to the fourth power of the temperature gradient. The qualitative predictions of the theory have been confirmed by numerical experiments, but important quantitative differences remain. For example, the numerical experiments indicate that the eddy heat flux is even more sensitive to the mean temperature gradients than predicted by the theory.

Numerical experiments have also been performed to test the relevance for inhomogeneous flows of the flux/gradient relationship, or “diffusivity,” determined by the homogeneous model. Initial work along these lines is very encouraging (y_u). For the baroclinically unstable jets considered in this work, the homogeneous diffusivity predicts the eddy potential vorticity flux remarkably well as long as the jet is at least several radii of deformation wide, as illustrated in Fig. 1.8. The homogeneous theory

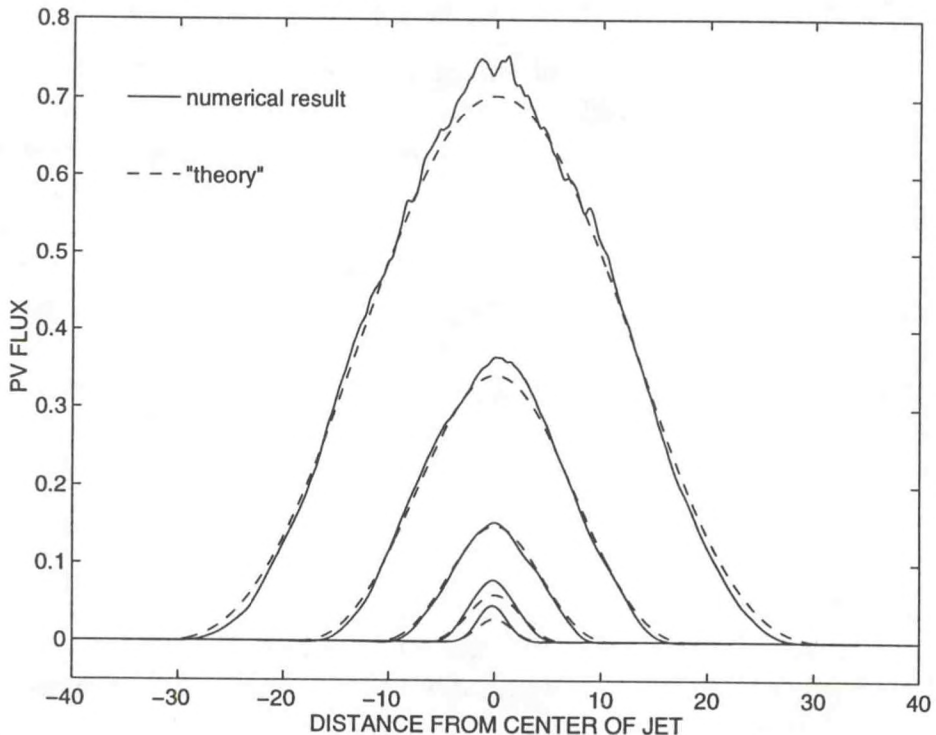


Fig. 1.8 The eddy potential vorticity fluxes in the lower layer of a two-layer model of a baroclinically unstable jet. Solid lines are the numerical results and dotted lines the predictions of a diffusive theory in which the diffusivity is determined by numerical calculations with a homogeneous model. The different sets of lines correspond to jets of different widths. Distance on the horizontal axis is measured in radii of deformation.

consistently underpredicts the amplitude of the eddy fluxes when the unstable jet is only a few radii of deformation wide. Possible explanations for this behavior are under investigation.

A primitive equation model of a baroclinically unstable jet, in which the parameters have been chosen to be similar to those observed for the Antarctic Circumpolar Current (ACC), is being analyzed to help in determining how eddy flux closures developed in the context of quasi-geostrophic (QG) theory can best be applied to primitive equation models. Important issues arise near the surface, where the convergence of vertical eddy buoyancy fluxes are generally important. This term does not appear in QG models. Care must also be taken in relating the horizontal potential vorticity flux in the QG model to the isopycnal flux in the primitive equation model. These results suggest a formulation of an eddy-flux closure scheme for z-coordinate ocean models that is different in important respects from the Gent-McWilliams scheme currently being utilized by several ocean modeling groups.

Study has also begun of a quasi-geostrophic wind-driven two-layer model to study the implications of diffusive theories for the relationship between the vertical shear and wind stress in such a system.

1.3.1.2 The Effects of Latent Heating on Eddy Statistics

The analysis of the effects of latent heat release on the time-averaged baroclinic eddy fluxes in several idealized models is nearing completion. Since the effects of latent heating increase in a warmer climate, these models should suggest new ways of analyzing GCM simulations of the climatic response to increasing greenhouse gas concentrations. Work has progressed on a two-layer quasi-geostrophic model and an idealized GCM. The comparison between these two models promises to be valuable in isolating different mechanisms by which latent heating affects eddy statistics. Given the success described in 1.3.1.1 in using diffusive approximations for eddy fluxes based on homogeneous turbulence models, the study of a moist two-layer homogeneous turbulence model has also been initiated.

1.3.1.3 Storm Tracks

The seasonal cycle of the North Pacific storm-track has become the focus of considerable interest because of its counter-intuitive behavior: while the maximum strength of the north-south temperature gradient occurs in January, maximum energy levels occur in November and March. Therefore, it is difficult to understand this seasonal cycle in terms of a theory in which the strength of the storm track is simply a function of the local baroclinicity. This and related problems are being addressed from several perspectives, discussed below.

Two competing arguments for this "mid-winter minimum" are 1) a reduction of upstream disturbances seeding the Pacific storm track in midwinter, and 2) faster advection of disturbances through the Pacific, allowing less time for growth. A two-layer QG model has been formulated to study the competition between these two mechanisms in a simple dynamical context. Experiments are currently underway examining the sensitivity of this model's storm track to the upstream seeding.

A spherical primitive equation model, linearized about a zonally asymmetric time mean flow is being used to study linear aspects of the same problem in a more realistic context. Linear explanations for storm track structure have historically focused on normal modes, but an alternative stochastic approach has shown considerable promise. In this approach, one initializes the linear model with an ensemble of randomly chosen initial conditions and integrates only for a few days. This model has been applied to a zonally symmetric problem in which the storm track is displaced meridionally by changing the surface drag in an idealized dry GCM. (The storm track moves polewards when the surface drag is decreased in strength.) This linear stochastic algorithm picks up some aspects of the model's qualitative behavior.

Barotropic models of the upper troposphere have shown a surprising ability to predict the rough position of storm tracks, without any information regarding the baroclinic wave sources. Two such models have been analyzed. In the first (a collaborative study with S. Lee at Penn State), a barotropic model is relaxed to a zonally asymmetric flow, becomes unstable, generates high frequency transients in a way that is still only poorly understood, and organizes the transients into localized maxima that resemble the observed oceanic storm tracks. In the second, a linear barotropic model is subjected to stochastic initial conditions as described above and produces enhanced variance in the regions of the oceanic jets. The implications of this ability of upper tropospheric barotropic dynamics to organize eddy activity into storm tracks even in the absence of localized baroclinic sources remains unclear.

PLANS FY96

Work will continue on problems related to baroclinic equilibration, storm track dynamics, latent heating effects of eddies, and geostrophic turbulence, using a variety of idealized models.

1.3.2 Generation of Tropical Transient Waves

Y. Hayashi

D. Golder

ACTIVITIES FY95

Over the past three decades, a number of theories have been proposed to explain low- and high-frequency tropical waves such as tropical intraseasonal oscillations (TIOs), superclusters, cloudclusters, Kelvin and mixed Rossby-gravity waves, and gravity waves. These theories can be classified into instability and random-forcing theories. Neither theory, however, adequately explains the wavenumber-frequency spectral distribution, structure, and generation of these waves. On the other hand, these waves have been reasonably well simulated by GFDL general circulation models with moist convective adjustment (1118).

In an effort to improve on these theories, wave-generation mechanisms have been proposed (1272) to unite the instability and random-forcing theories as follows. The modeled TIOs grow essentially through the evaporation-wind feedback mechanism, while the remaining waves amplify essentially through "saturation-triggering mechanism." The latter mechanism hypothesizes that transient waves coupled with moist convection are amplified by random heat pulses. The heat pulses, in turn, are produced by the abrupt onset of moist convection triggered by intermittent saturation in the presence of any pre-existing unstable stratification.

A numerical study of tropical transient waves has been conducted in order to examine the united wave-generation mechanisms. For this purpose, control experiments have been performed using an idealized nine-level R21 spectral model with moist convective adjustment. The model uses prescribed globally uniform distributions of sea-surface temperatures and insolation conditions, thereby excluding stationary waves and extratropical baroclinic waves. However, even this idealized model produced tropical transient waves. When wind fluctuations in the parameterized surface fluxes of latent and sensible heat were eliminated, the TIOs were profoundly weakened, consistent with evaporation-wind feedback theory, while other waves were only slightly affected. Subsequently, the moist convective adjustment scheme was modified to neutralize any conditionally unstable stratification that would otherwise develop during periods of nonsaturation. All tropical waves then disappeared in spite of the presence of moisture convergence, in contrast to wave-CISK theory. These results were consistent with the united wave-generation mechanisms.

On the other hand, a theoretical study of tropical transient waves has also been conducted in order to examine these mechanisms. For this purpose, the scheme of moist convective adjustment was artificially partitioned into two consecutive

processes of diagnostic and prognostic adjustments. Diagnostic adjustment neutralizes, upon saturation, any conditionally unstable stratification that has developed during periods of nonsaturation. Prognostic adjustment continually neutralizes any conditionally unstable stratification that is hypothetically possible during saturation. The heating due to diagnostic adjustment is a function of moisture and temperature, while that due to prognostic adjustment a function of large-scale variables such as moisture convergence and evaporation. Incorporating only the prognostic-adjustment process in a linear model of Kelvin waves, multiple vertical modes were obtained. These eigenmodes included a strongly unstable wavenumber one 40-50 day mode, and weakly unstable wavenumber one 25-30 and 10-20 day modes for plausible values of the model's adjustable parameters. When the surface fluxes of latent and sensible heat were eliminated, these modes did not amplify in the absence of the saturation-triggering mechanism. These results were also consistent with the united wave-mechanisms.

PLANS FY96

Further experiments will be conducted using the idealized model to examine the nonlinear effects of condensation, evaporation, and advection. The results from the idealized model will be re-examined with the use of a realistic model.

1.3.3 NOAA/University Joint Study of the Maintenance of Regional Climates and Low Frequency Variability in GCMs

I. Held *M.J. Nath*
N.-C. Lau *P. Phillipps*

ACTIVITIES FY95

A collaboration between GFDL, NOAA/Climate Diagnostic Center, MIT, the Universities of Washington, Chicago, and Illinois, and the Lamont Doherty Earth Observatory has continued its study of the interrelated problems of stationary waves, storm tracks, low-frequency variability, and the response of the atmosphere to perturbations in boundary forcing. The group has collaborated in designing experiments to be performed at GFDL.

Significant synergy has developed among researchers in two problem areas in particular. A 100,000-day integration of the 9-level R15 model, using perpetual January insolation and fixed sea surface temperatures, has generated two important studies at the University of Washington regarding the structure of atmospheric low frequency variability. These studies complement work using this same model at GFDL (see section 6.2.4). In addition, researchers at Illinois, Penn State, and Washington have focused on the dynamics of the zonal mean flow in a variety of the consortium

experiments and in observations. There is currently significant disagreement about the extent to which eddy feedbacks help to maintain the low frequency variability of the zonal mean flow, a central issue in developing simple theories for this mode of oscillation. This zonally symmetric mode is an important component of observed intraseasonal variability in the Southern Hemisphere. Furthermore, there are indications from these studies that the North Atlantic and North Pacific Oscillations may be the Northern winter's analogs of this mode, suggesting that this study will ultimately improve our understanding of those patterns of variability as well.

A series of long R15 integrations on the response to extratropical Atlantic SSTs has been completed (yv), in collaboration with Yochanan Kushnir (Columbia University), with discouraging results - the responses are too small to be statistically robust. A similar study has now been initiated with the R30 model, and initial results from a 10-year perpetual January integration using an Atlantic SST anomaly are more encouraging, although longer integrations will be needed to study the robustness of the response. It appears that the larger eddy momentum fluxes in the R30 model may permit the generation of larger barotropic responses through reorganization of these fluxes.

The generation of a series of GCM integrations with idealized boundary conditions has continued, using the 14-level R30 model and a dry model with various resolutions. These are being utilized within GFDL and by other researchers to study storm track dynamics (see section 1.3.1.1). Some of these integrations are also being utilized by researchers at the University of Chicago to study the maintenance of the relative humidity distribution within the troposphere.

PLANS FY96

Work will continue on both idealized and realistic GCM integrations, in collaboration with several university scientists. In collaboration with the Experimental Prediction Group, new higher resolution (R30 or T42) integrations will be performed to replace the R15 ensemble of integrations in which the atmospheric model is run for 40 years with observed sea surface temperatures. Integrations with similar or higher resolution idealized models will continue to focus on storm track, stationary wave, and midlatitude SST interactions.

1.4 PLANETARY ATMOSPHERES

G.P. Williams

ACTIVITIES FY95

The Jovian atmospheres have close dynamical ties with Earth's atmosphere and oceans and exhibit conventional meteorological and oceanographic processes - jets, eddies, and vortices. Although Jupiter seems to behave like a larger, faster-spinning Earth, significant differences occur because of its unbounded vertical structure. To examine the structural factor and improve the definition and understanding of the circulation, 3-D primitive equation (PE) models are used to try to reproduce the various turbulent and coherent phenomena.

The main problem in defining Jupiter's meteorology is that the nature and extent of the atmosphere and its motions are not known for the region below the clouds. The main hypothesis invoked - that the atmospheric circulation is relatively shallow and driven by baroclinicity - has been examined with a wide range of GFD models. The present study extends these models by considering the influence of the vertical structure more specifically.

To understand and define Jupiter's circulation requires that fundamental questions concerning the stability and genesis of vortices and jets be addressed. In particular, we need to know: 1) why vortices exist and why they last so much longer on Jupiter than in the oceans; 2) what processes generate and control the various vortex sets seen in the various anticyclonic zones; 3) how the various jets are generated in low and midlatitudes for unbounded atmospheres, in a way that is consistent with vortex stability and genesis.

Answers to these questions have been found that are mutually consistent, that define the vertical structure of the motions, and show how the multiple jets are produced and generate vortex sets in their turn.

1.4.1 Stability and Genesis of Vortex Sets

Planetary vortices occur in Earth's oceans near the Gulf Stream and in Jupiter's atmosphere between the anticyclonic zones where they last for decades or centuries. This longevity is explained by calculations with the primitive equation model that isolate the parameters and structures for which vortices last indefinitely. The solutions suggest that Jupiter's motions extend only over a thin layer, 30-50 km in depth, but are bounded by an abyss of 500-1000 km depth. Further calculations have isolated the jet forms whose instabilities generate such stable vortices.

A variety of evolutionary paths have been found, most but not all of which lead to single vortex states. The paths become more complex in heated systems when vortex regeneration becomes a factor. Forced systems also lead to a new vortex form that resembles the terrestrial blocking phenomenon. When multiple vortex sets are produced at different latitudes they have the same scales as the Great Red Spot, the Large Ovals, the Small Ovals, etc., becoming smaller with increasing latitude.

1.4.2 Stability and Genesis of Jet Sets

Calculations with the primitive equation model subject to heating functions appropriate for Jupiter's atmosphere produce different types of jet streams in midlatitudes, low latitudes, and at the equator. In particular, baroclinic instabilities are seen to be capable of generating multiple midlatitude jets even in unbounded atmospheres. Some of these jets can generate vortices. All flow phenomena have realistic scales and amplitudes, and long time scales.

1.4.3 Model Development

Isolating the Jovian parameters and structures and simulating the circulation is difficult because the dynamics is highly nonlinear. Consequently, many calculations were needed to solve the problems definitively. Such a long sequence of calculations was made feasible by GFDL's highly interactive computing system and by the form of the model and graphics programs. The model and analysis programs are constantly modified as the system evolves to achieve the level of accuracy, efficiency, interactiveness, and animation needed for comparing multiple solutions.

PLANS FY96

Further calculations will be made to produce global circulations that achieve a fuller synthesis of the various jets and vortex sets. Additional study of the processes underlying the genesis of the different jets and vortices will also be carried out.

The primitive equation models and analysis programs will be further developed, as needed, to extend and refine the understanding and simulation of deep atmosphere circulations and their terrestrial connection.

2. RADIATION AND CLOUDS

GOALS

To investigate the characteristics of convection-cloud-radiative interactions on a variety of space and time scales, leading to the understanding of their role in weather, climate and climate change.

To use satellite and other meteorological observations for diagnostic analyses of climate processes, and for evaluating and improving physical parameterizations employed in general circulation models.

To study fundamental aspects of atmospheric radiative transfer, and to investigate the climatic effects of natural and anthropogenic radiatively-active trace gases and aerosols.

ACTIVITIES FY95

2.1 SOLAR SPECTRUM

*S.M. Freidenreich V. Ramaswamy
J. Li*

2.1.1 Multiple-Scattering Approximation

A new delta-four stream spherical harmonic expansion approximation has been derived (yc) that improves considerably the accuracy of the multiple-scattering solution, compared to the traditional delta-Eddington approximation. The computational time for this analytic approximation is little more than that required for two-stream approximations. For conservative cloud properties, this method is free from singularity problems and its accuracy has been tested for a wide range of optical depths.

The new formulation has been combined with the GFDL line-by-line (LBL) algorithm to investigate the solar spectral interactions involving water vapor and water drops in stratus clouds. The role of water vapor is seen to be very important when comparing the absorption due to homogeneous and vertically inhomogeneous clouds. In particular, the heating rates in an inhomogeneous cloud are substantially higher than in a homogeneous cloud. The near-infrared reflection of an inhomogeneous cloud exhibits differences in some spectral regions compared to its homogeneous

counterpart. These differences could account for a small fraction of the apparent anomaly inferred from direct observations of water clouds.

2.1.2 Parameterizations

A new multi-band, exponential-sum-fit parameterization that uses the delta-Eddington approximation has been developed and tested for accuracy based on the “benchmark” calculations, and has been implemented in the “modular” SKYHI GCM. The new scheme is based on partitioning the solar spectrum into several distinct bands, in contrast to the Lacis-Hansen parameterization previously employed. The band structure, shown in Fig. 2.1, is guided by the necessity of considering the spectrally-dependent properties of the various atmospheric absorbers and scatterers in the solar spectrum. To illustrate this point, Fig. 2.1 also shows the spectral variations of four important parameters within each band: the incoming solar flux at the top of the atmosphere; the total gaseous optical depth; the drop coalbedo; and the clear-sky reflectivity at the top-of-the-atmosphere. The total gaseous optical depth is a measure of the molecular absorption, with the relevant absorbing gases indicated. The drop coalbedo, which is a measure of water drop absorption, is obtained for a typical stratus cloud using Slingo’s parameterization for the single-scattering properties of water drops. The clear-sky top-of-the-atmosphere reflectivity is a measure of the influence of molecular (Rayleigh) scattering.

In the $0.2 \mu\text{m} < \lambda < 0.31 \mu\text{m}$ (ultra-violet, or UV) spectral region, the principal factor affecting the disposition of the solar flux is O_3 absorption. In the $0.31 \mu\text{m} < \lambda < 0.68 \mu\text{m}$ (UV and visible) region where absorption by water drops and molecules is relatively small, Rayleigh scattering of the incident radiation dominates the interactions and thus becomes the main determinant of the band structure in this region. For the $\lambda > 0.68 \mu\text{m}$ (infrared) spectral region, the partitioning of the spectrum into bands is governed by the locations of the main gaseous absorption bands (principally H_2O , and to a lesser extent, CO_2). Note in particular the partitioning of the H_2O absorption in the $2.4 \mu\text{m} < \lambda < 4.0 \mu\text{m}$ region into 3 smaller bands; this choice is dictated by the manner in which spectral changes occur in the drop absorption over this region. Beyond $4 \mu\text{m}$ (not shown), where larger spectral variations in drop and gaseous properties occur, the small solar insolation makes any further partitioning unnecessary.

In general, for any band, the parameterization consists of an average of the spectrally-varying optical properties. While molecular scattering and O_3 absorption consist of straightforward arithmetic means of the scattering and absorption coefficients, respectively, in the band under consideration, the line absorption by H_2O and CO_2 are represented by a sum of exponential terms that are functions of the absorber strength in that band. For the entire spectrum, a total of 72 such terms are required as an optimal choice, balancing the need to have a high accuracy against

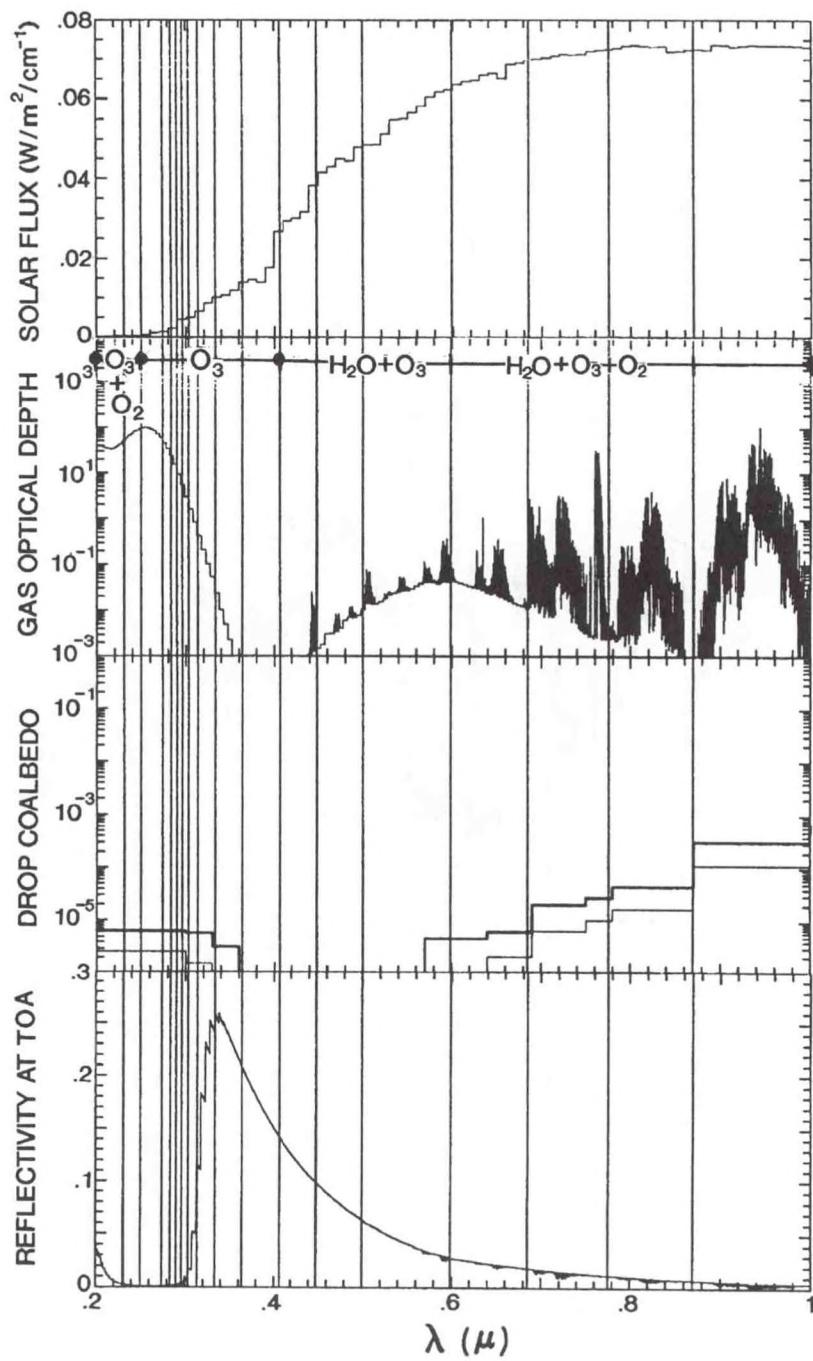


Fig. 2.1a Spectral dependence ($\text{W/m}^2 \text{ cm}^{-1}$) of the incoming solar flux between 0.2 and 1 μm wavelength at the top-of-the-atmosphere (TOA), the gaseous optical depth, the drop coalbedo of a typical water cloud, and the clear-sky reflectivity. Also shown are the delineation of the band structure adopted to construct a new shortwave parameterization for GCMs. The gases contributing to the absorption in each band are also shown.

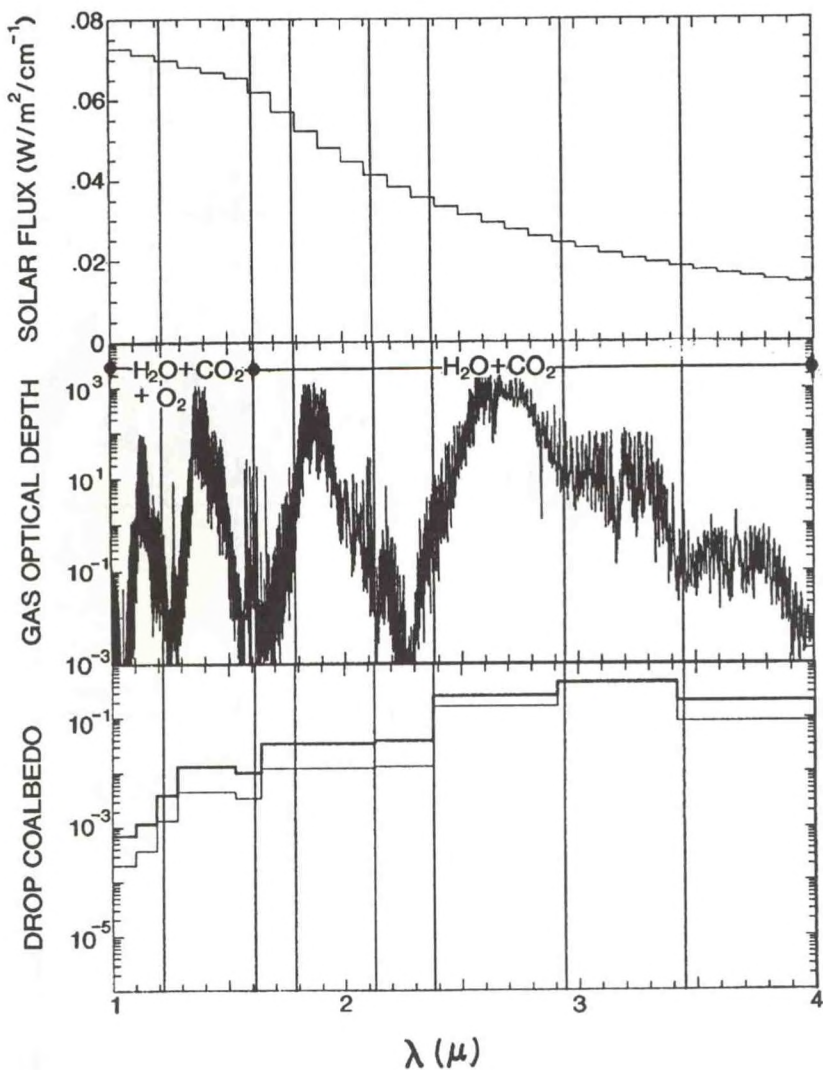


Fig. 2.1b Same as Fig. 2.1a, but for near-infrared wavelengths greater than 1 μm . Reflectivity at TOA in the near-infrared is negligible and hence is not shown.

the computational burden incurred. Fluxes and heating rates from this new parameterization have been compared with line-by-line computations. For overcast sky situations, in general, the error in the flux absorbed by clouds is < 10%, and the error in the surface and top-of-the-atmosphere flux is < 2%. For clear-sky conditions, the error in absorbed flux is generally < 2% and the error in the layer heating rates is < 15%.

2.1.3 H_2O and CO_2 Effects in the Stratosphere

Experiments were conducted using the fixed-dynamical heating model (A94/P95) to investigate the effect of improved broadband CO_2 and H_2O parameterizations on the stratospheric thermal profile (xy). Fig. 2.2 shows the zonally-averaged difference in the heating rate and the resulting temperature change for July conditions due to the improved broadband parameterizations. The sensitivity of temperature to H_2O and CO_2 is manifested clearly in the middle and lower stratosphere. In addition, differences in the temperature response due to heating perturbations by CO_2 -only and H_2O -only were examined. Both gases contribute significantly to the total temperature response in the lower stratosphere. The heating contribution due to H_2O is strongly peaked in the lower stratosphere, while for CO_2 the peak heating occurs in the upper stratosphere. It was found that the temperature response for a given layer in the stratosphere depends significantly on the vertical profile of the solar heating perturbations, a consequence of the longwave radiative exchange process. The fixed-dynamical model temperature response exceeds 2K near the tropopause in the high latitudes of the summer hemisphere.

2.1.4 Benchmark Computations

Changes in the absorbed solar flux were analyzed using the newer 1992 HITRAN line catalog for CO_2 and H_2O . For H_2O , there is a reduction in the absorbed flux of about 2% ($\sim 4\text{W/m}^2$ for an overhead sun) with most of it due to a reduction in the number of lines between 6200 and 9700 cm^{-1} . The additional absorbed flux due to new lines discovered for wavenumbers beyond 18000 cm^{-1} comprises only an additional 0.2 W/m^2 for an overhead sun case. For CO_2 , there is a reduction of its contribution to atmospheric absorption by about 10%. Additional sets of reference calculations involving multiple cloud systems were generated for purposes of analyzing the accuracy of the new shortwave parameterization.

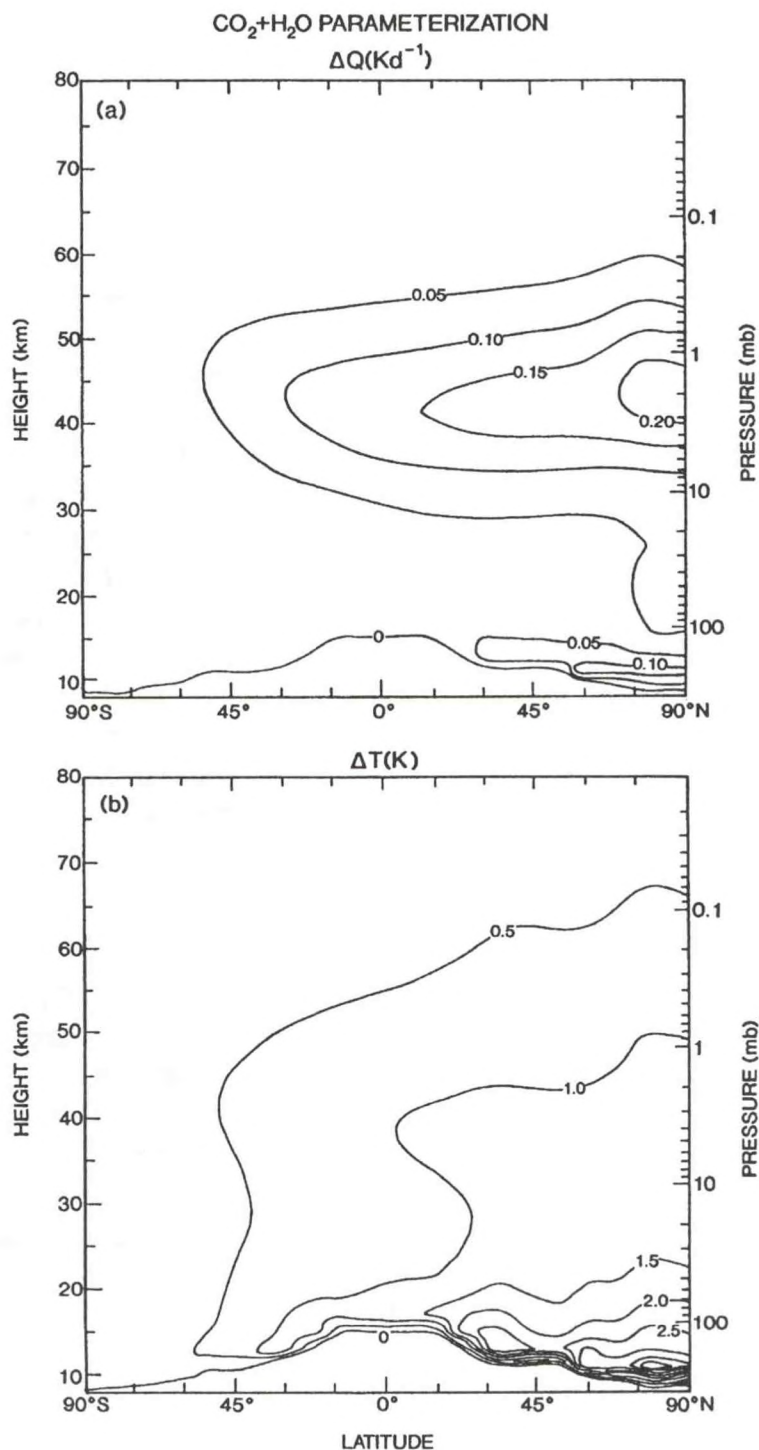


Fig. 2.2 Change in the (a) heating rate and (b) temperature due to improvements in the broadband parameterization of the solar absorption by H₂O and CO₂. The temperature change is computed using the Fixed Dynamical Heating assumption. The improved parameterization leads to a general warming of the global middle and lower stratosphere.

2.2 LONGWAVE SPECTRUM

V. Ramaswamy M.D. Schwarzkopf

2.2.1 Parameterization

The GFDL longwave radiative transfer algorithm (1034) has been modified to include the effects of CH₄, N₂O, and the halocarbons (F11, F12, F113, and F22). The accuracy of the new parameterization has been tested by comparing the fluxes and heating rates computed for standard ICRCCM (InterComparison of Radiation Codes in Climate Models project) atmospheric profiles with results using the GFDL line-by-line (LBL) algorithm. The change in the net infrared flux at the tropopause and the top of the atmosphere due to introduction of these trace species is computed by the parameterization with an accuracy of ~10%. The code has been incorporated into the "modular" GFDL SKYHI GCM.

2.2.2 Comparison of Line-by-Line Calculations with Observations

For the first time, radiances obtained using the GFDL (LBL) algorithm have been compared with measured radiances. The measurements are taken from spectrally detailed, clear-sky surface radiance observations made as part of the SPECTRE (Spectral Radiation Experiment) campaign, together with simultaneous measurement of the atmospheric temperature and constituent profiles. Four specific cases incorporating a wide range of temperatures and water vapor amounts have been analyzed. The LBL calculations have been performed using two representations of the H₂O vapor continuum, the first being the same as that used in the GFDL GCM parameterizations (termed the "Roberts" continuum), and the second a substantially different technique developed recently (termed the "CKD" continuum)¹. Fig. 2.3 illustrates the differences between the computed and observed radiances for two of the cases with the largest and smallest H₂O amounts. The newer continuum parameterization gives substantially better results, especially above 1200 cm⁻¹ (a region for which the Roberts continuum is not formulated) and for the high water vapor case.

PLANS FY96

The fluxes and heating rates in the new shortwave parameterization for the SKYHI GCM will be compared with that from the older scheme. Comparisons of fluxes with satellite observations will also be made. The SKYHI GCM will be run with the new parameterization and the effects on the model's simulation will be evaluated. Tests will

1. Clough, S.A., F.X. Kneizys, and R.W. Davies, Line shape and the water vapor continuum, *Atmospheric Research*, 23, 229-241, 1989.

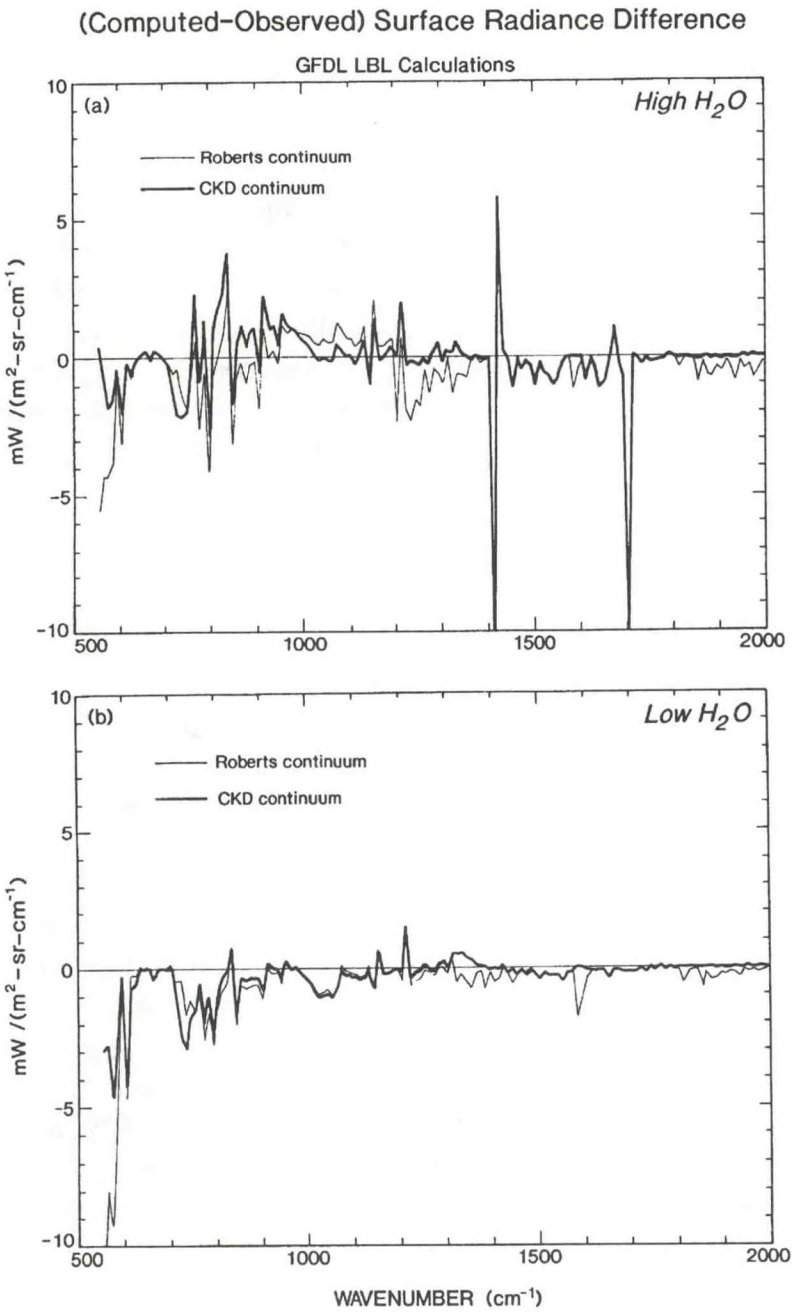


Fig. 2.3 Difference between computed and measured radiances in the infrared spectrum for two different ((a) high and (b) low) water vapor profiles. The computations are GFDL line-by-line calculations using two different assumptions of the water vapor continuum and are based on observed profiles of the trace gases. The measurements were conducted during the SPECTRE experiment. The sharp spikes at 1410 and 1700 cm^{-1} are due to instrument problems. The newer (CKD) continuum treatment yields a better agreement with the measured spectral radiances.

be conducted to determine the differences in accuracy and computational time between the various multiple-scattering approximations for cloud radiative treatments.

Analysis of the differences between LBL and observed radiances will continue. The calculations will be extended to additional cases involving different atmospheric soundings.

The GFDL longwave radiative parameterization will be modified to incorporate the newer H₂O vapor continuum formulation. Results will be compared to surface radiances and to clear-sky outgoing longwave radiances from satellite measurements. The revised parameterization, after appropriate testing, will be incorporated into the Laboratory's GCMs.

2.3 CONVECTION-CLOUDS-RADIATION-CLIMATE INTERACTIONS

2.3.1 Cumulus Parameterization

L. Donner

ACTIVITIES FY95

Interactions between cumulus convection and atmospheric radiation represent a difficult and important problem in the study of climate and climate change. Cumulus convection interacts with atmospheric radiation through several processes; among the most significant are the controls on the vertical distribution of water vapor exerted by cumulus convection and feedbacks involving clouds in convective systems with both short-wave and long-wave radiation. To address these problems in the context of general circulation models (GCMs), a parameterization for cumulus convection, which provides a physical basis for treating radiative interactions, has been developed (1133).

The water budget provided by this cumulus parameterization permits the calculation of the ice contents of the stratiform anvils associated with convective systems (z1). As noted in A94/P95, comparison with extremely limited field observations of anvil ice has been favorable. The focus has recently been on comparison of parameterized ice with ice simulations using the GFDL limited-area nonhydrostatic (LAN) model. The early stages of convective systems simulated using the LAN model are characterized by less ice than predicted by the cumulus parameterization, as may be reasonable since the anvil-formation process has not operated long enough to produce maximum ice contents.

The relative importance of mass fluxes and vertical velocities in the parameterization have also been examined. Both are important and are independent of each other to some degree. This result underscores the importance of treating both

mass fluxes and vertical velocities in cumulus parameterizations, which is a distinguishing feature of the parameterization described in (1133).

PLANS FY96

The parameterization will be incorporated in the SKYHI GCM and used to force its thermal and moisture fields. In conjunction with a new parameterization for nonconvective ice clouds recently added to SKYHI, this will result in a new, interactive treatment of high clouds in SKYHI. The impact of the new treatments for clouds and convection on radiative forcing and climate sensitivity in SKYHI will undergo initial examination.

2.3.2 Limited-Area Nonhydrostatic Model Development

L. Donner *T. Reisin*
R. Hemler *C. Seman*
V. Ramaswamy

ACTIVITIES FY95

The processes treated by the cumulus parameterization described in 2.3.1 are under study using the Lipps-Hemler (885) limited-area nonhydrostatic (LAN) model that has been used for investigations of radiative-convective equilibria in the two-dimensional mode (1183). Many of the dynamic, thermodynamic, microphysical, and radiative properties central to the parameterization are difficult to observe or have been observed only in limited synoptic situations. The LAN, in three-dimensional, semi-prognostic mode, predicts these properties without requiring the hypotheses and assumptions in the cumulus parameterization and can be used to assess the validity of the parameterization hypotheses. Shortwave and longwave radiative transfer has been added to the three-dimensional LAN, and preliminary studies of the distribution of radiative forcing have been completed. Radiative forcing under some circumstances is quite large and exhibits large vertical gradients. Key determinants of radiative forcing are the mass and size distributions of liquid and ice. Implementation of new microphysics in LAN that will provide information on size distributions has begun (Fig. 2.4). Studies also continue to focus on the region in the east Atlantic studied during GATE [GARP (Global Atmospheric Research Program) Atlantic Tropical Experiment] and to examine the agreement between LAN integrations and field observations. Analysis is focused on the distribution of cumulus vertical velocities and the microphysical properties of the cumulus cells and stratiform anvils simulated by the LAN, since the treatments of these processes represent unique aspects of the cumulus parameterization described above and are critical for studying interactions between cumulus convection and radiation. The heat and water-vapor budgets of modeled convective systems are also undergoing examination. These budgets have been compared with those from the cumulus parameterization (1297).

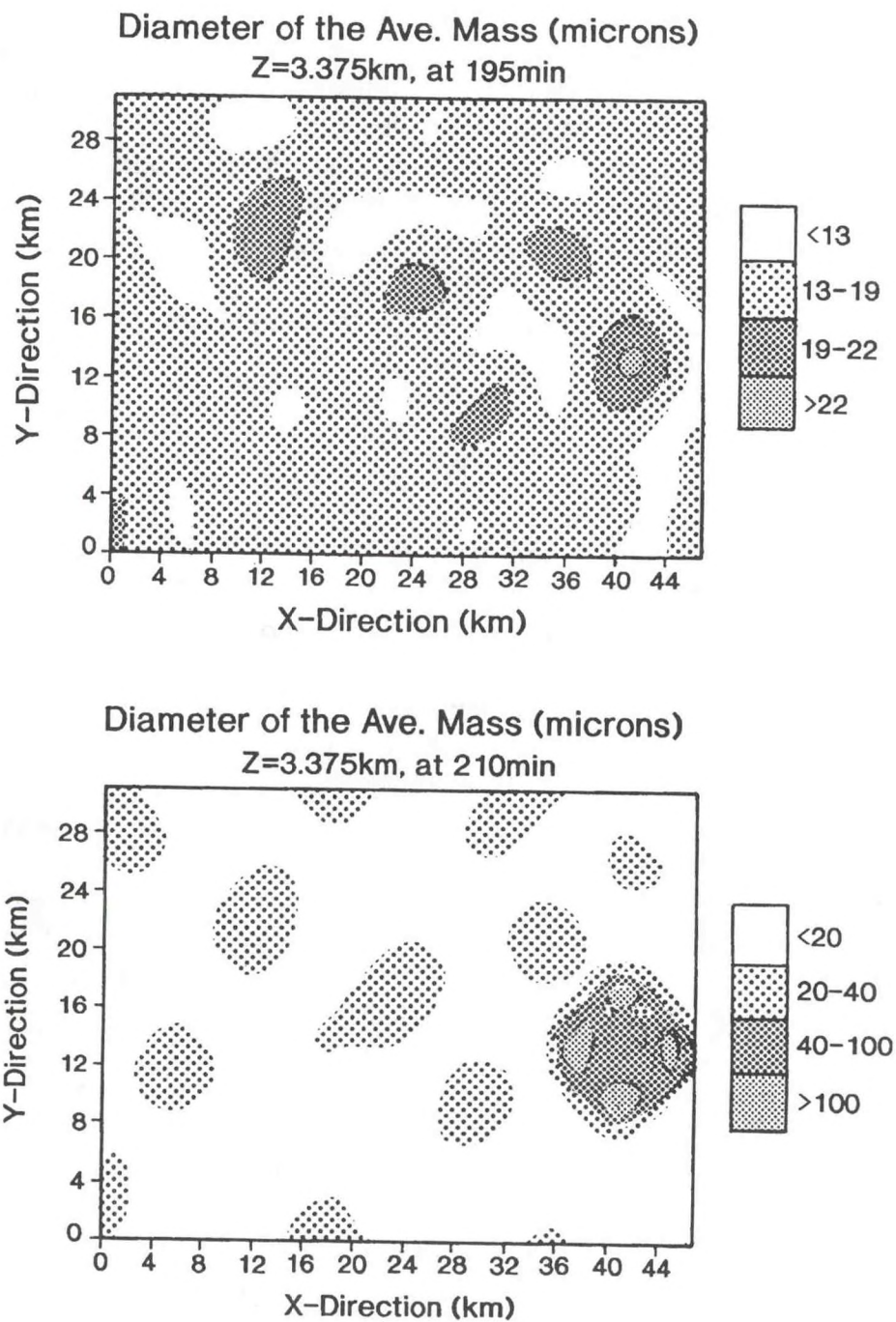


Fig. 2.4 Distribution of drop sizes at indicated times and height using the GFDL LAN model with the new microphysics parameterization. This is among the first calculations of drop sizes in a convective-system model and will permit a new generation of studies on cloud-radiation interactions.

PLANS FY96

The emphasis of the LAN studies will be placed on the temporal evolution of convective systems under conditions of imposed large-scale forcing for a complete life cycle of a tropical convective system. A larger domain will be used for this integration. Particular attention will be directed toward interactions involving radiative transfer and the relationships between cumulus-scale updrafts and stratiform anvils. The microphysical parameterization in the LAN will continue to undergo development, especially for ice processes, which are important in the anvil simulations. Open boundary conditions for three-dimensional integrations will be incorporated.

2.3.3 Radiative-Convective Equilibria with Explicit Moist Convection

I. Held

D.-Z. Sun

ACTIVITIES FY95

A study of the resolution-dependence of radiative-convective equilibrium on explicit two-dimensional moist convection has continued. Experiments have been performed in which the microphysics has been removed entirely, with condensed rainwater simply falling out of the atmosphere immediately and with realistic radiative transfer replaced by a simple Newtonian cooling. The domain averaged horizontal winds have been fixed with a small vertical shear to avoid issues related to the QBO-like oscillations described in A94/P95. Equilibria have been obtained with horizontal resolutions of 1 km, 2 km, 5 km, and 100 km. The resolution dependence of this model is found to be very similar to that of the model with warm rain microphysics and more complex radiative transfer, with indications of convergence of the mean humidity and especially the temperature profiles once the resolution reaches 2 km or less. Encouraged by this agreement, this simpler model is being used to take a closer look at the maintenance of the mean temperature profile.

There continues to be disagreement within the community as to the extent to which the tropical temperature profile is constrained by the moist adiabatic lapse rate. Conditional available potential energy (CAPE) is a convenient measure of the departure from the moist adiabat. The value of CAPE predicted by this two-dimensional model without microphysics has been computed for various values of the surface temperature from 25°C to 35°C and with 1, 2 and 5 km horizontal resolution. CAPE increases by a factor of 2 to 4 as temperatures increase from 25°C to 35°C. (The precise values are rather strongly dependent on the choice of cloud base for the computation of the reference moist adiabat.) CAPE is somewhat less sensitive to temperature at 5 km resolution than at 1 km. These changes in CAPE are large enough to have important ramifications for cloud microphysics in more realistic models.

Comparisons are also being conducted with a two-dimensional hydrostatic model with convective adjustment, using forcing and boundary conditions identical to those used in the non-hydrostatic model. To first approximation, changes in relative humidity and in CAPE when surface temperature is increased are similar to those in the non-hydrostatic simulations. On the other hand, the spatial organization of the convection is very sensitive to details in the parameterization and the boundary condition.

PLANS FY96

Further sensitivity studies will be conducted with the 2-D model. Experiments with a domain extending through the stratosphere will be initiated to examine the model's QBO-like oscillation more fully. Exploratory 3-D simulations of radiative-convective equilibria in small domains will also be initiated.

2.3.4 Atmospheric Ice Clouds

L. Donner

R. Hemler

C. Seman

B. Soden

J. Warren

ACTIVITIES FY95

To gain a better understanding of the climatic role of atmospheric ice clouds, a parameterization for their ice content (Heymsfield and Donner, 1990)² has been incorporated in the SKYHI GCM. The parameterizations which have been incorporated deal with 1) ice in saturated layers, in which deposition from vapor to ice and gravitational settling are in equilibrium, and 2) ice in subsaturated layers, in which settling ice sublimates. These parameterizations have also been linked to the hydrological cycle of SKYHI. Unlike many other cloud parameterizations, very little of the ice reaches the surface as precipitation. Most of the ice in a given cloud eventually sublimates, and the ice clouds can persist across model time steps. Another novel feature of the parameterization is its prediction of cloud vertical extent, which is not limited to the vertical resolution of the GCM. This parameterization has also been used to calculate both solar and longwave radiative transfer in SKYHI. Variations in ice-particle sizes are parameterized based on field observations. Large-scale variations in both ice content and particle sizes are important for regional variations in cloud albedo and emissivity.

SKYHI integrations using this parameterization are now undergoing analysis and comparison with satellite observations. The principal observed regions of large-

2. Heymsfield, A.J., and L.J. Donner, A scheme for parameterizing ice-cloud water content in general circulation models, *J. Atmos. Sci.*, 47, 1865-1877, 1990.

scale cirrus are largely captured in the SKYHI integrations, although details of geographic location differ in some cases. These differences are apparently largely related to differences between certain large-scale circulation features in SKYHI and analyses based on observations.

The roles of the variables which control the behavior of the parameterization have been studied using aircraft observations of ice in field programs. Temperature and vertical velocity are primary controls. There are indications that the role played by these variables differs as horizontal scale varies from those typically studied in field programs to those resolved in GCMs and reported in satellite cloud climatologies. In a simple experiment, parameterized ice water contents were calculated using temperature and vertical velocities at scales typical of those in field programs. The ice contents were subsequently averaged to scales typical of GCMs. These ice contents differed from ice contents calculated using temperatures and vertical velocities at GCM scales in a manner qualitatively similar to differences between satellite-inferred ice-cloud properties and parameterized ice-cloud properties, where the parameterized ice contents were calculated using analyzed temperatures and vertical velocities at GCM scales (z1). This result suggests that some of the errors in the GCM parameterization result from neglecting sub-grid variations in the variables which control ice content.

PLANS FY96

The role of ice clouds in SKYHI will be analyzed with respect to their impact on climate and climate sensitivity, their radiative forcing of the earth-atmosphere system, and their agreement with satellite observations. Attempts will be made to relate the differences between the simulated and observed ice distributions to the approximations used, and the deficiencies in the GCM's large-scale fields which control ice-cloud formation. Satellite data, used for comparison with the SKYHI results, will be reassessed in light of revised interpretations of some of the satellite observations, which have resulted from recently completed field studies of satellite cloud-property retrievals.

2.3.5 Interactions Between Water Vapor, Radiation, and Circulation

B. Soden

ACTIVITIES FY95

The tropics exhibit large regional variations in moisture which primarily reflect differences in the large-scale circulation. However, these variations in moisture greatly influence the radiative heating of the atmosphere, which in turn influences the patterns of tropical circulation. To help understand the interactions between water vapor, radiation, and the atmospheric circulation, a sensitivity experiment was

performed using a version of the GFDL climate GCM to study the global atmospheric response to tropical radiative heating due to water vapor. The initial experiment examined the impact of regional variations in radiative heating by total column moisture. At each grid box within the 30°N-30°S tropical belt, the water vapor concentration used to determine the infrared radiative heating was replaced with the tropical-mean water vapor for that level determined from a 5-year control run. Preliminary results indicate a significant atmospheric response to the perturbations in moist-radiative heating, including a warming of the tropics by ~2 K, a reduction in the strength of the Hadley circulation by 25%, a strengthening and equatorward shift in the midlatitude jets, and related changes in the Ferrell and Walker circulations.

PLANS FY96

Analysis of results and further sensitivity experiments will be performed.

2.3.6 GCM Studies of Cloud Radiative Effects

C.-T. Chen

V. Ramaswamy

ACTIVITIES FY95

An investigation has been conducted of the impact of cloud radiative treatments using a version of the GFDL Climate GCM with fixed sea surface temperature and cloud distributions (1187). It was found that the influences due to water vapor absorption and water drop extinction not only lead to important differences in the disposition of the solar flux absorbed in the atmosphere and at the surface, but also affect the energy and moisture balance at the surface (wq). Thus, biases in the solar radiative treatment initiate radiative flux differences at the surface and in the atmosphere. These, in turn, affect the vertical velocity and precipitation patterns, which are accompanied by changes in the terms comprising the land surface heat (e.g., latent heat) and moisture (e.g., soil moisture) balances. Such effects are, in general, different for the tropical and midlatitude land areas. It is concluded that deficiencies in the spectrally intricate interactions of water substance with solar radiation impacts the simulation of the atmosphere and the land surface processes.

Analyses of GCM experiments involving globally uniform and spatially localized perturbations in the microphysical properties of low clouds performed in A94/P95 have continued. It was found that, despite the near-constancy of the global-mean temperature sensitivity (i.e., surface temperature change-to-forcing ratio) to a variety of radiative forcings, the responses on a regional scale are different for the various forcings. The equator-to-pole temperature gradient, when normalized with respect to the global-mean temperature change, differs for the various experiments (zn). There is a distinct difference in the high latitude temperature changes between the

experiments leading to a "warm" and those leading to a "cold" climate (zi). In particular, an experiment that mimics the estimates of the midlatitude anthropogenic sulfate aerosol forcing over the past 100 years yields a response near the equator in the precipitation fields that is not noticeable when the forcing is globally uniform.

Further experiments were conducted using the fixed-cloud distribution model described in (1187) and along the lines described in A94/P95. In particular, a series of GCM experiments were conducted to examine if the climate responses to albedo and greenhouse perturbations of the sort posed by tropospheric aerosols and trace gas increases, respectively, over the past 100 years are linearly additive. Three experiments were performed: an increase in CO₂ only corresponding to the past 100 years, an increase in planetary albedo (simulated by increasing low cloud albedo) yielding the same forcing as the increase in CO₂ but with an opposite sign, and with the two forcings present simultaneously. The results indicate the following: the global-mean surface temperature change in the combined experiment follows expectations from the net zero forcing in that it is zero. Even on a zonal-scale, important climate features are linearly additive, such as high latitude sea-ice extent, temperature, and water vapor profiles.

PLANS FY96

Further analyses of the GCM results will continue, including the examination of the water vapor, albedo and lapse rate feedbacks, and the regional responses in the various radiative forcing experiments.

2.4 DIAGNOSTIC ANALYSES USING SATELLITE OBSERVATIONS

R. Fu *B. Soden*

2.4.1 Tropospheric Water Vapor and the Infrared Radiation Budget

Using a random strong line model, satellite observations of the upwelling radiance in the 6.3 μm water vapor absorption band were used to characterize the climatological variations of upper, middle, and lower tropospheric relative humidity for 1979-1992 (za). The resulting analyses clearly illustrate the role of the large-scale circulation in regulating the location and temporal variation of tropospheric water vapor. Peak relative humidities occur along the ITCZ, with minima over the subtropics, reflecting the ascending and descending branches of the Hadley cell. Interannual variations reveal a coherent anomaly pattern which extends throughout the tropics and which reflect changes in the Hadley and Walker circulation associated with the El Niño/Southern Oscillation.

TOVS water vapor radiances were also combined with ERBE measurements of the outgoing longwave radiation to examine the relationship between tropospheric water vapor and atmospheric greenhouse trapping (aa). In the tropics, increases in the atmospheric trapping are strongly correlated with increased middle and upper tropospheric relative humidity. The rapid increase in atmospheric trapping at high SSTs (> 300 K) is associated with both an increase in upper tropospheric water vapor and an increase in continuum absorption. In the midlatitudes, variations in atmospheric trapping were found to be only weakly related to variations in tropospheric relative humidity, but strongly coupled to variations in tropospheric lapse-rate. This result illustrates the importance of temperature, in addition to water vapor, in controlling the outgoing longwave radiation (OLR).

2.4.2 Deep Convection and Upper Tropospheric Humidity

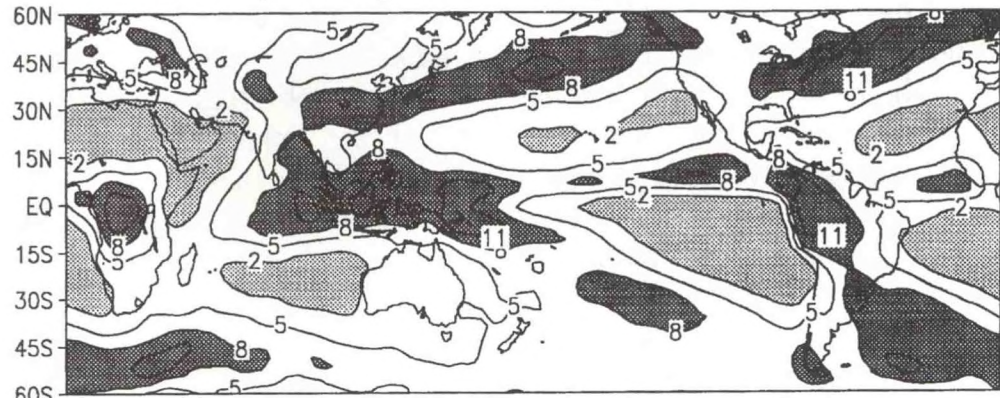
Satellite measurements of the upwelling $6.7 \mu\text{m}$ radiance from TOVS, together with cloud property information from ISCCP, were used to analyze the climatological interactions between deep convection and upper tropospheric humidity (xs). Enhanced tropical convection was found to be associated with increased upper tropospheric relative humidity (Fig. 2.5), and this correlation holds over a wide range of space and time scales. These results, combined with those in 2.4.1, provide, at least for the tropics, a picture which is consistent with a positive correlation between deep convection, upper tropospheric humidity and the greenhouse effect. Comparison with simulations from the GFDL climate model indicate that the model is qualitatively successful in capturing the observed relationships between convection and upper tropospheric moisture. This evidence lends credibility to the approach of using the GFDL GCM to predict upper tropospheric water vapor feedback, despite the model's relatively simplified treatment of moist convective processes.

In extratropical regions, temporal variations in upper tropospheric humidity exhibit little relationship to local variations in deep convection, suggesting the importance of other dynamical processes in determining changes in upper tropospheric moisture for this region. Analysis of interannual variations reveals a significant correlation between anomalies in midlatitude relative humidity and tropical Pacific convection, suggesting a potential remote influence on midlatitude moisture due to tropical convection. Comparison of the observed interactions with GFDL GCM simulations revealed a similar, but slightly weaker, pattern of remote forcing.

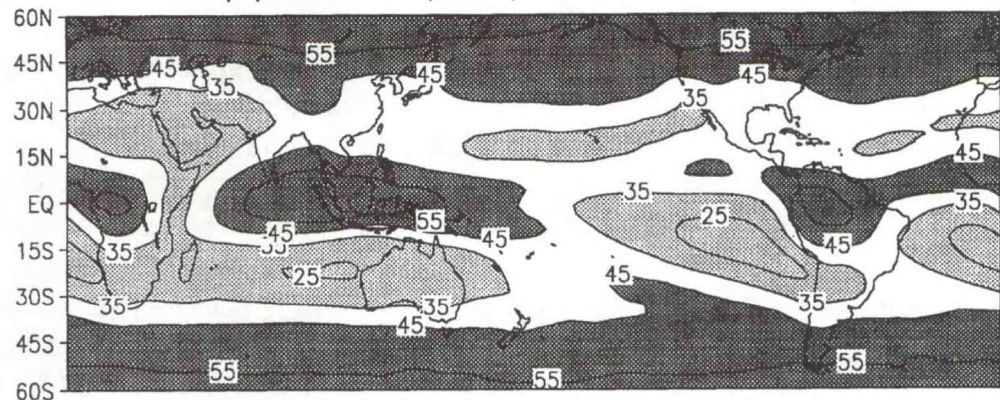
2.4.3 Moisture Transport Diagnostics from Satellite Imagery

A pattern tracking algorithm has been developed, tested, and applied to GOES $6.7 \mu\text{m}$ radiance measurements to identify moisture trajectories from successive (hourly) water vapor imagery (Fig. 2.6). These trajectories characterize the upper tropospheric wind field and agree well with *in situ* measurements (rms errors of $\sim 4\text{-}5$ m/s). The satellite-derived winds have been combined with contemporaneous

Frequency of Deep Convection



Upper Tropospheric Humidity



Greenhouse Parameter

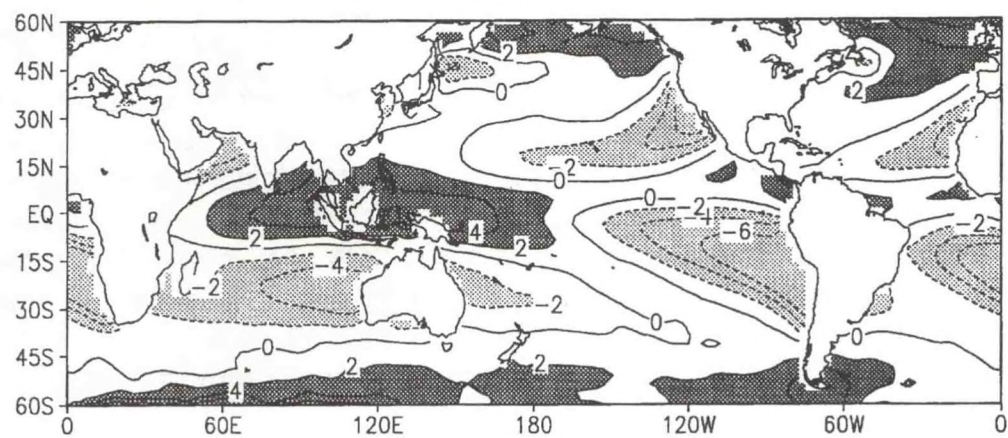


Fig. 2.5 Frequency of deep convection (top), upper-tropospheric humidity (middle), and dynamical greenhouse parameter (bottom). Contour intervals are 3% (top), 10% (middle), and 2% (bottom). Positive interrelationship between deep convection, upper tropospheric humidity and the greenhouse effect is consistent with climate model predictions.

Upper Tropospheric Relative Humidity and Pattern Displacement “Winds”

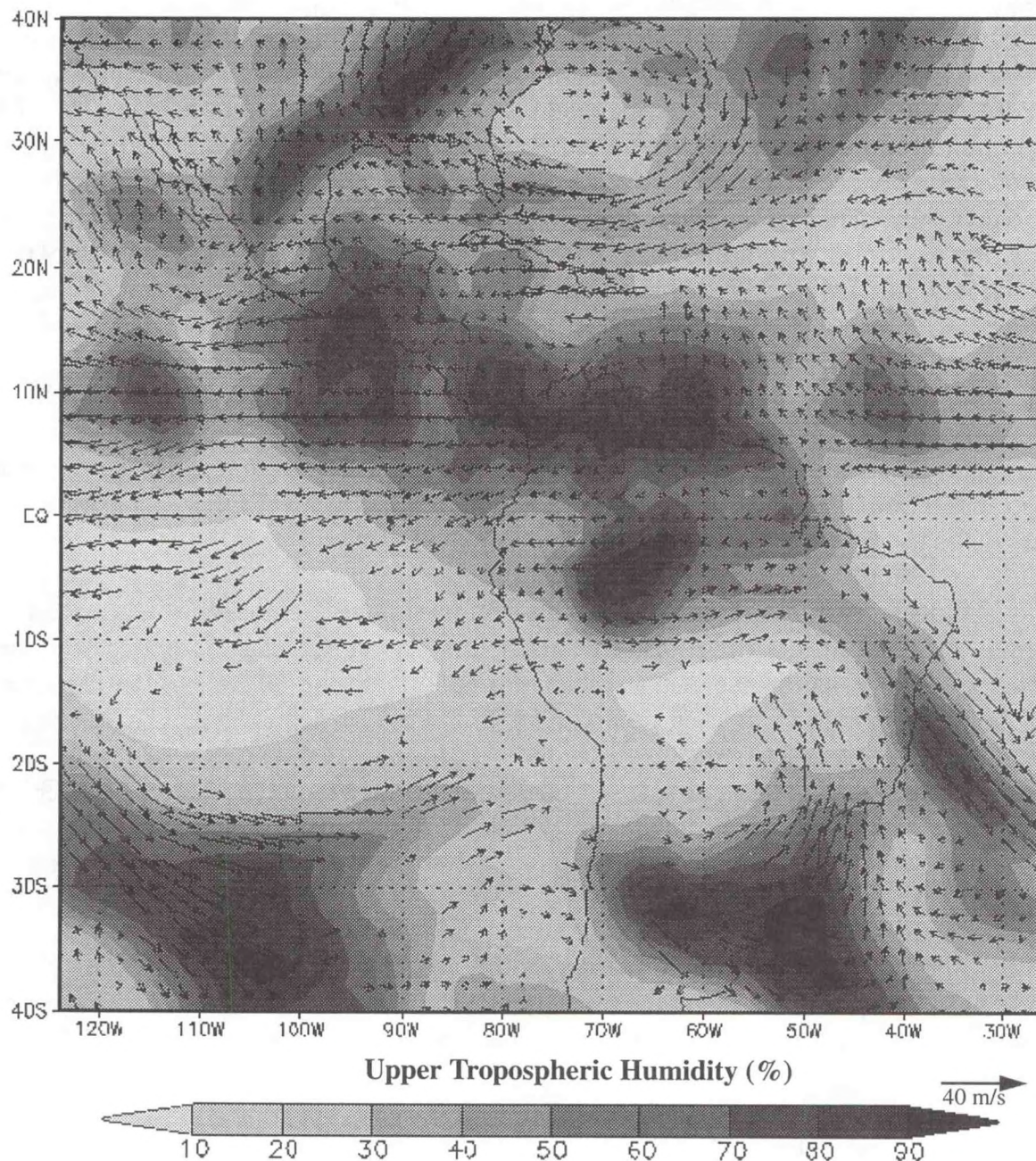


Fig. 2.6 A snapshot of the upper tropospheric relative humidity (shaded) and corresponding wind fields (vectors) for 00 GMT August 25, 1987, deduced entirely from GOES water vapor imagery. This approach provides insight into the processes which control the temporal evolution of upper tropospheric moisture.

information on upper tropospheric moisture and cloud cover to yield climatological diagnostics concerning the transport, horizontal trajectories, and Lagrangian statistics of the upper tropospheric moisture field and their relation to the formation and dissipation of clouds. A unique feature of this dataset is that the wind, cloud, and moisture parameters are all derived entirely from satellite imagery. Preliminary analysis indicates that upper level dynamics exert a strong influence upon the upper level moisture field. In the tropics, maximum moisture and cloudiness coincide with areas of strong upper level divergence. The subtropics are characterized by upper level convergence, which leads to subsidence and a drying of the upper troposphere. Additionally, moisture divergence from the tropics is found to be an important source of water vapor for the subtropics. This is a valuable new tool in diagnosing the distribution and temporal evolution of upper tropospheric moisture and cloudiness.

PLANS FY96

Further analysis of the upper tropospheric moisture transport and cloud formation processes from GOES water vapor imagery will be performed. Attempts will also be made to apply the feature tracking algorithm to GOES "split-window" radiances for diagnosing column integrated moisture transport.

Water vapor imagery from the new series of GOES satellites will be used to derive multi-level wind and moisture parameters during select periods of hurricane activity. Techniques for assimilating this information into the GFDL hurricane model will be developed to study their potential for improving hurricane forecasts.

High spatial and temporal resolution measurements from GOES and TOVS will be used to characterize the mesoscale variability of the upper tropospheric moisture field and examine the synoptic scale interactions between deep convection and upper tropospheric moisture.

Additional comparisons between model simulations and satellite observations of select atmospheric hydrologic components will be made to evaluate the impact of modifications to physical parameterizations and vertical resolution in the model.

2.5 EFFECT OF CHANGES IN ATMOSPHERIC COMPOSITION

*J.D. Mahlman
R. Orris*

*V. Ramaswamy
M.D. Schwarzkopf*

ACTIVITIES FY95

2.5.1 Simulation with Additional Trace Gases

The new "modular" GFDL SKYHI GCM has been used to study the changes in stratospheric climate due to inclusion of the radiative effects of present-day concentrations of CH_4 , N_2O , and the halocarbons. So far, three years of model integrations have been performed. Fig. 2.7b indicates that, in the tropical regions, the time-averaged lower stratospheric temperatures increase by $\sim 1\text{K}$, while a comparable decrease is observed in the vicinity of the stratopause. A Fixed Dynamical Heating calculation (Fig. 2.7a) indicates that the GCM patterns in these regions are similar to that expected from a radiative response. However, there are other regions of differences between the two model calculations, indicating that changes in dynamics also contribute to the GCM's response due to adding the additional greenhouse gases. Other features of note in the GCM simulations are an increase in the lower stratospheric water vapor, and a strengthening of the stratospheric Brewer-Dobson circulation.

2.5.2 Temperature Changes Due to the Observed 1979-1990 Ozone Loss

Analysis of lower stratospheric and upper tropospheric temperature changes simulated by the SKYHI 3° latitude experiment with the observed global ozone depletion indicates that temperature decreases extend to ~ 200 mb in the tropics and to about 300 mb in higher latitudes (Fig. 2.8a). These changes may be compared to the observed 1963-1988 temperature changes from (1270) (Fig. 2.8b). The comparisons, especially the close correspondence in the location of the "zero-change" contour, suggest that the reduction in stratospheric ozone may account substantially for this feature. More specifically, the loss of ozone in the lower stratosphere yields a cooling that extends well into the upper troposphere.

A computation using a one-dimensional radiative-convective model with appropriate values for CO_2 , CH_4 and N_2O and CFC concentrations has confirmed that the cooling tendency in the lower stratosphere due to ozone reduction greatly exceeds the tendency due to changes in other species over the entire 1765-1990 period (Fig. 2.9). Since the global ozone changes are known to have occurred only since about 1980, this represents a rapid global climate change compared to, say, the changes expected at the surface due to greenhouse gas increases. Further, the ozone loss and the accompanying temperature decrease were completely unanticipated at the start of the 1980s and thus have been a surprise in the context of climate change.

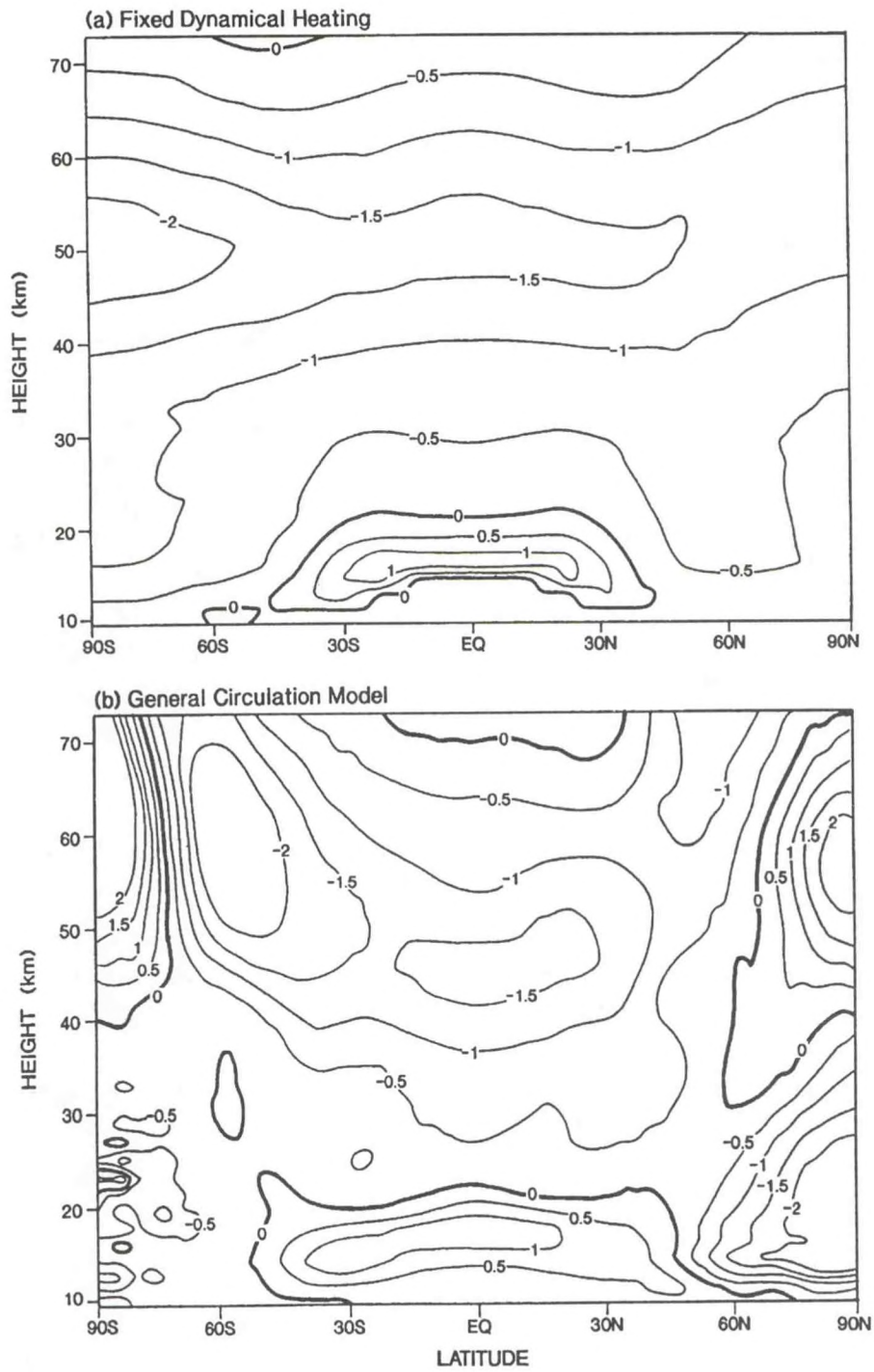


Fig. 2.7 Simulation of the temperature change due to incorporation of present-day concentrations of CH_4 , N_2O and CFCs. (a) Fixed Dynamical Heating calculation and (b) SKYHI GCM simulation. Note the warming of the lower stratospheric region in both simulations due to the addition of the trace gases.

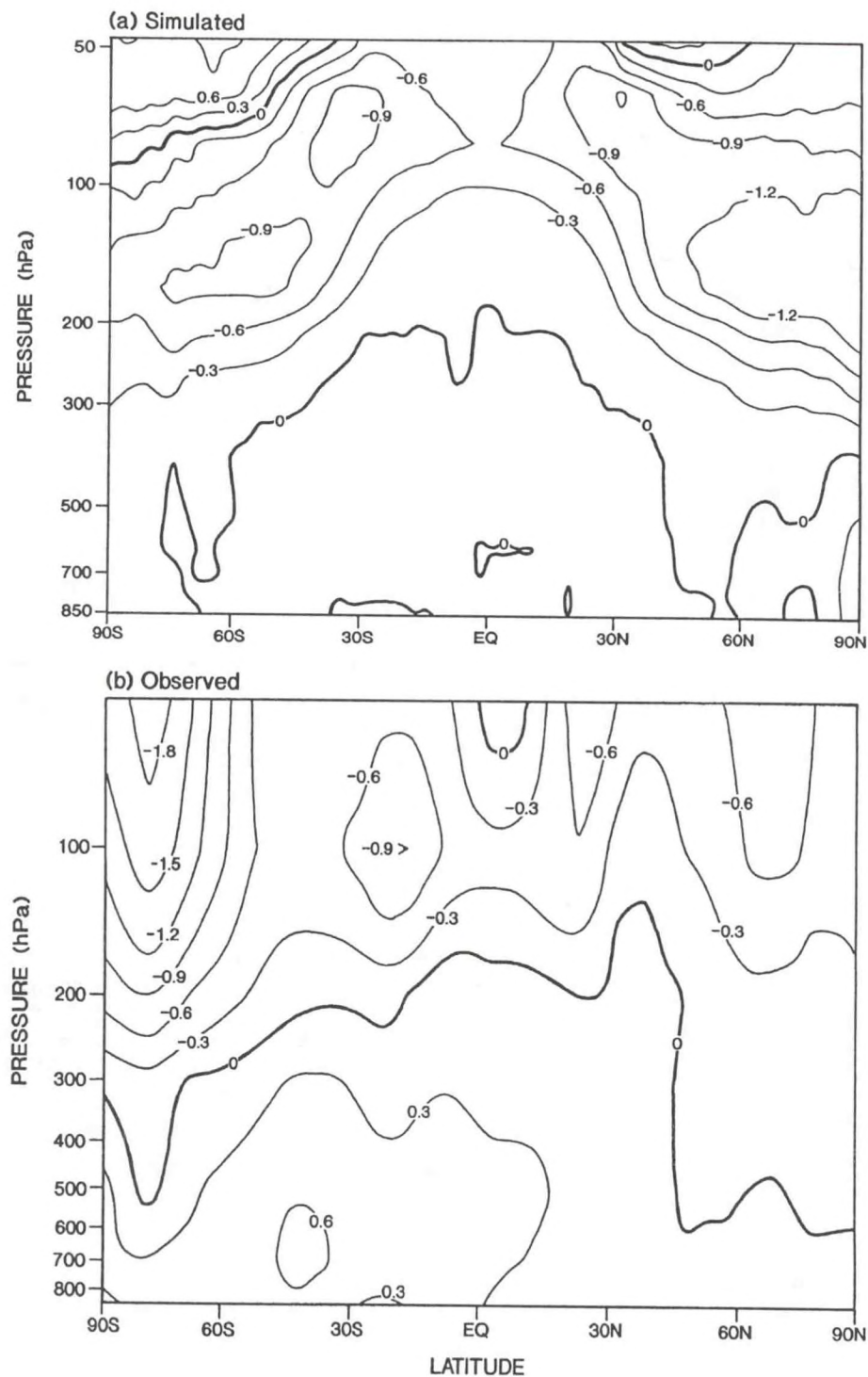


Fig. 2.8 Height-latitude profile of the temperature change (a) as obtained from the SKYHI GCM simulation with imposed global ozone losses derived from satellite observations, and (b) the difference between the two periods (1978-87) and (1963-1972) as analyzed from radiosonde observations. The results suggest that the reduction in stratospheric ozone may account substantially for the observed temperature decrease in the lower stratosphere and upper troposphere.

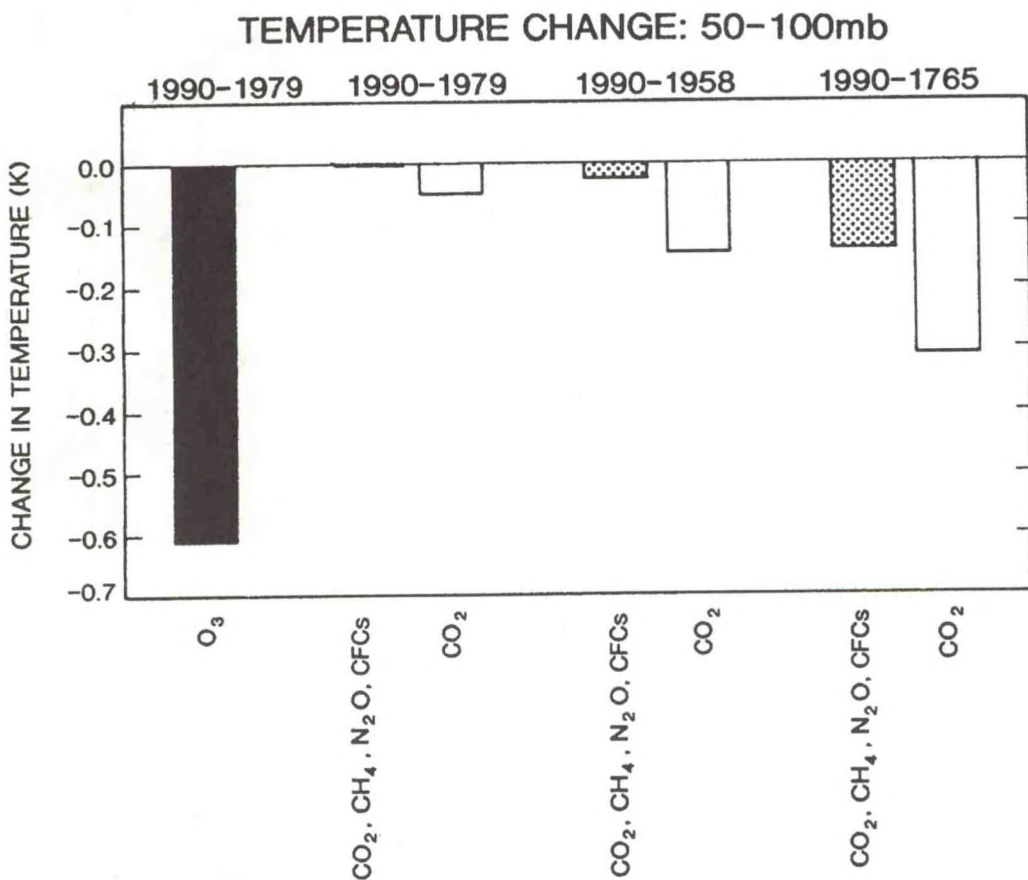


Fig. 2.9 Change in lower stratospheric (50-100 mb) temperature due to different considerations of trace gases and for three different time periods: lower stratospheric ozone change (1979-1990), CO_2 alone and along with other well-mixed greenhouse gases over the 1979-1990, 1958-1990 and 1765-1990 periods. The results confirm that the lower stratospheric cooling due to the 1979-1990 ozone loss greatly exceeds that due to the other species over the entire 1765-1990 period.

2.5.3 Intercomparison of Radiative Forcing Due to Ozone Losses

GFDL has participated in an intercomparison of the computed changes in solar and infrared heating rates and fluxes and associated temperature changes in the stratosphere due to changes in ozone (zt). In the case of stratosphere-only ozone loss, results for all six models show a negative radiative forcing of the surface-troposphere system. Temperature changes in the lower stratosphere are similar for all models. The unanimity amongst the models firmly establishes the conclusion that the observed global stratospheric ozone loss has exerted a negative forcing of the climate system.

2.5.4 Ozone-Temperature Relation in the Stratosphere

Work has continued on a study of the radiative consistency of ozone and temperature observations in the middle and upper stratosphere. Monthly, zonal averages of the Upper Atmosphere Research Satellite (UARS) Microwave Limb Sounder (MLS) ozone and temperature datasets, and LIMS and NMC temperature datasets were added to those previously examined. The MLS ozone was found to be within 5-10% of the older datasets in the middle and upper stratosphere. However, the observed MLS temperatures are 5-8K colder than the older (pre-“ozone hole” period) temperature datasets in the tropical middle stratosphere, where there is assumed to be very little interannual variability. No explanation for these rather large differences has been suggested.

Temperatures derived from the Fixed Dynamical Heating (FDH) model calculations, which employs dynamical heating rates obtained from the 1° SKYHI GCM and uses the MLS ozone rather than the older ozone data as input, are in closer agreement with the older temperature dataset, but quantitative differences still exist between the modeled and observed temperatures. The modeled temperature using MLS ozone is warmer than the observed MLS temperature in the tropics at 2 mb by 5-8K, and is colder than the observed MLS temperature by 4-6K in the midlatitudes of the summer hemisphere at pressures between 0.5-20 mb. This is an improvement compared to the temperature differences found when the older ozone datasets were used as input in the FDH model and then compared with the older temperature data. Differences as large as 10-12K in magnitude were found in the case of the older data, and were fairly uniform with latitude at pressure levels between 2-20 mb.

In assessing the uncertainties of the FDH calculations, an important contribution has been identified as arising due to the interannual variability of the 1° SKYHI GCM dynamical heating rates. The FDH temperatures in the tropics using two different years of dynamical heating rates differ by as much as 5K for winter conditions. The model's dynamical variability is likely associated with changes at the higher northern latitudes. Both the GCM's dynamical heating rates and the available observations are limited in their temporal extent, and this could be an important factor in the evaluation of the radiative consistency.

PLANS FY96

The run with additional trace gases will continue in order to obtain longer-term statistics. Analysis will also continue and will include an assessment of the statistical significance of the results. The results will be compared to those already obtained for a doubling of CO₂ and those investigating the decadal ozone losses.

Attempts will be made to quantify the uncertainty of the temperature change due to the uncertainties in the knowledge of the vertical profile of ozone changes over the last decade. FDH and GCM simulations with different profiles of ozone loss will be undertaken to assess the effect on the global stratospheric thermal profile. Temperature changes obtained from the current experiment will be compared to those obtained from GCM simulations of realistic CO₂ and other trace gas changes.

The FDH investigation of the ozone-temperature radiative consistency problem will be completed, including the effort to quantify the contributions due to different factors. Possible causes include the radiative properties of the constituents, radiative transfer methods, input ozone data, input temperature data, and dynamical heating rates.

3. MIDDLE ATMOSPHERE DYNAMICS AND CHEMISTRY

GOALS

To understand the interactive three-dimensional radiative-chemical-dynamical structure of the middle atmosphere (10-100 km), and how it influences and is influenced by the regions above and below.

To understand the dispersion and chemistry of atmospheric trace gases.

To evaluate the sensitivity of the atmospheric system to human activities.

3.1 ATMOSPHERIC TRACE CONSTITUENT STUDIES

<i>W.L. Chameides*</i>	<i>W.J. Moxim</i>
<i>A.I. Hirsch</i>	<i>S. Oltmans**</i>
<i>P.S. Kasibhatla*</i>	<i>J.R. Olson***</i>
<i>A. Klonicki</i>	<i>L.M. Perliski</i>
<i>H. Levy II</i>	<i>S. Taubman</i>
<i>J.D. Mahlman</i>	

* *Georgia Institute of Technology*

** *Climate Monitoring and Diagnostics Laboratory/NOAA*

*** *NASA Langley Research Center*

ACTIVITIES FY95

3.1.1 ZODIAC¹ Global Chemical Tracer Model Development

In recognition of the computational cost, chemical complexity and inherent empirical nature of explicit photochemical schemes for the polluted boundary layer (such as the one described in A94/P95), two types of empirical parameterizations of O₃ production in the polluted boundary layer are being examined. Both take advantage of the quasi-linear correlation between the observed concentrations of O₃ and oxidized nitrogen species. In the first, the slope of this correlation [O₃ production factor] can be thought to represent the balance between the catalytic production of O₃

1. ZODIAC was the first "high resolution" (2.4° latitude) general circulation model constructed at GFDL. It is used today to provide the winds for the GFDL GCTM.

by nitrogen oxides [NO_x] and the loss of the NO_x catalyst through oxidation, integrated over the lifetime of the parcel. Since both the total reactive nitrogen [NO_y] and NO_x are simulated in the GFDL ZODIAC Global Chemical Transport Model (GCTM), the residual [$\text{NO}_y - \text{NO}_x$] representing oxidized NO_x can be multiplied by this O_3 production factor to give the enhancement of O_3 above a background value. One challenge in developing this production factor (commonly called the OPE, or Ozone Production Efficiency), is that it varies with NO_x , sun angle, and the presence of isoprene. Therefore, it is necessary to collect data from a wide distribution of sites to get some idea of the variation of the OPE. Unfortunately, the number of sites measuring O_3 , NO_x , and NO_y for the entire summer season is small. So far, some progress has been made in the northern midlatitudes and areas of tropical biomass-burning. In the second approach, the rate of O_3 production in the polluted boundary layer is assumed to be directly proportional to the rate of oxidation of NO_x to nitric acid [HNO_3]. The proportionality constant is chosen to give realistic levels of summertime O_3 in the polluted boundary layer of the eastern US and realistic correlations between pollution generated O_3 and CO downwind of the eastern US source region. This extremely simple parameterization was used in the North Atlantic study discussed in 3.1.4. An extension of this simple parameterization, where the proportionality constant is itself assumed to be a function of NO_x concentration, is under development.

As another part of the tropospheric O_3 simulation effort, a global source of isoprene was added to the ZODIAC GCTM. Isoprene is a biogenic non-methane hydrocarbon (NMHC) that plays an important role as an O_3 precursor near the surface due to its widespread emission and its high reactivity compared to most anthropogenic NMHCs. The isoprene source, 500×10^{12} grams of carbon total annual emission, was taken from the Global Emissions Inventories Activity (GEIA) program. In the GCTM simulation, isoprene was emitted into the lowest model layer, with flux values updated every six hours. The emitted isoprene was then transported by the GCTM winds and destroyed by reaction with the hydroxyl radical (OH), which was calculated off-line. By including isoprene in the O_3 simulation, a more complete picture of tropospheric O_3 formation and improved insight on biosphere-atmosphere interactions is expected.

The development of a gas phase dry deposition parameterization that responds more realistically to changes in meteorological variables and surface properties continues. The algorithm has the standard three components [Ra , Rb , and Rc], which are analogous to resistance elements arranged in series. Ra , the resistance the gas molecules face in their transport to the surface, is an aerodynamic resistance related to atmospheric stability, and Rb is a sublaminar resistance corresponding to molecular diffusion close to the surface. Algorithms for both are generally based on standard parameterizations of boundary layer turbulent transport and diffusion. Rc , the surface resistance, depends on the surface characteristics and is more complicated. Its parameterization, which depends on ecosystem type and

condition (season, heat stress, light conditions) and temperature, is empirically derived from available surface measurements. An intercomparison of this three-resistance algorithm and the current GCTM algorithm is still in progress.

In an extension of last year's WCRP Intercomparison of boundary-layer and cumulus transport, the GCTM was used to perform simulations of radon (a short-lived noble gas with an e-folding radioactive decay time of 5.5 days and a continental source), and lead-210 (a product of the radioactive decay of radon which rapidly attaches to aerosols and thus has its atmospheric lifetime controlled by dry deposition at the earth's surface and removal by precipitation). This controlled experiment was performed as a contribution to a WCRP-sponsored model intercomparison test of transport and deposition in global chemical transport models. Tables, plots and time-series data for simulated radon concentrations, lead-210 concentrations and lead-210 deposition were submitted to the organizing committee for intercomparison with other GCTM simulations, as well as with available observations. Just as for the previous intercomparison, preliminary results suggested that GFDL's GCTM still compares favorably with other models.

3.1.2 SKYHI Chemical Model Development

3.1.2.1 Stratosphere

Over the past several years, a stratospheric chemistry module has been developed for use in the modular SKYHI model to provide the opportunity to study in detail three-dimensional transport of trace species and chemical/transport interactions. Although preliminary simulations will emphasize the model's ability to simulate observed distributions of important stratospheric trace species, the eventual goals are a completely interactive simulation of dynamical, radiative and chemical processes in the atmosphere, and the simulation of long-term ozone trends and their effect on climate.

A stratospheric chemistry module has been developed which employs simple Euler differencing to accurately predict the mixing ratios of trace species at time steps of up to 30 minutes. The new module deals with the stiffness inherent in atmospheric chemical systems by defining chemical families characterized by relatively long lifetimes in comparison to the integration time step, and rapid interchange between member species. To capture the rapid response of stratospheric chemistry to the diurnal variation of solar radiation, trace species which are partitioned from a parent species or solved in equilibrium during daylight (when chemical lifetimes tend to be rather short) now may be time-marched during night (when chemical lifetimes tend to be long). This flexibility allows for relatively accurate simulations of diurnal processes for some chemical family members defined in the model (*e.g.*, O_x (O, O_3), NO_x (N, NO, NO_2), and HO_x (H, OH, HO_2)). Other species may be computed by time marching or equilibrium expressions depending on local chemical lifetimes; examples of these are

NO_3 , N_2O_5 , HNO_4 and H_2O_2 . A methane-oxidation source of H_2O has now been added to the model, with the primary methane oxidation products solved in equilibrium. Halogens are currently not treated in the SKYHI photochemistry module, although a one-dimensional version of the module does include chlorine and bromine. The planned addition of halogen chemistry to SKYHI will approximately double the number of reactions and photoreactions included in the model (currently about 60).

The kinetic rate coefficients and absorption cross sections used in the chemical scheme described above are taken from the 1992 JPL (Jet Propulsion Laboratory) recommendations. Recently, improved Schumann-Runge band and NO photolysis parameterizations were added to the photochemical scheme. This model improvement was necessary because photolysis of NO, which results in formation of an N atom, is an important upper stratospheric loss of reactive nitrogen through the reaction of N and NO to form N_2 .

Due to the high computational cost of calculating photolysis frequencies for photolytically-active atmospheric species concurrently with the GCM execution, a scheme was implemented in which photolytic rates are pre-computed using a matrix inversion radiative transfer model for a specified zonally-averaged seasonal ozone/temperature distribution, and are stored as arrays varying with solar zenith angle. Since climatologies of temperature, pressure and ozone are used, the number of interpolations required is reduced to only one variable, solar zenith angle. Although this method of computing photolysis rates saves CPU time, it does not take into account the possible variations in actinic flux due to changing overhead ozone column. Without this response to ozone variations, the chemical scheme will not exhibit ozone increases below depleted regions due to increased UV transmission, the so-called "self-healing" effect. Therefore, an updated photolysis rate calculation will be included in future model runs. This algorithm will likely include an additional interpolation with respect to overhead ozone column abundance.

A non-halogenated atmosphere greatly simplifies the three-dimensional photochemical simulation. Since most of the chlorine present in today's stratosphere is anthropogenic, a non-halogenated atmosphere may resemble the pre-industrial stratosphere provided that pre-industrial values of such chemical source gases as CH_4 , H_2 and N_2O (which are not integrated on line in this model) are also used. A background distribution of N_2O has therefore been defined by using a long-term average SKYHI simulation of N_2O scaled to the tropospheric pre-industrial value of 288 ppb estimated by IPCC. Likewise, a background distribution of atmospheric CH_4 varying with latitude and altitude has been calculated by using the SKYHI N_2O distribution scaled to the tropospheric CH_4 value of 800 ppb. Calculated species were initialized with either observations (e.g., the CIRA climatological dataset for ozone) or 2-D chemical model calculations.

After an initial model integration of one year at low horizontal resolution ($5^\circ \times 6^\circ$ latitude/longitude), it was concluded that the chemical and advective schemes produce seasonal results that are in qualitative agreement with observations for O_3 and NO_x (A94/P95), although the simulated circulation at this low resolution is not very realistic. The model has since been run at higher horizontal resolution ($3^\circ \times 3.6^\circ$) for over two years of model time. Based on these calculations, several important conclusions have been reached, as summarized in the following paragraphs.

Figure 3.1 shows the calculated zonal average ozone for June. The mixing ratio distribution looks reasonable except at the winter high latitudes where the calculated ozone exceeds observed values by about 60% in region near $60^\circ S$ between 2.0 and 5.0 hPa. A similar problem shows up during the Northern Hemisphere winter at high latitudes although, due to the fact that the northern polar vortex is more dynamically disturbed than its Southern Hemisphere counterpart, the feature is not as localized and extends into higher latitudes. These differences in the calculated ozone

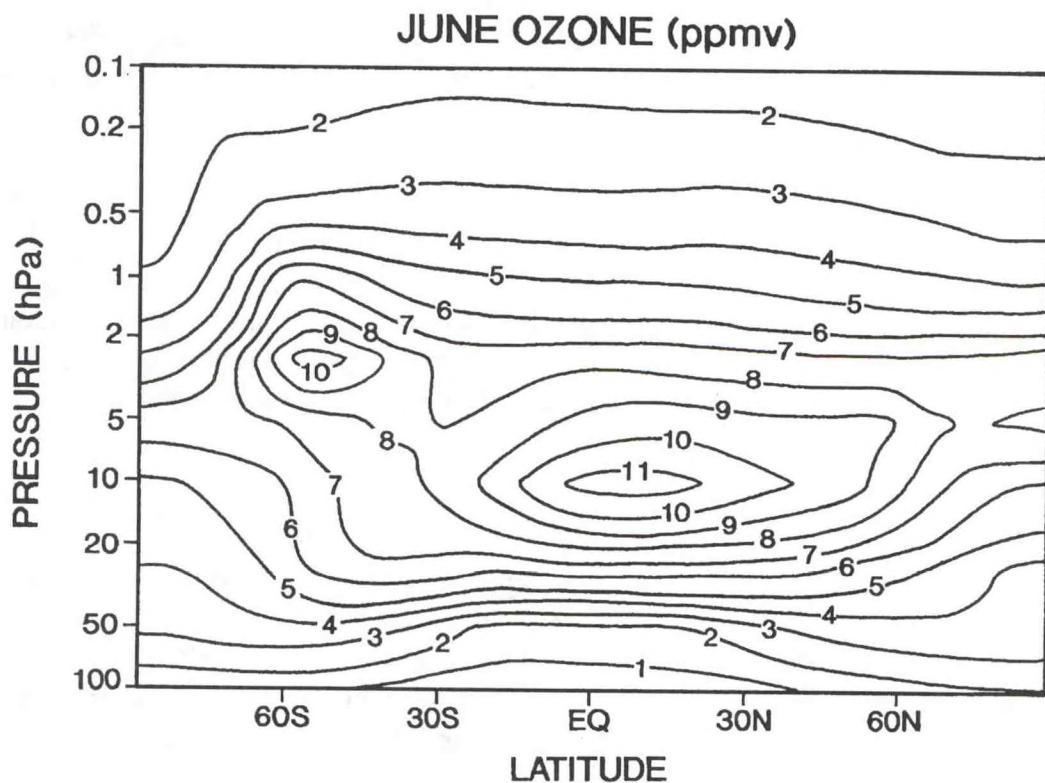


Fig. 3.1 Monthly-average ozone for June calculated with SKYHI. The results are consistent with observations, except between 2 and 5 hPa at $60^\circ S$, where concentrations exceed observed values by about 60%. These differences in the calculated ozone distributions are related to the model's cold pole bias, a problem common to all general circulation models.

distributions are related to the model's cold pole bias, a problem common to all general circulation models. The modeled temperatures are 10° to 40° colder than observations at 5 hPa in the Southern Hemisphere winter at polar latitudes, and 5° to 10° colder in the Northern Hemisphere. The colder temperatures slow the temperature-dependent odd-oxygen loss processes locally, shifting the photochemical balance of ozone towards production, which continues to occur (albeit slowly) near 60 degrees latitude. This results in ozone mixing ratios that are high compared to observations. Solution of this problem will involve warming the polar winter regions, probably by including a physically based gravity wave drag parameterization.

Although the methane oxidation source included in the photochemical model does gradually increase the water vapor mixing ratios at high altitudes, water vapor is still too low in the lower stratosphere (compared to observations) by a factor of 3 to 5. This problem is of special concern to the photochemistry because water vapor is the source of reactive hydrogen, which plays an important role in stratospheric chemistry since it determines the rates of formation of sinks for reactive nitrogen, chlorine, and bromine, and since reactive hydrogen itself catalytically destroys ozone. Furthermore, in regions where heterogeneous chemistry is important, hydrogen chemistry dominates the photochemical ozone loss. Therefore, it is important to get the correct water vapor distribution in a stratospheric photochemical model.

SKYHI's low water vapor in the lower stratosphere is directly related to the model's cold temperatures at the tropical tropopause where temperatures are about 5K too cold. This situation may be improved by the addition of more radiatively-active trace gases to the radiative transfer algorithm. A new radiative transfer code including N₂O and CFC's, for example, resulted in a temperature increase of about 2K at the tropical tropopause. Also, improved treatment of high altitude cirrus clouds will likely further warm the upper troposphere.

3.1.2.2 Troposphere

One reasonable approach to developing a tropospheric chemical module for SKYHI is to build on the existing stratospheric chemistry module. To this end, a collaboration was initiated with Jennifer Olsen and Jack Fishman at NASA Langley to develop a tropospheric chemistry module for SKYHI that can later be installed into the Langley GCM. The first step in this project was to update the one-dimensional version of the stratospheric chemistry module so that it corresponds exactly to the photochemical scheme currently being used in SKYHI. The next task was to test the new one-dimensional model's ability to reproduce the results from a recent IPCC tropospheric photochemical model intercomparison and to explore the limits at which the model does not seem to perform well. As an example, it was discovered that the current photochemical scheme does not accurately simulate photochemistry in the

case of a plume containing high levels of reactive nitrogen. It is likely that an assumption leading to a particular partitioning relation between the members of the NO_x or O_x chemical families which works in the stratosphere is inappropriate under tropospheric conditions. Such assumptions must be evaluated in detail in order to get the photochemical scheme to work correctly in the troposphere.

The next stage in the development of a tropospheric photochemical module for SKYHI will be to add PAN, which has been shown to be an important reservoir of reactive nitrogen (3.1.3), to the chemical scheme. The tropospheric photochemical module could then be run in SKYHI with the addition of the NO_x source distributions described in 3.1.3. This should yield some potentially very interesting and useful results.

3.1.2.3 Analysis Code Development

An analysis package is currently under development for use at GFDL and elsewhere in conjunction with the SKYHI GCM. This package is intended to be an easy-to-use tool that will aid researchers in the manipulation, analysis, and visualization of large SKYHI datasets within the larger context of a scientific research project. The code will automatically adjust for different spatial resolution SKYHI data, and will calculate zonal integrals (*e.g.*, temperature, kinetic energy, momentum transport), vertical column integrals, and zonal and global averages. Three-dimensional quantities such as potential vorticity can also be derived. Meridional transport and vertical fluxes of all SKYHI data are also available, and a chemistry module can calculate "fast chemistry" tracer mixing ratios for at least seven chemical species as well as sources and sinks for all chemical species.

The output from this package can be used by the GrADS two-dimensional plotting package or can be converted for use in Vis5D, which can generate three-dimensional renderings of data which can be very useful in viewing the three-dimensional structure of features in deforming cyclone and planetary waves.

An experimental world wide web interface (<http://www.gfdl.gov/~sjt/grads.html>) has been created that allows a remote user to view the pre-analyzed data using a web browser such as Netscape or Mosaic. In effect, this is a point and click interface that allows a new user of SKYHI to immediately view SKYHI fields without having any pre-existing knowledge of SKYHI or the analysis package.

3.1.3 Tropospheric Reactive Nitrogen in the ZODIAC GCTM

To help evaluate the GFDL ZODIAC GCTM simulation of reactive global nitrogen species, a comparison between observations and simulation results was performed. Observations were obtained for a wide variety of locations and seasons using data from 12 special observation programs, a number of ship cruises, and

several fixed site measurement stations. NO_x , PAN, and NO_y statistics were then derived for observations at pressure levels corresponding to those in the GCTM. Corresponding reactive nitrogen concentrations were gathered from the simulation along the mission flight paths and time series were extracted for the appropriate time window.

In the atmospheric boundary layer, simulated peroxyacetyl nitrate [PAN] was found to be concentrated over the continental sites of NO_x emissions, primarily the midlatitudes in the northern hemisphere and the subtropics in the southern hemisphere. In the free troposphere, simulated PAN is distributed relatively zonally throughout the northern hemisphere, with the maximum levels found in the coldest regions. In the southern hemisphere, the maximum levels are found in a belt from the equator to 30°S and stretching from South America to Australia. Overall, the model simulations were found to be in general good agreement, in both vertical structure and seasonality, with most of the observations discussed above, particularly in the remote oceanic regions where PAN plays a critical role in determining NO_x levels. However, there are some discrepancies in the mid-troposphere during NH summer, during the spring in the SH, and at Alert, Canada during winter. Specifically, the ABLE3b measurements over eastern Canada and the TRACE-A PAN measurements over the South Atlantic are as much as 100% higher than the simulated values, while the simulated PAN mixing ratios at Alert during winter are at least 50% higher than observed.

The spatial and temporal distribution for a global three-dimensional time-dependent lightning source of NO_x was constructed based on: a) ZODIAC GCTM deep moist-convection statistics; b) observations of cloud-to-cloud and intra-cloud lightning fractions and the vertical distribution of lightning discharge; and c) empirical/theoretical estimates of relative lightning frequency resulting from deep moist-convection over ocean and over land. By comparing tropospheric NO_x simulations from the GCTM with measurements of NO_x and/or NO_y [see discussion above] in the mid- and upper-troposphere (where lightning is a major, if not dominant, source), it was possible to estimate the annual global emission of NO_x from lightning to be between 2 and 6 TgN/year, with a most probable range of 3 to 5 TgN/year. While these amounts are much less than many previous estimates, lightning remains the single largest source of NO_x in the mid and upper troposphere for a latitude belt running from 30°N to 30°S and a major source, even in the lower troposphere, of NO_x over the remote oceans. It is also an important contributor to summertime free-tropospheric NO_x levels over the midlatitudes of both hemispheres.

3.1.4 Tropospheric Ozone in the GCTM

The concentration of tropospheric ozone, which controls the chemical reactivity of the lower atmosphere and is a significant greenhouse gas, is thought to

have increased significantly over the last 100 years in a number of regions, possibly throughout much of the globe. Two major questions must be addressed: 1) What is the relative importance of ozone transport from the stratosphere to the net chemical production in the troposphere; and 2) What are the relative contributions of natural and anthropogenic sources of ozone precursors to any chemical production of ozone in the troposphere.

Collaborations continue with colleagues involved in the ongoing Air Ocean Chemistry Experiment [AEROCE] over the North Atlantic, which is focusing on measurements of tropospheric ozone as well as its chemical precursors and tracers of atmospheric transport. In particular, a program of ozonesonde measurement and analysis continues, and an AEROCE field campaign (including aircraft measurements of key ozone precursors, surface measurements and ozonesondes) is being prepared for the spring of 1996.

A photochemical box model with carbon monoxide [CO] and methane [CH₄] chemistry has been modified to calculate the net contribution from chemical production less chemical destruction [hereafter, ozone tendency] of tropospheric ozone. This model was used to investigate the effects of temperature, radiation, humidity, and concentration of NO_x, ozone, and CO on ozone production and destruction. Ozone tendencies were also calculated as a function of altitude, with special attention paid to the upper troposphere. At 200mb in July and in the midlatitudes, ozone tendencies were found to be much smaller (not more than 2ppb/day) than at the surface, where they could reach over 30ppb/day for some NO_x values. The main factors responsible for the sharp decrease of the tendencies with height appear to be a decrease in humidity and temperature. Lower humidity strongly affects the concentration of NO_x at which the ozone tendency switches sign from negative to positive. Again for the summertime midlatitudes, at 200mb the crossover levels of NO_x were in the range of [10ppt-30ppt], while at the surface they were much larger [50ppt-100ppt].

Some initial attempts were undertaken to calculate net ozone tendencies for the globe as a whole. Using observed zonally averaged CO, temperature, and humidity, summer ozone tendencies were calculated for specified NO_x and ozone values at a number of latitudes and pressure surfaces. These tendencies can then be used to construct preliminary three-dimensional fields of ozone tendency by interpolating global fields of GCTM-produced ozone and NO_x to the precalculated set of tendencies. The global fields of ozone tendencies show a strong correlation to the fields of NO_x, with low values over the ocean where NO_x is low and high values in NO_x source regions.

To better understand the impact of reactive hydrocarbons on ozone tendencies, a version of the photochemical box model was run which treats the detailed gas phase

photochemistry of the reactive hydrocarbons with a reduced set of reactions. For NO_x higher than 50 ppt, the calculated ozone tendencies increased substantially when reactive hydrocarbons were included. For ~1 ppb NO_x , this increase is especially strong and, for the summertime, the tendencies can be as much as a factor of ten higher. Ozone production was also found to be sensitive to levels of isoprene, a natural reactive hydrocarbon. Adding only 50 ppt of isoprene resulted in a near doubling of the positive ozone source rate for high levels [>750 ppt] of NO_x .

The GCTM was also used to study the three-dimensional structure of the tropospheric ozone (O_3) distribution over the North Atlantic Ocean during summer. The model included a simplified representation of summertime O_3 photochemistry appropriate for Northern Hemisphere midlatitudes (*i.e.*, pre-calculated ozone for the free troposphere and a simple parameterization of ozone formation in the polluted boundary layer), and was evaluated by comparing simulated O_3 mixing ratios to summertime O_3 measurements taken in and near the North Atlantic Ocean basin. The model successfully reproduced: a) the means and standard deviations of ozonesonde measurements over North America at 500 mb; b) the statistical characteristics of surface O_3 data at Sable Island off the coast of North America and at Bermuda (western North Atlantic); and c) the mean mid-tropospheric O_3 measured at Bermuda and at the Azores (eastern North Atlantic). The model underestimated surface O_3 in the eastern North Atlantic, overestimated O_3 in the lower free troposphere over the western North Atlantic, and also had some difficulty simulating the observed temporal variance in the upper tropospheric ozonesonde measurements over North America. An examination of the mean summertime O_3 distribution simulated by the model shows a significant continental influence on boundary-layer and free-tropospheric O_3 over the western North Atlantic.

The GCTM model has also been exercised using a pre-industrial NO_x emission scenario. A comparison of present-day and pre-industrial simulations found that anthropogenic NO_x emissions have significantly perturbed the summertime tropospheric O_3 levels over most of the North Atlantic (A94/P95). Present-day O_3 levels in the lower troposphere over the North Atlantic are estimated to be at least twice as high as corresponding pre-industrial O_3 levels. The summertime anthropogenic impact is even substantial in the mid-troposphere, where modeled present-day O_3 mixing ratios are at least 50% higher than pre-industrial O_3 levels.

3.1.5 Transport Studies

The transport of PAN, combined with its unique temperature sensitivity, result in chemical lifetimes varying from several days near the Earth's surface to nearly a month in the upper troposphere. This, in turn, produces high mixing ratio values in the winter mid- and high-latitudes of the free troposphere. However, the amount of NO_x stored as PAN in the global troposphere never exceeds two days of tropospheric NO_x

emissions from all known sources. Nonetheless, the chemistry and transport of PAN results in a removal of sequestered NO_x from its point of emission and a subsequent release of NO_x in remote regions of the globe due to thermal decay. This transfer significantly impacts the global distribution of tropospheric NO_x . Model results indicate that by including PAN chemistry, NO_x values over remote oceanic areas increase by a factor of 2 to 5. This increase suggests a possible shift in the ozone chemistry of these regions from one of net destruction to one which is ozone-neutral or ozone-producing.

A trajectory analysis of local synoptic scale (1-2 day) NO_x events in the oceanic lower troposphere indicated that subsidence of PAN from aloft, followed by thermal decomposition, is the usual sequence of events. However, when examining a larger geographical area over a longer time frame, it is difficult to determine whether the increase in NO_x results from sinking of PAN from above or from boundary layer advection of PAN from its source regions. In order to quantify the difference, an experiment was designed which allowed PAN chemistry to take place only in the model's boundary layer. The results showed, by comparison with a complete chemistry run, that from late fall through spring, subsidence of PAN into the boundary layer accounts for more than 70% of the NO_x found over the eastern half of the Pacific and Atlantic ocean basins.

The springtime arctic troposphere is known to contain elevated levels of a range of pollutants, including hydrocarbons and reactive nitrogen (mainly PAN). It has been suggested that the southward flow of arctic air during spring may provide the necessary precursors for photochemical ozone production over the north Atlantic and Pacific basins. The GCTM's integral of PAN and NO_x was examined for storage north of 60N. This suggested a possible southward springtime flux of PAN, since a March-April PAN maximum is followed by a rapid decrease in May, without any corresponding increase in NO_x . In addition, an analysis of PAN chemistry in the Atlantic and Pacific regions has shown that, during spring, NO_x increases by a factor of 2 to 5 south of 50N. However, it was not possible to identify the enhancement due solely to the venting of arctic PAN.

A reexamination of the south Atlantic wintertime NO_x bloom was carried out using a new biomass burning source (provided by the NASA Langley Research Center). The new source was based on observed periods of biomass burning in Africa and South America. The old source was determined by the GCTM-generated climatology of the dry season over these geographical areas. This new source results in a shift in time of the maximum total biomass source from July to September, although the total NO_x produced over this period is essentially the same. The temporal change in the release of NO_x (from a time of strong model transport to one of weaker transport) reduces the NO_x maximum at 835MB over the south Atlantic by a factor of two. Even so, this region may still be one of positive ozone tendencies. This issue will

be further investigated when model integrations of ozone and its chemistry are completed.

3.1.6 Atmospheric Sulfur Chemistry and Transport in the GCTM

The GCTM was used to assess the global distribution of sulfur compounds resulting from anthropogenic activities. The latest inventory of SO_x emissions were incorporated into the model. Gas-phase conversion of SO₂ to SO₄ was calculated using specified temporally-varying, three-dimensional OH fields. A simplified representation of the aqueous-phase conversion of SO₂ to SO₄ was also included in the model. Comparisons with surface data at a number of sites in North America suggests that the model reproduces sulfate mixing ratios to within a factor of 2, and is also successful in reproducing the general features of the seasonal cycle in surface sulfate concentrations. However, a similar comparison with data from Europe reveals a significant discrepancy between modeled and observed surface sulfate mixing ratios. In particular, the modeled mixing ratios exhibit a strong seasonality with a summer maximum, a feature which is absent in the observations. The cause of this discrepancy is currently being investigated. The GCTM-simulated seasonally-varying, column-sulfate burden is being developed as a basis for calculating the seasonal variation of the direct radiative forcing of sulfate aerosols.

A zero-dimensional box model has been developed to simulate the cycling of sulfur gases, as well as the formation, growth, and removal of aerosols in the marine boundary-layer. The model includes representations of various physical, chemical, and aerosol microphysical processes, and is being used to investigate possible relationships between dimethyl sulfide fluxes and cloud condensation nuclei (CCN) concentrations in the marine environment.

PLANS FY96

SKYHI runs with stratospheric chemistry will continue, using a version of the model that includes a parameterization of the stratospheric quasi-biennial oscillation (QBO) developed at GFDL (3.2.8). The purpose of this study will be not only to continue assembling a climatology of chemical simulations of the stratosphere, but also to evaluate the three-dimensional photochemical model by comparing the calculated ozone QBO with observations. Issues such as the interaction between photochemistry, radiation and dynamics for both the equatorial and extra-tropical QBOs may also be explored.

Several experiments are also planned to test the various advection schemes currently available in the modular SKYHI by comparing the evolution of various tracers using several different schemes. The test tracers will be H₂O, N₂O, NO_y, CFC-11, as well as CO₂, Rn, Pb²¹⁰ and possibly Kr. The advection schemes that will be

used for this study are the hybrid second and fourth order centered differencing scheme currently employed in SKYHI, the SKYHI pseudo-fourth order scheme, the Lin semi-Lagrangian scheme, and a hybrid van Leer/semi-Lagrangian scheme.

The tracers used in the advection scheme experiment will also be used to obtain a more detailed understanding of SKYHI's transport properties. In particular, CFC-11 and CO₂ will be used to study interhemispheric transport, while Pb²¹⁰ will be used to assess the validity of the moist removal processes in the model.

Halogen chemistry will be added to SKYHI and a model run simulating the stratosphere will be initiated to investigate the degree to which today's chlorine levels influence ozone amounts.

Improvements to the photochemical scheme will continue. These include adding an interpolation of photolysis rates for the overhead ozone column and updating photolysis rates and kinetic rate coefficients to recent laboratory data. In addition, interim fixes for both the water vapor and the cold pole problems will be added to the GCM, permitting a more reasonable simulation of stratospheric chemistry.

PAN will be added to the current photochemical scheme in the troposphere, and a simulation using SKYHI which includes reactive nitrogen source distributions will be initiated.

The ongoing revision of the SKYHI analysis code to include additional zonal integral calculations and other derived quantities as individual research requirements demand will continue. In the next year, the analysis code will be fully tested through use in a variety of research projects listed above.

Analysis of the ZODIAC GCTM's global and regional budgets of tropospheric reactive nitrogen and the relative contributions of natural and pollution sources will be completed.

A gas-phase photochemical box model will be used to calculate tropospheric ozone photochemical tendencies for the entire globe and for all seasons. The ZODIAC GCTM will use these ozone tendencies, along with ozone transported from the stratosphere and a parameterized formation of ozone in the polluted boundary layer, to calculate the distribution of ozone throughout the troposphere and to determine the natural and anthropogenic contributions to its tropospheric global budget.

Work will continue on the GCTM's transport from the springtime Arctic, and an attempt will be made to quantify the influence of Arctic pollution.

Both the North Atlantic Regional Experiment (NARE) and AEROCE should supply measurements of photochemically-active species during the winter-spring in the North Atlantic region. These will be used to help evaluate both the anthropogenic and natural contributions to tropospheric ozone and the export of pollution from the Arctic.

3.2 ATMOSPHERIC DYNAMICS AND CIRCULATION

*K. Hamilton J.D. Mahlman
R. Hemler R.J. Wilson
C. Kerr P.W. Jones*****

*****Los Alamos National Laboratories/DOE*

3.2.1 SKYHI Model Development

The first of several planned physics upgrades to SKYHI has been made. A new radiation package with options to include up to 9 radiative gases has been included in the modular version of SKYHI. This package requires, as input, the output of separate cloud, astronomy, ozone and surface characteristics (albedo) modules, which have been created in SKYHI. Specification of these physical properties in separate modules outside of the radiation package provides additional modularity and facilitates easier modification and experimentation with these parameterizations.

The vertical diffusive transport of tracers is now determined by the moist Richardson number in saturated layers, rather than by the dry Richardson number used previously. This scheme provides a more realistic representation of the vertical transport of tracers in moist convectively unstable layers.

The SKYHI code now has the ability to utilize a variety of tracer transport schemes, including: centered second-order, centered pseudo-fourth order, semi-Lagrangian, and a hybrid semi-Lagrangian/vanLeer flux correction scheme. These schemes can be assigned to individual tracers for comparative evaluation. SKYHI may now also be integrated without including any tracers. The number and characteristics of the archive files that are saved for later analysis may now be easily defined and modified, allowing a user to customize the archive files that are created in a given experiment.

A number of improved physical process packages have been prepared for extended SKYHI evaluative testing. These include: an updated radiation code that incorporates a wide suite of additional greenhouse gases; an improved ozone climatology (see 2.5.4) based on a variety of observations; elimination of dry convective adjustment through the use of the SKYHI Richardson number diffusion

parameterization; addition of moist Richardson effects to diagnose vertical mixing of tracers in moist convection; and an initial attempt at producing prognostic clouds in SKYHI.

3.2.2 SKYHI Control Integrations and Basic Model Climatology

The control integration using a 40-level $1^\circ \times 1.2^\circ$ latitude-longitude version of the SKYHI model was continued. The portion of this integration completed on the Cray YMP (with no changes in model formulation) now extends for over 22 months. This has allowed the June-August and December-February climatologies for the $1^\circ \times 1.2^\circ$ model first published in (1274) to be updated to include two years of data (ye). The integrations for 30-day periods in June and January were repeated with hourly archiving of selected fields.

3.2.3 Studies of Diurnal Variability

Analysis is continuing on a multiyear $3^\circ \times 3.6^\circ$ SKYHI integration with a diurnal cycle. Aspects of the long-term mean, zonal-mean circulation in the diurnal run have been compared with results from a diurnally-averaged control integration. The differences in general have been found to be quite small.

The significance of latent heat release in forcing the upward-propagating diurnal tide is the subject of a collaboration with J. Forbes (University of Colorado) and M. Hagan (NCAR). An analysis of the diurnal harmonic of rainfall at a large number of individual stations has been used to produce suggested global distributions of diurnal latent heat forcing. These will be employed in a linear model for the diurnal tide that includes a realistic zonal mean state.

3.2.4 High Horizontal Resolution Integration with SKYHI

An integration of a version of the 40-level SKYHI model with $0.6^\circ \times 0.72^\circ$ latitude-longitude resolution was started on the Los Alamos CM5 massively parallel computer and has now proceeded for two months. Analysis has begun on the results with a focus on how the mean flow and gravity wave field in the stratosphere and mesosphere differ from those in the 1° and lower resolution versions of the model.

3.2.5 Resolved Gravity Waves in the SKYHI Model

Analysis of the resolved gravity wave field in the SKYHI control simulations has continued. In particular, some attempts have been made to compare the high frequency variations in the SKYHI simulations with observations in the middle atmosphere. This kind of comparison is hampered by the lack of global observations on sufficiently small space and time scales. Earlier work (1120) focused on comparisons between the statistics of the vertical profiles of temperature and horizontal wind in the model simulations and in historical rocketsonde data (useful for

the ~30-60 km altitude range). An exciting development in recent years has been the deployment of Rayleigh lidars at several sites. These instruments have the capability of measuring the vertical temperature profile in the range ~30-80 km at quite high vertical and temporal resolution. The lidar at the Observatoire de Haute Provence (OHP) in France has operated for several years, enabling the group there to publish fairly extensive results concerning the high frequency variations in temperature at that location. Fig. 3.2a shows a typical height-time temperature section obtained from the 1° SKYHI model simulation at the grid point closest to OHP. The results are shown for five consecutive days and are presented as anomalies from the five day mean at each level. This figure can be compared with similar sections published by the OHP group. Many of the basic features seen in this figure are also apparent in the results from the OHP lidar, notably the peak range of temperature excursions in the mesosphere ($\sim 25^{\circ}\text{C}$) and the clear dominance of downward phase propagation. The observations do show more variability at somewhat higher frequencies than seen in the model, however. The OHP group has computed a measure of wave activity in their observations, namely the available potential energy density associated with the temperature variations. Their results (average over 15 km height intervals) are compared with the same quantity derived from the simulated temperatures at the SKYHI grid point closest to OHP in Fig. 3.2b. This indicates that the model is able to produce a realistic degree of gravity wave variability in the midlatitude stratosphere and mesosphere (supporting the earlier conclusions obtained on the basis of comparisons with rocketsondes). Some preliminary results concerning the high frequency variability in the SKYHI mesosphere are presented in (ye).

3.2.6 Sensitivity of the Middle Atmospheric Gravity Wave Field to Changes in the Moist Convection Parameterization

It has been shown (e.g., 1153) that moist convection plays a very important role in exciting the vertically-propagating gravity waves seen both in the tropical and extratropical middle atmosphere of the SKYHI model. Some experiments have been undertaken to examine the sensitivity of the simulated gravity wave field to some rather arbitrary changes introduced into the convection parameterization. A set of 38-day integrations of the $2^{\circ} \times 2.4^{\circ}$ SKYHI model with several such modifications has now been completed. One set of changes was designed to make the moist convective eddy momentum flux in the midlatitude mesosphere in the last 30 days of two adjustment somewhat less abrupt. This was accomplished by having the convective parameterization restore towards a linear combination of the actual (pre-adjustment) lapse rate and the moist convective lapse rate. A second kind of modification was designed to couple the convection more directly to the large-scale boundary layer convergence. In particular, one run simply retained the standard moist convection algorithm, but only activated it at grid points at which the vertical velocity was upward at the third model level from the bottom. Preliminary analysis suggests that the middle atmospheric gravity wave field is not greatly affected by these changes in the

a

SKYHI "OHP" Temperature

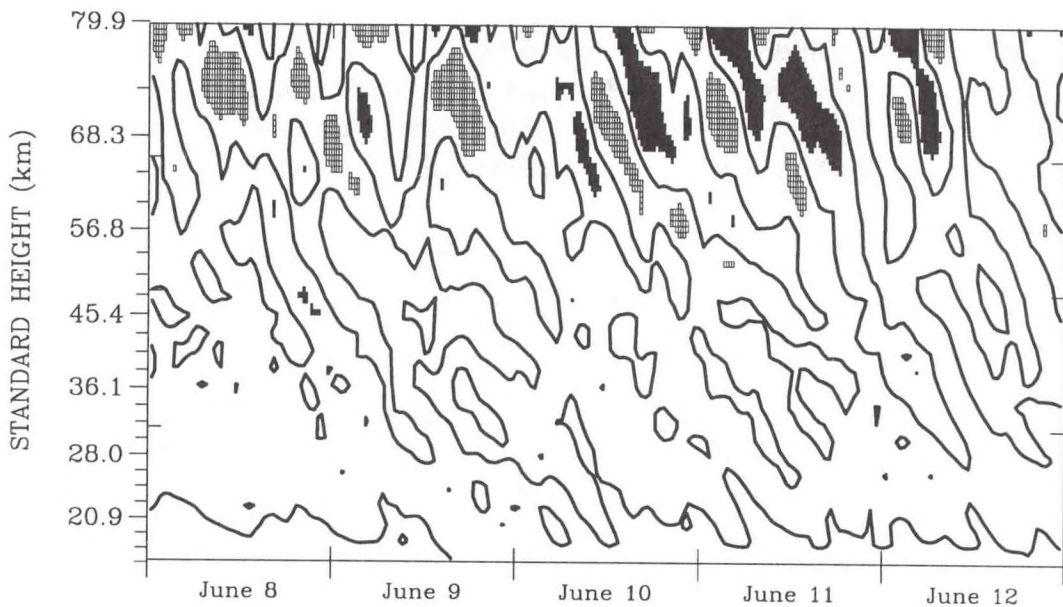
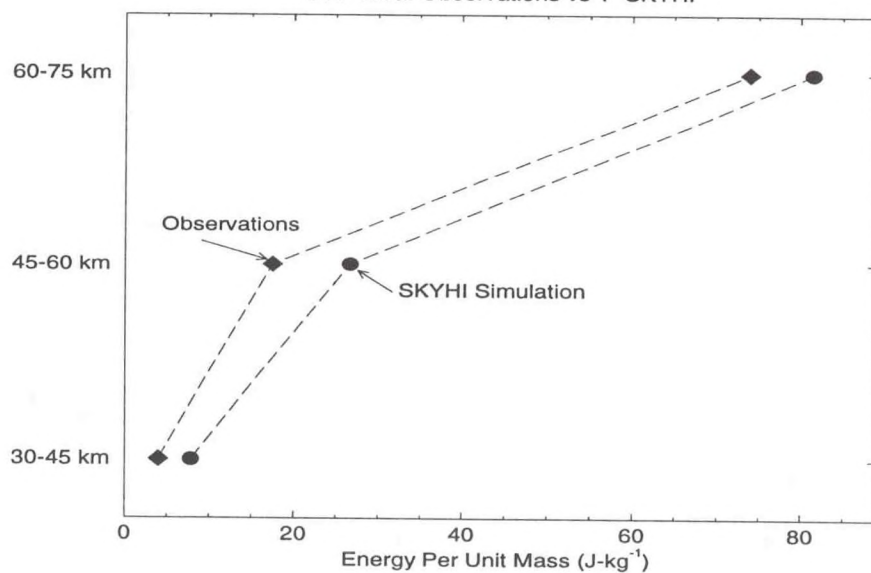
**b**June Mean Gravity Wave Activity Near 44°N, 6°E
OHP Lidar Observations vs 1° SKYHI

Fig. 3.2 (a) Temperature anomalies at the grid point corresponding to Observatoire de Haute Provence (OHP) over 5 days of simulation with the 1° SKYHI model. The zero contour is shown, along with regions where the temperature anomaly is $>10^\circ\text{C}$ (dark shading) or $<-10^\circ\text{C}$ (light shading). (b) Comparison of estimated gravity wave energy density based on OHP lidar observations and the 1° SKYHI simulation. The results show that the model is capable of producing a realistic degree of gravity wave variability.

convection. As an example, Fig. 3.3 shows the zonal wavenumber spectrum of vertical integrations, one with the standard convective adjustment and one with the vertical velocity switch.

The focus of the analysis thus far has been on the spectrum of resolved gravity waves. It will also be interesting to analyze the global-scale equatorial waves that are excited in simulations with various modifications to the moist convection parameterization. To this end, some considerably longer integrations will be performed on the Cray C90.

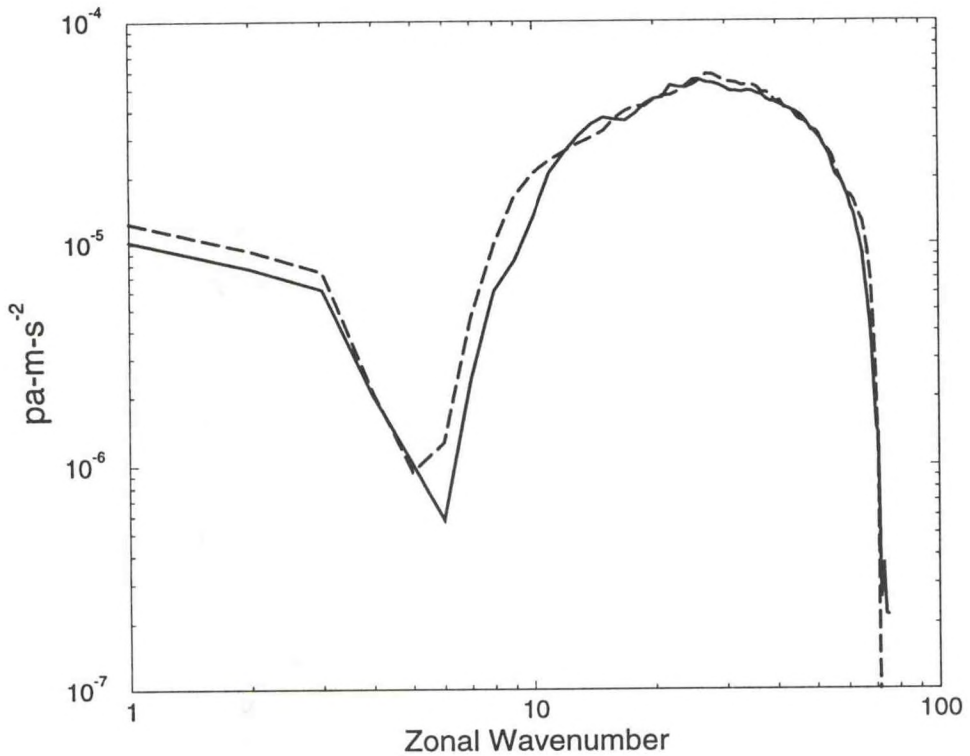


Fig. 3.3 The vertical momentum flux $\overline{u'w'}$ per zonal wavenumber at the second highest model level (~73 km) along the 45°S latitude circle in two integrations performed with the $2^\circ \times 2.4^\circ$ SKYHI model. The solid curve gives the results from the control run employing the standard moist convective adjustment, while the dashed curve shows results for a model with the moist convection allowed to act only at grid points where the vertical velocity was upwards at the third model level from the bottom. Results in each case represent the average over 30 days (June 8-July 6) in runs starting from identical initial conditions on June 1 and indicate that the middle atmospheric gravity wave field is not greatly affected by changes in the convection scheme.

3.2.7 Experiments with Simple Models of Wave Propagation

In collaboration with E. Manzini of the Max Planck Institute, Hamburg, a study of linear wave propagation in arbitrary zonal mean flows is being conducted. The

model being used is a modification of that described in (1153), and this model is now running efficiently on the CRAY C90 in Hamburg. The focus of these calculations is on examining the propagation of global-scale equatorial waves through realistic mean flows. The observed mean flow in the tropical stratosphere is known to display both very strong vertical shears and very rapid transition. Both these features render suspect the usual theoretical treatments of the vertical propagation of equatorial waves. The present calculations can easily be performed at extremely fine spatial and temporal resolution, and thus will provide a direct indication of the effects of mean flow transience and strong mean flow shear on the wave structure.

Simple nonlinear 2-D and 3-D models of wave propagation are being developed. These will be applied in a study of the evolution of a spectrum of vertically-propagating gravity waves. The results will be used to evaluate the value of proposed parameterizations of the effects of gravity waves on the large scale circulation.

3.2.8 GCM Simulation with an Imposed Tropical Quasi-biennial Oscillation

An integration using the $3^\circ \times 3.6^\circ$ SKYHI model with an imposed zonal momentum source designed to force a realistic quasi-biennial oscillation (QBO) in the tropical stratosphere has proceeded for about 10 years. It appears that the specification of the momentum source has succeeded in producing a mean flow evolution at low latitudes that closely resembles the observed QBO, while avoiding any noticeable discontinuity between the tropical and subtropical mean flow. Analysis of this experiment will shed light on several important questions. Given the realistic radiative transfer algorithms used in the model, the contribution of the residual mean meridional circulation to the mean momentum balance should be diagnosed very accurately. This in turn will lead to an unambiguous determination of how much total eddy forcing of the mean flow is required to account for the QBO. A related issue is the extent to which the required eddy mean flow forcing is supplied by the resolved motions in the model. The preliminary results in this regard are very interesting. It appears that during the westerly acceleration phase, the eddies produced by the model can in fact account for the mean flow accelerations equatorward of $\sim 5^\circ$, but not for regions further from the equator. The parameterized subgrid scale mechanical dissipation also appears to be a significant factor in the mean zonal momentum budget of the lower stratosphere in this experiment.

Another issue that will be addressed with the results from this simulation is the QBO modulation of transport between the tropics and higher latitudes. Given the likely role of quasi-stationary planetary waves in producing mixing across the subtropics, it seems reasonable to suppose that this mixing could be strongly modulated by the location of the zero wind surface. The present experiment should allow a direct diagnosis of this effect in a 3-D model with rather realistic mean flow evolution through

the QBO. The dynamical effects of the tropical QBO on higher latitudes will also be examined.

3.2.9 Observations and GCM Simulation of the Ozone Quasi-biennial Oscillation

The observational study of the ozone QBO using the Nimbus-7 Total Ozone Mapping Spectrometer (TOMS) data was completed. The study described in A93/P94 was updated using the full record of the TOMS data (1978-1993). The results support a view of the ozone QBO that had been proposed earlier on the basis of Dobson spectrophotometer measurements of total ozone at an array of individual stations (922). In particular, it seems that very near the equator (say equatorward of $\sim 15^\circ$) the ozone QBO is largely symmetric about the equator and is in phase with the QBO in zonal wind. As one proceeds to higher latitudes the interaction of the QBO and the annual cycle comes to dominate. This is most naturally interpreted as a QBO modulation of along-isentropic mixing associated with the seasonal cycle of quasi-stationary planetary waves. The combination of the direct QBO effect and the QBO modulation of the annual cycle leads to a very complicated latitude-time section of the TOMS total ozone field. As part of the present work it was shown that much of the very irregular behavior disappears when the field is simply decomposed in components symmetric and antisymmetric about the equator. It was further shown that the power spectrum of the symmetric component has a single peak near that of the dynamical QBO, while the spectrum of the antisymmetric component has peaks corresponding to the beat frequencies of the annual and QBO components (1301).

The QBO forcing described in 3.2.8 has now been incorporated into the SKYHI version with stratospheric chemistry, as discussed in 3.1.2. An integration with this model designed to cover several cycles of the QBO has commenced. The results will be used to examine the ozone QBO forced by the dynamical QBO. The issues raised in the observational study of the ozone QBO will be addressed through a detailed analysis of the results from this simulation.

3.2.10 Tropical Waves Observed in High-Resolution Radiosonde Data

Global scale, relatively long period (~ 3 -15 days) equatorial waves are thought to be very important components of the circulation in the equatorial lower stratosphere. Unfortunately, direct observation of these components is hindered by the rather short vertical wavelengths that are anticipated for these waves. Depending on the mean winds, the theoretically predicted vertical wavelengths for the equatorial waves expected to dominate in the lower stratosphere can vary from less than 1 km to several km. Such short vertical scales are too small to be resolved in satellite radiometer observations. The balloon-borne radiosonde data as conventionally archived at mandatory and significant levels is only able to resolve the very longest of the equatorial waves. The most detailed investigations of these waves remain the

original studies from 25 years ago that employed data archived at ~1 km resolution from special observing campaigns in the tropical Pacific.

Fortunately, the radiosonde systems deployed at many stations now have the capability of taking data at very high resolution. In an important recent development, the US Weather Bureau has begun to archive data from almost all its stations at 6-second (~30 m) intervals. This is now being done at several stations in the tropical Pacific. As part of the TOGA-COARE special observing period (November 1992-March 1993), the data at six US National Weather Service stations in the tropical Western Pacific were archived at 6-second resolution. These data have now been obtained and a project to investigate equatorial waves has started. Fig. 3.4 shows a very preliminary analysis of some of these data. In particular, the top panel (Fig. 3.4a) shows a single temperature sounding from Koror (7°N) presented at 50 m resolution. The presence of quite short vertical scale fluctuations in the upper troposphere and lower stratosphere is quite striking. The bottom panel (Fig. 3.4b) shows high-passed versions of the temperature profiles at 12-hour intervals through an eight day period. The presence of short wavelength fluctuations coherent over several days is evident. The next step will be to correlate the short vertical scale fluctuations observed at different stations.

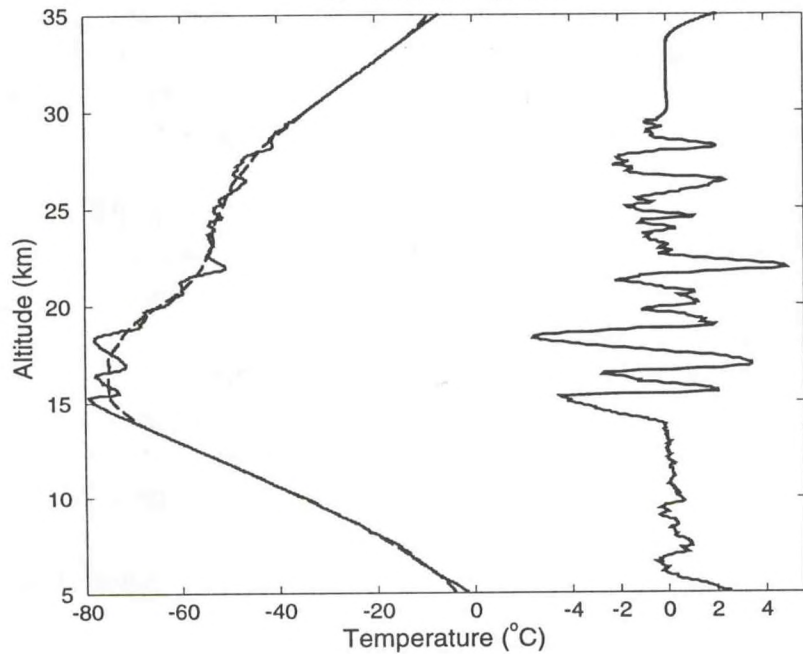
A brief review of some issues involved in analysis of high resolution balloon data is presented in (ag).

3.2.11 SKYHI Simulations with an Imposed Kelvin Wave Forcing

A set of $3^\circ \times 3.6^\circ$ SKYHI model experiments was described in A94/P95 in which a single upward-propagating monochromatic Kelvin wave was excited by an imposed arbitrary heating. Work has continued on analysis of these experiments, with a focus on understanding the mechanisms responsible for the dissipation of wave activity. Some new experiments have been prepared and will be run on the CRAY C90. In particular, experiments in which the seasonal cycle of the mean wind and temperature are suppressed will provide an even simpler case for the diagnosis of the wave activity budget of the imposed wave. It is also planned to repeat some of the experiments with the $2^\circ \times 2.6^\circ$ SKYHI model to see if the more complete explicit representation of the gravity wave spectrum at higher resolution leads to an enhanced dissipation of the global-scale Kelvin wave.

aKoror (7°N , 134°E) Temperature Profile

00z November 1, 1992

**b**

High-Passed Temperatures

12-Hourly Soundings November 1-8, 1992

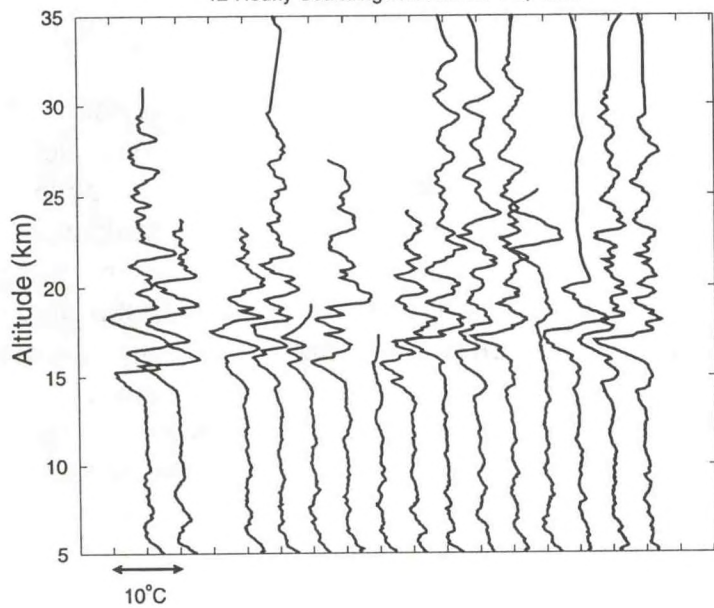


Fig. 3.4 (a) Instantaneous temperature sounding at Koror during the TOGA-COARE period (solid) and a smoothed profile (dashed). The curve on the right is the difference (high-passed) profile. (b) A set of high-passed temperature profiles at Koror taken at 12-hour intervals over 8 days (third profile is missing). Curves are displaced rightward 5° each 12 hours. The results reveal the presence of fluctuations which are coherent over several days.

3.2.12 Dynamics of the Martian Atmosphere

Work has continued on the development of a Martian GCM adapted from the SKYHI model. The model now incorporates the surface physics for the CO₂ cycle as well as radiation physics appropriate for a variably dusty atmosphere. A companion 2-D radiative-convective equilibrium model has also been developed for examining radiative and surface physics processes in greater detail. Simulated climate results are consistent with available observations and with those from the NASA/Ames Martian GCM. Prominent features of the zonal mean circulation are an intense winter hemisphere westerly jet of great depth and a shallow subtropical westerly jet in the summer hemisphere. The latter jet is associated with the lower branch of the Hadley circulation and is similar to the westerly jet associated with the Indian summer monsoon. The large scale topography of Mars modulates the low-level, cross-equatorial flow in the form of western boundary currents. The strength and depth of the Hadley cell circulation depends on the opacity of the atmosphere. For large dust loadings, the model produces a warm winter polar atmosphere similar to that observed.

Further investigations have been carried out on the nature and role of the thermal tides which are a prominent feature of Martian weather. For example, near-surface winds associated with the tides, and modified by local topographic slopes, are likely to play a significant role in dust raising and transport. It has been demonstrated that thermal tides are responsible for forcing westerly zonal mean zonal wind at the equator at altitudes of 10-30 km. Longitudinally-varying surface thermal inertia, topography and aerosol distribution all can contribute to the excitation of a near-resonant diurnal Kelvin wave which may strongly modulate the Martian tidal fields. The main features of the seasonal cycle of tidal surface pressure oscillations observed by the Viking landers can be understood in the context of this resonance phenomenon. It appears that one must postulate significant geographical and temporal variations in atmospheric dust concentration in order to reproduce the observed time series of surface pressure at both lander sites. Simulations with the GCM using interactive dust transport suggest that the dust distributions required to explain the tidal observations are actually quite plausible. Investigation is beginning on the nature of the baroclinic eddies in the simulations. As inferred from the lander surface data, these eddies are very regular by terrestrial standards and show sensitivity to atmospheric aerosol amounts. Interhemispheric differences in eddy activity suggest an important role for topography. Some basic features of the model simulation and an extensive discussion of the diurnal tide are given in (zm).

PLANS FY96

An updated version of the basic physics package for the SKYHI model will be incorporated. This will include the new radiative transfer code, an improved ozone climatology, and a simple form of prognostic cloudiness.

Integrations of SKYHI will be performed at high spatial resolution. Analysis of the $0.6^\circ \times 0.72^\circ$ integration on the Los Alamos CM5 will be continued and some new experiments with both high vertical and horizontal resolution will be run on the GFDL Cray C90.

Integrations of SKYHI with parameterizations of stratospheric and mesospheric gravity wave drag will be undertaken.

Investigation of the diurnal cycle in the SKYHI model will continue. The sensitivity of the calculated thermal forcing of diurnal tides to the assumed water vapor, ozone and cloud distributions will be investigated.

The SKYHI experiments with imposed QBO forcings will continue. The QBO in the ozone field simulated in the model version with stratospheric chemistry will be studied and compared with available observations.

The comparison of small-scale wind and temperature variations in the SKYHI GCM with lidar, rocket and radar observations will continue.

The observational study of wave motions in the tropics using the high-resolution TOGA-COARE data will continue.

Analysis of simple linear and nonlinear model vertical wave propagation experiments will continue. New, higher resolution SKYHI integrations with imposed monochromatic wave sources will be performed.

The work on Martian dynamics will be completed.

4. EXPERIMENTAL PREDICTION

GOALS

To develop methods of stochastic dynamic prediction capable of extracting as much useful forecast information as possible from numerical prediction models given imperfectly observed initial conditions.

To develop and improve numerical models of the atmosphere-ocean-land system in order to produce useful forecasts with lead times of several weeks, months, seasons or years.

To understand the limits of predictability of the ocean-atmosphere system with emphasis on quantifying the amount of useful forecast information that could be available at lead times of several weeks, months, seasons or years.

To develop methods for the assimilation of ocean observations into dynamical models in order to improve predictions of the ocean and atmosphere.

4.1 STOCHASTIC DYNAMIC PREDICTION

*J. Anderson K. Miyakoda
S. Griffies W. Stern
V. Hubeny*

ACTIVITIES FY95

4.1.1 Selection of Initial Conditions for Ensembles

A number of simple dynamical systems were studied in order to better understand how to select initial conditions for ensemble forecasts. It was demonstrated that one must take into account details of the model's dynamics in addition to information about the statistics of observational error. Using only information about the observational error can lead to a significant underestimate of the variability in both the ensemble initial conditions and forecasts (x_i); this phenomenon may explain the inability of operational ensemble forecasts to produce the observed variance. Methods developed in simple low-order dynamical systems have been

extended to a study of the dynamics of a three-level, global quasi-geostrophic model. The attractor of this model was found to be surprisingly complex, suggesting that extension of the ensemble initial condition selection techniques will be challenging.

4.1.2 Methods for Interpretation and Validation of Ensemble Forecasts

A method for evaluating the potential predictive utility of an ensemble of forecasts was developed (yd). The method uses information about the entire forecast distribution to determine if a particular ensemble forecast can be distinguished from a long term control climate. If such a distinction is possible, the ensemble forecast can potentially be used to produce a forecast that is superior to the climatological control forecast. The method was validated in simple dynamical systems and then applied to an ensemble of Atmospheric Model Intercomparison Project (AMIP) ten-year model simulations (4.3.2.4).

A method for evaluating whether a set of ensemble forecasts is consistent with the verifying observations was developed (yy). The method uses the ensemble forecast values of a particular quantity to define a set of bins into which the corresponding observation can be placed. Given a large set of ensemble forecasts, the verifying observation should fall into each of the bins with uniform probability. The new method was applied to simple dynamical systems where it was discovered that the addition of information about the observational error distribution may be vital for verifying short range forecasts. This method was also applied to an ensemble of AMIP integrations (4.3.2.4).

4.1.3 Theoretical Limits of Predictability

Classical predictability experiments that have long been used as baselines for evaluating the limits of predictability of the atmosphere were reexamined using new insights gained from the study of dynamical systems. Experiments with low order models compared the apparent limits of predictability with and without additional information about the dynamics of a particular system. It was discovered that naive attempts to evaluate the limits of predictability in this fashion can produce answers that are quite different from the correct results. Extension of these results may lead to a reevaluation of the limits of atmospheric predictability.

4.1.4 Norms for Dynamical Systems

There is currently no objective definition of the distance between dynamical states. Such a distance, or norm, is required for defining notions such as stability and predictability. Recent work in the areas of statistical physics and information theory, however, have employed ideas from differential geometry in hopes of garnering a deeper understanding of such norms. Theoretical research is currently underway with

the goal of assessing these new ideas and their implications for atmospheric prediction and predictability.

PLANS FY96

Potential predictive utility and ensemble consistency diagnostics will be applied to additional model simulations and coupled model forecasts. Results related to selection of initial conditions will be extended to more realistic higher order forecast models. Investigation of natural norms for geophysical fluid dynamics (GFD) problems will be continued.

4.2 DEVELOPMENT OF MONTHLY TO SEASONAL FORECAST MODELS

<i>J. Anderson</i>	<i>J. Ploshay</i>
<i>C. T. Gordon</i>	<i>A. Rosati</i>
<i>S. Griffies</i>	<i>J. Sirutis</i>
<i>R. Gudgel</i>	<i>R. Smith</i>
<i>C. Kerr</i>	<i>W. Stern</i>
<i>V. Larichev</i>	<i>A. Weill-Zrahia</i>
<i>K. Miyakoda</i>	<i>B. Wyman</i>
<i>R. Pacanowski</i>	

ACTIVITIES FY95

4.2.1 Atmospheric Models

4.2.1.1 Global Grid Point Model

An initial version of a B-grid atmospheric general circulation model (AGCM) has been completed. The B-grid provides a more logical and efficient arrangement of grid points for the global model than previous E-grid models. The model design emphasizes flexibility and modularity of the model's physical parameterizations (4.2.1.5), and initial tests have demonstrated that the model has a climate that is comparable to those of other GCMs.

A six year integration of the E45L18 Global Eta E-grid Model has been completed for both the sigma and eta vertical coordinates (wh). The global tropospheric circulation did not differ greatly between the two integrations, perhaps due to the relatively low resolution. The eta coordinate appeared to be superior in the following respects: 1) large-scale stationary circulation in the Northern Hemisphere; 2) spatial and temporal variation of blocking frequency; 3) some regional precipitation distributions; 4) vertical motion fields over steep topography. In the Northern Hemisphere polar night stratosphere, the eta coordinate produced a polar vortex with much stronger zonal winds and colder temperatures.

4.2.1.2 Spectral Model Improvements

Participation in AMIP highlighted some key weaknesses in the spectral AGCM, including excessive precipitation over the western Pacific during June-July-August (JJA) period and an unrealistic southward suppression of the western Indian monsoon. Improvements to the surface, boundary layer and cloud prediction parameterizations were made in an attempt to improve this situation and reduce the even larger biases which occur when the AGCM is coupled to the ocean. However, only limited improvements were obtained, highlighting the extreme difficulty of improving the climate of coupled GCMs.

A T63L18 version of the atmospheric GCM has been produced. A 10 year AMIP integration with this model is underway to investigate the impact of increased horizontal resolution on the quality of the model simulation.

4.2.1.3 Development of Subgrid Scale Parameterizations

Code for the Relaxed Arakawa-Schubert (RAS) convection scheme has been obtained, incorporated into the spectral model, and is currently being tested and tuned. Based on preliminary tests, RAS requires less than half the computations needed for the full Arakawa-Schubert scheme.

4.2.1.4 Modular Physics Packages

A specification for modular grid point physics packages which can be readily exchanged between different GCMs has been formulated. The physical parameterizations that are used in the E-grid version of the Global Eta Model (4.2.1.1) have been converted into modules conforming to this specification in which all user interaction with the modules is through well-defined argument lists. Major parameterizations produced so far include moist convective adjustment (MCA), large scale condensation, Mellor-Yamada turbulent closure, Monin-Obukhov similarity theory, surface temperature prediction, and surface hydrology. These modules have been tested in both the B-grid and E-grid versions of the Global Eta Model. A modular version of the Arakawa-Schubert cumulus parameterization scheme used in the spectral model has also been created.

4.2.1.5 Modular Spectral Dynamical Core

Preliminary versions of the spectral dynamical core of the proposed modular spectral model have been completed and are undergoing tests. Efforts are underway to test the core in a number of different spectral models and to port the core to a variety of parallel programming environments.

4.2.2 Ocean Model

4.2.2.1 Maintenance of Equatorial Thermocline

Maintaining a tight equatorial thermocline consistent with observations has proven to be difficult in coupled ocean-atmosphere models. Because equatorial thermocline displacement is highly correlated with tropical sea surface temperature (SST) anomalies, its accurate representation is of prime importance when forecasting El Niño-Southern Oscillation (ENSO) events. An effort is underway to gain a better understanding of subgrid-scale ocean processes and to assess their effects on both tropical and extratropical forecasting skill. Idealized process studies using limited-basin ocean-only models, combined with fully coupled GCM simulations and forecasts, are being investigated. Preliminary studies of the off-equatorial dynamics are also underway in an effort to understand their impact on midlatitude ocean and coupled responses.

4.2.2.2 Sensitivity to Subgrid Scale Parameterizations

Physically based subgrid-scale parameterizations have been implemented for use in the ocean portion of the coupled forecast model (wn). Smagorinsky nonlinear momentum mixing, Mellor-Yamada turbulence closure, and the Pacanowski-Philander Richardson number vertical mixing are currently available. In addition, closure schemes thought to be relevant for parameterizing the effects of geostrophic eddies on tracers are being investigated (wu).

4.2.3 Land Surface Model

The Simple Biospheric (SiB) Model has been implemented in the spectral model. A soil-vegetation-atmosphere transfer model is under development and will be incorporated into the spectral model. This model should yield the benefits of including the effects of vegetation on the surface fluxes and will be significantly more efficient than the full SiB model.

4.2.4 Coupled Atmosphere-Ocean-Land Models

The B-grid atmospheric model has been modified so that its grid points are collocated with grid points from the higher resolution ocean B-grid. This modification has been made to allow a more straightforward coupling between the atmosphere and ocean models.

PLANS FY96

A limited number of atmosphere-only and fully-coupled model runs will be performed to evaluate the impacts of AGCM resolution (T63 versus T42) and convective schemes on both the coupled-model forecasts and atmosphere-only

simulations. The spectral model will then be frozen and development of a new modular spectral model will be expedited by combining the existing modular spectral core and modular physics packages.

The B-grid atmospheric model will undergo further testing before being coupled to the ocean model. The climate of the both the atmosphere-only and coupled models will be studied and compared to those for the spectral atmospheric model. Comparison of the eta and sigma coordinate E-grid models will be completed by performing a series of high resolution integrations and assessing their climates.

A set of studies combining the results of idealized process models for the ocean with results from the fully coupled forecast model will be undertaken. The goal is to gain an understanding of the particular physical processes as well as their relative importance in producing realistic simulations and skilled forecasts. The response of the midlatitude ocean to these parameterizations, especially those schemes aimed at parameterizing tracer transport by geostrophic eddies, will be examined.

Development of a number of subgrid scale parameterizations will continue including the impacts of sulfate aerosols and of marine stratocumulus clouds. The RAS and MCA convective schemes will undergo additional refinement, and alternative schemes for land surface processes will be examined. A 10 year integration will be made with the SiB model in the spectral AGCM to establish its climatology, and to compare it with the bucket model hydrology currently being used. A bucket model with a variable bucket depth will also be implemented and tested.

4.3 ATMOSPHERIC AND OCEANIC PREDICTION AND PREDICTABILITY

<i>J. Anderson</i>	<i>A. Rosati</i>
<i>C.T. Gordon</i>	<i>J. Sirutis</i>
<i>S. Griffies</i>	<i>R. Smith</i>
<i>R. Gudgel</i>	<i>W. Stern</i>
<i>K. Miyakoda</i>	<i>F. Vitart</i>
<i>J. Ploshay</i>	<i>B. Wyman</i>

ACTIVITIES FY95

4.3.1 Coupled Model Prediction

4.3.1.1 ENSO (El Niño Southern Oscillation) Forecasts

Forecasts were made with a number of variations of the atmospheric model physics. Emphasis was placed on evaluating the impact of two atmospheric convection schemes: Moist Convective Adjustment and Arakawa-Schubert.

Additional ensemble members and cases are necessary before a final evaluation of these schemes can be completed.

4.3.1.2 Improvement of Seasonal Cycle

Since ENSO appears to be closely coupled to the annual cycle (wn), an effort has been made to improve the coupled model's seasonal cycle in the tropical Pacific. A large part of the systematic error in the eastern tropical Pacific was found to be due to a poor representation of the marine stratocumulus clouds. Multiyear integrations have been performed to test the coupled model's sensitivity to predicted low cloud amount versus a specified monthly mean climatology derived from ISCCP (International Satellite Cloud Climatology Project). In runs with the Arakawa-Schubert cumulus parameterization, the SST in the eastern tropical Pacific cools by approximately 2K and the annual cycle is much stronger with the ISCCP clouds than with clouds predicted (Fig. 4.1). These results are related to the model's inability to adequately simulate marine stratocumulus clouds. It was also noted that some cooling spreads to the western Pacific along a narrow equatorial belt, apparently due to a dynamical feedback mechanism.

4.3.2 Atmospheric Predictability

4.3.2.1 Impacts of Clouds and Radiation

A parameterization of marine stratocumulus clouds based upon a linear regression method (A94/P95, section 4.1.1) has been tested in a 40 year integration with the T30 spectral atmospheric GCM. The simulation of marine stratocumulus clouds off the west coasts of North and South America is noticeably more realistic using this parameterization than previous parameterizations (1097).

Results from one month integrations suggest that the negative bias in the spectral model's zonal mean short-wave radiation at the surface in the tropics can be reduced significantly by specifying a latitudinally varying single scattering albedo which decreases linearly with the near-surface zonal mean saturation mixing ratio.

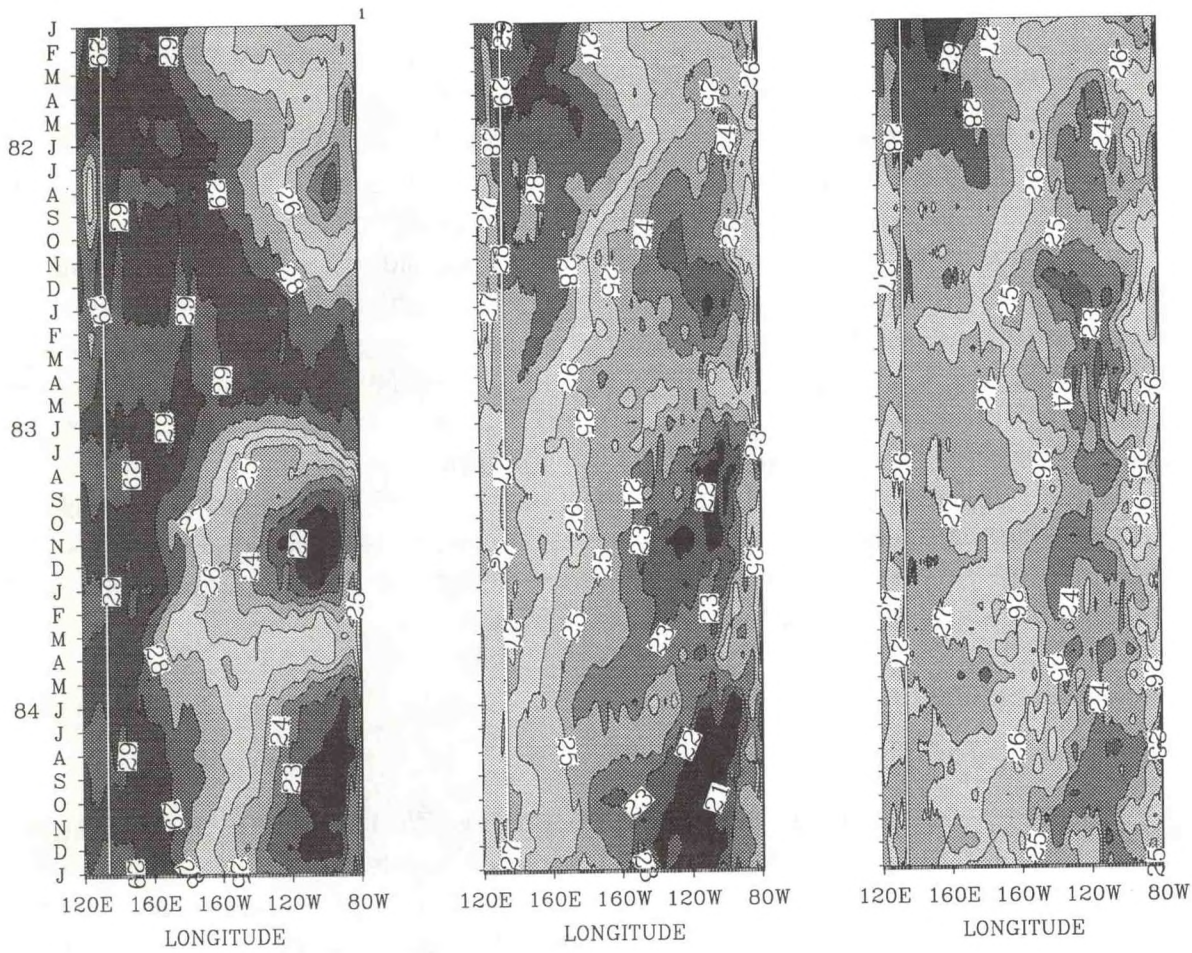


Fig. 4.1 Longitude time-sections of monthly mean sea surface temperature (C) on the equator: Reynold's analysis (left); coupled model with specified ISCCP low clouds over ocean (center); coupled model with predicted low clouds (right). The integration with the ISCCP clouds produces a considerably stronger seasonal cycle in the eastern tropical Pacific.

4.3.2.2 Intraseasonal Variability

Tropical intraseasonal oscillations (TIO) in the T42L18 AMIP integrations have been assessed using a single model simulation during the period January through June of each year from 1980 to 1988. In addition, all nine members of the ensemble were analyzed for January through June in 1983 and 1984. In the time mean, the model appears to have a dominant eastward propagating mode with period close to 30 days while observed modes appear to have periods from 45 to 60 days. However, the considerable interannual scatter in the GCM (with periods near 60 days for some years), combined with significant frequency and amplitude scatter between ensemble members within a given year, indicates the need for an ensemble approach to understanding and forecasting the TIO.

4.3.2.3 Interannual Variability

The eastward propagation of the ENSO signal in the spectral model and in the atmosphere has been investigated using a variety of techniques including rotated complex principle component analysis and Hayashi space-time spectral analysis.

Studies of the T42 AMIP ensemble have shown that the interannual variability of individual simulations is robust only for the tropical Pacific. Outside of this region, the increasing scatter among individual ensemble members clearly suggests that an ensemble approach is required to properly assess interannual variability (zs).

The surface heat budget from the 40 year AGCM simulation has been compared to the Comprehensive Ocean-Atmosphere Data Set (COADS) analyzed fluxes. Overall, the model and COADS monthly mean anomalies over the equatorial Pacific are fairly well correlated, especially during the 1980's. The model exhibits upper tropospheric warming during each ENSO event that is zonal in character, consistent with the observations. A warming trend in global mean (land plus sea) surface temperature of approximately 0.8K in 15 years which starts in 1974 is roughly twice as large as the trend in the observed global mean SST. Rather large interdecadal variations are found in the eastward propagation of the modeled monthly mean anomalies of zonal wind across the equatorial Pacific.

The potential predictability of the tropical disturbances produced in the AMIP ensemble integrations of the T42 atmospheric model is being investigated. An automatic procedure for tracking model tropical disturbances has been applied to this ensemble and to ECMWF observations. A variety of statistics describing the model generated tropical disturbances have been examined; these include frequency, track, duration and intensity.

4.3.2.4 Feasibility of Seasonal Forecasts

Studies of the feasibility of seasonal forecasts have continued via 10 year and 40 year GCM integrations. Seasonal mean results from ensembles of AMIP integrations (at both T30L18 and T42L18) have been analyzed using both the reproducibility ratio (1300) and an improved measure, predictive utility (yd). Results confirm significant potential predictability throughout much of the tropics and for selected regions outside the tropics, such as the southeast U.S., including northeast Brazil. It is apparent that much of the potentially predictable signal results from the El Niño events of 1982-83 and (to a lesser extent) 1986-87. The 40 year integrations are intended to increase the sample size of ENSO events in order to enhance the robustness of the potential predictability and teleconnection patterns derived from the AMIP integrations. For example, a T30L18 40-year GCM integration demonstrates a strong relationship between the southern oscillation index (SOI) and anomalous winter precipitation over the southeast U.S. (Fig. 4.2). Lesser areas of potential predictive

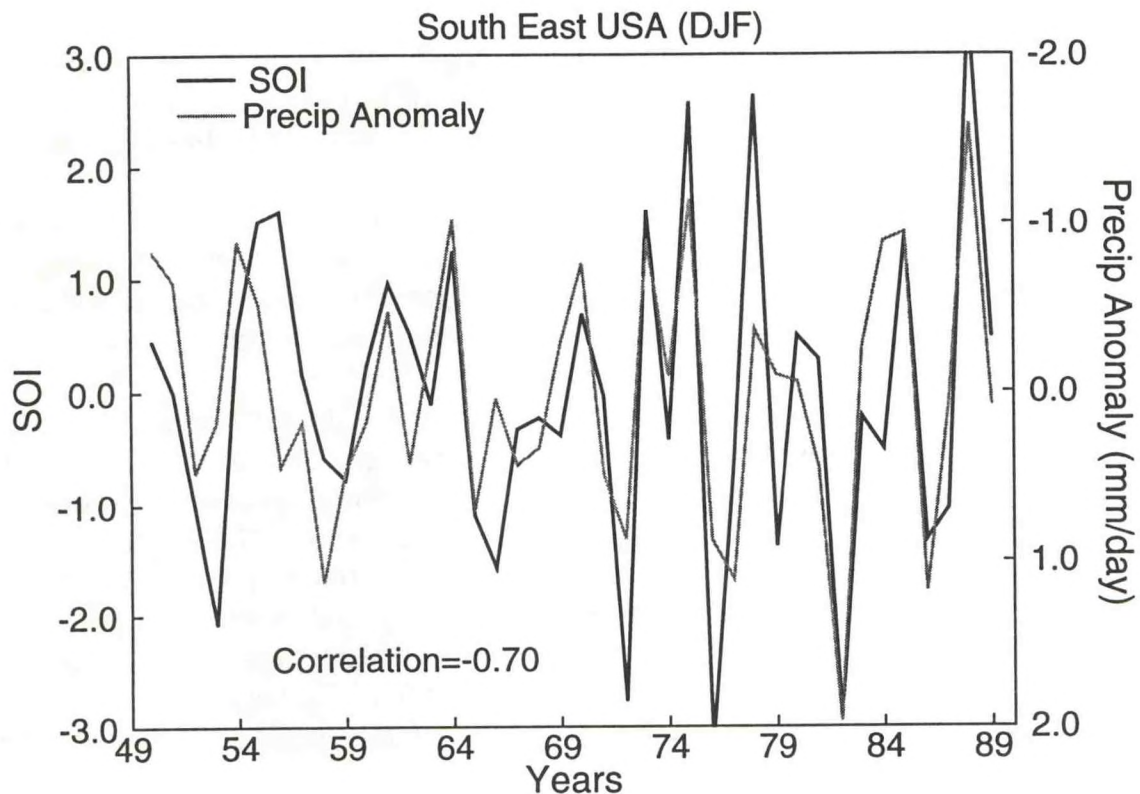


Fig. 4.2 Time series of December-January-February mean precipitation anomaly over the southeast United States and the Southern Oscillation Index (SOI) from a 40 year atmospheric model simulation. The negative of the precipitation anomaly is plotted to highlight the significant correlation between the series.

utility were found during years with normal or cold tropical Pacific SSTs, suggesting that useful long range forecasts may be possible for some areas of the extratropics in most years.

4.3.3 Ocean Predictability

The predictability of the ocean in the coupled-model system is being investigated by performing a series of integrations with identical ocean initial conditions but slightly perturbed atmospheric initial conditions. The impacts of model resolution and physics parameterizations in both the atmosphere and ocean are also being investigated through a number of companion integrations in which these factors are varied. In order to better assess how well the model is performing in various configurations, an analysis package employing various prediction indices is being developed.

PLANS FY96

The frozen version of the current spectral model (see plans for section 4.2) will be used to produce a suite of atmosphere-only and coupled-model runs with consistent resolution and parameterizations. These runs will be designed to address fundamental questions about coupled model predictability, including the relation to the predictability of the individual atmospheric and oceanic components, the impacts of coupling frequency, and whether fully coupled models are essential to the prediction problem. Additional runs with single element changes to selected physical parameterizations, including convection schemes and clouds, will be used to more clearly elucidate the role of these processes in coupled model prediction.

In collaboration with the Climate Dynamics group, an ensemble of 40 to 50 year AGCM integrations will be produced at R30L18 and/or T42L18 resolution. This will serve as the basis for further study of the feasibility of seasonal prediction including validation of regional seasonal mean anomalies. Additional multi-decadal runs with the current spectral AGCM will assess the impact of different SST datasets on the atmospheric response. Of particular interest will be the feasibility of drought forecasts in those regions that demonstrate significant potential predictability within the AGCM.

Analysis of the tropical intraseasonal oscillations in the AMIP ensembles will be expanded to include all nine members.

The relationship between model tropical disturbances and observed tropical storms, and its implications for seasonal and interannual prediction, will be investigated using the AMIP ensemble.

Process studies to better understand the mechanisms of the annual cycle in the coupled model will continue. As the model's seasonal cycle is improved, forecasts will be made to try to understand the role of the annual cycle in interannual variability.

4.4 OCEAN DATA ASSIMILATION

<i>A. Rosati</i>	<i>M. Harrison</i>
<i>S. Griffies</i>	<i>K. Miyakoda</i>
<i>R. Gudgel</i>	<i>J. Poshay</i>

ACTIVITIES FY95

The ocean data assimilation (ODA) system is used to initialize the ocean component of the coupled model forecast system and to verify ocean forecasts. The predictive skill of the sea surface temperature anomaly fields in coupled-model forecasts has been found to be highly dependent on the ocean initial conditions, and

this skill is much greater when the ocean initial conditions come from an assimilation which includes subsurface thermal data (1308).

Improvements to Current Assimilation Methodology

The ODA system was expanded to include data from COADS and the TOGA/TAO (Tropical Ocean Global Atmosphere/Tropical Atmosphere Ocean Array) moorings.

Assimilation of Altimeter Data

Using a statistical method based on correlating sea surface height with subsurface temperature, the satellite altimetry data from the Topographic Experiment (TOPEX) for October 1992 through December 1993 was assimilated into the ocean model. Analysis of the assimilation methodology, as well as the relative impacts of altimetry data and *in situ* observations, is ongoing.

Coupled Model Assimilation

A fully coupled air-sea data assimilation system was developed and tested. A number of 13 month coupled model forecasts were run from the 10 day assimilated initial conditions to assess the impact of the coupled assimilation.

Decadal Data Assimilation

The ocean data assimilation system was run for the period 1979 through 1994 (1308) and the resulting analysis product was compared to independent analyses. Special attention was given to the tropical Pacific, especially the El Niño signature (xt). This assimilation produced initial conditions which were used for coupled model forecast integrations (yz).

PLANS FY96

A reanalysis for the 1985-1994 period will be made with many new features. The ocean model will be based on MOM2 and the vertical resolution will be increased to 50 levels and atmospheric forcing will come from the NMC reanalysis project. A new quality control procedure is being developed that will process multiple datasets and data types. Continued development of the ODA system will focus on improving the error statistics as well as the methodology for the assimilation of altimetry data. As the ODA system is modified, coupled model forecasts will be made to assess the impact of the changes and to evaluate the value of various data sources (e.g., TAO moorings and TOPEX data).

5. OCEANIC CIRCULATION

GOALS

To develop a capability to predict the large-scale behavior of the World Ocean in response to changing atmospheric conditions through detailed, three-dimensional models.

To identify practical applications of oceanic models to human marine activities by the development of a coastal ocean model.

To incorporate biological effects in a coupled carbon-cycle/ocean GCM.

To study the dynamical structure of the ocean through detailed analyses of tracer data.

5.1 OCEAN-ATMOSPHERE INTERACTIONS

<i>A. Bush</i>	<i>N.-C. Lau</i>
<i>L. Goddard</i>	<i>T. Li</i>
<i>B. Goswami</i>	<i>S. Masina</i>
<i>D. Gu</i>	<i>R.C. Pacanowski</i>
<i>G. Lambert</i>	<i>S.G.H. Philander</i>

ACTIVITIES FY95

The prediction of climate fluctuations on seasonal and interannual time scales, of which the Southern Oscillation between El Niño and La Niña is a prominent example, requires coupled ocean-atmosphere GCMs (general circulation models) that are capable of a realistic simulation of the spectrum of observed variability. The persistence of unusually warm conditions in the tropical Pacific over the past several years, a phenomenon not anticipated by any of the models currently in use for the prediction of El Niño, underlines the need for realistic coupled GCMs. The failure of the models now being used is attributable, in part, to their specification of the time-averaged state and the seasonal cycle on the basis of measurements over a certain period. Over a longer period, low frequency variations can change the effective background states, as they did during the early 1990's. Coupled GCMs capable of reproducing realistically the time-averaged state, the seasonal cycle, the interannual and decadal fluctuations should also be capable of coping with such low frequency

variations. The development of improved GCMs requires ancillary studies with simpler models, and also the analysis of measurements, to elucidate the phenomena that are involved in the fluctuations.

5.1.1 The Seasonal Cycle Simulated with Coupled GCMs

A curious feature of the tropics, with which all coupled GCMs have trouble, is the observed climatic asymmetry relative to the equator in the eastern tropical Atlantic and Pacific. Observations show that the warmest surface waters and heaviest rainfall are north of the equator. Most of the simulations produce essentially symmetrical distributions of these properties about the equator. A study (ak) with a coupled GCM forced with annual mean solar radiation demonstrated that low-level stratus clouds which form over the cold waters off Peru are involved in a positive feedback that contributes to the observed asymmetry. Another curious feature of the eastern tropical Pacific and Atlantic is the presence on the equator of an annual harmonic, despite the fact that the sun "crosses" the equator twice a year. A new study (aj) showed that it is possible to explain the annual harmonic given the asymmetry of the time-averaged state. This annual cycle was explored using a simplified coupled model in which the mean state was specified.

Although the coupled GCM behaves well in response to annual mean solar radiation, it yields unrealistic results when it attempts to simulate the seasonal cycle. These results are very sensitive to the parameterization of low-level stratus clouds. To check whether those clouds are indeed the source of the problems, they were simply specified. Although the simulation gains significantly in realism -- the asymmetry relative to the equator is recovered -- sea surface temperatures (SSTs) are too low by approximately 2°C throughout the tropics, and the cold tongue along the equator is too prominent. The problem appears to be related to the heat flux across the ocean surface, rather than dynamical processes in the ocean, because an increase in the heat flux by a 4% increase in the solar constant improves the SSTs significantly. A change in the parameterization of evaporation is now being explored.

5.1.2 Studies of Decadal Variability

Persistent warm conditions in the tropical Pacific were observed in the early 1990s, as well as from 1976-1982. They lasted for several years, far longer than a typical El Niño event. These warm conditions appear to be part of decadal variations that modulate the Southern Oscillation. Measurements from the TOGA/TAO array have been analyzed in collaboration with scientists at PMEL (Seattle) in order to get more information about this low frequency signal and its effect on the seasonal and interannual fluctuations. It appears that the seasonal cycle in and below the equatorial thermocline is distinct from that in the upper ocean and has pronounced decadal variability. For example, seasonal variations in temperature at a depth of 100 m on the equator are negligible before 1989, but are prominent thereafter. This indicates that

dramatic changes have occurred in the manner in which winds over the western equatorial Pacific affect oceanic conditions in the eastern part of the basin, presumably because of changes in the structure of the winds.

A hybrid coupled model has been used to explore the decadal variability. The oceanic component of the hybrid model is a GCM, but the atmospheric component is a simple Gill-type model that predicts wind anomalies in response to SST anomalies. The mean winds, which are specified, can be altered to determine how they affect the Southern Oscillation. Weaker time-averaged easterlies throughout the tropics are found to cause persistent warming in the eastern part of the ocean basin and in a Southern Oscillation with a much reduced amplitude.

Reduced easterlies throughout the tropics are usually associated with changes in subtropical winds. These winds, in turn, influence the depth of the equatorial thermocline (v_d), a key feature that controls air-sea interactions in low latitudes. The link between the tropics and subtropics via the wind occurs instantaneously, but the oceanic link involves time lags. The way in which this distinction contributes to the decadal variation is being explored using simple coupled ocean-atmosphere models.

5.1.3 Development of Nested Models

The eastern tropical Pacific and the tropical Americas have a number of features that are poorly resolved by atmospheric models because they have small spatial scales and large gradients. These include the ITCZ, the Andes mountains, the SST front just north of the equator, and the thin layer of stratus clouds over the cold waters off Peru. A high-resolution limited-area model (LAM), acquired from the mesoscale group, has been imbedded in an R30 atmospheric model to cope with these features. The LAM is centered on the tropical Americas, and its boundary conditions are generated by the R30 model which runs independently of the LAM. Thus far, this tool has been used to explore the influence of the Andes. In the R30 spectral model, it is best to suppress these mountains because they interfere with the winds over the oceanic coastal zone where the upwelling of cold water is important. A study with LAM indicates that, because the temperature difference between land and sea causes winds that are parallel to the coast, the mountains are of secondary importance and can, to a first approximation, be neglected. It is only during periods of high SSTs in the eastern tropical Pacific, when the land-sea contrast is much reduced, that the effect of the mountains becomes significant.

PLANS FY96

The development of coupled GCMs capable of realistic simulations of the tropical climate will continue. The focus will be on elimination of the cold bias in SSTs, through improved parameterization of oceanic mixing processes. The matter of cloud

parameterization will be addressed once realistic SSTs can be obtained using specified low level clouds. Studies of decadal variations by means of simplified coupled models will continue, as will the development of nested models.

5.2 WORLD OCEAN STUDIES

5.2.1 Nutrient Dynamics in the Equatorial Zone

S. Carson

J.R. Toggweiler

ACTIVITIES FY95

A simple ecosystem model (1155,1166) has been coupled with a high-resolution model of the equatorial Pacific (758) to study the dynamics of nutrient cycling. The ecosystem model is used to simulate both the uptake of nitrate by organisms in the equatorial euphotic layers and the remineralization of sinking detrital particles at depths below. The coupled biological/physical model has also been used to study the ways in which inorganic nitrate is introduced to the equatorial upwelling system and the ways in which remineralized nitrate returns to the upper ocean (yf). This project was initiated as part of the JGOFS (Joint Global Ocean Flux Study) Equatorial Pacific Process Study, the field phase of which was completed in 1992.

It had previously been reported that nitrate concentrations in model runs forced by the actual 1992 monthly mean COADS winds tended to be much higher than observed nitrate concentrations. These results were obtained while using a drag coefficient that gave reasonable nitrate concentrations with climatological monthly mean winds from the 1950-1979 period. Additional model runs have been made to explore this discrepancy. It was found that a wind climatology derived from the 1980-1992 period produced higher nitrate concentrations than those derived using the standard 1950-1979 climatology. The difference, however, was not sufficient to fully explain the elevated nitrates in the runs using the actual 1992 winds.

The temporal drift of model surface nitrate concentrations over the period 1980-1992 was examined in comparison to the drift in climatologically forced runs. It was found that in runs forced with winds from actual years, there was a significant upward drift of the surface nitrate concentrations over the whole period. This indicates that the elevated nitrates during 1992 are mainly due to the use of the actual monthly mean winds instead of average monthly mean winds. This appears to be a result of the greater variability in the forcing field derived from the actual winds.

Examination of upward fluxes of nitrate through specific subsurface areas shows that the fluxes are both greater in magnitude and much more variable in model runs forced by 1992 winds than in those forced by 1950-1979 climatological winds. It

appears that the greater upward transport of nitrate in the model forced by actual winds, coupled with the tendency of the ecological model to trap nutrients in the upper levels, lead to an increased build up of nitrate in the model euphotic zone. Thus, the very high levels of nitrate found in the model forced by winds from any specific year in the period 1980-1992 are the result of two factors: 1) the climatologically stronger winds of that period; and 2) the model effects of using wind forcing that is more variable than climatological mean winds.

The sensitivity of surface nitrate concentrations to higher month-to-month variability in the wind field points to a major problem with the ecosystem model. The main problem seems to be the treatment of detritus and the fact that the existing model does not take into account the disappearance of oxygen when detrital organic nitrogen is remineralized back to nitrate. The existing scheme for detritus (1155, 1166) is based on an assumption that detrital material is composed of particles which sink quickly with respect to the time it takes for detrital material to decompose. Thus, the existing scheme was written so that detritus simply sinks and does not advect laterally with upper ocean currents. The sensitivity of the model to variable winds seems to be due to the fact that the decomposition of detrital material in sinking particles is too localized near the equator, such that nitrate remineralized from decomposing detritus is immediately reintroduced into the upper levels via upwelling, leading to still more organic production. This suggests that a large fraction of the detrital material in the real ocean is composed of dissolved organic material which, by definition, does not sink and advects laterally with ocean currents. This assertion is strongly supported by observations made during the field program.

There is one big problem with this idea. A model with weakly sinking or non-sinking detritus leaves the tropical ocean without its main export mechanism (sinking particles) for balancing the input of upwelled nitrate. It has been suggested (yf) that a system with minor nitrogen losses due to sinking particles will evolve to the point where oxygen is depleted within the thermocline north and south of the equator. When oxygen disappears, specialized microbes begin using nitrate as an oxygen source for breaking down organic material (denitrification). Denitrification may turn out to be the main sink for tropical nitrate.

PLANS FY96

Two relatively straightforward modifications of the model are planned to address these problems. The first is to alter the treatment of detritus in the model so that detritus can advect with upper ocean currents. The second modification is to have the model predict oxygen concentrations so that denitrification can be included as a nitrate sink. It is not at all obvious that the model will produce anoxia where it is observed to occur (off Peru and Central America) in order to balance its nitrate budget. Work will continue on incorporating carbon and ^{14}C in the model.

5.2.2 Water Masses and Thermohaline Circulation

B. Samuels

J.R. Toggweiler

ACTIVITIES FY95

While oceanographers usually think of deep-water formation in the North Atlantic as a process driven mainly by the ocean's gain and loss of heat, recent work (1313) has shown that changes in the wind stress over the circumpolar belt of the Southern Ocean can change the amount of deep water being formed in the North Atlantic. This result has led to an attempt to formulate a new mechanism for driving the ocean's thermohaline circulation in which wind forcing, continental geometry, and bottom topography in the Southern Ocean are critical factors.

The key to the new mechanism is a demonstration that a major part of the energy which is tapped to maintain the thermohaline circulation is produced by the forces driving the Antarctic Circumpolar Current (ACC). The ACC takes on a critical role because it flows through a zonal channel which is continuous around the world. Within the channel, the ACC is constrained to lose momentum by pressure gradient forces built against deep topographic ridges spanning the channel. This means that the vertical shear in the ACC's eastward flow and the north-south density contrast across the ACC have to extend far down into the ocean's interior. This is another way of saying that a large pool of available potential energy (APE) is maintained in the ocean because of dynamic constraints on the zonal flow of the ACC.

The size of the ocean's APE pool and its effect on the thermohaline circulation are determined by three factors which are externally imposed. First, the wind stress driving the ACC determines the amount of momentum that must be removed. Second, the depth of the submerged ridges across the zonal channel determines the depth to which the eastward flow and the density anomalies across the ACC must extend. Third, the surface density contrast across the ACC determines the maximum density contrast across the current and the maximum vertical shear in the eastward flow. The north-south density contrast and the vertical shear in the interior must satisfy these boundary conditions.

The long-range overturning (1313) which links Southern Ocean winds and deep-water formation in the North Atlantic falls out of the interplay between the three external factors and the density contrast across the ACC. Deep water formed in the North Atlantic flows out of the Atlantic directly into the ACC. The outflow is accelerated toward the east as it moves into latitudes with less planetary angular momentum. The deep eastward flow encounters the submarine ridges in the circumpolar belt, leading to a removal of zonal momentum from the ACC. Thus, the long-range overturning volumetrically links the northward Ekman drift at the surface with the outflow of

Atlantic deep water into the ACC and explicitly relates the input of momentum by the wind stress with the loss of momentum at the bottom.

By suppressing the possibility of deep water formation in the North Atlantic, it is easy to illustrate why this long-range overturning is an energetically favorable solution. Without the deep outflow from the Atlantic, the loss of momentum from the ACC is weak and the ACC becomes stronger. This causes the density contrast across the ACC to extend to a greater depth, creating more APE in the ocean. Without the deep outflow, the removal of momentum by bottom pressure forces is not very efficient, and the wind pumps more APE into the system. If the long-range overturning is then switched on (by making deep-water formation possible in the North Atlantic), two things happen. The same wind work which formerly pumped up the APE in the ACC now goes into kinetic energy associated with meridional overturning. Second, the thermocline shoals globally, meaning that the system as a whole operates at a lower level of potential energy.

This new mechanism also provides an explanation for the abyssal overturning associated with bottom waters formed around Antarctica. Again, one normally thinks of the abyssal overturning as a process driven by the thermal and haline forces associated with bottom water formation. However, the overturning of the ocean's bottom waters has two rather odd properties which are not consistent with bottom water formation as the sole driving mechanism. First, the volume of water flowing northward away from Antarctica at 30°S is about 10x greater than the volume of bottom water actually formed, *i.e.*, only 1/10 of the bottom water flow has had contact with the ocean's surface. Second, the poleward flow (or return flow) which balances the northward flow of bottom water occurs at mid-depth, not near the surface. According to the proposed mechanism, the overturning of the ocean's bottom waters also works off the APE associated with the ACC and is only indirectly related to the formation of bottom water.

It is easy to illustrate how the ACC drives the mid-depth poleward flow by systematically deepening the ocean of a GCM. Basically, deeper topographic obstructions produce a stronger ACC and more north-south density contrast. This increases the total level of APE in the deep ocean and provides for an enhanced exchange of water properties across the ACC. This enhanced exchange makes deep waters north of the ACC denser than deep waters at mid-depth generally, and induces a relatively large volume of mid-depth water to flow poleward and sink north of the ACC. At this point, the sinking mid-depth water joins the small quantity of new bottom water flowing northward away from Antarctica. An abyssal overturning operating in this fashion explains the origin of the water mass known as Circumpolar Deep Water (CDW) and explains why CDW has such low radiocarbon and low CFC levels. This behavior also illustrates that coarse-resolution model oceans need to maintain

substantially higher levels of APE than the real ocean in order to produce a realistic bottom water circulation.

Figure 5.1 shows two meridional sections of APE in the ocean. The upper section is derived from the Levitus dataset; the lower section is derived from the ocean group's standard 4° ocean model. The deep-reaching feature at 60° S is present in both panels and is due to anomalously dense water poleward of the ACC. Without the ACC, this feature would disappear because the whole deep ocean would be filled with water with the same density. The ocean must maintain a substantial density contrast across the ACC, with relatively low-density water to the north, in order that the ACC can maintain its momentum balance.

PLANS FY95

The proposed mechanism is most easily illustrated using the ocean's energy balance. This requires a new set of diagnostics to determine the sources and sinks of available potential energy. Following the work of Oort et al. (1223), a complete description of the APE cycle is being developed for MOM. This work is nearly completed. The new diagnostics will then be applied to a whole series of model experiments to illustrate key elements of the theory.

5.2.3 Using CFCs as Ocean Tracers

K. Dixon

ACTIVITIES FY95

Anthropogenic chlorofluorocarbons (CFCs) dissolved in seawater have been used in an analysis of the GFDL model. Comparing simulated CFC distributions to observations gathered by researchers at NOAA/PMEL and elsewhere allows one to assess the model's ventilation of ocean waters on decadal time scales. The rate at which CFC concentrations in surface waters approach saturation is determined by a gas transfer "piston velocity" (κ). The time scale for CFCs in the ocean's mixed layer to adjust to atmospheric CFC concentrations is generally less than one month, although uncertainties exist as to how best to estimate gas transfer velocities from environmental variables, such as wind speed.

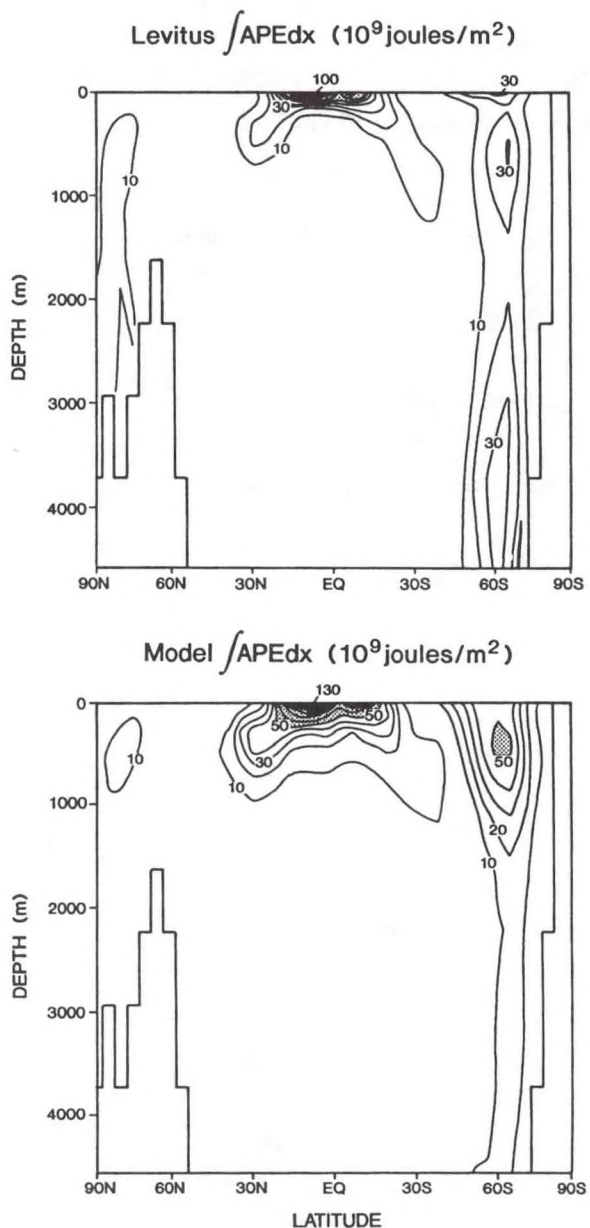


Fig. 5.1 Meridional sections showing the zonally integrated available potential energy of the world ocean. Top panel is derived from the Levitus climatology. Bottom panel is derived from the O-Group's standard 4° ocean model (1313). This figure shows that the APE fields in the model and in the real ocean contain common features, in particular, the enhanced levels of APE in the deep ocean near 60°S , *i.e.*, just south of the Antarctic Circumpolar Current.

To study the sensitivity of model-predicted CFC levels to uncertainties in κ , model simulations were run using two published methods of estimating κ . The first formulation yielded piston velocities which were only 55% to 60% of that produced by

the second method. Between 30°S and 30°N (where CFC levels in surface waters are very close to saturation), model-predicted CFC levels exhibited very little sensitivity to the method chosen to estimate κ . In this zone, the two gas exchange formulations produced mean surface CFC fluxes, F , that agreed to within one percent. In contrast, substantial sensitivities were found in areas affected by rapid and deep ocean ventilation. For example, poleward of 50°S, the slower κ values resulted in F values only 82% as large as those computed using the larger κ values. And where CFCs penetrate below 1500 m depth in the higher latitudes of the Southern Hemisphere, smaller κ values yielded CFC levels that were only about 65% to 75% that of those predicted using the second formulation.

These results suggest that while comparisons of observed and simulated oceanic CFC distributions are quite useful in assessing an ocean model's ability to produce observed patterns of ocean ventilation, uncertainties associated with the parameterization of gas transfer velocities hinder quantitative assessments in areas influenced by rapid ventilation.

PLANS FY96

Model sensitivities to CFC air-sea gas exchange parameterizations will continue to be explored, and will focus on the coupled model's Southern Ocean. This area is of particular interest because rapid ocean ventilation there has been found to markedly influence greenhouse warming patterns in coupled model simulations.

5.2.4 High-Resolution North Atlantic Studies

W. Hurlin

ACTIVITIES FY95

Analysis of the potential vorticity distribution within a high resolution North Atlantic Model showed remarkable agreement with observations. In addition, the results show that the subpolar front can act as a strong barrier to the mixing of tracers between the Labrador Basin and the rest of the North Atlantic. Given this barrier to mixing, it is unclear how deep water formed in the Labrador Basin contributes to the global thermohaline circulation. If deep-water formation occurs in the center of the Labrador Basin, it is difficult for Labrador water to reach the deep western boundary current south of Newfoundland, where the Labrador signal can spread to the rest of the ocean. If deep-water formation occurs within the Labrador Current system, a southward propagation of Labrador water seems more feasible.

PLANS FY96

An investigation into Labrador Basin mixing processes is planned, beginning with a phenomenological study of the Great Salinity Anomaly, a multiyear freshening signal which propagated through the Denmark Straits into the Labrador Basin as a near-shelf signal. This study will also contribute to an understanding of the importance of coastal processes with respect to the hypothesized central Labrador Basin formation of deep water. Other areas of investigation include near-shelf deep-water formation, as well as tracer mixing across the subpolar frontal barrier. These simulations should shed light on the appropriateness of traditional mixing parameterizations in a realistic basin and a near-Rossby radius modeling environment.

5.2.5 Thermohaline Circulation Stability

T. Delworth *M. Winton*
W. Hurlin

ACTIVITIES FY95

The deep Atlantic overturning is one of the main heat transporting circulations of the climate system and it is important to understand its potential for variability. One question that arises is: Why was the formation of North Atlantic Deep Water (NADW) apparently quite variable during the last glacial period, but relatively stable over the most recent 10,000 year warm period (the Holocene)? This is particularly surprising since freshwater forcing of the circulation (a possible source of variability) was likely reduced in the cold glacial climate.

The reduced stability of the glacial circulation might have been caused by convective instability induced by the colder climate, such that a larger portion of the net freshening region in the high-latitude North Atlantic was occupied by water at near freezing temperatures. Under these circumstances, seasonal cooling may be unable to overcome the stratifying effects of precipitation and ice melt, resulting in the formation of an extensive halocline. Preliminary results from a two-dimensional ocean model coupled to an energy balance atmospheric model show that NADW formation is favored by a warm climate. In FY96, an experiment will be run to see if this also holds true for a three-dimensional global ocean model coupled to a simple energy balance type atmospheric model.

Although the Holocene has not been subject to the dramatic climate changes seen in glacial times, there are observations showing significant interdecadal variation in North Atlantic SSTs and surface pressure patterns. The structure of the temperature and pressure patterns supports the interpretation that the ocean is forcing the atmosphere rather than the reverse. Long integrations of a coupled global climate

model show continuous, small amplitude, NADW variability associated with SST variability similar to observed variations (1182). The mechanism responsible for the model variability has not been clearly identified. One hypothesis is that the variability is forced by stochastic variations in the overlying atmosphere (wm). The variability might also be related to a dynamical instability found in flat-bottom, ocean-only models forced with fixed buoyancy fluxes or weak restoring of surface buoyancies¹.

PLANS FY96

In FY96, diagnostic experiments are planned to pin down the precise mechanism. One experiment will involve forcing the ocean component of the coupled model with fixed buoyancy fluxes of varying magnitudes. Another experiment will involve forcing the ocean model with a simple stochastic atmosphere. These experiments should help in evaluating the potential for the model variability to occur in nature.

The temperature and salinity fields of the North Atlantic contain patterns that can only be resolved by high resolution models -- for example, the confinement of large freshwater stocks shoreward of the continental slope. This structure may be important to the stability characteristics of NADW formation. On the other hand, high resolution models are too inefficient to find the global steady state in which potential instabilities are expected to occur. As part of the high-resolution modeling effort, two questions will be posed: 1) to what extent can a limited region model with boundary conditions be expected to reproduce the stability behavior of a more complete model; 2) how does the freshwater over the continental shelves mix into the interior and influence deep water formation in the convective gyres? The long term goal is to evaluate the stability of the global scale circulation in a model that resolves potentially important small-scale processes such as eddies and coastal circulations.

5.2.6 North Atlantic Thermohaline Circulation Predictability

*K. Bryan
S. Griffies*

E. Tziperman

ACTIVITIES FY95

Decadal variability of the North Atlantic thermohaline circulation (THC) has been documented in observations and in the GFDL coupled ocean-atmosphere climate model (1182). A major goal of current research programs, such as NOAA's Atlantic Climate Change Program and the World Ocean Circulation Experiment, is to quantify the ability to forecast such low-frequency climate fluctuations. This goal is

1. Winton, M., On the role of horizontal boundaries in parameter sensitivity and decadal-scale variability of coarse-resolution ocean general circulation models, *J. Phys. Oceanogr.*, in press, 1995.

consistent with a quest to forecast such variability for the purposes of establishing decadal climate trends, as well as to distinguish natural variability from possible anthropogenic effects. A research effort is therefore underway to characterize the predictability of the GFDL climate model's thermohaline variability in hopes of gaining insight into the forecasting of such natural phenomena.

As a first step towards this characterization, the predictability of the North Atlantic THC variability has been established for two ensembles of nine 30-year experiments (y_h). Each ensemble consists of a model ocean with initial conditions underneath a series of model atmospheres chosen randomly from the model's climatology. This experimental design is motivated by the large characteristic time scale separation between the THC (years to decades) and the atmospheric surface forcing (days to weeks). Furthermore, this scale separation suggests that the predictability deduced from these ensembles will provide an upper limit to the model's THC predictability. The results of the ensemble study indicate that the rapidly decorrelating portion of the THC contains predictability for roughly 1.5 years, whereas the slower portion has predictability for roughly 5-7 years. These relatively short predictability times indicate the strong dependence of the model's THC on the stochastic atmospheric forcing.

PLANS FY96

The ensemble experiments contain a wealth of information concerning the predictability of various climate signals in the model. For example, further analysis of the dynamic topography in the North Atlantic is underway for the purpose of diagnosing the predictability of oceanic patterns more accessible to observational measurement, yet still indicative of the long time and large scale oceanic variability. Quantifying the predictability of the dynamical topography's principle components will lend insight into the growth in error for various spatial scales.

The ensemble experiments, combined with a box model process study (wm), point to the relevance of a linear stochastic perspective for understanding the thermohaline variability simulated in the GFDL climate model. Namely, the model's low frequency North Atlantic variability is indicative of a highly damped linear oscillator (the thermohaline circulation) driven by random forcing (the atmospheric synoptic variability). This framework is being further tested with experiments in which the frequency of coupling between the oceanic and atmospheric portions of the model is altered. The idea is to progressively isolate different parts of the atmospheric variability spectrum in order to determine the frequency range which contributes most strongly to the ocean's low-frequency response.

5.2.7 Modeling Mesoscale Eddies in the Ocean

*K. Bryan
J. Dukowicz**

R. Smith
A.-M. Treguier*

**Los Alamos National Laboratory*

ACTIVITIES FY95

Cyclones and anticyclones play a key role in atmospheric climate and are usually included explicitly in climate models. The equivalent phenomena in the ocean are mesoscale eddies, such as meanders in the Gulf Stream or time-dependent waves in the Antarctic Circumpolar Current. The climatic role of these eddies is not as well understood, and they are only included explicitly in the highest resolution ocean circulation models. To gain a better understanding of the role of mesoscale eddies, an analysis of a very high resolution ocean circulation model calculation is being carried out in cooperation with scientists at Los Alamos National Laboratory. The goal of this analysis is to determine if it is possible to design an accurate parameterization of mixing by mesoscale eddies in ocean models of lower resolution.

Preliminary results from this analysis indicate that present closure schemes for representing mesoscale eddies provide an inadequate description of the results from a high resolution model. In particular, nonlocal effects are very important mechanisms for distributing mesoscale energy away from sources.

PLANS FY96

The results of the mesoscale eddy analysis will be used to design new parameterization schemes for representing the mixing effects of mesoscale eddies in ocean climate models.

5.3 MODEL DEVELOPMENT

*C. Goldberg
S. Griffies*

*V. Larichev
R.C. Pacanowski*

ACTIVITIES FY95

MOM 2 is ready for release to the general oceanographic community. A substantial documentation, user's guide and reference manual, has been prepared which details all equations and options. The release version of MOM 2 includes an implementation of the Gent-McWilliams isopycnal mixing scheme.

Recent efforts in model development have focused on the generation of noise within the model, especially with regard to the isopycnal mixing tensor. Experiments have been carried out using an idealized equatorial basin, and noise spontaneously occurs when isopycnal slopes reach their maximum allowable value. The reasons are not clearly understood. Noise also is generated near boundaries and topography without the use of the isopycnal mixing tensor. Simple one-dimensional advection-diffusion equations have been used as analogues for exploring the mechanism of noise generation under various types of boundary conditions. One surprising result is that the test case has been integrated with zero diffusion without noise, in violation of simple Peclet arguments.

PLANS FY96

In anticipation of further developments with isopycnal mixing, the diffusion parameterization of Held and Larichev (yw) which predicts variable isopycnal diffusion coefficients has been implemented within MOM 2. However, these coefficients need to be restricted to regions of possible baroclinic instability, and this is not done in the current implementation. Further work is necessary along these lines.

Also underway is an implementation of the implicit free surface scheme developed at Los Alamos National Laboratory which is cleaner, more understandable, and thoroughly documented.

5.4 COASTAL OCEAN MODELING AND DATA ASSIMILATION

5.4.1 Data Assimilation and Model Evaluation Experiments

T. Ezer

G.L. Mellor

ACTIVITIES FY95

The Data Assimilation and Model Evaluation Experiments (DAMEE) is a Navy sponsored project aimed at the assessment of nowcast/forecast capabilities of several high resolution ocean models (1299), one of which is the Princeton Ocean Model (POM). The first phase of the project has focused on the Gulf Stream system and has been completed in FY95. Considerable nowcast and forecast skill in predicting variations in the Gulf Stream system has been demonstrated using an efficient altimeter data assimilation scheme (1249). The scheme uses an optimal interpolation approach and a vertical correlation technique to project surface data onto subsurface fields. Recently, the data assimilation scheme has been extended to include other sources of satellite-derived data such as SST and Gulf Stream frontal position data (xf). Experiments show how a combination of different data sources improve the nowcast compared to using only a single source of data. The second phase of the

project, data assimilation over the entire North Atlantic basin, has just started with the set-up of a new high-resolution North Atlantic model.

PLANS FY96

The data assimilation methodology, previously developed for regional models, will be tested for the North Atlantic Ocean. Model resolution will be further refined, and intercomparisons will be performed with other models which will use the same data for forcing and assimilation.

5.4.2 The East Coastal Forecast System

P. Chen *G.L. Mellor*
T. Ezer

ACTIVITIES FY95

This project, with support from NOAA's Coastal Ocean Program, is a cooperative effort between Princeton University, GFDL, the National Meteorological Center (NOAA/NMC), and the National Ocean Service (NOAA/NOS). The Princeton Ocean Model is forced by NMC's operational meso-scale atmospheric model (Eta model), in order to provide continuous nowcast and forecast information for the U.S. east coast. The East Coast Forecast System has been in operation since August, 1993, providing daily 24-hour forecasts of oceanic fields (zb). To identify potential users, some of the forecasts are available to the public through the Internet (<http://www-aos.princeton.edu/htdocs/pom/CFS>).

Evaluation of the results shows considerable skill in the prediction of subtidal coastal sea level changes, such as storm surges. Considerable biases found in the air-sea fluxes of the atmospheric model motivated improvements in the boundary layer formulation of the atmospheric model, and required the implementation of new flux calculations and bias correction in the forcing fields used by the ocean model. Several system enhancements were tested on a parallel, non-operational, system at Princeton, and will be implemented in the operational system at NMC. They include for example the addition of river runoffs, tidal forcing, surface pressure forcing and improved mixed layer dynamics.

PLANS FY96

Research will focus on the development and implementation of an operational data assimilation system as an integral part of the East Coast Forecasting System. This effort will build on previous experience in data assimilation, but will require accessing and processing of data in real-time. Further improvements in the atmospheric and oceanic models are planned. Efforts will be started to develop

regional high-resolution models for bays and estuaries, to be nested in, or forced by, the large-scale forecasting system.

5.4.3 North Atlantic and Arctic Climate Studies

T. Ezer

G.L. Mellor

ACTIVITIES FY95

An extension of the Princeton Ocean Model (POM) to the entire Atlantic Ocean and the Greenland sea has been implemented in cooperation with scientists from Goddard/NASA under the support of the Atlantic Climate Change Program (ACCP). The new model produces quite realistic meridional circulation, heat transport, and Gulf Stream separation. Variation in wind stress and the corresponding changes in Ekman transport have been found to be responsible for variations in ocean overturning and meridional heat flux on time-scales ranging from seasonal to interannual and interdecadal (an). A comparison with previous diagnostic calculations of interdecadal changes based on pentadal climatological data (1327) reveals the important role played by the seasonal and interannual variations of the wind in affecting interdecadal climatic changes.

Because of the use of the incompressible fluid and the Boussinesq approximation in all ocean models, variations of sea level due to seasonal or climatological heating or cooling are not calculated exactly. Therefore, a study with a non-Boussinesq version of POM has been used to derive ways to correct global and regional models for non-Boussinesq effects associated with heating and cooling (zc).

PLANS FY96

Long-term simulations with higher resolution Atlantic and Arctic models will continue in order to study the influence of the high latitude dynamics and water formation on the climatology of the Atlantic.

5.4.4 Modeling the Mediterranean Outflow

J. Jungclaus

G.L. Mellor

ACTIVITIES FY95

The outflow of the salty Mediterranean water through the Strait of Gibraltar, down the continental slope and into the North Atlantic has been investigated with a high resolution calculation using the sigma coordinate Princeton Ocean Model. Some of the observed characteristics of the outflow, such as the 'nose' shape of the velocity profile and the shear in the bottom boundary layer, are simulated very well. The time-

dependent evolution of the density current and the spreading of the Mediterranean water mass into the Atlantic ocean seem to be affected by lateral diffusion as well as by advective eddy transport that is triggered by the interaction of the deep flow with the overlying water layers.

PLANS FY96

The instability of an initially bottom trapped density current within a stratified environment will be studied in more detail using both idealized and realistic topographies. Studies with an enlarged model domain that includes the Strait of Gibraltar and the Alboran Sea will be carried out to investigate the exchange flow between the Mediterranean and the Atlantic. These will include realistic forcing and focus on the time-dependency of the Mediterranean outflow.

5.5 CARBON SYSTEM

5.5.1 Ocean Carbon Cycle

S. Fan *J. Olszewski*
*F. Joos** *S. Pacala***
C. Le Quéré *J. Sarmiento*
R. Murnane

** University of Bern, Switzerland*

***Dept. of Ecology and Evolutionary Biology, Princeton University*

ACTIVITIES FY95

A new Carbon Modeling Consortium (CMC) was initiated with support from the NOAA Office of Global Programs. The CMC has the long term goal of developing an integrated carbon system model capable of providing assessments of future oceanic and terrestrial biosphere sinks for anthropogenic carbon. The strategy that will be followed is to make use of existing atmospheric, oceanic, and terrestrial measurements in combination with models to improve our understanding of carbon source and sink processes. The CMC includes collaborators from AOML, PMEL, and CMDL, as well as from several non-NOAA institutions. A first meeting of the CMC Scientific Steering Committee was held in September 1995, and the decision was made to focus the first year of the project on making a new estimate of the mean anthropogenic carbon balance for the period 1980-87.

A series of new calculations were carried out in support of an IPCC (Intergovernmental Panel of Climate Change) model comparison study of a range of scenarios for controlling future atmospheric CO₂ content (1288). The future uptake of

anthropogenic carbon by the terrestrial biosphere was estimated with a simple terrestrial model, calibrated using a model/data estimate of terrestrial uptake of anthropogenic carbon since the beginning of the industrial revolution. The ocean uptake was estimated with a perturbation carbon model coupled to the GFDL ocean model (1084). The results of this simulation suggest that uptake by the ocean and terrestrial biosphere could be roughly equal and account for more than three-quarters of the anthropogenic carbon over the next three centuries.

The oceanic uptake of anthropogenic carbon was estimated with an improved ocean model that includes the full carbon chemistry equations and the impact of biological processes on the carbon distribution. This model takes up 9.2% more anthropogenic carbon than the perturbation model (1288) due primarily to an improved simulation of carbon chemistry. If biological processes are removed from the model, the uptake increases by 5.1% due to a change in the carbon holding capacity of surface waters. These results were used to analyze the carbon budget of the North Atlantic in combination with observational constraints (1320).

The use of three-dimensional ocean models for scenario estimates of anthropogenic carbon uptake is very costly in terms of computer time. Previous studies have attempted to characterize the ocean model behavior by use of an oceanic response function to a pulse input to the atmosphere. This response function can then be used to inexpensively calculate a wide range of oceanic uptake scenarios. However, this approach suffers from the serious problem that the carbon chemistry determining the air-sea CO_2 balance is highly non-linear with respect to the CO_2 concentration. Predictions made using the atmospheric response function can differ by several tens of percent from predictions made with the full ocean model. A new technique has been developed which gets around the non-linear chemistry problem by explicitly modeling the air-sea equilibration, and combining this with a surface to deep ocean exchange function estimated from the response of the model to a pulse input in the ocean surface layer. This new simplified model can reproduce the ocean GCM results to within a few percent (ap).

PLANS FY96

The major focus of research over the following year will be to lay the groundwork for the first year CMC study of the anthropogenic carbon balance for the period 1980-87. The transport of CO_2 by the atmosphere will be evaluated for a wide range of source/sink distributions using the GFDL SKYHI atmospheric transport model. Methods will be developed for obtaining a new estimate of the anthropogenic carbon budget based on the results of the SKYHI simulations combined with the results of ocean carbon model simulations and atmospheric and oceanic observational constraints provided by members of the CMC.

A coupled atmosphere-ocean climate model of the impact of global warming will be used to study the feedback between greenhouse warming and the oceanic carbon cycle.

The results of the new ocean carbon cycle model which utilizes full chemistry equations and biological processes will be analyzed, including a study of the ^{13}C isotope distribution that has important implications for both anthropogenic transient and paleoceanographic studies.

5.5.2 Ocean Carbon Cycle

<i>R. Armstrong</i>	<i>G. Hurtt***</i>
<i>J. Dengg</i>	<i>R. Murnane</i>
<i>V. Garcon**</i>	<i>J. Sarmiento</i>
<i>N. Gruber*</i>	<i>R. Slater</i>

* University of Bern, Switzerland

** C.N.R.S., Toulouse, France

*** Dept. of Ecology and Evolutionary Biology, Princeton University

ACTIVITIES FY95

Progress was made on the development of surface ocean ecosystem models for use in understanding and monitoring the oceanic role in the global carbon cycle. A range of sensitivity studies were carried out in an ocean GCM using an early version of an ecosystem model containing one phytoplankton, one zooplankton, bacteria, and four forms of nitrogen (1175). The addition of multiple size classes was found to have a large impact on the simulations and also suggested how the role of micronutrient limitation might be included in ecosystem models (1253). A first attempt was made to assimilate satellite observations of ocean color into the ocean GCM (1294). This study showed that only the multiple size class model had sufficient flexibility to simulate the wide range of chlorophyll standing crop observations. A major emphasis of ongoing research is to develop a new family of simplified ecosystem models based on a rigorous calibration with existing observations at the JGOFS Bermuda time series station (ya) as well as other locations.

Progress was also made on using thorium trace metal and other observational constraints to develop and calibrate models of recycling of organic matter in the deep ocean (1206, 1207, ww). The stoichiometric ratio of various elements in organic matter was estimated as a function of depth using GEOSECS observations of the inorganic concentrations (1235), and the results were shown to give realistic simulations in an ocean GCM biogeochemistry model (ac). A description of a new simplified model of the ocean developed some years ago for biogeochemical studies

was published (1318). This HILDA model has already seen wide use by the IPCC as the standard model for estimates of oceanic carbon uptake.

PLANS FY96

Work on simplifying biogeochemical cycling models and calibrating the models with data assimilation techniques will continue. The present model assumes that the availability of nitrogen limits algal growth. However, for diatoms silicon is also a limiting nutrient, and certain algae can fix nitrogen gas into ammonium that can be used for growth. Other groups of organisms precipitate calcium carbonate, altering the alkalinity of the water and its ability to dissolve carbon dioxide. These reasons are the motivation for considering model structures with multiple algal taxa with biogeochemically distinct effects.

A biogeochemical model of organic matter production will be coupled to an eddy-resolving ocean general circulation model of the North Atlantic driven by synoptic wind forcing. The main points of interest will be the effects of higher resolution in space and time on biogeochemical cycles, the physical mechanisms controlling oceanic biological production and tracer transport, and the ability of the model to reproduce observed properties of the marine system.

The study of observed carbon and nutrient distributions will be continued with a new analysis of the nitrate and total carbon distribution that aims to identify the components of these tracer distributions that result from denitrification and the anthropogenic transient, respectively.

5.5.3 Measurements

<i>R. Key</i>	<i>C. Sabine</i>
<i>G. McDonald</i>	<i>J. Sarmiento</i>
<i>R. Rotter</i>	

ACTIVITIES FY95

Members of the Ocean Tracer Laboratory made carbon system measurements on World Ocean Circulation Experiment (WOCE) cruises to the Indian Ocean beginning in December 1994. An underway pCO₂ measurement system, which will be on board the ship for almost 13 continuous months, has performed well and has shown excellent agreement with another independent measurement system as well as calculated pCO₂ from carbon system measurements. The Ocean Tracer Lab also had responsibility for all of the carbon system measurements on leg I9N which went from Fremantle, Australia to Colombia, Sri Lanka. During this leg approximately 2600 (55% of the total samples collected) discrete water samples were analyzed for both total CO₂ and total alkalinity.

An analysis of carbon system parameters from a WOCE cruise to the South Pacific details the different contributions of heat and water fluxes and new production to the observed changes in $p\text{CO}_2$ along a section. The most important factors affecting $p\text{CO}_2$ along the sections are heat flux and new production, which oppose each other in their effect on $p\text{CO}_2$ along the section.

PLANS FY96

The first part of FY96 will see the completion of field work for the WOCE Indian Ocean program. The underway $p\text{CO}_2$ system will continue, and new carbon system measurements will be obtained on leg I10 in November. By the time the Indian Ocean work is completed, members from the lab will have completed a total of approximately 20 man-months at sea over 13 calendar months.

5.6 NITROUS OXIDE

J. Sarmiento *P. Suntharalingham*

ACTIVITIES FY95

The ocean is a significant source of atmospheric nitrous oxide (N_2O), but large uncertainties attend the estimated magnitude of this source, its spatial and temporal distribution, and the processes involved in marine N_2O formation. These issues have been investigated using two separate approaches. The first involves the development of a model of the oceanic N_2O cycle embedded in an ocean general circulation model. N_2O is treated as a non-conserved tracer, and is subject to biological sources and sinks as well as gas-exchange at the ocean surface. The modeled N_2O source function is based on observed correlations below the euphotic zone between excess N_2O and oxygen utilization. Simulation results indicate that this model successfully reproduces the large-scale features of the observed distribution. The estimated N_2O flux to the atmosphere is 5 Tg N per year.

The second approach involves the use of existing oceanic N_2O observations to construct maps of surface N_2O concentrations, and to derive estimates of the global oceanic N_2O flux. Correlations between surface N_2O and local physical and biological properties have been investigated, and a variety of statistical models ranging from simple linear regressions to more sophisticated curve fitting techniques have been employed in estimating the N_2O distribution. The flux of N_2O to the atmosphere estimated from the mapped N_2O distribution is 3.8 to 4.0 Tg N per year. This result, and the results of the model simulation, are within the IPCC estimated ocean flux of 1-5 Tg N per year, out of an implied total global source of 13-20 Tg N per year.

PLANS FY96

Work will continue on the ocean N₂O model. The N₂O source function will be refined to reflect observational results indicating the dependence of oceanic N₂O formation and consumption processes on local oxygen concentration.

5.7 OCEAN CIRCULATION TRACERS

*H. Figueroa R. Rotter
R. Key J. Sarmiento
G. MacDonald J.R. Toggweiler*

ACTIVITIES FY95

For the past 4 years, the Ocean Tracer Laboratory has been the principal U.S. laboratory responsible for collection and interpretation of radiocarbon samples in the WOCE Hydrographic Program. The laboratory participated in the WOCE survey of the Indian Ocean and collected large volume samples for standard beta counting techniques and small volume samples for analysis by accelerator mass spectrometry.

The Ocean Tracer Lab continues to make major contributions to radiocarbon studies in the World Ocean Circulation Experiment. The radiocarbon program has responsibility for all of the Indian Ocean WOCE legs except for the first. This has entailed one person on legs I9N, I8N5E, I3, I4I5W, and I7N for a total of 8 man-months at sea since the beginning of 1995.

A model study of the mechanisms of thermocline ventilation in the North Atlantic was completed (ad).

PLANS FY96

The radiocarbon sampling program will continue to sample all of the remaining legs in the Indian Ocean program (I1, I2 and I10). Finally, during May and June, 1996, samples for radiocarbon analysis will be collected from WOCE Antarctic section S4 between Capetown and Fremantle. The radiocarbon samples will be returned to the AMS facility at WHOI for analysis. Interpretation of the most extensive ocean radiocarbon data set will begin as measurements are completed.

6. OBSERVATIONAL STUDIES

GOALS

To determine and evaluate the physical processes by which the earth's climate and the atmospheric and oceanic general circulations are maintained in the mean, and by which they change from year to year and from decade to decade, using all available observations.

To compare results of observational studies with similar diagnostic studies of model atmospheres and model oceans developed at GFDL and thereby develop a feedback to enhance understanding in both areas.

6.1 ATMOSPHERIC DATA PROCESSING

<i>M. Bauer</i>	<i>A. Raval</i>
<i>J.R. Lanzante</i>	<i>M. Rosenstein</i>
<i>A.H. Oort</i>	<i>B.J. Soden</i>

ACTIVITIES FY95

6.1.1 Processing of Daily Upper-Air Data

The TD54 radiosonde dataset, which consists of early upper-air observations (~ mid-1940s to early 1960s card deck data), was returned in a reorganized and reformatted version to Roy Jenne at NCAR, together with information regarding the detailed characteristics of the formats, problems encountered, and corrections made. This effort represents the culmination of years of intense efforts on the part of the Observational Studies Group. This ~ 4 GB dataset consists of over five million individual observations and is intended for incorporation into the database being used in the NMC/NCAR Reanalysis Project.

A set of new, previously unavailable twice-daily Chinese radiosonde data (T , T_d and Z) for the period 1954-57 was reformatted. Copies of the data were provided to R. Jenne at NCAR and E.C. Kung at the University of Missouri. These data will be included in the NCAR data archive and are also to be used in the NMC Reanalysis Project.

6.1.2 Comparison of Daily Radiosonde and Satellite Measures of Upper Tropospheric Humidity

A project has been initiated to compare the statistical characteristics of daily observations of radiosonde and satellite upper tropospheric humidity measurements. Radiosonde instruments are known to have particular difficulty in measuring humidity in very dry conditions, whereas satellite humidity measurements are hindered by the presence of extensive cloud cover, which are typically associated with very moist conditions. This work addresses the geographical and seasonal aspects of these relative observing biases using a limited global network of "high quality" radiosonde stations (*i.e.*, the network of Jim Angell) and the TIROS (Television and InfraRed Observational Satellite) Operational Vertical Sounder (TOVS) data from a single satellite (NOAA10) during the period 1987-91. Initial results suggest that the satellite "clear sky" bias is most pronounced in the deep tropical convective zones and appears to "follow" the seasonal north-south migration of these zones.

6.1.3 Processing and Distribution of Monthly Mean Rawinsonde Data

Many groups inside and outside the U.S. have requested and received copies of various parts of the GFDL observational data archives, mainly for use in climate and climate-change related research. Copies of one of the largest data archives, the "GFDL Monthly Rawinsonde Station Statistics" for the period May 1958-December 1989, were sent to the National Climatic Data Center for internal use and for distribution to other groups such as NCAR and Atmospheric Environmental Research, Inc.

The basic programs to assess and error-check the twice daily rawinsonde observations for the post-1989 period have been successfully rewritten for the Cray YMP supercomputer, and the follow-up program to compute monthly station statistics and prepare them for mapping through use of the GFDL interpolation algorithm, ANAL95, has been completed.

Development of the objective analysis scheme for global monthly mean fields, called ANAL95, has continued. The approach which was finally chosen is very simple, elegant, and easy to use, and reproduces the results from the old (ANAL68) scheme very well (a key requirement for updating the existing climate archives). Many tests were performed to validate and assess the sensitivity of the analyses to the choice of parameters, such as the radius of influence for each station and the degree of smoothing. The results were also compared with independent analyses from the ECMWF. A "Guide for the Use of ANAL95" has been written which describes the workings of ANAL95 as well as the validation tests performed. All these developments have prepared the way for updating the GFDL climate archives for the period after 1989.

PLANS FY96

The comparison between daily radiosonde and satellite observations of upper tropospheric humidity will continue in an effort to document and better quantify each set's relative measurement biases.

Attempts will be made to identify and adjust both sets of observations in order to eliminate or reduce the influence of artificial (*i.e.*, non-climatic) changes. Revised trend estimates will be made and consistency between the radiosonde and satellite observations will be assessed.

Collaboration will begin with Dian Gaffen of the Air Resources Laboratory (ARL) and Ted Habermann of the National Geophysical Data Center (NGDC) to combine advanced statistical and data analysis techniques with a unique compilation of "meta-data" describing historical changes in global radiosonde instruments recently created at ARL in an attempt to improve the quality of upper air temperature measurements and subsequently to estimate temperature trends.

The "Guide for the Use of ANAL95" will be put on the World Wide Web to make it available for wider use in the scientific community. ANAL95 is a flexible scheme for constructing global horizontal analysis at a regular longitude-latitude grid from irregularly spaced monthly (or longer term) mean station values.

The GFDL monthly-mean rawinsonde statistics and global climate analyses of the troposphere and lower stratosphere will be updated and extended through the period 1990 through 1994, providing a continuous set of analyses from May 1958 through December 1994.

6.2 CLIMATE OF THE ATMOSPHERE

<i>M.W. Crane</i>	<i>J.P. Peixoto*</i>
<i>G. Gahrs</i>	<i>P. Peng</i>
<i>J.R. Lanzante</i>	<i>M. Rosenstein</i>
<i>N.-C. Lau</i>	<i>B.J. Soden</i>
<i>M.J. Nath</i>	<i>D.-Z. Sun</i>
<i>A.H. Oort</i>	<i>J.J. Yienger</i>

**University of Lisbon, Portugal*

ACTIVITIES FY95

6.2.1 Radiosonde and Satellite Observations of Upper Tropospheric Water Vapor and Its Trends

Comparison of radiosonde and satellite climatologies of upper tropospheric water vapor for the period 1979-1991 revealed significant differences in the regional distribution of upper tropospheric relative humidity (zh). These discrepancies exhibited a distinct geographical dependence which was found to be the result of differences in radiosonde instrumentation used by different countries (Fig. 6.1). Specifically, radiosondes equipped with goldbeaters skin humidity sensors (found primarily in the former Soviet Union, China and eastern Europe) report a systematically moister upper troposphere relative to the satellite observations, whereas radiosondes equipped with capacitive or carbon hygristor sensors (found at most other locations) report a systematically drier upper troposphere. The bias between humidity sensors was found to be roughly 15-20% in terms of the relative humidity, being slightly greater during summer than during winter and greater in the upper troposphere than in the middle troposphere. However, once the instrumentation bias is accounted for, regional variations of satellite and radiosonde upper tropospheric relative humidity were shown to be in good agreement.

The impact which the limited spatial coverage of the radiosonde network has upon the moisture climatology was examined and found to introduce systematic errors of 10-20% relative humidity over data sparse regions of the tropics. One implication of this finding is that the present radiosonde network may lack sufficient coverage in the eastern tropical Pacific to adequately detect ENSO-related variations in upper tropospheric moisture.

Upper Tropospheric Humidity

JJA 1989

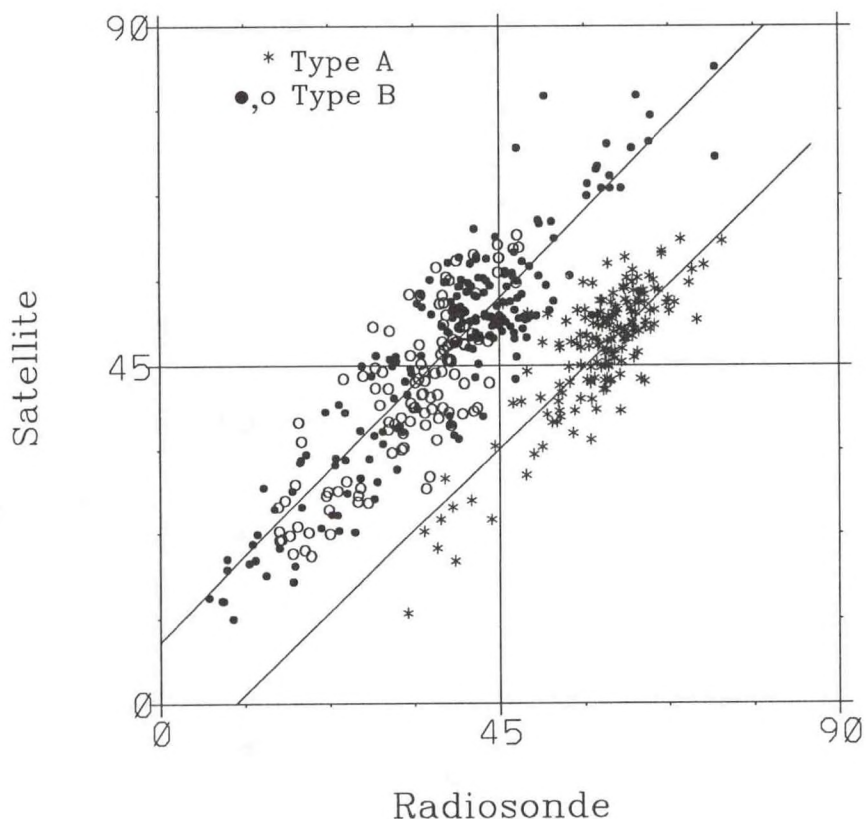


Fig. 6.1 Scatter plot of radiosonde versus satellite Upper Tropospheric Humidity categorized by sensor type for June-August 1989. Stars indicate goldbeaters skin sensors (Type A). Filled circles denote capacitive humidity sensors and open circles denote carbon hygristor sensors (Type B). The diagonal lines represent least-squares fits calculated separately for Type A and Type B sensors, and show that the two types of sensors yield consistently different measurements, explaining some of the regional differences in "observed" upper tropospheric humidity.

Humidity measurements from the global network of radiosonde stations and TOVS from 1979-91 were used to estimate linear trends in upper tropospheric humidity (UTH). In view of concerns regarding the quality of these data, techniques drawn from the fields of resistant, robust and nonparametric statistics (x_r , xx) have been employed to minimize the effects of outliers, non Gaussian data, etc. Straightforward application of linear trend analysis to the radiosonde and satellite observations resulted in what appear to be rather large, significant trends over many geographical areas. However, the lack of consistency between the radiosonde and

satellite trend patterns suggested that there may be other effects which were not taken into account.

In the case of radiosonde data, the trends were often observed to vary considerably over short distances and sometimes change dramatically across political boundaries. In addition, examination of selected time series suggests that apparent trends are often characterized by what appear to be abrupt changes or discontinuities. These discontinuities may be due to changes in radiosonde instrumentation and recording practices.

A time series of a TOVS-based middle tropospheric humidity (MTH) index, which has considerable overlap in the vertical with the UTH index, was also employed in the trend analyses. Examination of the time series and objective statistical tests suggest that the satellite-derived trends are due in large part to discontinuities which sometimes occur when one satellite is "retired" and replaced by another in the same series. So, much of the "observed" trend may not be real.

6.2.2 15-Year Global Climatology of Relative Humidity

In spite of the shortcomings, limitations, and errors of the existing radiosonde network, it has nevertheless been possible to assemble a reliable description of the main characteristics of the relative humidity distribution in the atmosphere (zp). This new information is very useful in assessing GCM and convective parametrization results.

The global distribution of relative humidity at various levels show that the distributions are not zonally uniform, and extrema are observed at all latitudes. The dry subtropical belts are very well defined, and the ocean-land contrast is also quite apparent. The general pattern of relative humidity is similar at all levels, but its magnitude decreases with altitude. The zonal mean profiles of relative humidity at various levels show that the relative humidity decreases rapidly with height in the lower troposphere, but at a slower rate above 700 mb. The profiles also show a well-defined maximum in the equatorial zone and minima around 30°N and 30°S. The land-sea contrast and variations related to the orographic relief are very clear. The seasonal analyses are not substantially different from the annual analyses, but are slightly shifted toward the summer pole.

The saturation deficit and the dew point depression have also been evaluated. Cross sections of the saturation deficit show that the maxima are found in the middle to lower troposphere at subtropical latitudes (consistent with the relative humidity minima mentioned above), being most intense in the Northern Hemisphere during the summer season.

The temporal variability of the relative humidity due to transient eddies exhibits a bimodal structure with a midlatitude maximum near the 700 mb level in each hemisphere. The stationary eddy distributions are less pronounced than the transient ones and do not change substantially from one season to another.

The current climatology was verified using several independent sources of humidity data. COADS data was used to obtain independent analyses of the relative humidity over the ocean surface. Satellite observations from the Stratospheric Aerosol and Gases Experiment (SAGE) were used for validation at the 300 mb level. Furthermore, the results have also been compared with operational analyses of relative humidity by the ECMWF. Given the obvious connection between relative humidity and cloudiness, a recent cloud climatology for various types of clouds was also used as a consistency check. In each case, the comparison provided increased confidence in the current rawinsonde-based representation of the mean climatology of relative humidity in the atmosphere.

6.2.3 Long-Term Variability in the Hadley Circulation and Its Connection to ENSO

The variability in the strength of the tropical Hadley cells has been investigated using the GFDL global upper air wind analyses for the period January 1964-December 1989 (yq). Several measures of the intensity of the zonal-mean cells have been analyzed, but the main focus has been on the maximum in the meridional stream function in the northern and southern tropics. The stream function was computed from the observed monthly-mean cross sections of the zonal-mean meridional wind component. Significant seasonal variations have been found in the strength, latitude, and height of the maximum stream function for both Hadley cells, as illustrated in Fig. 6.2. Significant correlations have also been found between these two cells and the El Niño Southern Oscillation phenomenon. During episodes of warm sea surface temperature anomalies in the eastern equatorial Pacific (El Niño), the cells tend to strengthen, while during episodes of cold anomalies they tend to weaken. Furthermore, the anomalies in the strength of the Hadley cells are strongly and inversely correlated with the anomalies in the strength of the Walker Oscillation. These results represent important new observational evidence of the role of Hadley and Walker Oscillations in the general circulation.

6.2.4 Simulation of Atmospheric Variability in Very Long GCM Integrations

As part of the NOAA/Universities collaborative effort to understand the nature of atmospheric variability using GCM tools, an 100,000 day experiment was conducted using climatological SST and perpetual January conditions. The large sample size provided by this long-term experiment allowed for the computation of stable statistics and detailed descriptions of various atmospheric fluctuations with long time scales. Diagnosis of the model output revealed the existence in the model atmosphere of slowly-varying phenomena with well-defined spatial patterns and

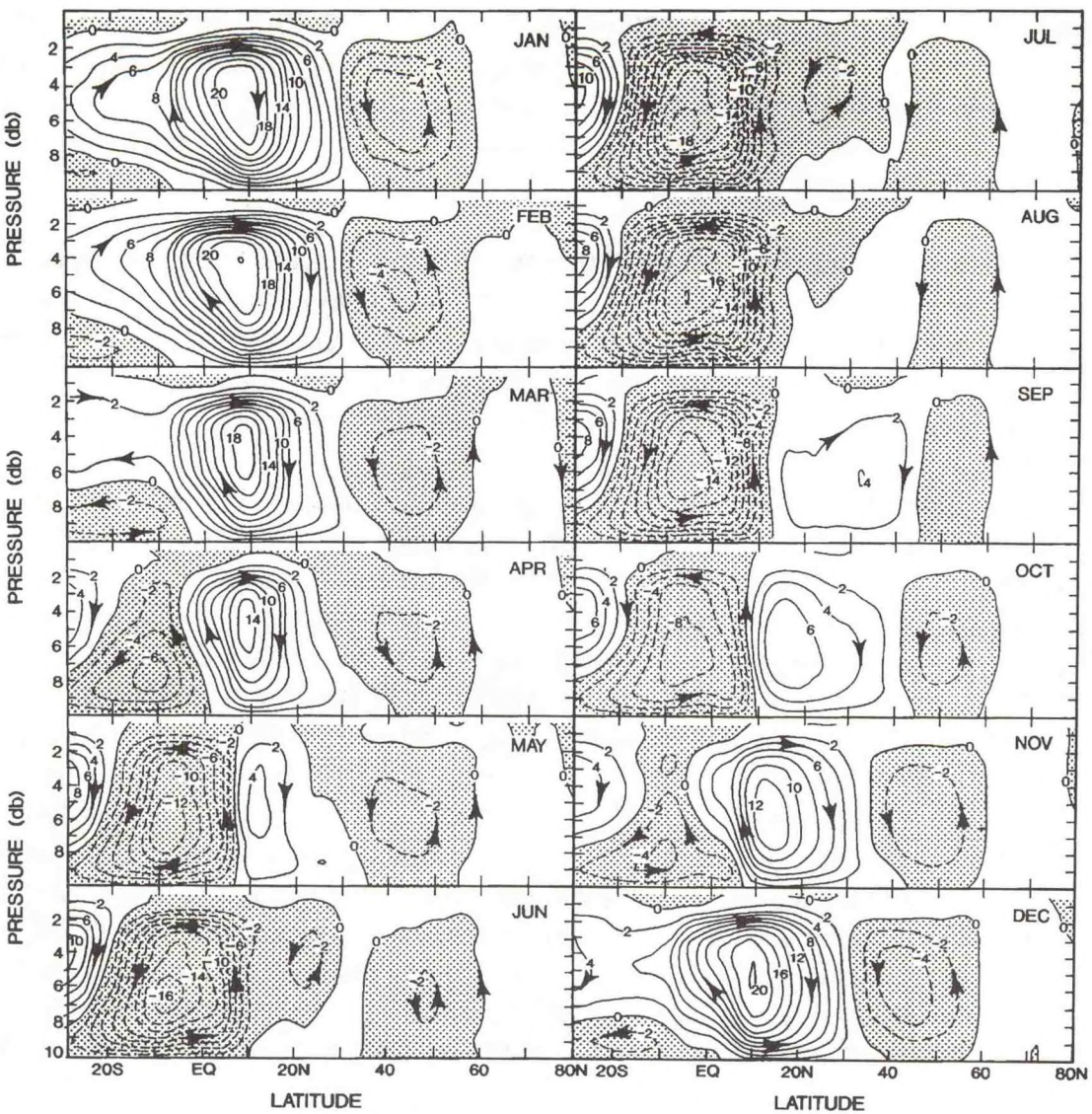


Fig. 6.2 Annual cycle of the zonal-mean meridional stream function ψ in units of $10^{10} \text{ kg s}^{-1}$ for the 1964-89 mean conditions. Over the entire domain 30°S - 80°N the stream function was computed directly from the observed mean meridional component of the wind, $[\mathbf{v}]$, with the only imposed constraint being that vertically integrated mass transport vanishes to ensure conservation of mass. The results show the well-known growth of the Hadley cell in the winter hemisphere and its decline in the summer hemisphere, as well as the (previously unknown) seasonal cycle in the midlatitude Ferrel cell with a maximum in northern winter.

temporal evolution, some of which are similar to observed features in the extratropical Northern Hemisphere. Particularly noteworthy is the existence in the model atmosphere of a mode of variability with a strong zonal symmetry and a probability distribution function of temporal coefficients of this mode exhibiting pronounced

skewness. Investigations have begun on the extent to which this phenomenon can be attributed to the nonlinear interactions between the slowly varying component of the atmospheric flow and the high-frequency synoptic-scale transient disturbances. Another feature of interest is the occurrence in the simulation of well-defined westward propagating waves in the high latitudes of the Northern Hemisphere. The characteristic period and spatial pattern of these waves are in agreement with those deduced from observational data.

A second integration of 40,000 day duration, in this case allowing for interaction between the atmosphere and a simple mixed layer ocean model inserted in extratropical grid points, has been completed. Comparison of the variability statistics for this run with those for the 100,000 day run described above will clarify the role of midlatitude air-sea interaction on atmospheric variability.

It has been found that a large fraction of upper tropospheric zonal mean zonal wind variability on inter-monthly or longer time scales can be explained by a few leading modes. To what extent these modes are related to variability of stationary eddies has not yet been fully resolved. In order to study these problems, winter data from a 100-year GCM experiment without interannual variability in SST forcing has been examined. Several coherent modes of the zonal mean and eddy wind fields were found using various statistical techniques, but these could explain only a small portion of the eddy variability. A steady linear barotropic model was then used to diagnose these relationships, and two distinct processes accounting for the linkage between the zonal mean and eddy fluctuations were suggested. The first possibility is that some eddy patterns are associated with local zonal wind anomalies, which in turn lead to perturbations in the zonal mean zonal wind. The other possibility is that zonal wind anomalies give rise to eddy anomalies through interaction with the climatological stationary eddies. The contribution of topographic forcing accompanying the anomalous zonal wind to the genesis of the eddies was found to be weak.

6.2.5 Hydrological Cycle Over Deserts

A preliminary study of the hydrological budget over the Sahara desert region, based on the new four-times daily NMC/NCAR Reanalysis for the years 1985-1989, shows an excess of evaporation over precipitation, confirming the long-standing, but controversial, results of Starr and Peixoto¹. The present result, that the Sahara desert region may indeed be a source of water vapor, implies that there must be either substantial subsurface flows of water into the region or a depletion of "fossil" water from below the desert, as speculated by Starr and White.

1. Starr, V.P., and J.P. Peixoto, On the global balance of water vapor and the hydrology of deserts, *Tellus*, 10, 188-194, 1958.

PLANS FY96

Investigations of the radiosonde and satellite climatologies of upper tropospheric water vapor will continue, concentrating on a comparison of trends over the last 15 years.

The origin of the highly skewed, zonally-symmetric mode appearing in the extended GCM integrations will be further investigated by examining the dependence of the mean flow-eddy interactions on the polarity of the low-frequency anomaly. The temporal evolution of various quasi-stationary and propagating modes in the model atmosphere will be documented using trajectories of representative indices of such spatial structures in multi-dimensional reference frames, such as those corresponding to the leading principal components.

Additional very long GCM runs will be conducted by prescribing SST anomalies in the tropical oceans having similar autocorrelation statistics as the observations, but also allowing the atmospheric responses thus generated to interact with simple mixed layers in the extratropical oceans.

6.3 AIR-SEA INTERACTIONS

<i>I.M. Held</i>	<i>A.H. Oort</i>
<i>J. Lanzante</i>	<i>P. Peng</i>
<i>N.-C. Lau</i>	<i>M. Rosenstein</i>
<i>M.J. Nath</i>	

ACTIVITIES FY95

6.3.1 Lag Relationships Involving Tropical SSTs

A long historical record (1870s-1980s) of tropical SST data from the Comprehensive Ocean-Atmosphere Data Set (COADS) was used to examine the lag relationships between different locations in the global tropics which occur primarily in the context of El Niño-Southern Oscillation (ENSO) variability (zv). Application of Complex Principal Component (CPC) analysis suggested a number of relationships which were confirmed using other simpler techniques. The primary relationships were found in different sub-samples of the period of record as well as in a different source for the SSTs (Global Ocean Surface Temperature Atlas, or GOSTA). These analyses confirm, as reported elsewhere in the literature, that ENSO-related SST anomalies appear first in the eastern tropical Pacific and then spread westward into the central tropical Pacific. Subsequently, SST anomalies of similar sign appear in certain areas in the tropical Indian and western tropical North Atlantic. These more remote anomalies, which typically appear about 6 months after the initial warming, are similar

to the response found in GCM experiments examined by Lau and Nath (1256). Furthermore, it was found that the remote response in the Atlantic is more variable than for the other relationships; in other words, the Atlantic response does not always occur as expected, but those involving the Pacific and Indian Oceans almost always follow a similar sequence during the ENSO cycle.

6.3.2 Role of the Atmospheric Bridge in Linking Tropical Pacific ENSO Events to Extratropical SST Anomalies

A study (zy) has been completed on the role of the atmospheric circulation as a "bridge" between sea surface temperature (SST) anomalies in the tropical Pacific and concomitant changes in the midlatitude northern oceans. The key processes associated with this atmospheric bridge are described using output from four independent GCM simulations subjected to month-to-month SST variations observed in the tropical Pacific during the 1946-88 period. (This set of experiments will be referred to as the "TOGA" runs.) During prominent SST episodes in the tropical Pacific, extratropical perturbations in the simulated atmospheric temperature, humidity, and wind fields lead to changes in the latent and sensible heat fluxes across the air-sea interface at the midlatitude oceans. These anomalous fluxes, in turn, result in warming or cooling of the underlying ocean, as illustrated in Fig. 6.3.

The fidelity of the atmospheric bridge mechanism has been evaluated by driving a motionless, 50-m deep oceanic mixed layer model at individual grid points with the local surface fluxes generated in the TOGA runs. The negative feedback of the mixed layer temperature anomalies on the imposed flux forcing has been taken into account by a linear damping term with a five month dissipative time scale. The results demonstrate that this simple system is capable of reproducing the basic spatial and temporal characteristics of the observed SST variability in the North Pacific and western North Atlantic.

The two-way air-sea feedbacks associated with the atmospheric bridge were investigated by performing four additional 43-year runs as modified versions of the TOGA experiment: instead of prescribing climatological SST conditions outside the tropical Pacific, these new "TOGA-ML" runs predict the ocean temperature by allowing the atmosphere to interact fully with the same mixed layer model mentioned above. Spectral and autocorrelation analyses performed on the surface flux and mixed layer temperature data indicate that an analogy can be drawn between midlatitude ocean-atmosphere interaction and the stochastic framework of a first-order Markov process, with the red-noise response of mixed layer temperature being driven by the white-noise atmospheric forcing in the presence of linear damping.

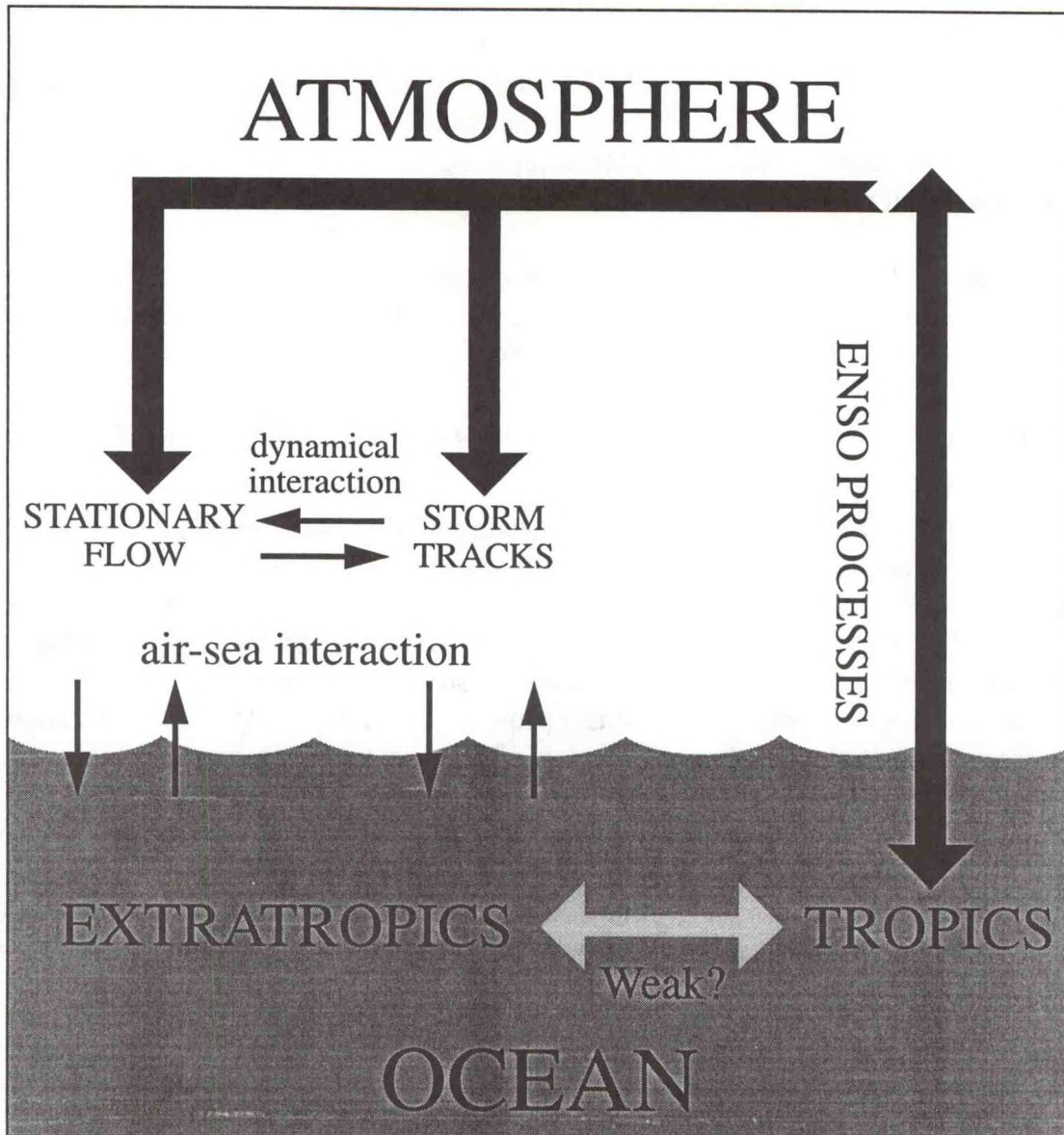


Fig. 6.3 Schematic diagram depicting role of the atmospheric "bridge" in linking SST variation in the tropical and extratropical oceans. The bold dark arrows illustrate the pathways through which tropical SST anomalies exert remote influences on the midlatitude atmosphere. The resulting atmospheric fluctuations, in turn, drive oceanic anomalies in the extratropics through local air-sea interaction.

The amplitude of near-surface atmospheric anomalies appearing in the TOGA-ML runs is significantly higher than that in the TOGA runs. This finding implies that, in the TOGA-ML scenario, the midlatitude oceanic responses to atmospheric driving could, in turn, exert positive feedbacks on the atmosphere, thereby reinforcing the air-sea coupling. The enhanced mutual atmosphere-ocean interactions operating in

TOGA-ML were observed to lengthen the typical duration of persistent meteorological episodes in that experiment. A comprehensive survey was conducted of this persistence time scale as simulated in TOGA, TOGA-ML, and several other experiments subjected to prescribed SST forcing at various sites. Model scenarios in which observed tropical Pacific SST anomalies act in conjunction with SST perturbations in middle latitudes (either prescribed or predicted) are seen to produce the highest frequency of persistent events.

A review (zx) has been completed summarizing the current understanding of the relative roles of tropical SST anomalies, extratropical SST anomalies and internal atmospheric variability in interannual fluctuations of the coupled air-sea system.

6.3.3 Ensemble GCM Experiments Subjected to SST Anomalies for Specific ENSO Events

As part of the collaborative project among NOAA and university investigators to diagnose the impact of boundary conditions on atmospheric variability, an ensemble of 16 GCM runs has been created for each of the 1968-73, 1981-83 and 1986-89 ENSO cycles. For each episode, the individual members of the ensemble are initiated from independent atmospheric conditions, but are subjected to the same evolution of the near-global SST anomaly pattern. The model output from this suite of integrations exhibits a notable degree of variability among the individual samples for a given ENSO event. The dominant mode of inter-sample variability appears related to the principal mode of internal variability of the model atmosphere, as deduced from a 100-year control run subjected to climatological SST conditions. The impact of variations in the zonal mean flow and tropical heat sources and sinks on such inter-sample variability have been investigated using both statistical analysis and linear stationary wave modeling.

PLANS FY96

The physical mechanisms contributing to prolonged persistence and enhanced frequency of anomalous episodes due to ocean-atmosphere coupling in the extratropics will be identified by diagnosing the day-to-day variations of the relevant meteorological and oceanographic parameters as simulated in the TOGA-ML experiment during selected outstanding events.

The dynamical origin of the inter-sample fluctuations in the model response to a given SST scenario will be investigated. The relative importance of internal variability of the model atmosphere and changes in the thermal forcing originating from the tropics will be assessed.

6.4 SATELLITE DATA

M.W. Crane
L.P. Dritt
N.-C. Lau

A.H. Oort
A. Raval
B.J. Soden

ACTIVITIES FY95

6.4.1 Relationships Between the Formation of Stratiform Clouds and the Ambient Circulation

The occurrence of stratus cloud decks over the eastern subtropical oceans, as identified from daily cloud analyses produced by the International Satellite Cloud Climatology Project (ISCCP), has been found to be strongly correlated with prominent changes in the large-scale atmospheric circulation, as inferred from wind, pressure, temperature and humidity analyses produced by the European Centre for Medium-Range Weather Forecasts (ECMWF). Of particular interest is the coincidence of enhanced subtropical maritime stratus cloud cover with strong low-level cold advection, increased surface wind speed, increased subsidence, and strengthening of the static stability in the lower troposphere. The change in static stability is primarily governed by the temperature change (due to subsidence) at 700 and 850 mb, rather than by temperature change near sea level. These results offer a comprehensive and objective description of the favorable meteorological environment for the formation of maritime boundary-layer clouds. The physical consistency among findings based on the independent ISCCP and ECMWF datasets lends credence to the reliability of satellite cloud products for studying various types of circulation systems.

6.4.2 Circulation Features Associated With Propagating Deep Convective Clouds in Subtropical Frontal Zones

The prevalent modes of variability of deep convective cloud cover (as depicted in the ISCCP archives) in the summertime subtropical frontal zones in East Asia, South America/South Atlantic and South Pacific have been documented using extended empirical orthogonal function (EEOF) analysis. The leading EEOF modes of deep convection in these regions appear as eastward propagating wave-like disturbances with characteristic spatial shapes and time scales. The atmospheric circulations (as deduced from the concurrent ECMWF analyses) exhibit well-defined phase relationships with the convective cloud bands. Such relationships are helpful in understanding the synoptic processes associated with heavy rain episodes in the subtropical frontal zones, such as the Mei-Yu (Plum Rain) phenomena in China during late spring and early summer.

6.4.3 Patterns of Cloud Cover in Midlatitude Cyclones

Using composite techniques similar to those developed in a recent study of the organization of the satellite-derived cloud field in synoptic scale circulation systems (1309), synoptic cloud reports from surface observers have been analyzed to determine the spatial distribution of various cloud types associated with wintertime cyclones in the extratropical North Atlantic. The findings are consistent with those deduced from satellite measurements, suggesting that data from space-borne instruments might be reliably used to characterize atmospheric structures associated with synoptic disturbances, especially in otherwise data-sparse regions. Diagnosis of the surface observations of precipitation and cloud types also indicates the existence of spatial displacements between centers of maximum precipitation and centers of maximum cloudiness.

PLANS FY96

Cloud patterns (as deduced from both satellite and surface datasets) associated with disturbances over land will be contrasted against the corresponding patterns over ocean. Wintertime and summertime cloud patterns accompanying cyclonic disturbances will also be compared.

The fine structure of cloud cover associated with various types of cloud regimes, including stratus decks, subtropical frontal zones, tropical continental convection and extratropical baroclinic cyclones, will be explored using high-resolution (in space and time) satellite cloud products.

7. HURRICANE DYNAMICS

GOALS

To understand the genesis, development and decay of tropical disturbances by investigating the thermo-hydrodynamical processes using numerical simulation models.

To study small-scale features of hurricane systems, such as the collective role of deep convection, the exchange of physical quantities at the lower boundary and the formation of organized spiral bands.

To investigate the capability of numerical models in predicting hurricane movement and intensity, and to facilitate their conversion to operational use.

7.1 HURRICANE PREDICTION SYSTEM

*M.A. Bender R.E. Tuleya
Y. Kurihara C.-C. Wu*

ACTIVITIES FY95

7.1.1 The 1994 Hurricane Season

The GFDL Hurricane Prediction System was run at the National Center for Environmental Prediction (NCEP, formerly the National Meteorological Center) in a parallel test mode during the 1994 hurricane season on a supercomputer Cray Model C-90 (A94/P95). Predictions were performed for 60 Atlantic cases and 148 eastern/central Pacific cases of tropical cyclones at all development stages, from tropical depressions to hurricanes. Also, experimental predictions were conducted for 19 cases of typhoons in the western Pacific. Average track forecast errors in the Atlantic and the eastern/central Pacific basins are presented and compared to other hurricane models in Table 7.1. The GFDL system performed very well up to 36 hours and was superior to all other models at 48 and 72 hours. In the case of Hurricane Gordon, a storm with a complicated track, it successfully predicted, three days in advance, the storm's westward movement through the Florida Strait and the subsequent recurvature to the northeast and across the Florida peninsula. The recurvature of Hurricane Rosa and its landfall on the west coast of Mexico was also

**TABLE 7.1 Hurricane track forecast errors in the 1994 hurricane season.
Average errors (in km, compared with operational positions)
for all cases including tropical depressions.**

Atlantic basin

Model	GFDL	VBAR	QLM	BAMM	A90L	CLIPER
12h (60 cases)	111	102	111	110	113	124
24h (53 cases)	186	185	220	194	201	258
36h (45 cases)	248	243	293	294	251	359
48h (39 cases)	322	348	415	442	348	491
72h (28 cases)	464	581	822	844	564	746

Eastern/Central Pacific basin

Model	GFDL	QLM	BAMM	P91L	CLIPER
12h (148 cases)	82	94	93	86	78
24h (138 cases)	146	162	169	147	149
36h (126 cases)	198	247	237	206	232
48h (111 cases)	249	340	303	256	292
72h (77 cases)	351	460	451	360	424

accurately predicted. In this case the newly implemented storm tracking algorithm over high mountain regions functioned well.

Extensive post season analysis was carried out. Despite the demonstrated skill of the GFDL forecast system, some biases were revealed in the storm track and intensity. In particular, an overestimation of the intensity of weak storms suggests a need for some improvement in the model initialization method.

7.1.2 The 1995 Hurricane Season

In Fig. 7.1, the average track forecast errors of the GFDL system for all 282 cases in 1993 and 1994 seasons are compared against the previously operational QLM model. Given its strong performance during the 1994 hurricane season, the GFDL system was adopted as the official hurricane forecast model at the NCEP for the 1995 hurricane season.

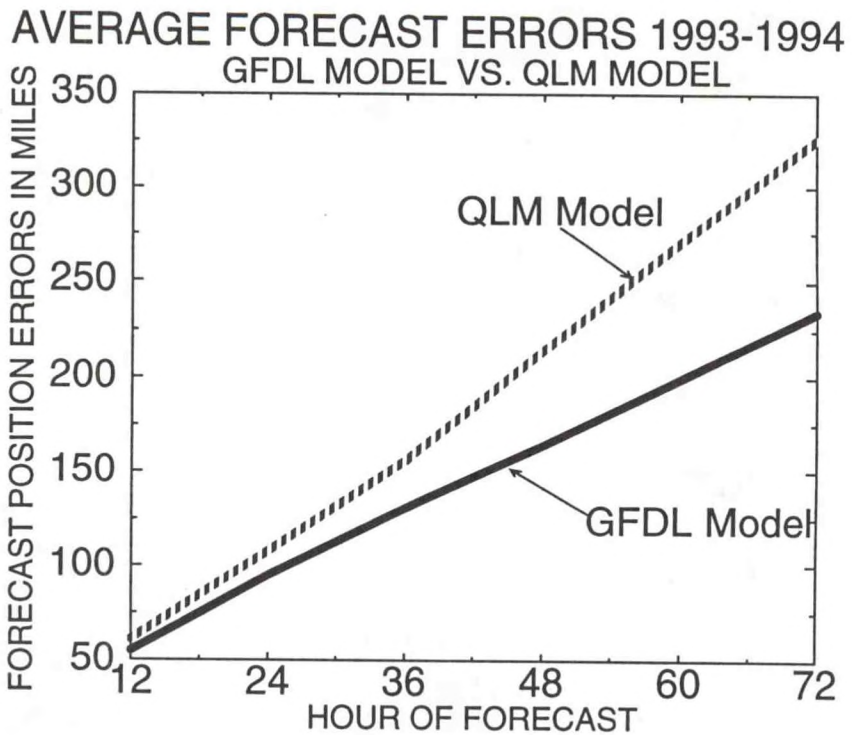


Fig. 7.1 Comparison of average forecast position errors (in miles) between the QLM model and the GFDL model. Errors for 282 cases in the Atlantic and eastern/central Pacific in the 1993 and 1994 hurricane seasons are averaged.

Implementation of the system as a fully operational tool involved extensive coding changes in order to conform with operational requirements. The hurricane model, originally developed as a research tool, was successfully transferred to NCEP as a fully operational prediction system that includes data input from the National Hurricane Center (NHC) and from the NCEP global models, model initialization by vortex specification, and delivery of forecast results to NHC. Fig. 7.1 indicates the expected average improvement in the dynamical model guidance provided by NCEP to NHC.

Performance of the GFDL system at NCEP has been carefully monitored and thus far in the 1995 hurricane season, the prediction skill of this system has been superior to other models. The same system has also been in use for experimental predictions of typhoons in the western Pacific.

A cooperative effort is underway to run the GFDL system at the Fleet Numerical Meteorology and Oceanography Center (FNMOC), U.S. Navy, at Monterey. Results from this work are expected to yield useful information regarding the sensitivity of

predictions to the analysis used to define the initial conditions, an issue relating to the potential use of ensemble forecasts.

PLANS FY96

Performance of the GFDL system in the second half of the 1995 hurricane season will be carefully monitored and post-season analysis of the forecast results will be conducted. Work to upgrade the prediction system will begin with the formulation of a new initialization technique to specify a more realistic vortex.

7.2 OBSERVING SYSTEM

*S.J. Lord** *R.E. Tuleya*

**National Center for Environmental Prediction*

ACTIVITIES FY95

Previous studies using the GFDL multiply-nested movable mesh (MMM) hurricane model have demonstrated a positive impact of Omega Dropwindsondes (ODW) observations on tropical cyclone track forecasts. Two additional cases of Hurricane Emily (1993) and one additional case of Andrew (1992) were examined over the past year. Results of the track prediction for these new cases also showed a positive impact of ODW (au).

The impact of the ODW observations on intensity forecasts using the GFDL model was also examined and the results show a small positive impact, especially for the two to three day period. However, the validity of model physics and accuracy of vortex initialization are still serious problems in the effort to improve the skill of intensity forecasts.

PLANS FY96

The numerical results obtained from the ODW impact study will be finalized and will include an analysis of the case-to-case variability of ODW impact.

7.3 BEHAVIOR OF TROPICAL CYCLONES

ACTIVITIES FY95

7.3.1 Evolution of Tropical Cyclones

P.J. Reas *R.E. Tuleya*

Changes in the structure of tropical cyclones at landfall were studied through analysis of simulation experiments for the cases of Hurricane Hugo (1989) and Bob (1991). A pool of cool air was discovered beneath the landfalling storms, a phenomenon also found in observational studies. This feature was found to be associated with enhanced upward motion in addition to evaporational cooling of the land surface.

A diurnal oscillation of tropical convection was discovered in a tropical zonal belt model. An examination of the mechanisms responsible for this signal and its implication on tropical cyclogenesis has begun. Also, the utilization of this tropical zonal belt model in studying tropical cyclone formation and its sensitivity to climatic or other environmental conditions has started.

PLANS FY96

Investigation of the processes of tropical cyclone genesis and decay will continue for certain real data cases. Numerical studies of the influence of larger scales on tropical cyclone formation may be initiated using a tropical zonal belt model.

7.3.2 Scale Interaction

Y. Kurihara *C.-C. Wu*

An investigation of the interaction between tropical cyclones and the surrounding environment was conducted using two numerical experiments, one with and the other without an initial tropical cyclone. Hurricanes Bob (1991), Gilbert (1988) and Andrew (1992) comprised the test suite. The experiment design used was the same as that from previous studies (1281), with the results interpreted from a potential vorticity (PV) perspective.

An analysis of the PV budget revealed that, in the case of Hurricane Bob, condensational heating within the vortex resulted in a redistribution of the PV, causing a PV sink in the upper part of the vortex and a PV source in the lower part. This tendency was largely compensated for by upward transport of positive PV from the lower levels to the upper levels. These two effects, shown in Fig. 7.2, were the major terms in the PV budget in the vortex region. However, their net effect is an increase in

the upper level negative PV anomaly during the vortex intensification period. This result underscores the importance of accurate representation of the heating profile in hurricane models.

The current study also revealed that the negative potential vorticity anomaly at upper levels in Hurricane Bob was, at first, exported by the outflow from the vortex region to the surroundings and later by the large-scale flow as well. The effect of the PV anomaly on the movement of the storm itself was evaluated by computing the nonlinear balanced flows associated with the PV perturbation at different levels as well as with the background mean PV. A notable contribution to the steering of the storm from the upper level PV anomaly was found. The results indicate a need for enhanced observations as well as accurate analyses of upper level winds as inputs to deterministic hurricane models.

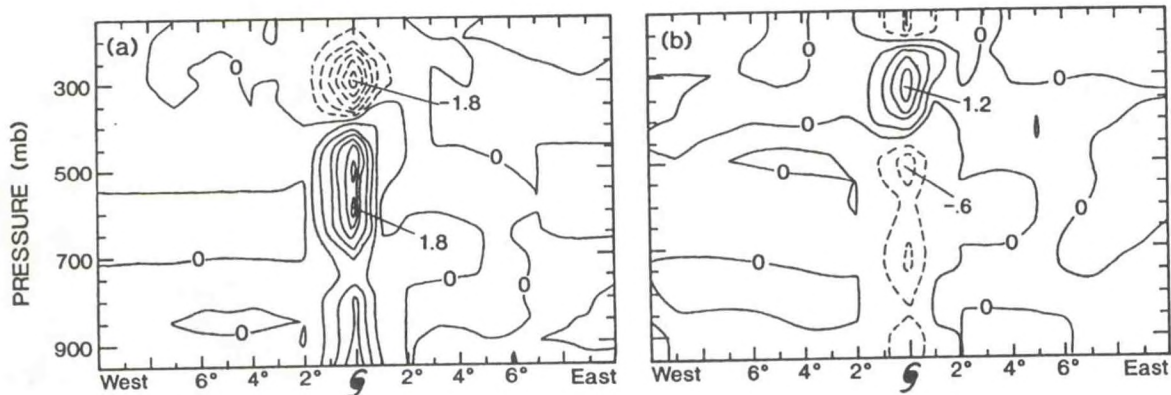


Fig. 7.2 West-east cross section of a 12-hour forecast of Hurricane Bob (1991) at 0000UTC 18 August 1991. The change of potential vorticity due to (a) condensational heating and (b) vertical advection are shown. Unit is PVU/12-hour, contour interval is 0.3 PVU/12-hour and negative values are indicated by dashed lines. Note that while the two effects compensate to some extent, there remains a net reduction of PV at upper levels and a net gain in mid- and low-levels.

PLANS FY96

A study focusing on the impact of orography of different scales on the behavior of tropical cyclones will be initiated.

7.3.3 Tropical Cyclone - Ocean Interaction

*M.A. Bender
I. Ginis**

Y. Kurihara

**University of Rhode Island*

ACTIVITIES FY95

A coupled model consisting of the GFDL hurricane model and the Princeton ocean model was constructed in order to study the effect of tropical cyclones on the structure of the ocean, particularly that of the mixed layer, and its feedback mechanism influencing the storm behavior. This coupling effect was facilitated by the specification of both lateral and bottom boundaries in the Princeton ocean model. A preliminary test of the coupled model has been proceeding.

PLANS FY96

A cyclone-ocean interaction study will continue for Hurricane Gilbert (1988) which exhibited several interesting features and for which extensive ocean observations are available.

7.4 STRUCTURE OF TROPICAL CYCLONES

*M.A. Bender
Y. Kurihara*

ACTIVITIES FY95

Asymmetric structure, in particular its quasi-steady component in the eyewall region and vicinity, was identified in both the divergence field and the precipitation distribution in a series of idealized simulation experiments using the GFDL MMM hurricane model (A94/P95). The quasi-steady features are generally masked by transient components of large amplitude, but become clear when extended model integrations are appropriately analyzed.

Previously generated numerical results were analyzed further and a strong relationship was found between the asymmetry pattern and the winds relative to the storm motion near the vortex center. These relative winds were associated with the asymmetric wind of the beta gyres, the environmental flow, or some combination of the two. A possible mechanism linking the relative wind to the formation of asymmetries was hypothesized which involves divergence patterns induced by the relative wind in the vicinity of the eyewall.

PLANS FY96

Structures of real tropical storms will be investigated. Findings from such a study may prove useful in the development of a new initialization technique for hurricane models.

7.5 MODEL IMPROVEMENT

M.A. Bender *P.J. Rears*
Y. Kurihara *R.E. Tuleya*

ACTIVITIES FY95

Implementation of the GFDL prediction system at NCEP as the official hurricane prediction model required extensive coding changes and the throughput of the system has been much improved. An NCEP technical memo on the GFDL MMM forecasting system was prepared.

Analysis tools were developed to verify forecast intensity and track prediction. Software to automate computation of error statistics of the GFDL and other models was prepared. To ascertain the regional characteristics of the track error, a preliminary evaluation of the spatial distribution of the forecast biases was made.

In preparation for the next generation prediction system, an investigation was initiated to improve the present cumulus parameterization method.

PLANS FY96

Work will begin to formulate a new method of vortex specification and to improve the cumulus parameterization scheme.

8. MESOSCALE DYNAMICS

GOALS

To produce accurate numerical simulations of mesoscale processes in order to understand what role synoptic scale parameters play in their generation and evolution.

To understand the dynamics of mesoscale phenomena and their interaction with larger and smaller scales.

To determine the practical limits of mesoscale predictability by means of sensitivity studies using numerical simulations of mesoscale phenomena.

8.1 THE LIFE CYCLE OF MIDLATITUDE CYCLONES

*E. Chang** *L. Polinsky*
I. Orlanski *J. Sheldon*

**M.I.T.*

ACTIVITIES FY95

8.1.1 Cyclone Evolution Along Storm Tracks

A number of recent studies have indicated that sea surface temperature gradients and dispersion of upper level wave energy are the major processes affecting cyclonic development along storm tracks (1177). The type of cyclonic development, its structure, explosiveness, and other properties depend mainly on the intensity of surface baroclinicity and upper level energy dispersion. Along the storm tracks, the ratio of these two effects varies considerably. As a consequence, the dynamics of cyclone development are expected to be different at, for instance, the entrance and exit of storm tracks. North America is flanked by two major storm tracks: the Pacific storm track, which ends over the west coast, and the Atlantic storm track, which begins on the east coast. Differences in 24h and 48h forecast skills in these two regions can be attributed in part to the type of cyclonic development.

An understanding of the nature of cyclone development along storm tracks has implications beyond short range forecasts. It has recently been shown that cyclone-

scale wave packets are prevalent in storm tracks (1144). The individual eddies that compose the packet have a life cycle of a few days, the entire packet has a lifetime on the order of a few weeks. Understanding the environmental conditions that support these packets could have a direct bearing on extending the predictability of those systems. An ongoing investigation aims to characterize the behavior of cyclones in the observed entrance and exit regions of storm tracks, as well as identify the environmental conditions most conducive to the formation and maintenance of packets. Idealized storm track simulations are being used to quantify the role of surface boundary forcings such as surface drag, enhanced baroclinicity, and topography. Preliminary results suggest that localized surface drag and/or baroclinicity modifies the magnitude of the eddy kinetic energy but not the zonality of the storm track itself, whereas isolated mountain chains can have a profound effect on the distribution of cyclones along the storm track.

8.1.2 Wavelet Analysis for Detection of Baroclinic Packets in Storm Tracks

One basic difficulty in the analysis of cyclone evolution along storm tracks is the identification of wave packets in the presence of complex flows characterized by different scales. A new analysis technique based on wavelet decomposition shows promise as a powerful tool for such detection. The wavelets used in this analysis are orthogonal and act like band-pass filters of Fourier components. Each wavelet can represent a band of wavenumbers and an individual wavelet may contain a full packet of waves if they are present in the signal. The time evolution of the wavelet amplitude which characterizes the packet can denote precisely the length and speed of the packet along the storm track. Application of this analysis of the idealized storm track simulations successfully distinguished between baroclinic waves characterized by high and low wavenumbers and clearly identified the propagation speed of individual eddies as well as baroclinic wave packets.

8.1.3 Energy Flux and Group Velocity in Baroclinic Waves

Although some of the difficulties in using time filters to detect wave activity can be overcome (1154), other methods currently employed for analyzing wave activity are not well-suited to the detection of downstream development in high frequency, synoptic scale waves. However, given the fact that the convergence of energy fluxes can be a good indicator for development of an energy center (*i.e.*, a new eddy), knowledge that downstream development is operating in localized regions of a storm track is of paramount importance in identifying areas which are ripe for cyclone development. A promising approach has been identified in a recently completed study which shows that the eddy energy flux, when normalized by the total eddy energy and modified to take the effects of a variable Coriolis parameter into account, gives a very good approximation to the group velocity of a system. This new formulation needs to be tested in different regions around the globe, particularly in the Pacific storm track where considerable downstream energy flux has been found (1310).

8.1.4 Stages in the Energetics of Baroclinic Systems

Local energetics has been used in conjunction with several idealized and case studies to develop a comprehensive picture of "downstream baroclinic evolution." This viewpoint offers a complementary alternative to the more conventional descriptions of cyclone development. Additional insights are made possible largely because the local energetics approach permits one to define an energy flux vector which accurately describes the direction of energy dispersion and quantifies the role of neighboring systems in local development. In this new view, the development of a system's energetics is divided into three stages. In *Stage 1*, a pre-existing disturbance well upstream of an incipient trough loses energy via ageostrophic geopotential fluxes directed downstream through the intervening ridge, generating a new energy center there. In *Stage 2*, this new energy center grows vigorously, at first due to the convergence of these fluxes, and later by baroclinic conversion as well. As the center matures, it begins to export energy via geopotential fluxes to the eastern side of the trough, initiating yet another energy center there. In *Stage 3*, this newest energy center continues to grow while that on the western side decays due to dwindling energy fluxes from the older upstream system and also as a consequence of its own export of energy downstream. As the eastern energy center matures, it exports energy further downstream, and the sequence begins anew.

Midlatitude and high-latitude case studies were used to test the limits to which this conceptual sequence might apply. One of the cases used was the notorious "Blizzard of '93". It was shown that, despite the extraordinary magnitude of some of the events, the evolution of the trough associated with the storm fits the conceptual picture of downstream baroclinic evolution quite well, with geopotential fluxes playing a critical role in its development (xk).

PLANS FY96

Studies of the environmental conditions that favor downstream baroclinic evolution will continue, as will efforts at correlating the structure of eddy activity with the local environmental characteristics at the entrance and exit of storm tracks. The relationship between the stability and deformation of the monthly mean flow and its ability to support different regimes of eddy activity, including packets, will remain a focus of investigation. Additional tests of wavelet analysis will use data from observed storm tracks. Attempts to identify, if possible, a case (or cases) of cyclogenesis which does not owe its initial development to geopotential flux convergence will continue, targeting perhaps the entrance of the Pacific storm track where baroclinicity is high and there is a dearth of upstream disturbances.

8.2 SENSITIVITY STUDIES OF MIDLATITUDE CYCLONES

G. Balasubramanian *I. Orlanski*
S. Garner *J. Sheldon*

8.2.1 The Blizzard of '93

The results from various case studies up to this point seem to indicate that downstream fluxes are an inseparable contributor to the development of all energy centers associated with baroclinic systems (7.1.4). However, it is not clear whether the fluxes are always necessary for the initial development of a disturbance, or whether baroclinic conversion alone could, in some cases, prove to be an adequate mechanism to initiate such a disturbance. In an effort to determine whether an event could be precipitated by purely baroclinic means, local energetics were analyzed in the so-called Blizzard of '93, which moved up the east coast of the U.S. on 13-14 March 1993, setting numerous records in terms of snowfall, temperatures, and sea-level pressures. However, it was found that even in an event as explosive as this, geopotential fluxes played a key role. First, fluxes from a decaying system over the Pacific converged over the west coast and initiated the development of an energy center there, altering the basic flow and causing the jet stream to push south into Mexico. Second, fluxes from the new energy center over northern Mexico were strongly convergent over the Texas gulf coastal region, initiating strong development of an energy center. This energy center, in turn, subsequently tapped into the baroclinicity of a weakly stable area over the Gulf of Mexico. Strong local baroclinic conversion combined with continued convergence of fluxes from the energy center on the west side of the trough (itself maintained by baroclinic conversion in the sinking cold air) produced the spectacular strengthening of this record-breaking storm (xk).

A numerical simulation of the event, initialized at 00Z 12 March reproduced the storm with a high degree of fidelity, and provided additional insight by revealing these important processes at a higher spatial and temporal resolution than that available from the analyses.

In order to estimate the deterioration of the simulation as a function of initialization times, a series of solutions were calculated starting every 12 hours from 00Z 10 March. As expected, the quality of the simulations worsened for longer forecast times. What was especially interesting was that this degradation was particularly abrupt for the case initialized at 00Z 10 March. The poor quality of this simulation was traced to a failure to reproduce the processes associated with the southward extension of the jet over Mexico 24-48 hours beforehand. This deficiency was found to be a consequence of a much weaker than observed cyclone over the central Pacific, which the analysis showed to be the source of the fluxes. As discussed above (8.1.4), this result demonstrates the pervasive role played by geopotential fluxes in the flow of energy through a series of disturbances, as well as

the value of using geopotential fluxes as a diagnostic tool for analyzing deficiencies in numerical simulations and forecasts.

8.2.2 Nonlinear Baroclinic Wave Equilibration

The interaction between baroclinic eddies and the zonal-mean or time-mean circulation has implications for the jet stream, storm tracks, stationary wave patterns and blocking events. An idealized study of nonlinear baroclinic wave equilibration in different initial environments and geometries illuminates this interaction in the case of normal-mode development (ai). There is a stark difference in the equilibration between spherical and Cartesian models, with spherical simulations producing much more anticyclonic zonal-mean wind shear and shorter-lived eddies (Fig. 8.1). (It should be noted, however, that the larger anticyclonic shear can be engineered within either model by manipulating the barotropic shear in the initial state.) The main dynamical difference between the two types of equilibration lies in the strength of the positive feedback between the barotropic decay of the eddy and the acceleration of the zonal-mean wind (which occurs first at low levels and then at upper levels). The strength of the feedback is determined by the shape of the normal mode and the spherical modification of the mean wind tendency due to momentum fluxes.

Traditional analysis using transformed zonal-mean equations obscures this process by combining the eddy momentum forcing of the low-level jet with the forcing by the mean meridional circulation. Only the former is significantly different in the two

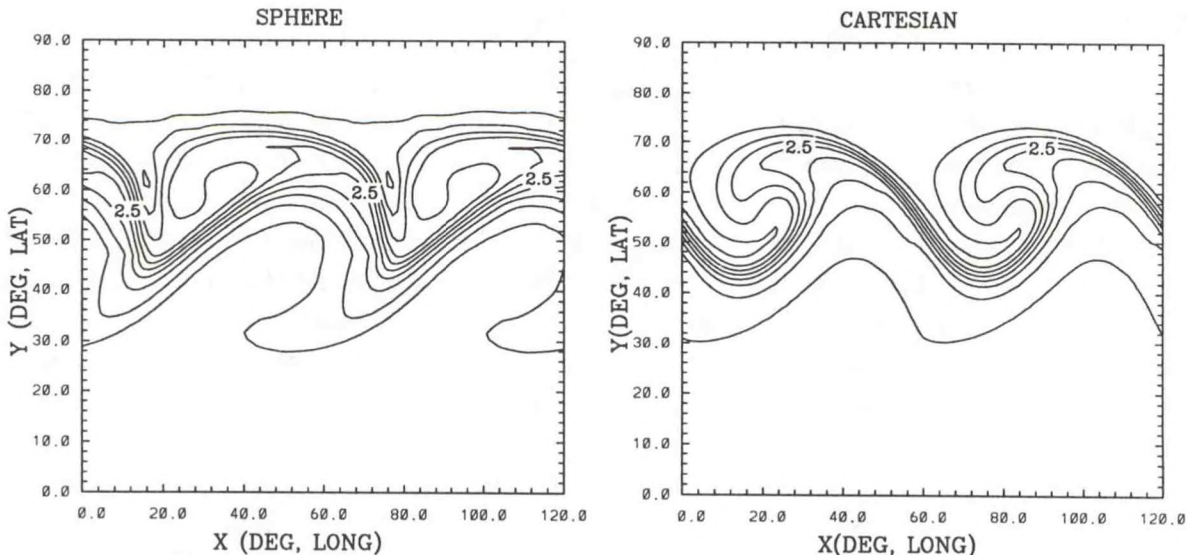


Fig 8.1 The potential vorticity (PV) on the 320K potential temperature surface on day 7 in the spherical (left) and Cartesian (right) models. The contour interval is 0.5 PV unit (1 PV unit = $1 \times 10^{-6} \text{ m}^2 \text{ s}^{-1} \text{ K kg}^{-1}$). Both models were initialized with similar linearly unstable basic-state PV distributions. The wave breaks anticyclonically on the sphere and it rolls up cyclonically in the Cartesian model.

types of equilibration. This study has also produced a heuristic understanding of the shape of baroclinic normal modes in the presence of a planetary vorticity gradient, different geometries, and horizontal shear.

PLANS FY96

Since numerical simulations have been found to provide the best "dataset" for elaborate analysis of cyclone evolution, efforts will continue toward improvement of the physics packages of the models in order to obtain the most accurate simulations, especially with respect to drag over mountainous terrain and its potential similarity to empirically derived drag coefficients over water. The sensitivity of the Blizzard simulations to surface and latent heating effects, and to initialization, will be further investigated. The analysis of cyclone evolution in different geometries will be extended, including a systematic study to compare frontal evolution in high-resolution spherical and Cartesian models. The mechanism responsible for the stronger wrap-up of the warm front in the Cartesian geometry (and the weaker one in the spherical geometry) will be analyzed. An attempt will also be made to link the eddy momentum fluxes to the type of fronts that develop in baroclinic waves.

8.3 TOPOGRAPHIC INFLUENCES IN ATMOSPHERIC FLOWS

S. Garner

B. Gross

8.3.1 Blocking and Frontogenesis Due to Topography

The nature of blocking by orography has been investigated in the case of a rotating baroclinic atmosphere using a highly idealized two-dimensional model. The blocked baroclinic solutions differ from blocked barotropic solutions in two ways: there is no permanent far-upstream influence and the flow near the obstacle never becomes steady. Permanent blocking in the presence of background rotation is possible only in the case of warm advection. Shallow fronts that form as a consequence of the blocking bear some resemblance to observed fronts in certain coastal regions. The mountain drag in blocked, rotating solutions is comparable to that in blocked, nonrotating solutions obtained with much stronger static stability.

A weakly nonlinear analysis of baroclinic orographic blocking has shown that the barrier enhancement due to warm advection stems from an additional zonal momentum flux divergence in the baroclinic linear mountain waves. The additional flux is associated with larger meridional velocities created by a larger angle between phase lines and ambient angular momentum surfaces. Another nonlinearity arises from the tilting of the horizontal temperature stratification into the vertical, in phase with the vertical motion field. However, the nonlinear temperature flux divergence was found to be much less important than the momentum flux divergence.

8.3.2 Resolved Topographic Drag in Global Models

One of the most perplexing systematic errors in global model simulations of the present climate is the overly strong upper-tropospheric mean westerlies in the Northern Hemisphere. Many modelers have resorted to a parameterized representation of unresolved gravity-wave drag as a way of weakening the time-mean westerlies. Unfortunately, it is not well known how closely the total wave-drag forcing needed to produce a realistic correction corresponds to that which exists in the real atmosphere. At least one recent study suggests that there is a huge discrepancy.

Since wave drag is the result of a complex interaction between large-scale circulations and mesoscale terrain features, the answer to this question will require high-resolution simulations in deep, planetary-scale domains, but with 25 km resolution in the horizontal and 500 m resolution in the vertical. For this purpose, the hydrostatic Zeta model has been modified to include fully compressible nonhydrostatic dynamics and spherical geometry (8.4.2). These modifications are required by the depth and horizontal size of the domain in the planned experiments.

PLANS FY96

The importance of nonhydrostatic effects and compressibility in mesoscale circulations will be assessed, with a particular effort toward improving the simulation of circulations around topographic features. Analysis will continue of the total wave-drag forcing in high-resolution simulations of the interaction between large-scale circulations and mesoscale terrain features. The development of both hydrostatic and nonhydrostatic model adjoints will aid in determining the sensitivity of model solutions to topography and other physical influences.

8.4 MODEL DEVELOPMENT

*G. Balasubramanian L. Polinsky
B. Gross J. Sheldon
I. Orlanski*

ACTIVITIES FY95

8.4.1 Improvements to the Hydrostatic Zeta Model

The primitive equation Zeta model uses the terrain-following coordinate

$$Z = e^{-\epsilon \left(\frac{z-h(x,y)}{H-h(x,y)} \right)},$$

where $h(x,y)$ represents the topographic height and H is the height of the rigid lid. The original version of the model is dry, inviscid, and adiabatic (except that weak second-order diffusion is included to control noise), and employs the hydrostatic and Boussinesq approximations. A complete description of the model has been provided (1200). Parameterizations of radiative forcing and surface drag have been introduced into the hydrostatic model in order to more realistically examine the effects of baroclinicity and surface friction on cyclone development and its long-term statistics within storm tracks.

8.4.2 The Nonhydrostatic Compressible Zeta Model

A three-dimensional, nonhydrostatic, fully compressible version of the hydrostatic Zeta model has been constructed to investigate mesoscale atmospheric circulations and for evaluating nonhydrostatic and compressibility effects by direct comparison with the hydrostatic Zeta model. The current version of the nonhydrostatic compressible model uses velocity as a dependent variable and expresses advection as second or fourth order finite-differences rather than in flux form. The vertical pressure gradient and vertical divergence of vertical velocity are integrated semi-implicitly in the vertical. Other features of the model include Richardson-number dependent vertical mixing and a constant flux layer at the surface. A time-split version of the model is also available. The three-dimensional model has been verified against the hydrostatic Zeta model with idealized simulations of barotropic and baroclinic instability.

8.4.3 Model Intercomparisons

The addition of the nonhydrostatic Zeta model to several other two- and three-dimensional hydrostatic and nonhydrostatic models provides a suite of tools with which a variety of atmospheric phenomena can be explored. In particular, nonhydrostatic and compressibility effects can now be assessed in three-dimensional flows. Such an assessment was made in order to verify the nonhydrostatic Zeta model by comparing hydrostatic and nonhydrostatic simulations of idealized barotropic and baroclinic instability. A linear stability analysis shows that the growth rates for both instabilities decrease with compressibility, as measured by the inverse acoustic phase speed. An examination of the perturbation energy equations indicate that the work done against elasticity during compression represents a source of perturbation internal energy and a sink of perturbation kinetic energy, thereby diminishing the growth rate. Simulations of barotropic and baroclinic instability with the nonhydrostatic compressible Zeta model are nearly identical to those using the hydrostatic Boussinesq Zeta model, but show that relatively slower growth continues well into the nonlinear regime (Fig. 8.2).

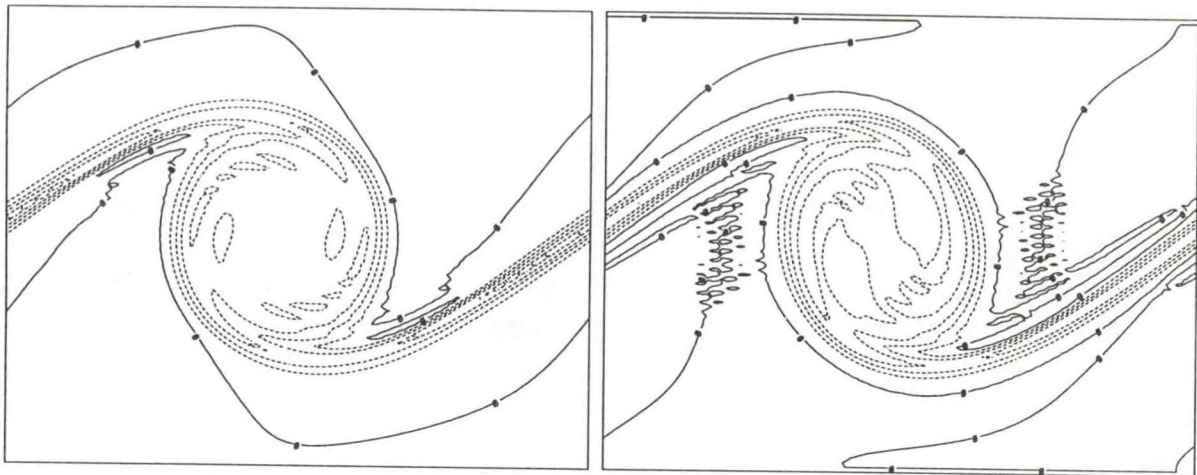


Fig. 8.2 Vorticity in the compressible barotropic simulation after five days of integration (left) and in the Boussinesq simulation after four days of integration (right). The contour interval is $1 \times 10^{-5} \text{ s}^{-1}$ and dashed contours indicate negative values. The domain size is 7680 km in the zonal direction and 6000 km in the meridional direction. The basic zonal flow is a bounded uniform shear layer 1000 km wide meridionally centered in the domain. The acoustic phase speed in the compressible solution is 120 m s^{-1} .

In order to simplify model intercomparisons, initialization procedures that allow the output from one model to be input by another are being developed. One such method currently being pursued transforms the results of the hydrostatic Boussinesq Zeta model for input into the Limited Area HIBU Model (LAHM) by means of potential vorticity inversion. One key difficulty in this process is the solution of the nonlinear balance system in spherical coordinates (for LAHM) using the potential vorticity calculated on a β -plane (in the Zeta model). Once this difficulty is overcome, this methodology can be used for other model data transformations.

PLANS FY96

Moist processes and boundary layer physics will be incorporated into both the hydrostatic and nonhydrostatic Zeta models. High resolution (10-20 km) nonhydrostatic simulations of baroclinic waves will facilitate the investigation of phenomena such as frontal collapse and equilibration and the role of nonhydrostatic circulations in the development and decay of these systems. The adjoints of the hydrostatic and nonhydrostatic Zeta models will be developed, and sensitivity studies will be undertaken to clarify the features most important to the aforementioned development, equilibration, and decay processes.

9. COMPUTATIONAL SERVICES

GOAL

To provide a computational facility to support research conducted at GFDL with emphasis on supercomputing and interactive capabilities for developing, running, and analyzing numerical models and on file serving capabilities for managing large amounts of data.

9.1 COMPUTER SYSTEMS

<i>P. Baker</i>	<i>L. Umscheid</i>
<i>L. Lewis</i>	<i>R. White</i>
<i>T. Taylor</i>	<i>W. Yeager</i>

ACTIVITIES FY95

The Request for Proposal for the Scientific Computer System to replace the Cray Y-MP was issued in October 1994. Live Test Demonstrations were viewed by a Technical Evaluation Board for the computational, data archiving, and scalable components of each proposed system. After discussions with all the offerors and a very competitive Best and Final Offer process, the contract was awarded to Cray Research Inc., in May 1995. The 63 month contract calls for an initial installation of a C916/16 system and phased delivery of a subsequent T90 system. Archiving capability for over 124 terabytes of data, additional rotating storage, upgrades to the I/O subsystem, and a T3E scalable system will be delivered over the life of the contract. The computational power, as demonstrated by an extensive set of benchmark programs, will increase in phases from approximately 6 to 16 times a Y-MP/8. The initial C90 system has 16 processors, 256 megawords (MW) of central memory, one gigaword of solid state disk, 355 gigabytes of rotating storage, and two robotic silos for tape media. This C90 system started acceptance testing on August 24, 1995. Within 12 hours of being made generally available to scientific users, the system was at 98% utilization.

In addition to the new C90, GFDL's computer facility includes: a Cray Y-MP with 8 processors, 64 MW of central memory, 256 MW of solid state storage, and 45 gigabytes of rotating storage; three Sun Microsystems and two Silicon Graphics (SGI) servers; and a variety of text and graphics printers. Distributed throughout GFDL are 116 desktop workstations including 17 SGI Indigo2 R4400XZs, 34 SGI Indigo

R4000XZs, 12 SGI 4D/35s, 34 SGI 4D/25s, 5 Sun SPARCstation-1s, and 14 Sun 3/50s. The workstations, servers, and Y-MP are inter-connected by eight Ethernet segments and two Network Systems Corporation (NSC) routers; the C90, Y-MP, and two Sun servers are inter-connected by a Fiber Distributed Data Interface (FDDI) network which connects to the Ethernet network through one of the NSC routers.

The SGI Indigo2 R4400XZ workstations that were installed this year are the most powerful desktop workstations ever available to GFDL scientists. Indigo and Indigo2 workstations now comprise more than half of GFDL's SGI workstations. A significant amount of data analysis that previously required a supercomputer is now being run on these very powerful workstations. An Indigo2 with three times the memory and disk capacity was connected to the FDDI network for use as a public workstation and compute server capable of transferring and analyzing extremely large datasets generated on the C90.

A major upgrade of the IRIX operating system was installed on all SGI workstations. Two additional color PostScript printers were acquired to meet the increasing demand for color hardcopy and transparency output. A network backup system for backing up local workstation disk drives was ordered. A three-year contract to provide GFDL's Internet connection was awarded.

The number of user processor hours for each month and the accumulative amount of total archive data in billions of bytes for the Y-MP are shown in Table 9.1. The system utilization indicated in the table is the highest ever achieved. The record number of user processor hours resulted primarily from the doubling of central memory in August 1994 and improved disk I/O efficiency in several programs.

Table 9.2 shows the same information as Table 9.1, but for the new C90. The number of user processor hours achieved in September indicates nearly full utilization of the C90 and is approximately double a typical Y-MP month due to having twice the number of processors.

Table 9.1 Cray Y-MP User Processor Time and Amount of Total Archive Data

Month	Hours	Gigabytes
Oct 94	5,765	11,073
Nov 94	5,349	10,595
Dec 94	5,601	10,940
Jan 95	5,722	11,181
Feb 95	5,134	10,975
Mar 95	5,719	11,175
Apr 95	5,070	11,071
May 95	5,659	11,168
Jun 95	5,629	11,313
Jul 95	5,760	11,471
Aug 95	6,027	11,770
Sep 95	5,548	11,669

Table 9.2 Cray C90 User Processor Time and Amount of Total Archive Data

Month	Hours	Gigabytes
Aug 95 ¹	2,664	200
Sep 95	11,325	1,092

¹ Partial month beginning Aug. 18

PLANS FY96

Data archiving on the C90 will be carefully monitored in order to determine how best to utilize the two different types of proposed tape media (IBM 3490E compatible and helical scan). The high capacity helical scan tapes will be delivered in October 1995, four months ahead of the original schedule. In April 1996, the C90 will be replaced by a T932/16 system with approximately 1.5 times the computational power of the C90 (9 times a Y-MP/8). Central memory will also be increased from 256 MW

to 512 MW. Since the T90 system will use IEEE floating point arithmetic, as opposed to the proprietary Cray format on the C90, and since it will be necessary to convert programs from Fortran 77 to Fortran 90, preparation for the transition to the T90 will include training for users and test time on an off-site T90 system which will be made available by Cray Research. The 40-processor T3E scalable system will be installed in August 1996. GFDL will continue to operate the Y-MP as long as it remains advantageous for research and is cost-effective for the government.

The network backup system ordered near the end of FY95 will be implemented. The SGI software server will be upgraded to a faster model. All servers not presently connected to the FDDI network will be connected via an Ethernet-FDDI switch. New hardware and software maintenance contracts for the SGI workstations will be negotiated. Pending availability of funds, older Sun workstations will continue to be replaced with SGI workstations. An analysis of printer utilization will be undertaken with the goal of redeploying or replacing some of the black-and-white PostScript printers.

9.2 DATA MANAGEMENT AND VISUALIZATION

J. Sheldon *R. White*
H. Vahlenkamp

ACTIVITIES FY95

An effort has been initiated to design and assemble an integrated data management and visualization infrastructure for the Laboratory using a carefully managed approach which will be more efficient, avoid unnecessary duplication of effort, and enable the Laboratory to take advantage of technologies that might otherwise have been overlooked. Efforts in this first year have concentrated on defining current capabilities and requirements, identifying potential software and hardware solutions that will address both immediate and strategic needs, and beginning to implement some specific high priority elements.

Several data formats were examined on the basis of portability, self-describability, and support from existing data analysis and visualization packages. The "netCDF" package was chosen, primarily because of its wide acceptance in the meteorological and oceanographic community as well as by data analysis and visualization/plotting packages, particularly NCAR graphics. A number of tools were located, developed, and/or outlined to facilitate the reading, writing, and editing of netCDF files. These include a concise set of "interface" routines for which the user need only satisfy an argument list in order to read and write netCDF files.

A fairly exhaustive survey was also conducted of applicable plotting/visualization packages. The packages were divided into 4 levels which reflect their sophistication and expected use. While it was not possible to select a clear "winner" in each of these categories, a limited number of packages were identified which would accomplish the intended goals. The new, casual, or infrequent users will especially appreciate two packages ("Freud" and "cxIsoSlice") which employ graphical interfaces (GUI's) to specify how to view data and/or generate basic plots. The "Scian" package is very "Mac-like" and can produce simple 3-D surfaces and 2-D slices quite easily. Eventually, NCAR Graphics, with its new command language and GUI, will likely satisfy a very broad spectrum of users.

The SGI/NAg "Explorer" package was tentatively adopted as the high-end 3,4-D visualization package and used with great success to generate a variety of impressive color figures. While use of this package is much more demanding of the user, its flexible analysis and graphics power is commensurately greater as well. Some of the visualizations produced using Explorer have revealed many features of research interest, such as the path of air parcels in the eye of a hurricane. In addition, a number of these visualizations have appeared in both print and broadcast media, as well as in the annual report of the High Performance Computing and Communication (HPCC) program and in several DOC/NOAA/ERL presentations and press briefings. In support of efforts utilizing Explorer, a wide variety of modules (approximately 40) were developed for ingesting, manipulating, and rendering data.

One aspect of visualization and presentation which has received particular attention over the past year is animation, culminating in the development of "TkAniMaker." TkAniMaker's primary purpose is to simplify the task of transferring an animation to videotape. Using a graphical interface, it performs all the functions which previously required writing a complex script consisting of specific time codes and commands. A "preview" feature, which creates either an MPEG or SGI "movie" file, allows the author to review what the animation will look like before "printing" to tape.

PLANS FY96

Efforts will continue toward addressing infrastructure needs identified during the past year. The variety of tools for editing and manipulation netCDF files will be enhanced and consolidated into a small number of utilities which will be far easier to use. Individualized support will be provided to users needing to write/read netCDF files. User adoption of Explorer will be promoted by providing several pre-programmed applications and individual "driving lessons." The availability and development of various visualization packages will be monitored, particularly those in the "publication quality" class which is such a state of flux. GUI's will be developed for several of the more obtuse system utilities (e.g., "cpio," "find"), making them far more

usable by the user population as a whole, and serving as examples of how GUI's can be used as "accelerators" for a variety of general and user-specific functions.

APPENDIX A

GFDL STAFF MEMBERS

and

AFFILIATED PERSONNEL

during

Fiscal Year 1995

Jerry D. Mahlman, Director
Betty M. Williams, Secretary

Bruce B. Ross, Assistant Director
Joan M. Pege, Management Analyst

PERSONNEL SUMMARY

September 30, 1995

GFDL/NOAA

Full Time Permanent (FTP)	81
Part Time Permanent (PTP)	3
Intermittent (INT)	1
National Oceanic and Atmospheric Administration (NOAA) Corps	1

PRINCETON UNIVERSITY (PU)

AOS Program Scientists	12
Graduate Students	11
Professors	3
Research Scientists	2
Research Staff	7
Support Staff	3
Technical Staff	8
UCAR Fellows	1
Visiting Senior Research Scientist	1

OTHER INSTITUTIONS

U.S. Geological Survey (USGS)	2
University Corporation for Atmospheric Research (UCAR)	3

VENDORS

Cray Research Inc. Computer Support Staff	4
IBM Research Staff	1

TOTAL **144**

CLIMATE DYNAMICS

Manabe, Syukuro	Senior Scientist at GFDL	FTP
Baker, David F.	Graduate Student	PU
Broccoli, Anthony J.	Meteorologist	FTP
Delworth, Thomas L.	Meteorologist	FTP
Hall, Alexander	Graduate Student	PU
Hayashi, Yoshikazu	Meteorologist	FTP
Golder, Donald G.	Meteorologist	FTP
Held, Isaac M.	Senior Scientist at GFDL	FTP
Chen, Shuo	Graduate Student	PU
Larichev, Vitaly	AOS Program Scientist	PU
Phillipps, Peter J.	Meteorologist	FTP
Sun, Dezheng	AOS Program Scientist	PU*
Swanson, Kyle	AOS Program Scientist	PU
Treguier, Anne Marie	AOS Program Scientist	PU*
Weill-Zrahia, Anne	AOS Program Scientist	PU
Zhang, Jiawei	Graduate Student	PU*
Zhang, Yunqing	Graduate Student	PU
Zhang, Zhojun	AOS Program Scientist	PU
Ip, Chi Fong	AOS Program Scientist	PU*
Knutson, Thomas R.	Meteorologist/Management Associate	FTP
Milly, P.C.D.	Hydrologist	RA**
Dunne, Krista	Physical Scientist	RA**
Numaguchi, Atsushi	AOS Program Scientist	PU
Robock, Alan	AOS Program Scientist	PU*
Spelman, Michael J.	Meteorologist	FTP
Stouffer, Ronald J.	Meteorologist	FTP
Wetherald, Richard T.	Meteorologist	FTP
Williams, Gareth P.	Meteorologist	FTP

*Affiliation terminated prior to September 30, 1995.

**United States Geological Survey (USGS) on detail to GFDL.

RADIATION AND CLOUDS

Ramaswamy, V.	Physical Scientist	FTP
Donner, Leo J.	Physical Scientist	FTP
Reisin, Tamir	AOS Program Scientist	PU
Seman, Charles J.	Physical Scientist	FTP
Freidenreich, Stuart	Meteorologist	FTP
Li, Jiangnan	AOS Program Scientist	PU
Orris, Rebecca	Graduate Student	PU
Schwarzkopf, M. Daniel	Meteorologist	FTP
Soden, Brian J.	Physical Scientist	FTP

MIDDLE ATMOSPHERE DYNAMICS AND CHEMISTRY

Mahlman, Jerry D.	Director	FTP
Goldberg, Charles	Scientific Visitor	UCAR
Hamilton, Kevin P.	Meteorologist	FTP
Wilson, Robert J.	Meteorologist/Graduate Student	FTP/PU
Hemler, Richard S.	Meteorologist	FTP
Goldberg, David	Student	PTT*
Kerr, Christopher L.	Scientific Visitor/Computer Scientist	UCAR*/IBM
Levy II, Hiram	Physical Scientist	FTP
Hirsch, Adam	Technical Staff	PU
Klonecki, Andrzej	Graduate Student	PU
Moxim, Walter J.	Meteorologist	FTP
Perliski, Lori	Physical Scientist	FTP
Taubman, Steven J.	Scientific Visitor	UCAR

*Affiliation terminated prior to September 30, 1995.

EXPERIMENTAL PREDICTION

Anderson, Jeffrey L.	Meteorologist	FTP
Miyakoda, Kikuro [†]	Supervisory Research Meteorologist	FTP*
Gordon, Charles T.	Meteorologist	FTP
Hubeny, Veronika	Summer Student	PU*
Ploshay, Jeffrey J.	Meteorologist	FTP
Rosati, Anthony J.	Physical Scientist	FTP
Gudgel, Richard G.	Meteorologist	FTP
Sirutis, Joseph J.	Meteorologist	FTP
Stern, William F.	Meteorologist	FTP
Smith, Robert G.	Computer Assistant	FTP
Vitart, Frederic	Graduate Student	PU
Wyman, Bruce L.	Meteorologist	FTP

[†] Former Project Leader, retired 6/30/95.

OCEANIC CIRCULATION

Toggweiler, John R.	Oceanographer	FTP
Carson, Steven R.	Physical Scientist	FTP
Dixon, Keith W.	Meteorologist	FTP
Griffies, Stephen	UCAR Fellow	PU
Harrison, Matthew	Research Associate	NOAA**
Hurlin, William J.	Meteorologist	FTP
Pacanowski, Ronald C.	Oceanographer	FTP
Samuels, Bonita L.	Oceanographer	FTP
Winton, Michael	Oceanographer	FTP

*Affiliation terminated prior to September 30, 1995.

**NOAA Corps, on assignment to GFDL.

OBSERVATIONAL STUDIES

Oort, Abraham H.	Meteorologist	FTP
Bauer, Michael P.	Visiting Graduate Student	PTT*
Lanzante, John	Meteorologist	FTP
Gahrs, Gregory	Summer Student	PU*
Lau, Ngar-Cheung	Meteorologist	FTP
Crane, Mark	Meteorologist	FTP
Nath, Mary Jo	Meteorologist	FTP
Peng, Peitao	AOS Program Scientist	PU
Raval, Ameet	Physical Scientist	INT*
Rosenstein, Melvin	Physical Science Technician	FTP*

HURRICANE DYNAMICS

Kurihara, Yoshio	Meteorologist	FTP
Bender, Morris A.	Meteorologist	FTP
Tuleya, Robert E.	Meteorologist	FTP
Rears, Patrick J.	Student	PTT*
Wu, Chun-Chieh	AOS Program Scientist	PU*

MESOSCALE DYNAMICS

Orlanski, Isidoro	Meteorologist	FTP
Balasubramanian, G.	AOS Program Scientist	PU
Garner, Stephen	Meteorologist	FTP
Gross, Brian	Physical Scientist	FTP
Polinsky, Larry	Meteorologist	FTP
Sheldon, John	Meteorologist/Graphics Specialist	FTP

*Affiliation terminated prior to September 30, 1995.

MANAGEMENT FRAMEWORK

Administrative and Technical Structure

Mahlman, Jerry D.	Director	FTP
Knutson, Thomas R.	Meteorologist/Management Associate	FTP
Ross, Bruce B.	Assistant Director	FTP
Haller, Gail T.	Library Technician	PTP
Amend, Beatrice E.	Office Automation Clerk	INT
Lewis, Lawrence J.	Leader, COMPUTER SYSTEMS	FTP
Marshall, Wendy H.	Editorial Assistant	FTP
Pege, Joan M.	Management Analyst	FTP
Raphael, Catherine	Scientific Illustrator	PTP
Sheldon, John	Meteorologist/Graphics Specialist	FTP
Vahlenkamp, Hans	Scientific Visitor	UCAR
Umscheid, Ludwig J.	Major Systems Specialist	FTP
Urbani, Elaine B.	Transportation Assistant	FTP
Uveges, Frank J.	Supervisory Computer Specialist	FTP
Byrne, James S.	Junior Technician	FTP
Shearn, William F.	Leader, COMPUTER OPERATIONS	FTP
Varanyak, Jeffrey	Scientific Illustrator	FTP
Williams, Betty M.	Secretary	FTP

Scientific Structure

Mahlman, Jerry D.	Director and Leader, MIDDLE ATMOSPHERE DYNAMICS AND CHEMISTRY	FTP
Anderson, Jeffrey L.	Leader, EXPERIMENTAL PREDICTION	FTP
Kurihara, Yoshio	Leader, HURRICANE DYNAMICS	FTP
Manabe, Syukuro	Leader, CLIMATE DYNAMICS	FTP
Oort, Abraham H.	Leader, OBSERVATIONAL STUDIES	FTP
Orlanski, Isidoro	Leader, MESOSCALE DYNAMICS	FTP
Ramaswamy, V.	Leader, RADIATION AND CLOUDS	FTP
Toggweiler, John R.	Leader, OCEANIC CIRCULATION	FTP

COMPUTER SYSTEMS

Lewis, Lawrence J.	Supervisory Computer Specialist	FTP
Baker, Philip L.	Computer Specialist	FTP*
Taylor III, Thomas E.	Computer Specialist	FTP
White, Robert K.	Computer Specialist	FTP
Yeager, William T.	Computer Specialist	FTP

COMPUTER OPERATIONS SUPPORT

Shearn, William F.	Operations Manager	FTP
Hopps, Frank K.	Supervisory Computer Operator	FTP
King, John T.	Lead Computer Operator	FTP
Duggins, Marsha	Peripheral Equipment Operator	FTP
Harrold, Renee M.	Computer Operator	FTP
Yacovelli, Deborah	Peripheral Equipment Operator	FTP
Hand, Joseph S.	Supervisory Computer Operator	FTP
Cordwell, Clara L.	Lead Computer Operator	FTP
Ledden, Jay H.	Computer Operator	FTP
Lim, Jennifer J.	Computer Operator	PTP
Pinter, Kristina D.	Computer Operator	PTT*
Schulze, Howard P.	Computer Operator	FTP*
Deuringer, James A.	Supervisory Computer Operator	FTP
Heinbuch, Ernest C.	Supervisory Computer Operator	FTP*
Krueger, Scott R.	Lead Computer Operator	FTP
Conover, Leonard J.	Lead Computer Operator	FTP*
Blakemore, Geneve	Computer Operator	FTP
Dahl, Tania	Computer Operator	FTP
Henne, Ronald N.	Computer Assistant	FTP

*Affiliation terminated prior to September 30, 1995.

ATMOSPHERIC AND OCEANIC SCIENCES PROGRAM

Philander, S.G.H.	Professor, Program Director	PU
Bryan, Kirk	Visiting Senior Research Scientist	PU
Callan, Johann V.	Technical Research Secretary	PU
Goddard, Lisa M.	Graduate Student	PU
Goswami, B.N.	AOS Program Scientist	PU*
Gu, Daifang	Research Staff	PU
Harper, Scott	Graduate Student	PU
Lambert, Gregory	Technical Staff	PU
Li, Tianming	AOS Program Scientist	PU*
Nicoletti, Mary Ann	Program Manager	PU*
Rossi, Laura	Program Manager	PU
Valerio, Anna	Technical Research Secretary	PU
Mellor, George	Professor Emeritus	PU
Chen, Ping	AOS Program Scientist	PU
Ezer, Tal	Research Staff	PU
Jungclaus, Johann	AOS Program Scientist	PU
Kim, Namsoug	Technical Staff	PU
Sarmiento, Jorge	Professor	PU
Armstrong, Robert	Research Staff	PU
Dengg, Joachim	AOS Program Scientist	PU
Fan, Song-Miao	Research Staff	PU
Figueroa, Horacio	Research Staff	PU*
Garcon, Veronique	Research Scientist	PU
Key, Robert M.	Research Scientist	PU
LeQuere, Corrine	Technical Staff	PU
McDonald, Gerard	Technical Staff	PU
Murnane, Richard J.	Research Staff	PU
Olszewski, Jason	Research Staff	PU
Rossmassler, Julie E.	Technical Staff	PU
Rotter, Richard	Technical Staff	PU
Sabine, Christopher L.	Research Staff	PU
Slater, Richard D.	Technical Staff	PU
Webb, Vincent	Graduate Student	PU

*Affiliation terminated prior to September 30, 1995.

CRAY RESEARCH INCORPORATED

Siebers, Bernard
Braunstein, Mark
Rao, Ramesh
Weiss, Ed

Analyst in Charge
Field Engineer
Applications Analyst
Engineer in Charge

APPENDIX B

GFDL

BIBLIOGRAPHY

1991-1995

GFDL PUBLICATIONS

This is a partial listing of GFDL publications. A copy of the complete bibliography can be obtained by calling (609) 452-6502, or by writing to:

Director
Geophysical Fluid Dynamics Laboratory
Post Office Box 308
Princeton, New Jersey 08542

- * (1019) Lau, K.-H., An Observational Study of Tropical Summertime Synoptic Scale Disturbances, Ph.D. Dissertation, Atmospheric and Oceanic Sciences Program, Princeton University, 1991.
- * (1020) Zhu, X., Spectral Parameters in Band Models with Distributed Line Intensity, *Journal of Quantitative Spectroscopy and Radiative Transfer*, 45(1), 33-46, 1991.
- * (1021) Xue, H.-J., Numerical Studies of Gulf Stream Meanders in the South Atlantic Bight, Ph.D. Dissertation, Atmospheric and Oceanic Sciences Program, Princeton University, 1991.
- * (1022) Milly, P.C.D., A Refinement of the Combination Equations for Evaporation, *Surveys in Geophysics*, 12, 145-154, 1991.
- (1023) Bryan, K., and R.J. Stouffer, A Note on Bjerknes's Hypothesis for North Atlantic Variability, *Journal of Marine Systems*, 1(3), 229-241, 1991.
- * (1024) Bard, E., M. Arnold, J.R. Toggweiler, P. Maurice, and J.-C. Duplessy, Bomb ^{14}C in the Indian Ocean Measured by Accelerator Mass Spectrometry: Oceanographic Implications, *Radiocarbon*, 31(3), 510-522, 1991.
- * (1025) Garner, S.T., The Nongeostrophic Structure of Baroclinic Waves and Its Relation to Fronts and Jet Streaks, *Journal of the Atmospheric Sciences*, 48(1), 147-162, 1991.
- * (1026) Randel, W.J., and I.M. Held, Phase Speed Spectra of Transient Eddy Fluxes and Critical Layer Absorption, *Journal of the Atmospheric Sciences*, 48(5), 688-697, 1991.
- * (1027) Wetherald, R.T., V. Ramaswamy, and S. Manabe, A Comparative Study of the Observations of High Clouds and Simulations by an Atmospheric General Circulation Model, *Climate Dynamics*, 5, 135-143, 1991.
- (1028) Tuleya, R.E., Sensitivity Studies of Tropical Storm Genesis Using a Numerical Model, *Monthly Weather Review*, 119(3), 721-733, 1991.
- * (1029) Lee, S., and I.M. Held, Subcritical Instability and Hysteresis in a Two-Layer Model, *Journal of the Atmospheric Sciences*, 48(8), 1071-1077, 1991.

*In collaboration with other organizations

- * (1030) Ramaswamy, V., M.D. Schwarzkopf, and S.C. Liu, Preface to JGR-ICRCCM Issue, *Journal of Geophysical Research*, 96(D5), 8921-8923, 1991.
- * (1031) Ramaswamy, V., and S.M. Freidenreich, Solar Radiative Line-by-Line Determination of Water Vapor Absorption and Water Cloud Extinction in Inhomogeneous Atmospheres, *Journal of Geophysical Research*, 96(D5), 9133-9157, 1991.
- * (1032) Fouquart, Y., B. Bonnel, and V. Ramaswamy, Intercomparing Shortwave Radiation Codes for Climate Studies, *Journal of Geophysical Research*, 96(D5), 8955-8968, 1991.
- * (1033) Ellingson, R.G., J. Ellis, and S. Fels, The Intercomparison of Radiation Codes Used in Climate Models: Long-Wave Results, *Journal of Geophysical Research*, 96(D5), 8929-8953, 1991.
- (1034) Schwarzkopf, M.D., and S.B. Fels, The Simplified Exchange Method Revisited: An Accurate, Rapid Method for Computation of Infrared Cooling Rates and Fluxes, *Journal of Geophysical Research*, 96(D5), 9075-9096, 1991.
- * (1035) Feigelson, E.M., B.A. Fomin, I.A. Gorchakova, E.V. Rozanov, Yu. M. Timofeyev, A.N. Trotsenko, and M.D. Schwarzkopf, Calculation of Long-wave Radiation Fluxes in Atmospheres, *Journal of Geophysical Research*, 96(D5), 8985-9001, 1991.
- (1036) Manabe, S., Studies of Glacial Climates by Coupled Atmosphere-Ocean Models: How Useful are Coupled Models?, in *Global Changes of the Past*, edited by R.S. Bradley, pp. 421-448, 1989 OIES Global Change Institute, Snowmass, CO, 24 July-4 August 1989, UCAR/Office for Interdisciplinary Earth Studies, Boulder, CO, 1989.
- * (1037) Peixoto, J.P., A.H. Oort, M. de Almeida, and A. Tome, Entropy Budget of the Atmosphere, *Journal of Geophysical Research*, 96(D6), 10,981-10,988, 1991.
- * (1038) Fels, S.B., J.T. Kiehl, A.A. Lacis, and M.D. Schwarzkopf, Infrared Cooling Rate Calculations in Operational General Circulation Models: Comparisons with Benchmark Computations, *Journal of Geophysical Research*, 96(D5), 9105-9120, 1991.
- * (1039) Karoly, D.J., and D.S. Graves, On Data Sources and Quality for the Southern Hemisphere Stratosphere, in *Dynamics, Transport and Photochemistry in the Middle Atmosphere of the Southern Hemisphere*, edited by A. O'Neill, pp. 19-32, NATO ASI Series C, Vol. 321, Kluwer Academic Press, 1990.
- * (1040) Lee, S., Baroclinic Wave Pockets in Models and Observations, Ph.D. Dissertation, Atmospheric and Oceanic Sciences Program, Princeton University, 1991.
- * (1041) Mitchell, J.F.B., S. Manabe, V. Meleshko, and T. Tokioka, Equilibrium Climate Change - and Its Implications for the Future, in *Climate Change, the IPCC Scientific Assessment*, edited by J.T. Houghton, G.J. Jenkins and J.J. Ephraums, pp. 137-164, Cambridge University Press, 1990.

*In collaboration with other organizations

(1042) Manabe, S., R.J. Stouffer, M.J. Spelman, and K. Bryan, Transient Responses of a Coupled Ocean-Atmosphere Model to Gradual Changes of Atmospheric CO₂, Part I: Annual Mean Response, *Journal of Climate*, 4(8), 785-818, 1991.

* (1043) Wallace, J.M., D.J. Baker, M.L. Blackmon, J.D. Mahlman, J. Blackmon, and J. Shukla, *Prospects for Extending the Range of Prediction of the Global Atmosphere*, National Research Council, National Academy Press, 33 pp., 1991.

* (1044) Mellor, G.L., and T. Ezer, A Gulf Stream Model and an Altimetry Assimilation Scheme, *Journal of Geophysical Research*, 96(C5), 8779-8795, 1991.

* (1045) Mellor, G.L., Notes and Correspondence: An Equation of State for Numerical Models of Oceans and Estuaries, *Journal of Atmospheric and Oceanic Technology*, 8, 609-611, 1991.

* (1046) Milly, P.C.D., Some Current Themes in Physical Hydrology of the Land-Atmosphere Interface, in *Hydrological Interactions Between Atmosphere, Soil, and Vegetation*, edited by G. Kienitz, P.C.D. Milly, M. Genuchten, D. Rosbjerg and W.J. Shuttleworth, pp. 3-10, International Association of Hydrological Sciences, 1991.

* (1047) Joos, F., J.L. Sarmiento, and U. Siegenthaler, Estimates of the Effect of Southern Ocean Iron Fertilization on Atmospheric CO₂ Concentrations, *Nature*, 349(6312), 772-775, 1991.

(1048) Sarmiento, J.L., Slowing the Buildup of Fossil CO₂ in the Atmosphere by Iron Fertilization: A Comment, *Global Biogeochemical Cycles*, 5(1), 1-2, 1991.

* (1049) Nuttle, W.K., J.S. Wroblewski, and J.L. Sarmiento, Advances in Modeling Ocean Primary Production and Its Role in the Global Carbon Cycle, *Advances in Space Research*, 11(3), 367-376, 1991.

* (1050) Joos, F., U. Siegenthaler, and J.L. Sarmiento, Possible Effects of Iron Fertilization in the Southern Ocean on Atmospheric CO₂ Concentration, *Global Biogeochemical Cycles*, 5(2), 135-150, 1991.

* (1051) Kasibhatla, P.S., H. Levy II, W.J. Moxim, and W.L. Chameides, The Relative Impact of Stratospheric Photochemical Production on Tropospheric NO_y Levels: A Model Study, *Journal of Geophysical Research*, 96(D10), 18,631-18,646, 1991.

(1052) Lipps, F.B., and R.S. Hemler, Numerical Modeling of a Midlatitude Squall Line: Features of the Convection and Vertical Momentum Flux, *Journal of the Atmospheric Sciences*, 48(17), 1909-1929, 1991.

(1053) Orlanski, I., and J. Katzfey, The Life Cycle of a Cyclone Wave in the Southern Hemisphere, Part I: Eddy Energy Budget, *Journal of the Atmospheric Sciences*, 48(17), 1972-1998, 1991.

* (1054) Cook, K.H., and A. Gnanadesikan, Effects of Saturated and Dry Land Surfaces on the Tropical Circulation and Precipitation in a General Circulation Model, *Journal of Climate*, 4(9), 873-889, 1991.

*In collaboration with other organizations

(1055) Bryan, K., Michael Cox (1941-1989): His Pioneering Contributions to Ocean Circulation Modeling, *Journal of Physical Oceanography*, 21(9), 1259-1270, 1991.

(1056) Hamilton, K., Climatological Statistics of Stratospheric Inertia Gravity Waves Deduced from Historical Rocketsonde Wind and Temperature Data, *Journal of Geophysical Research*, 96(D11), 20,831-20,839, 1991.

* (1057) Toggweiler, J.R., K. Dixon, and W.S. Broecker, The Peru Upwelling and the Ventilation of the South Pacific Thermocline, *Journal of Geophysical Research*, 96(C11), 20,467-20,497, 1991.

* (1058) Ramaswamy, V., and J.D. Mahlman, Climatic Effects of Trace Gases in the Atmosphere, *Proceedings of the CFC Issue and Greenhouse Effect, Asia-Pacific Conference*, Singapore, pp. 172-185, 1991.

* (1059) Boer, G.J., K. Arpe, M. Blackburn, M. Deque, W.L. Gates, T.L. Hart, H. le Treut, E. Roeckner, D.A. Sheinin, I. Simmonds, R.N.B. Smith, T. Tokioka, R.T. Wetherald, and D. Williamson, An Intercomparison of the Climates Simulated by 14 Atmospheric General Circulation Models, CAS/JSC Working Group on Numerical Experimentation, WCRP-58, WMO/TD No. 425, 1991.

* (1060) Orlanski, I., J. Katzfey, C. Menendez, and M. Marino, Simulation of an Extratropical Cyclone in the Southern Hemisphere: Model Sensitivity, *Journal of the Atmospheric Sciences*, 48(21), 2293-2311, 1991.

(1061) Orlanski, I., Atmospheric Fronts, in *Encyclopedia of Earth System Science*, edited by W.A. Nierenberg, Vol. 1, pp. 201-216, Academic Press, 1992.

* (1062) Manzini, E., A Numerical Study of the Middle Atmosphere Response to Tropical and Subtropical Tropospheric Heat Sources, Ph.D. Dissertation, Atmospheric and Oceanic Sciences Program, Princeton University, 1992.

(1063) Lau, N.-C., and M.J. Nath, Variability of the Baroclinic and Barotropic Transient Eddy Forcing Associated with Monthly Changes in the Midlatitude Storm Tracks, *Journal of the Atmospheric Sciences*, 48(24), 2589-2613, 1991.

(1064) Hemler, R.S., F.B. Lipps, and B.B. Ross, A Simulation of a Squall Line Using a Nonhydrostatic Cloud Model with a 5-km Horizontal Grid, *Monthly Weather Review*, 119(12), 3012-3033, 1991.

* (1065) Peixoto, J.P., and A.H. Oort, *Physics of Climate*, 520 pp., American Institute of Physics, New York, NY, 1992.

(1066) Cook, K.H., and I.M. Held, The Stationary Response to a Large-Scale Orography in a General Circulation Model and a Linear Model, *Journal of the Atmospheric Sciences*, 49(6), 525-539, 1992.

(1067) Manabe, S., M.J. Spelman, and R.J. Stouffer, Transient Responses of a Coupled Ocean-Atmosphere Model to Gradual Changes of Atmospheric CO₂, Part II: Seasonal Response, *Journal of Climate*, 5(2), 105-126, 1992.

*In collaboration with other organizations

- * (1068) Blain, C.A., and P.C.D. Milly, Development and Application of a Hillslope Hydrologic Model, *Advances in Water Resources*, 14(4), 168-174, 1991.
- * (1069) Najjar, R.G., J.L. Sarmiento, and J.R. Toggweiler, Downward Transport and Fate of Organic Matter in the Ocean: Simulations with a General Circulation Model, *Global Biogeochemical Cycles*, 6(1), 45-76, 1992.
- * (1070) Milly, P.C.D., Potential Evaporation and Soil Moisture in General Circulation Models, *Journal of Climate*, 5(3), 209-226, 1992.
- * (1071) Ramaswamy, V., M.D. Schwarzkopf, and K.P. Shine, Radiative Forcing of Climate from Halocarbon-Induced Global Stratospheric Ozone Loss, *Nature*, 355, 810-812, 1992.
- (1072) Toggweiler, J.R., Catalytic Conversions, *Nature*, 356, 665-666, 1992.
- * (1073) Milly, P.C.D., Land Surface Processes and Climate Variability, *EOS, Transactions*, American Geophysical Union, 73(15), 163, 1992.
- * (1074) Gordon, A.L., S.E. Zebiak, and K. Bryan, Climate Variability and the Atlantic Ocean, *EOS, Transactions*, American Geophysical Union, 73(15), 161, 164-165, 1992.
- (1075) Lau, N.-C., Book Review of "Teleconnections Linking Worldwide Climate Anomalies", *Science*, 256(5057), 682, 1992.
- * (1076) Lau, N.-C., S.G.H. Philander, and M.J. Nath, Simulation of ENSO-like Phenomena with a Low-Resolution Coupled GCM of the Global Ocean and Atmosphere, *Journal of Climate*, 5(4), 284-307, 1992.
- * (1077) Philander, S.G.H., R.C. Pacanowski, N.-C. Lau, and M.J. Nath, Simulation of ENSO with a Global Atmospheric GCM Coupled to a High-Resolution Tropical Pacific Ocean GCM, *Journal of Climate*, 5(4), 308-329, 1992.
- * (1078) Kushnir, Y., and N.-C. Lau, The General Circulation Model Response to a North Pacific SST Anomaly: Dependence on Time Scale and Pattern Polarity, *Journal of Climate*, 5(4), 271-283, 1992.
- (1079) Mahlman, J.D., Understanding Climate Change, Science and Policy Associates, Inc., *Report of Findings: Joint Climate Project to Address Decision Makers' Uncertainties*, edited by J.C. Bernabo and P.D. Eglinton, 16 pp., 1992.
- * (1080) Tziperman, E., W.C. Thacker, and K. Bryan, Computing the Steady Oceanic Circulation Using an Optimization Approach, *Dynamics of Atmospheres and Oceans*, 16(5), 379-403, 1992.
- * (1081) Neelin, J.D., M. Latif, M.A.F. Allaart, M.A. Cane, U. Cubasch, W.L. Gates, P.R. Gent, M. Ghil, C. Gordon, N.-C. Lau, C.R. Mechoso, G.A. Meehl, J.M. Oberhuber, S.G.H. Philander, P.S. Schopf, K.R. Sperber, A. Sterl, T. Tokioka, J. Tribbia, and S.E. Zebiak, Tropical Air-Sea Interaction in General Circulation Models, *Climate Dynamics*, 7(2), 73-104, 1992.
- * (1082) Wu, G., and N.-C. Lau, A GCM Simulation of the Relationship Between Tropical Storm Formation and ENSO, *Monthly Weather Review*, 120(6), 958-977, 1992.

*In collaboration with other organizations

- * (1083) Garner, S.T., and A.J. Thorpe, The Development of Organized Convection in a Simplified Squall-Line Model, *Quarterly Journal of the Royal Meteorological Society*, 118, 101-124, 1992.
- * (1084) Sarmiento, J.L., J.C. Orr, and U. Siegenthaler, A Perturbation Simulation of CO₂ Uptake in an Ocean General Circulation Model, *Journal of Geophysical Research*, 97(C3), 3621-3645, 1992.
- * (1085) Sarmiento, J.L., and U. Siegenthaler, New Production and the Global Carbon Cycle, in *Primary Productivity and Biogeochemical Cycles in the Sea*, edited by P. Falkowski, pp. 317-322, Plenum Press, New York, NY, 1992.
- * (1086) Sarmiento, J.L., and E. Sundquist, Revised Budget for the Oceanic Uptake of Anthropogenic Carbon Dioxide, *Nature*, 356, 589-593, 1992.
- * (1087) Sarmiento, J.L., and J.C. Orr, Three-Dimensional Simulations of the Impact of the Southern Ocean Nutrients Depletion on Atmospheric CO₂ and Ocean Chemistry, *Limnology and Oceanography*, 36(8), 1928-1950, 1991.
- * (1088) Sarmiento, J.L., Oceanic Uptake of Anthropogenic CO₂: The Major Uncertainties, *Global Biogeochemical Cycles*, 5(4), 309-313, 1991.
- * (1089) Herbert, T.D., and J.L. Sarmiento, Ocean Nutrient Distribution and Oxygenation: Limits on the Formation of Warm Saline Bottom Water in the Oceans over the Past 90 Years, *Geology*, 19, 702-705, 1992.
- * (1090) Orr, J.C., and J.L. Sarmiento, Potential of Marine Macroalgae as a Sink for CO₂: Constraints from a 3-D General Circulation Model of the Global Ocean, *Water, Air and Soil Pollution*, 64, 405-421, 1992.
- (1091) Bryan, K., Poleward Heat Transport in the Ocean: A Review of a Hierarchy of Models of Increasing Resolution, A Contribution to the Friberghs Herrgard Symposium, *Tellus*, 43AB, 104-115, 1991.
- * (1092) Ezer, T., and G.L. Mellor, A Numerical Study of the Variability and the Separation of the Gulf Stream, Induced by Surface Atmospheric Forcing and Lateral Boundary Flows, *Journal of Physical Oceanography*, 22(6), 660-682, 1992.
- * (1093) Ezer, T., G.L. Mellor, and D.-S. Ko, Nowcasting the Gulf Stream Structure with a Primitive Equation Model and Assimilation of Altimetry and SST Data, *Proceedings of MTS '91*, Marine Technology Society Meeting, 10-14 November 1991, New Orleans, LA, pp. 236-241, 1991.
- (1094) Holloway, L., Atmospheric Sun Protection Factor on Clear Days: Its Observed Dependence on Solar Zenith Angle and Its Relevance to the Shadow Rule for Sun Protection, *Photochemistry and Photobiology*, (56)2, 229-234, 1992.
- * (1095) Ramaswamy, V., and S.M. Freidenreich, A Study of Broadband Parameterizations of the Solar Radiative Interactions with Water Vapor and Water Drops, *Journal of Geophysical Research*, 97(D11), 11,487-11,512, 1992.

*In collaboration with other organizations

(1096) Stern, W.F., and J.J. Ploshay, A Scheme for Continuous Data Assimilation, *Monthly Weather Review*, 120(7), 1417-1432, 1992.

(1097) Gordon, C.T., Comparison of 30-Day Integrations with and without Cloud-Radiation Interaction, *Monthly Weather Review*, 120(7), 1244-1277, 1992.

* (1098) Verma, R.K., ENSO-Monsoon Linkages as Evidenced from Pacific SST Correlations with Monsoon Precipitation, *TOGA Notes*, 6, 1-3, 1992.

(1099) Broccoli, A.J., and S. Manabe, Reply to Evans, *Geophysical Research Letters*, 19(14), 1525-1526, 1992.

(1100) Mahlman, J.D., Assessing Global Climate Change: When Will We Have Better Evidence?, in *Climate Change and Energy Policy*, edited by L. Rosen and R. Glasser, pp. 17-31, American Institute of Physics, NY, 1992.

(1101) Ross, R.J., and Y. Kurihara, A Simplified Scheme to Simulate Asymmetries Due to the Beta Effect in Barotropic Vortices, *Journal of the Atmospheric Sciences*, 49(17), 1620-1628, 1992.

* (1102) Oltmans, S.J., and H. Levy II, Seasonal Cycle of Surface Ozone Over the Western North Atlantic, *Nature*, 358, 392-394, 1992.

(1103) Lipps, F.B., and R.S. Hemler, On the Downward Transfer of Tritium to the Ocean by a Cloud Model, *Journal of Geophysical Research*, 97(D12), 12,889-12,900, 1992.

* (1104) Ezer, T., D.-S. Ko, and G.L. Mellor, Modeling and Forecasting the Gulf Stream, *Marine Technology Society Journal*, 26(2), 5-14, 1992.

* (1105) Oey, L.-Y., T. Ezer, G.L. Mellor, and P. Chen, A Model Study of "Bump" Induced Western Boundary Current Variabilities, *Journal of Marine Systems*, 3(4/5), 321-342, 1992.

(1106) Ploshay, J.J., W.F. Stern, and K. Miyakoda, FGGE Reanalysis at GFDL, *Monthly Weather Review*, 120(9), 2083-2108, 1992.

* (1107) Held, I.M., and E. O'Brien, Quasigeostrophic Turbulence in a Three-Layer Model: Effects of Vertical Structure in the Mean Shear, *Journal of the Atmospheric Sciences*, 49(19), 1861-1870, 1992.

* (1108) Stephenson, D., and K. Bryan, Large-Scale Electric and Magnetic Fields Generated by the Oceans, *Journal of Geophysical Research*, 97(C10), 15,467-15,480, 1992.

* (1109) Garner, S.T., N. Nakamura, and I.M. Held, Nonlinear Equilibration of Two-Dimensional Eady Waves: New Perspective, *Journal of the Atmospheric Sciences*, 49(21), 1984-1996, 1992.

(1110) Mahlman, J.D., A Looming Arctic Ozone Hole?, *Nature*, 360, 209-210, 1992.

* (1111) Lau, K.-H., and N.-C. Lau, The Energetics and Propagation Dynamics of Tropical Summertime Synoptic Scale Disturbances, *Monthly Weather Review*, 120(11), 2523-2539, 1992.

*In collaboration with other organizations

(1112) Delworth, T., S. Manabe, and R. Stouffer, Interdecadal Variability of the Thermohaline Circulation in a Coupled Ocean-Atmosphere Model, *Proceedings from the Principal Investigators Meeting*, University of Miami, Miami, Florida, 9-11 March 1992, The Atlantic Climate Change Program, NOAA Climate and Global Change Program, Special Report #7, 1992.

* (1113) Lofgren, B., Sensitivity and Feedbacks Associated with Vegetation-Related Land Surface Parameters in a General Circulation Model, Ph.D. Dissertation, Atmospheric and Oceanic Sciences Program, Princeton University, 1993.

* (1114) Chang, E.K.M., Downstream Development of Baroclinic Waves, Ph.D. Dissertation, Atmospheric and Oceanic Sciences Program, Princeton University, 1993.

* (1115) Hamilton, K., and L. Yuan, Experiments on Tropical Stratospheric Mean-Wind Variations in a Spectral General Circulation Model, *Journal of the Atmospheric Sciences*, 49(24), 2464-2483, 1992.

* (1116) Orlanski, I., and E.K.M. Chang, Ageostrophic Geopotential Fluxes in Downstream and Upstream Development of Baroclinic Waves, *Journal of the Atmospheric Sciences*, 50(2), 212-225, 1993.

* (1117) Anderson, L.A., The Determination of Redfield Ratios for Use in Global Oceanic Nutrient Cycle Models, Ph.D. Dissertation, Atmospheric and Oceanic Sciences Program, Princeton University, 1993.

(1118) Hayashi, Y., and D.G. Golder, Tropical 40-50- and 25-30-Day Oscillations Appearing in Realistic and Idealized GFDL Climate Models and the ECMWF Dataset, *Journal of the Atmospheric Sciences*, 50(3), 464-494, 1993.

(1119) Ploshay, J., W. Stern, and K. Miyakoda, A Summary Report on FGGE Re-analysis at GFDL, *Data Assimilation Systems*, BMRC Research Report No. 27, pp. 29-53, Melbourne, Australia, 1991.

(1120) Hamilton, K., What We Can Learn from General Circulation Models about the Spectrum of Middle Atmospheric Motions, in *Coupling Processes in the Lower and Middle Atmosphere*, edited by E.V. Thrane et al., pp. 161-174, Kluwer Academic Publishers, 1992.

(1121) Manabe, S., and R.J. Stouffer, Reply to Comments on "Two Stable Equilibria of a Coupled Ocean-Atmosphere Model", *Journal of Climate*, 6(1), 178-179, 1993.

* (1122) Schwarzkopf, M.D., and V. Ramaswamy, Radiative Forcing due to Ozone in the 1980s: Dependence on Altitude of Ozone Change, *Geophysical Research Letters*, 20(3), 205-208, 1993.

(1123) Broccoli, A.J., and S. Manabe, The Effects of Orography on Midlatitude Northern Hemisphere Dry Climates, *Journal of Climate*, 5(11), 1181-1201, 1992.

* (1124) Oort, A.H., and H. Liu, Upper-Air Temperature Trends Over the Globe, 1958-1989, *Journal of Climate*, 6(2), 292-307, 1993.

* (1125) Chang, E.K.M., and I. Orlanski, On the Dynamics of a Storm Track, *Journal of the Atmospheric Sciences*, 50(7), 999-1015, 1993.

*In collaboration with other organizations

(1126) Bryan, K., Ocean Circulation Models, in *Strategies for Future Climate Research*, edited by M. Latif, pp. 265-285, Max Planck Institute fur Meteorologie, Hamburg, Germany, 1991.

(1127) Lau, N.-C., Climate Variability Simulated in GCMs, in *Climate System Modeling*, edited by K.E. Trenberth, pp. 617-642, Cambridge University Press, 1992.

(1128) Lanzante, J.R., A Comparison of the Stationary Wave Responses in Several GFDL Increased CO₂ GCM Experiments, *Proceedings of the Sixteenth Annual Climate Diagnostics Workshop*, Lake Arrowhead, CA, pp. 241-246, 1991.

* (1129) Milly, P.C.D., Sensitivity of the Global Water Cycle to the Water-Holding Capacity of Soils, *Proceedings of the Yokohama Symposium*, Yokohama, Japan, pp. 495-501, 1993.

* (1130) Savoie, D.L., J.M. Prospero, S.J. Oltmans, W.C. Graustein, K.K. Turekian, J.T. Merrill, and H. Levy II, Sources of Nitrate and Ozone in the Marine Boundary Layer of the Tropical North Atlantic, *Journal of Geophysical Research*, 97(D11), 11,575-11,589, 1992.

(1131) Held, I.M., Large-Scale Dynamics and Global Warming, *Bulletin of the American Meteorological Society*, 74(2), 228-241, 1993.

* (1132) Imbrie, J., E.A. Boyle, S.C. Clemens, A. Duffy, W.R. Howard, G. Kukla, J. Kutzbach, D.G. Martinson, A. McIntyre, A.C. Mix, B. Molfino, J.J. Morley, L.C. Peterson, N.G. Pisias, W.L. Prell, M.E. Raymo, N.J. Shackleton, and J.R. Toggweiler, On the Structure and Origin of Major Glaciation Cycles, 1. Linear Responses to Milankovitch Forcing, *Paleoceanography*, 7(6), 701-738, 1992.

(1133) Donner, L.J., A Cumulus Parameterization Including Mass Fluxes, Vertical Momentum Dynamics, and Mesoscale Effects, *Journal of the Atmospheric Sciences*, 50(6), 889-906, 1993.

(1134) Mahlman, J.D., Modeling Perspectives on Global Monitoring Requirements, *Proceedings of the NOAA Workshop on Assuring the Quality and Continuity of NOAA's Environmental Data*, Silver Spring, MD, December 1991, pp. 19-26, 1993.

* (1135) Murray, J.W., M.W. Leinen, R.A. Feely, J.R. Toggweiler, and R. Wanninkhof, EqPac: A Process Study in the Central Equatorial Pacific, *Oceanography*, 5(3), 134-142, 1992.

* (1136) Freidenreich, S.M., and V. Ramaswamy, Solar Radiation Absorption by CO₂, Overlap with H₂O, and a Parameterization for General Circulation Models, *Journal of Geophysical Research*, 98(D4), 7255-7264, 1993.

* (1137) Kasibhatla, P.S., H. Levy II, and W.J. Moxim, Global NO_x, HNO₃, PAN, and NO_y Distributions from Fossil Fuel Combustion Emissions: A Model Study, *Journal of Geophysical Research*, 98(D4), 7165-7180, 1993.

(1138) Held, I.M., and P.J. Phillipps, Sensitivity of the Eddy Momentum Flux to Meridional Resolution in Atmospheric GCMs, *Journal of Climate*, 6(3), 499-507, 1993.

*In collaboration with other organizations

(1139) Kurihara, Y., M.A. Bender, R.E. Tuleya, and R.J. Ross, Hurricane Forecasting with the GFDL Automated Prediction System, in *Preprints, 20th Conference on Hurricanes and Tropical Meteorology*, 10-14 May 1993, San Antonio, TX, pp. 323-326, American Meteorological Society, Boston, MA, 1993.

(1140) Ross, R.J., and Y. Kurihara, Hurricane-Environment Interaction in Hurricanes Gloria and Gilbert, *Preprints, 20th Conference on Hurricanes and Tropical Meteorology*, 10-14 May 1993, San Antonio, TX, pp. 27-30, American Meteorological Society, Boston, MA, 1993.

* (1141) Hakkinen, S., G.L. Mellor, and L.H. Kantha, Modeling Deep Convection in the Greenland Sea, *Journal of Geophysical Research*, 97(C4), 5389-5408, 1992.

* (1142) Sarmiento, J.L., Biogeochemical Ocean Models, in *Climate System Modeling*, edited by K. Trenberth, pp. 519-549, Cambridge University Press, Cambridge, MA, 1992.

* (1143) Sarmiento, J.L., and J.C. Orr, The Iron Fertilization Strategy, *Proceedings of the Conference "Oceans, Climate, Man"*, Fondazione, San Paolo, Italy, 1992.

* (1144) Lee, S., and I. Held, Baroclinic Wave Packets in Models and Observations, *Journal of the Atmospheric Sciences*, 50(10), 1413-1428, 1993.

(1145) Delworth, T., and S. Manabe, Climate Variability and Land Surface Processes, *Advances in Water Resources*, 16, 3-20, 1993.

(1146) Manabe, S., and R.J. Stouffer, Century-Scale Effects of Increased Atmospheric CO₂ on the Ocean-Atmosphere System, *Nature*, 364(6434), 215-218, 1993.

(1147) Kurihara, Y., M.A. Bender, and R.J. Ross, An Initialization Scheme of Hurricane Models by Vortex Specification, *Monthly Weather Review*, 121(7), 2030-2045, 1993.

(1148) Bender, M.A., R.J. Ross, R.E. Tuleya, and Y. Kurihara, Improvements in Tropical Cyclone Track and Intensity Forecasts Using the GFDL Initialization System, *Monthly Weather Review*, 121(7), 2046-2061, 1993.

(1149) Anderson, J.L., The Climatology of Blocking in a Numerical Forecast Model, *Journal of Climate*, 6(6), 1042-1056, 1993.

* (1150) Yuan, L., Statistical Equilibrium Dynamics in a Forced-Dissipative f-plane Shallow-Water Model, Ph.D. Dissertation, Atmospheric and Oceanic Sciences Program, Princeton University, 1993.

* (1151) Levy II, H., W.J. Moxim, and P.S. Kasibhatla, Impact of Global NO_x Sources on the Northern Latitudes, in *The Tropospheric Chemistry of Ozone in the Polar Regions*, edited by H. Niki and K.H. Becker, pp. 77-88, NATO ASI Series I, Vol. 7, Springer-Verlag, Berlin, 1993.

(1152) Kurihara, Y., Hurricanes and Atmospheric Processes, in *Relating Geophysical Structures and Processes: The Jeffreys Volume*, edited by K. Aki and R. Dmowska, pp. 19-26, Geophysical Monograph 76, IUGG, Vol. 16, American Geophysical Union, 1993.

*In collaboration with other organizations

- * (1153) Manzini, E., and K. Hamilton, Middle Atmospheric Traveling Waves Forced by Latent and Convective Heating, *Journal of the Atmospheric Sciences*, 50(14), 2180-2200, 1993.
- * (1154) Chang, E.K.M., Downstream Development of Baroclinic Waves as Inferred from Regression Analysis, *Journal of the Atmospheric Sciences*, 50(13), 2038-2053, 1993.
- * (1155) Sarmiento, J.L., R.D. Slater, M.J.R. Fasham, H.W. Ducklow, J.R. Toggweiler, and G.T. Evans, A Seasonal Three-Dimensional Ecosystem Model of Nitrogen Cycling in the North Atlantic Euphotic Zone, *Global Biogeochemical Cycles*, 7(2), 417-450, 1993.
- (1156) Toggweiler, J.R., and B. Samuels, Is the Magnitude of the Deep Outflow from the Atlantic Ocean Actually Governed by Southern Hemisphere Winds?, in *The Global Carbon Cycle*, edited by M. Heimann, pp. 303-331, NATO ASI Series I, Vol. 15, Springer-Verlag, Berlin, 1993.
- (1157) Toggweiler, J.R., and B. Samuels, New Radiocarbon Constraints on the Upwelling of Abyssal Water to the Ocean's Surface, in *The Global Carbon Cycle*, edited by M. Heimann, pp. 333-366, NATO ASI Series I, Vol. 15, Springer-Verlag, Berlin, 1993.
- * (1158) Matano, R.P., On the Separation of the Brazil Current from the Coast, *Journal of Physical Oceanography*, 23(1), 79-90, 1993.
- * (1159) Matano, R.P., and S.G.H. Philander, Heat and Mass Balances of the South Atlantic Ocean Calculated from a Numerical Model, *Journal of Geophysical Research*, 98(C1), 977-984, 1993.
- * (1160) Ezer, T., G.L. Mellor, D.-S. Ko, and Z. Sirkes, A Comparison of Gulf Stream Sea Surface Height Fields Derived from Geosat Altimeter Data and Those Derived from Sea Surface Temperature Data, *Journal of Atmospheric and Oceanic Technology*, 10(1), 76-87, 1993.
- * (1161) Hakkinen, S., and G.L. Mellor, Modeling the Seasonal Variability of a Coupled Arctic Ice-Ocean System, *Journal of Geophysical Research*, 97(C12), 20,285-20,304, 1992.
- * (1162) Nakamura, N., Momentum Flux, Flow Symmetry, and the Nonlinear Barotropic Governor, *Journal of the Atmospheric Sciences*, 50(14), 2159-2179, 1993.
- * (1163) Gerdes, R., A Primitive Equation Ocean Circulation Model Using a General Vertical Coordinate Transformation, 1: Description and Testing of the Model, *Journal of Geophysical Research*, 98(C8), 14,683-14,701, 1993.
- * (1164) Gerdes, R., A Primitive Equation Ocean Circulation Model Using a General Vertical Coordinate Transformation, 2: Application to an Overflow Problem, *Journal of Geophysical Research*, 98(C8), 14,703-14,726, 1993.
- * (1165) Sarmiento, J.L., Ocean Carbon Cycle, *Chemical and Engineering News*, 71, 30-43, 1993.

*In collaboration with other organizations

- * (1166) Fasham, M.J.R., J.L. Sarmiento, R.D. Slater, H.W. Ducklow, and R. Williams, Ecosystem Behavior at Bermuda Station "S" and Ocean Weather Station "India", A General Circulation Model and Observational Analysis, *Global Biogeochemical Cycles*, 7, 379-415, 1993.
- * (1167) Kasibhatla, P.S., NO_y from Sub-sonic Aircraft Emissions: A Global, Three-Dimensional Model Study, *Geophysical Research Letters*, 20(16), 1707-1710, 1993.
- (1168) Hamilton, K., A General Circulation Model Simulation of El Niño Effects in the Extratropical Northern Hemisphere Stratosphere, *Geophysical Research Letters*, 20(17), 1803-1806, 1993.
- * (1169) Ting, M.-F., and N.-C. Lau, A Diagnostic and Modeling Study of the Monthly Mean Wintertime Anomalies Appearing in a 100-Year GCM Experiment, *Journal of the Atmospheric Sciences*, 50(17), 2845-2867, 1993.
- * (1170) Armstrong, R.A., A Comparison of Index-Based and Pixel-Based Neighborhood Simulations of Forest Growth, *Ecology*, 74(6), 1707-1712, 1993.
- * (1171) Ramaswamy, V., and C.-T. Chen, An Investigation of the Global Solar Radiative Forcing Due to Changes in Cloud Liquid Water Path, *Journal of Geophysical Research*, 98(D9), 16,703-16,712, 1993.
- (1172) Hamilton, K., Notes and Correspondence: An Examination of Observed Southern Oscillation Effects in the Northern Hemisphere Stratosphere, *Journal of the Atmospheric Sciences*, 50(20), 3468-3473, 1993.
- * (1173) Siegenthaler, U., and J.L. Sarmiento, Atmospheric Carbon Dioxide and the Ocean, *Nature*, 365, 119-125, 1993.
- * (1174) Sarmiento, J.L., Atmospheric CO₂ Stalled, *Nature*, 365, 697-698, 1993.
- * (1175) Slater, R.D., J.L. Sarmiento, and M.J.R. Fasham, Some Parametric and Structural Simulations with a Three Dimensional Ecosystem Model of Nitrogen Cycling in the North Atlantic Euphoric Zone, in *Long-Term Monitoring of Global Climate Forcings and Feedbacks*, pp. 1-5, NASA Conference Publication 3234, 1993.
- * (1176) Stephenson, D.B., and I.M. Held, GCM Response of Northern Winter Stationary Waves and Storm Tracks to Increasing Amounts of Carbon Dioxide, *Journal of Climate*, 6(10), 1859-1870, 1993.
- (1177) Orlanski, I., and J. Sheldon, A Case of Downstream Baroclinic Development over Western North America, *Monthly Weather Review*, 121(11), 2929-2950, 1993
- (1178) Hamilton, K., Model Simulation of the Stratospheric Penetration of the Southern Oscillation, *Toga Notes*, 13, 7-11, 1993.
- * (1179) Xue, H.-J., and G.L. Mellor, Instability of the Gulf Stream Front in the South Atlantic Bight, *Journal of Physical Oceanography*, 23(11), 2326-2350, 1993
- (1180) Milly, P.C.D., An Analytic Solution of the Stochastic Storage Problem Applicable to Soil Water, *Water Resources Research*, 29(11), 3755-3758, 1993.

*In collaboration with other organizations

- * (1181) Imbrie, J., A. Berger, E.A. Boyle, S.C. Clemens, A. Duffy, W.R. Howard, G. Kukla, J. Kutzbach, D.G. Martinson, A. McIntyre, A.C. Mix, B. Molfino, J.J. Morley, L.C. Peterson, N.G. Pisias, W.L. Prell, M.E. Raymo, N.J. Shackleton, and J.R. Toggweiler, On the Structure and Origin of Major Glaciation Cycles, 2. The 100,000-year Cycle, *Paleoceanography*, 8(6), 699-735, 1993.
- (1182) Delworth, T., S. Manabe, and R.J. Stouffer, Interdecadal Variations of the Thermohaline Circulation in a Coupled Ocean-Atmosphere Model, *Journal of Climate*, 6(11), 1993-2011, 1993.
- * (1183) Held, I.M., R.S. Hemler, and V. Ramaswamy, Radiative-Convective Equilibrium with Explicit Two-Dimensional Moist Convection, *Journal of the Atmospheric Sciences*, 50(23), 3909-3927, 1993.
- * (1184) Xie, S.P., A. Kubokawa, and K. Hanawa, Evaporation-Wind Feedback and the Organizing of Tropical Convection on the Planetary Scale, Part II: Nonlinear Evolution, *Journal of the Atmospheric Sciences*, 50(23), 3884-3893, 1993.
- * (1185) Tziperman, E., and K. Bryan, Estimating Global Air-Sea Fluxes from Surface Properties and from Climatological Flux Data using an Oceanic General Circulation Model, *Journal of Geophysical Research*, 98(C12), 22,629-22,644, 1993.
- (1186) Mahlman, J.D., Monitoring Issues from a Modeling Perspective, in *Long-Term Monitoring of Global Climate Forcings and Feedbacks*, pp. 1-5, NASA Conference Publication 3234, 1993.
- * (1187) Chen, C.-T., Sensitivity of the Simulated Global Climate to Perturbations in Low Cloud Microphysical Properties, Ph.D. Dissertation, Atmospheric and Oceanic Sciences Program, Princeton University, 1994.
- * (1188) Nakamura, H., Notes and Correspondence: Horizontal Divergence Associated with Zonally Isolated Jet Streams, *Journal of the Atmospheric Sciences*, 50(14), 2310-2313, 1993.
- * (1189) Nakamura, H., and J.M. Wallace, Synoptic Behavior of Baroclinic Eddies during the Blocking Onset, *Monthly Weather Review*, 121(7), 1892-1903, 1993.
- (1190) Kurihara, Y., Surface Conditions in Tropical Cyclone Models, Modelling Severe Weather, paper presented at the Fourth BMRC Modelling Workshop, 26-29 October 1992, BMRC Research Report #39, edited by J.D. Jasper and P.J. Meighen, pp. 69-74, 1993.
- (1191) Kurihara, Y., R.E. Tuleya, M.A. Bender, and R.J. Ross, Advanced Modeling of Tropical Cyclones, *Proceedings of ICSU/WMO International Symposium on Tropical Cyclone Disasters*, 12-16 October 1992, pp. 190-201, Beijing, China, 1993.
- (1192) Manabe, S., and R.J. Stouffer, Multiple Century Response of a Coupled Ocean-Atmosphere Model to an Increase of Atmospheric Carbon Dioxide, *Journal of Climate*, 7(1), 5-23, 1994.

*In collaboration with other organizations

- * (1193) Mahlman, J.D., J.P. Pinto, and L.J. Umscheid, Transport, Radiative, and Dynamical Effects of the Antarctic Ozone Hole: A GFDL "SKYHI" Model Experiment, *Journal of the Atmospheric Sciences*, 51(4), 489-508, 1994.
- (1194) Manabe, S., R.J. Stouffer, and M.J. Spelman, Response of a Coupled Ocean-Atmosphere Model to Increasing Atmospheric Carbon Dioxide, *Ambio*, 23(1), 44-49, 1994.
- (1195) Held, I.M., Lectures on the General Circulation of the Atmosphere, *Proceedings of the Atmosphere-Ocean Dynamics and Interannual Climate Variability*, Friday Harbor Summer School, University of Washington, 19 July-21 August 1993, 35 pp., 1994.
- (1196) Delworth, T.L., Tracer Transport in a Quasi-Geostrophic Ocean Model, *Proceedings of the Atmosphere-Ocean Dynamics and Interannual Climate Variability*, Friday Harbor Summer School, University of Washington, 19 July-21 August 1993, 13 pp., 1994.
- * (1197) Hamilton, K., R.J. Wilson, and H. Vahlenkamp, Three-Dimensional Visualization of the Stratospheric Polar Vortex, *Canadian Meteorological and Oceanographic Society Bulletin*, 22(4), 4-6, 1994.
- * (1198) Bender, M., I. Ginis, and Y. Kurihara, Numerical Simulations of Tropical Cyclone-Ocean Interaction with a High-Resolution Coupled Model, *Journal of Geophysical Research*, 98(D12), 23,245-23,263, 1993.
- (1199) Tuleya, R., Tropical Storm Development and Decay: Sensitivity to Surface Boundary Conditions, *Monthly Weather Review*, 122(2), 291-304, 1994.
- (1200) Orlanski, I., and B.D. Gross, Orographic Modification of Cyclone Development, *Journal of the Atmospheric Sciences*, 51(4), 589-611, 1994.
- * (1201) Stouffer, R.J., S. Manabe, and K.Ya. Vinnikov, Model Assessment of the Role of Natural Variability in Recent Global Warming, *Nature*, 367, 634-636, 1994.
- * (1202) Bryan, K., and F.C. Hansen, A Toy Model of North Atlantic Climate Variability on a Decade to Century Time-Scale, in *Natural Climate Variability on Decade-to-Century Time Scales*, edited by D.G. Martinson, K. Bryan, M. Ghil, M.M. Hall, T.R. Karl, E.S. Sarachik, S. Sorooshian, and L.D. Talley, National Academy Press, Washington, DC, 1994.
- * (1203) Lau, N.-C., and K.-H. Lau, Simulation of the Asian Summer Monsoon in a 40-Year Experiment with a General Circulation Model, in *Proceedings of Second International Conference on East Asia and Western Pacific Meteorology and Climate*, 7-10 September 1992, edited by W.J. Kyle and C.P. Chang, pp. 49-56, World Scientific, Publishing Co., Singapore, 1993.
- * (1204) Xie, S.P., On Preferred Zonal Scale of Wave-CISK with Conditional Heating, *Journal of the Meteorological Society of Japan*, 72(1), 19-30, 1994.
- * (1205) Pavan, V., Parameter Study of the Statistically Steady-State of a Multi-Layer Quasi-Geostrophic Model, Ph.D. Dissertation, Atmospheric and Oceanic Sciences Program, Princeton University, 1994.

*In collaboration with other organizations

- * (1206) Murnane, R.J., J.K. Cochran, and J.L. Sarmiento, Estimates of Particle and Thorium Cycling Rate Constants in the Northwest Atlantic Ocean, *Journal of Geophysical Research*, 99(C2), 3373-3392, 1994.
- * (1207) Murnane, R., Determination of Thorium and Particulate Matter Cycling Parameters at Station P: A Re-analysis and Comparison of Least Squares Techniques, *Journal of Geophysical Research*, 99(C2), 3393-3405, 1994.
- * (1208) Chao, Y., and S.G.H. Philander, On the Structure of the Southern Oscillation, *Journal of Climate*, 6(3), 450-469, 1993.
- * (1209) Peixoto, J.P., and A.H. Oort, On the Forced Regime of the General Circulation of the Atmosphere, *Transactions of the Academy of Sciences*, Lisbon, Portugal, Vol. 32, pp. 111-148, 1993.
- * (1210) Peixoto, J.P., and A.H. Oort, The Forcing of the Zonal Mean State of the Atmosphere, *Transactions of the Academy of Sciences*, Lisbon, Portugal, Vol. 32, pp. 149-179, 1993.
- * (1211) Sun, D.-Z., and R.S. Lindzen, A PV View of the Zonal Mean Distribution of Temperature and Wind in the Extratropical Troposphere, *Journal of the Atmospheric Sciences*, 51(5), 757-772, 1994.
- * (1212) Ramaswamy, V., Perturbation of the Climate System due to Stratospheric Ozone Depletion, *Chemistry of the Atmosphere Symposium Proceedings*, Preprints, American Chemical Society, Division of Petroleum Chemistry, 37(4), 1546-1551, 1993.
- (1213) Knutson, T.R., and S. Manabe, Impact of Increasing CO₂ on the Walker Circulation and ENSO-like Phenomena in a Coupled Ocean-Atmosphere Model, in *Preprints, 6th Conference on Climate Variations*, 23-28 January 1994, Nashville, TN, pp. 80-81, American Meteorological Society, Boston, MA, 1994.
- (1214) Najjar, R.G., and R.J. Toggweiler, Reply to the Comment by Jackson, *Limnology and Oceanography*, 38(6), 1331-1332, 1993.
- * (1215) Liu, Z., Thermocline Forced by Varying Ekman Pumping, Part II: Annual and Decadal Ekman Pumping, *Journal of Physical Oceanography*, 23(12), 2523-2540, 1993.
- * (1216) Anderson, J.L., and H.M. van den Dool, Skill and Return of Skill in Dynamic Extended-Range Forecasts, *Monthly Weather Review*, 122(3), 507-516, 1994.
- * (1217) Liu, Z., Notes and Correspondence: Interannual Positive Feedbacks in a Simple Extratropical Air-Sea Coupling System, *Journal of the Atmospheric Sciences*, 50(17), 3022-3028, 1993.
- (1218) Donner, L.J., Radiative Forcing by Parameterized Ice Clouds in a General Circulation Model, in *Preprints, The 8th Conference on Atmospheric Radiation*, 23-28 January 1994, Nashville, TN, pp. 110-112, American Meteorological Society, Boston, MA, 1994.

*In collaboration with other organizations

(1219) Stouffer, R.J., The Geophysical Fluid Dynamics Laboratory (GFDL) Model Integration, in *An Intercomparison of Selected Features of the Control Climates Simulated by Coupled Ocean-Atmosphere General Circulation Models*, pp. 3-7, WCRP-82, WMO/TD No. 574, 1993.

(1220) Hamilton, K., Interdecadal Climate Variations Over the High-Latitude North Atlantic as Seen in 235 Years of Surface Air Temperature Data, *Canadian Meteorological and Oceanographic Society Bulletin*, 22(2), 11-14, 1994.

(1221) Lau, N.-C., Environmental Crisis of the Twenty-First Century: Air and Sunshine, Part I: (in Chinese), "Twenty-First Century" *Bimonthly*, No. 21, February 1994, pp. 69-76, published by Institute of Chinese Studies, Chinese University of Hong Kong, 1994.

(1222) Lau, N.-C., Environmental Crisis of the Twenty-First Century: Air and Sunshine, Part II: (in Chinese), "Twenty-First Century" *Bimonthly*, No. 22, April 1994, pp. 69-77, published by Institute of Chinese Studies, Chinese University of Hong Kong, 1994.

* (1223) Oort, A.H., L.A. Anderson, and J.P. Peixoto, Estimates of the Energy Cycle of the Oceans, *Journal of Geophysical Research*, 99(C4), 7665-7688, 1994.

* (1224) Strahan, S.E., and J.D. Mahlman, Evaluation of the GFDL SKYHI General Circulation Model using Aircraft N₂O Measurements: 1. Polar Winter Stratospheric Meteorology and Tracer Morphology, *Journal of Geophysical Research*, 99(D5), 10,305-10,318, 1994.

* (1225) Strahan, S.E., and J.D. Mahlman, Evaluation of the GFDL SKYHI General Circulation Model using Aircraft N₂O Measurements: 2. Tracer Variability and Diabatic Meridional Circulation, *Journal of Geophysical Research*, 99(D5), 10,319-10,332, 1994.

(1226) Hamilton, K., Modelling Middle Atmosphere Interannual Variability, *Proceedings of the Fifth Cospar Colloquium*, Columbia, MD, August 1993, edited by M. Teague, D. Baker and V. Papitashvi, pp. 751-757, Pergamon Press, 1994.

(1227) Milly, P.C.D., and K.A. Dunne, Sensitivity of the Global Water Cycle to the Water-Holding Capacity of Land, *Journal of Climate*, 7(4), 506-526, 1994.

(1228) Tziperman, E., J.R. Toggweiler, Y. Feliks, and K. Bryan, Instability of the Thermohaline Circulation with Respect to Mixed Boundary Conditions: Is it Really a Problem for Realistic Models?, *Journal of Physical Oceanography*, 24(2), 217-232, 1994.

* (1229) Matano, R.P., and S.G.H. Philander, On the Decay of the Meanders of Eastward Currents, *Journal of Physical Oceanography*, 24(2), 298-304, 1994.

* (1230) Raval, A., A. Oort, and V. Ramaswamy, Observed Dependence of Outgoing Longwave Radiation on Sea Surface Temperature and Moisture, *Journal of Climate*, 7(5), 807-821, 1994.

(1231) Phillipps, P.J., and I.M. Held, The Response to Orbital Perturbations in an Atmospheric Model Coupled to a Slab Ocean, *Journal of Climate*, 7(5), 767-782, 1994.

*In collaboration with other organizations

- * (1232) Gross, B.D., Frontal Interaction with Isolated Orography, *Journal of the Atmospheric Sciences*, 51(11), 1480-1496, 1994.
- * (1233) Boer, G., R. Colman, M. Dix, V. Galin, M. Helfand, J. Kiehl, A. Kitoh, W. Lau, X.-Z. Liang, V. Lykossov, B. McAvaney, K. Miyakoda, and S. Planton, Cloud Radiative Effects on Implied Oceanic Energy Transports as Simulated by Atmospheric General Circulation Models, PCMDI Report #15, UCRL-ID-116893, University of California, Lawrence Livermore National Laboratory, Livermore, CA, 1994.
- * (1234) Kasahara, A., A.P. Mizzi, and L.J. Donner, Diabatic Initialization for Improvement in the Tropical Analysis of Divergence and Moisture using Satellite Radiometric Imagery Data, *Tellus*, 46A(3), 242-264, 1994.
- * (1235) Anderson, L.A., and J.L. Sarmiento, Redfield Ratios of Remineralization Determined by Nutrient Data Analysis, *Global Biogeochemical Cycles*, 8(1), 65-80, 1994.
- * (1236) Sarmiento, J.L., and M. Bender, Carbon Biogeochemistry and Climate Change, *Photosynthesis Research*, 39, 209-234, 1994.
- (1237) Orlanski, I., Energy Dispersion vs. Baroclinic Conversion in the Life Cycle of Atmospheric Eddies, *Proceedings of the Life Cycle of Extratropical Cyclone Conference*, Bergen, Norway, 27 June-2 July 1994, 1994.
- * (1238) Ohfuchi, W., The Sensitivity of an Atmospheric General Circulation Model to Large Changes in Carbon Dioxide Level, Ph.D. Dissertation, Atmospheric and Oceanic Sciences Program, Princeton University, 1994.
- * (1239) Seman, C.J., A Numerical Study of Nonlinear Nonhydrostatic Conditional Symmetric Instability in a Convectively Unstable Atmosphere, *Journal of the Atmospheric Sciences*, 51(11), 1352-1371, 1994.
- * (1240) Colman, R.A., B.J. McAvaney, and R.T. Wetherald, Sensitivity of the Australian Surface Hydrology and Energy Budgets to a Doubling of CO₂, *Australian Meteorological Magazine*, 43, 105-116, 1994.
- * (1241) Molinari, R.L., D. Battisti, K. Bryan, and J. Walsh, The Atlantic Climate Change Program, *Bulletin of the American Meteorological Society*, 75(7), 1191-1199, 1994.
- * (1242) Milly, P.C.D., Climate, Soil Water Storage, and the Average Annual Water Balance, *Water Resources Research*, 30(7), 2143-2156, 1994.
- * (1243) Galloway, J.N., H. Levy II, and P.S. Kasibhatla, Year 2020: Consequences of Population Growth and Development on Deposition of Oxidized Nitrogen, *Ambio*, 23(2), 120-123, 1994.
- * (1244) Oltmans, S.J., and H. Levy II, Surface Ozone Measurements from a Global Network, *Atmospheric Environment*, 28(1), 9-24, 1994.
- * (1245) Chameides, W.L., P.S. Kasibhatla, J. Yienger, and H. Levy II, Growth of Continental-Scale Metro-Agro-Plexes, Regional Ozone Pollution, and World Food Production, *Science*, 264, 74-77, 1994.

*In collaboration with other organizations

(1246) Broccoli, A.J., and S. Manabe, Climate Model Studies of Interactions Between Ice Sheets and the Atmosphere-Ocean System, in *Ice in the Climate System*, edited by W.R. Peltier, Springer-Verlag, Berlin, NATO ASI Series I, Vol. 12, pp. 271-290, 1993.

* (1247) Soden, B.J., and L.J. Donner, Evaluation of a GCM Cirrus Parameterization using Satellite Observations, *Journal of Geophysical Research*, 99(D7), 14,401-14,413, 1994.

* (1248) Ezer, T., On the Interaction Between the Gulf Stream and the New England Seamount Chain, *Journal of Physical Oceanography*, 24(1), 191-204, 1994.

* (1249) Ezer, T., and G.L. Mellor, Continuous Assimilation of Geosat Altimeter Data into a Three-Dimensional Primitive Equation Gulf Stream Model, *Journal of Physical Oceanography*, 24(4), 832-847, 1994.

* (1250) Ezer, T., and G.L. Mellor, Diagnostic and Prognostic Calculations of the North Atlantic Circulation and Sea Level Using a Sigma Coordinate Ocean Model, *Journal of Geophysical Research*, 99(C7), 14,159-14,171, 1994.

* (1251) Mellor, G.L., T. Ezer, and L.-Y. Oey, The Pressure Gradient Conundrum of Sigma Coordinate Ocean Models, *Journal of Atmospheric and Oceanic Technology*, 11(4), 1126-1134, 1994.

* (1252) Koberle, C., and S.G.H. Philander, On the Processes that Control Seasonal Variations of Sea Surface Temperatures in the Tropical Pacific Ocean, *Tellus*, 46A, 481-496, 1994.

* (1253) Armstrong, R.A., Grazing Limitation and Nutrient Limitation in Marine Ecosystems: Steady State Solutions of an Ecosystem Model with Multiple Food Chains, *Limnology and Oceanography*, 39(3), 597-608, 1994.

* (1254) Scanlon, B.R., and P.C.D. Milly, Water and Heat Fluxes in Desert Soils, 2. Numerical Simulations, *Water Resources Research*, 30(3), 721-733, 1994.

* (1255) Navarra, A., W.F. Stern, and K. Miyakoda, Reduction of the Gibbs Oscillation in Spectral Model Simulations, *Journal of Climate*, 7(8), 1169-1183, 1994.

(1256) Lau, N.-C., and M.J. Nath, A Modeling Study of the Relative Roles of Tropical and Extratropical SST Anomalies in the Variability of the Global Atmosphere-Ocean System, *Journal of Climate*, 7(8), 1184-1207, 1994.

* (1257) Nakamura, H., Rotational Evolution of Potential Vorticity Associated with a Strong Blocking Flow Configuration over Europe, *Geophysical Research Letters*, 21(18), 2003-2006, 1994.

(1258) Broccoli, A.J., Learning From Past Climates, *Nature* (News and Views), 371, 282, 1994.

* (1259) Milly, P.C.D., Climate, Interseasonal Storage of Soil Water, and the Annual Water Balance, *Advances in Water Resources*, 17, 19-24, 1994.

*In collaboration with other organizations

- * (1260) Ramaswamy, V., and M.M. Bowen, Effect of Changes in Radiatively Active Species upon the Lower Stratospheric Temperatures, *Journal of Geophysical Research*, 99(D9), 18,909-18,921, 1994.
- * (1261) Xie, S.P., The Maintenance of an Equatorially Asymmetric State in a Hybrid Coupled GCM, *Journal of the Atmospheric Sciences*, 51(18), 2602-2612, 1994.
- (1262) Hamilton, K., Meteorology and Climatology, in *Encyclopedia of Applied Physics*, 10, 215-237, VCH Publishers, Inc., 1994.
- * (1263) Soden, B.J., S.A. Ackerman, D.O'C. Starr, S. H. Melfi, and R.A. Ferrare, Comparison of Upper Tropospheric Water Vapor from GOES, Raman Lidar, and Cross-chain Loran Atmospheric Sounding System Measurements, *Journal of Geophysical Research*, 99(D10), 21,005-21,016, 1994.
- * (1264) Xie, S.P., and S.G.H. Philander, A Coupled Ocean-Atmosphere Model of Relevance to the ITCZ in the Eastern Pacific, *Tellus*, 46A, 340-350, 1994.
- * (1265) Xie, S.P., Oceanic Response to the Wind Forcing Associated with the Intertropical Convergence Zone in the Northern Hemisphere, *Journal of Geophysical Research*, 99(C10), 20,393-20,402, 1994.
- (1266) Broccoli, A.J., Climate Model Sensitivity, Paleoclimate and Future Climate Change, in *Long-Term Climatic Variations*, edited by J.-C. Duplessy and M.-T. Spyridakis, NATO ASI Series I, Vol. 22, Springer-Verlag, Berlin, pp. 551-567, 1994.
- (1267) Toggweiler, J.R., The Ocean's Overturning Circulation, *Physics Today*, 47(11), 45-50, 1994.
- (1268) Knutson, T.R., and S. Manabe, Impact of Increased CO₂ on Simulated ENSO-Like Phenomena, *Geophysical Research Letters*, 21(21), 2295-2298, 1994.
- * (1269) Held, I.M., and M.J. Suarez, A Proposal for the Intercomparison of the Dynamical Cores of Atmospheric General Circulation Models, *Bulletin of the American Meteorological Society*, 75(10), 1825-1830, 1994.
- * (1270) Karoly, D.J., J.A. Cohen, G.A. Meehl, J.F.B. Mitchell, A.H. Oort, R.J. Stouffer, and R.T. Wetherald, An Example of Fingerprint Detection of Greenhouse Climate Change, *Climate Dynamics*, 10, 97-105, 1994.
- * (1271) Randall, D.A., R.D. Cess, J.P. Blanchet, S. Chalita, R. Colman, D.A. Dazlich, A.D. DelGenio, E. Keup, A. Lacis, H. Le Treut, X.-Z. Liang, B.J. McAvaney, J.F. Mahfouf, V.P. Meleshko, J.-J. Morcrette, P.M. Norris, G.L. Potter, L. Rikus, E. Roeckner, J.F. Royer, U. Schleise, D.A. Sheinin, A.P. Sokolov, K.E. Taylor, R.T. Wetherald, I. Yagai, and M.-H. Zhang, Analysis of Snow Feedbacks in 14 General Circulation Models, *Journal of Geophysical Research*, 99(D10), 20,757-20,771, 1994.
- (1272) Hayashi, Y., and D.G. Golder, Kelvin and Mixed Rossby-Gravity Waves Appearing in the GFDL "SKYHI" General Circulation Model and the FGGE Dataset: Implications for their Generation Mechanism and Role in the QBO, *Journal of the Meteorological Society of Japan*, 72(6), 901-935, 1994

*In collaboration with other organizations

(1273) Toggweiler, J.R., Vanishing in Bermuda, *Nature (News and Views)*, 372, 505-506, 1994.

(1274) Hamilton, K., R.J. Wilson, J.D. Mahlman, and L.J. Umscheid, Climatology of the SKYHI Troposphere-Stratosphere-Mesosphere General Circulation Model, *Journal of the Atmospheric Sciences*, 52(1), 5-43, 1995.

(1275) Hamilton, K., Interannual Variability in the Northern Hemisphere Winter Middle Atmosphere in Control and Perturbed Experiments with the GFDL SKYHI General Circulation Model, *Journal of the Atmospheric Sciences*, 52(1), 44-66, 1995.

* (1276) Yuan, L., and K. Hamilton, Equilibrium Dynamics in a Forced-Dissipative f-Plane Shallow Water System, *Journal of Fluid Mechanics*, 280, 369-394, 1994.

* (1277) Branstator, G., and I.M. Held, Westward Propagating Normal Modes in the Presence of Stationary Background Waves, *Journal of the Atmospheric Sciences*, 52(2), 247-262, 1995.

(1278) Garner, S.T., Permanent and Transient Upstream Effects in Nonlinear Stratified Flow over a Ridge, *Journal of the Atmospheric Sciences*, 52(2), 227-246, 1995.

* (1279) Held, I.M., R.T. Pierrehumbert, S.T. Garner, and K.L. Swanson, Surface Quasi-Geostrophic Dynamics, *Journal of Fluid Mechanics*, 282, 1-20, 1995.

* (1280) Liu, Z., and S.-P. Xie, Equatorward Propagation of Coupled Air-Sea Disturbances with Application to the Annual Cycle of the Eastern Tropical Pacific, *Journal of the Atmospheric Sciences*, 51(24), 3807-3822, 1994.

* (1281) Ross, R.J., and Y. Kurihara, A Numerical Study on Influences of Hurricane Gloria (1985) on the Environment, *Monthly Weather Review*, 123(2), 332-346, 1995.

* (1282) Xie, S.-P., On the Genesis of the Equatorial Annual Cycle, *Journal of Climate*, 7(12), 2008-2013, 1994.

* (1283) Burpee, R.W., J.L. Franklin, S.J. Lord, and R.E. Tuleya, The Performance of Hurricane Track Guidance Models With and Without Omega Dropwindsondes, *Preprint of 21st AMS Conference on Hurricanes and Tropical Meteorology*, 1995.

* (1284) Wu, C.-C., and K.A. Emanuel, Potential Vorticity Diagnostics of Hurricane Movement. Part I: A Case Study of Hurricane Bob (1991), *Monthly Weather Review*, 123(1), 69-92, 1995.

* (1285) Wu, C.-C., and K.A. Emanuel, Potential Vorticity Diagnostics of Hurricane Movement. Part II: Tropical Storm Ana (1991) and Hurricane Andrew (1992), *Monthly Weather Review*, 123(1), 93-109, 1995.

(1286) Manabe, S., R.J. Stouffer, and M.J. Spelman, Interaction Between Polar Climate and Global Warming, *Fourth Conference on Polar Meteorology and Oceanography*, Dallas, TX, 15-20 January 1995, American Meteorological Society, Boston, MA, pp. 1-9, 1995.

*In collaboration with other organizations

(1287) Hamilton, K., Aspects of Mesospheric Simulation in a Comprehensive General Circulation Model, in *The Upper Mesosphere and Lower Thermosphere: A Review of Experiment and Theory*, Geophysical Monograph 87, American Geophysical Union, pp. 255-264, 1995.

* (1288) Sarmiento, J.L., C. LeQuéré, and S.W. Pacala, Limiting Future Atmospheric Carbon Dioxide, *Global Biogeochemical Cycles*, 9(1), 121-137, 1995.

(1289) Lanzante, J.R., Circulation Response in GFDL Increased CO₂ Experiments and Comparison with Observed Data, *Proceedings of the Seventeenth Annual Climate Diagnostic Workshop*, Norman, OK, October 1992, pp. 248-253, 1993.

* (1290) Pierrehumbert, R.T., I.M. Held, and K.L. Swanson, Spectra of Local and Non-Local Two-Dimensional Turbulence, *Chaos, Solitons, and Fractals*, 4(6), 1111-1116, 1994.

* (1291) Willems, R.C., S.M. Glenn, M.F. Crowley, P. Malanotte-Rizzoli, R.E. Young, T. Ezer, G.L. Mellor, H.G. Arango, A.R. Robinson, and C.-C.A. Lai, Experiment Evaluates Ocean Models and Data Assimilation in the Gulf Stream, *EOS, Transactions*, American Geophysical Union, 75(34), 385,391,394, 1994.

* (1292) Moody, J.L., S.J. Oltmans, H. Levy II, and J.T. Merrill, Transport Climatology of Tropospheric Ozone: Bermuda, 1988-1991, *Journal of Geophysical Research*, 100(D4), 7179-7194, 1995.

* (1293) Gu, D., and S.G.H. Philander, Secular Changes of Annual and Interannual Variability in the Tropics During the Past Century, *Journal of Climate*, 8(4), 864-876, 1995.

* (1294) Armstrong, R.A., J.L. Sarmiento, and R.D. Slater, Monitoring Ocean Productivity by Assimilating Satellite Chlorophyll into Ecosystem Models, in *Ecological Time Series*, edited by T.M. Powell and J.H. Steele, pp. 371-390, 1995.

(1295) Kurihara, Y., M.A. Bender, and R.E. Tuleya, Performance Evaluation of the GFDL Hurricane Prediction System in the 1994 Hurricane Season, *Proceedings of the 21st Conference on Hurricanes and Tropical Meteorology*, Miami, FL, 24-28 April 1995, American Meteorological Society, Boston, MA, pp. 41-43, 1995.

* (1296) Zhang, J., Effects of Latent Heating on Midlatitude Atmospheric General Circulation, Ph.D. Dissertation, Atmospheric and Oceanic Sciences Program, Princeton University, 1995.

(1297) Donner, L.J., Validating Cumulus Parameterizations using Cloud (System)-Resolving Models, *Proceedings of the 21st Conference on Hurricanes and Tropical Meteorology*, Miami, FL, 24-28 April 1995, American Meteorological Society, Boston, MA, pp. 564-566, 1995.

(1298) Bender, M.A., Numerical Study of the Asymmetric Structure in the Interior of Tropical Cyclones, *Proceedings of the 21st Conference on Hurricanes and Tropical Meteorology*, Miami, FL, 24-28 April 1995, American Meteorological Society, Boston, MA, pp. 600-602, 1995.

*In collaboration with other organizations

(1299) Hayashi, Y., and D.G. Golder, The Generation Mechanism of Tropical Transient Waves: Control Experiments and a Unified Theory with Moist Convective Adjustment, *Proceedings of the 10th Conference on Atmospheric and Oceanic Waves and Stability*, Big Sky, MT, 5-9 June 1995, American Meteorological Society, Boston, MA, pp. 7-8, 1995.

(1300) Stern, W.F., and K. Miyakoda, Feasibility of Seasonal Forecasts Inferred from Multiple GCM Simulations, *Journal of Climate*, 8(5), 1071-1085, 1995.

(1301) Hamilton, K., Comment on "Global QBO in Circulation and Ozone. Part I: Re-examination of Observational Evidence," *Journal of the Atmospheric Sciences*, 52(10), 1834-1838, 1995.

* (1302) Gleckler, P.J., D.A. Randall, G. Boer, R. Colman, M. Dix, V. Galin, M. Helfand, J. Kiehl, A. Kitoh, W. Lau, X.-Y. Liang, V. Lykossov, B. McAvaney, K. Miyakoda, S. Planton, and W. Stern, Cloud-Radiative Effects on Implied Oceanic Energy Transports as Simulated by Atmospheric General Circulation Models, *Geophysical Research Letters*, 22(7), 791-794, 1995.

* (1303) Shine, K.P., Y. Fouquart, V. Ramaswamy, S. Solomon, and J. Srinivasan, Radiative Forcing, in *Climate Change 1994: Radiative Forcing of Climate Change*, Cambridge University Press, pp. 167-199, 1995.

* (1304) Shine, K.P., K. Labitzke, V. Ramaswamy, P. Simon, S. Solomon, W.-C. Wang, Radiative Forcing and Temperature Trends, WMO/UNEP Scientific Assessment of Stratospheric Ozone Depletion, 1994, Report #37, WMO, Global Ozone Research and Monitoring Project, 1995.

* (1305) Ginis, I., and G. Sutyrin, Hurricane-Generated Depth-Averaged Currents and Sea Surface Elevation, *Journal of Physical Oceanography*, 25(6), 1218-1242, 1995.

* (1306) Zavatarelli, M., and G.L. Mellor, A Numerical Study of the Mediterranean Sea Circulation, *Journal of Physical Oceanography*, 25(6), 1384-1414, 1995.

* (1307) Yienger, J.J., and H. Levy II., Empirical Model of Global Soil-Biogenic NO_x Emissions, *Journal of Geophysical Research*, 100(D6), 11,447-11,464, 1995.

(1308) Rosati, A., R. Gudgel, and K. Miyakoda, Decadal Analysis Produced from an Ocean Data Assimilation System, *Monthly Weather Review*, 123(7), 2206-2228, 1995.

(1309) Lau, N.-C., and M.W. Crane, A Satellite View of the Synoptic-Scale Organization of Cloud Cover in Midlatitude and Tropical Circulation Systems, *Monthly Weather Review*, 123(7), 1984-2006, 1995.

* (1310) Chang, E.K.M., and I. Orlanski, On Energy Flux and Group Velocity of Waves in Baroclinic Flows, *Journal of the Atmospheric Sciences*, 51(24), 3823-3828, 1994.

* (1311) Goddard, L., The Energetics of Interannual Variability in the Tropical Pacific Ocean, Ph.D. Dissertation, Atmospheric and Oceanic Sciences Program, Princeton University, 1995.

*In collaboration with other organizations

(1312) Mehta, V.M., and T.L. Delworth, Decadal Variability of the Tropical Atlantic Ocean Surface Temperature in Shipboard Measurements and in a Global Ocean-Atmosphere Model, *Journal of Climate*, 8(2), 172-190, 1995.

(1313) Toggweiler, J.R., and B. Samuels, Effect of Drake Passage on the Global Thermohaline Circulation, *Deep-Sea Research*, 42(4), 477-500, 1995.

(1314) Toggweiler, J.R., Anthropogenic CO₂ - The Natural Carbon Cycle Reclaims Center Stage, *Reviews of Geophysics*, (Supplement), 1249-1252, 1995.

(1315) Toggweiler, J.R., and B. Samuels, Effect of Sea Ice on the Salinity of Antarctic Bottom Waters, *Journal of Physical Oceanography*, 25(9), 1980-1997, 1995.

(1316) Lanzante, J.R., Analysis of Climate Data Using Resistant, Robust and Nonparametric Techniques: Some Examples and Some Applications to the Historical Radiosonde Record, *Proceedings of the Nineteenth Annual Climate Diagnostics Workshop*, College Park, MD, 14-18 November 1994, pp. 37-40, 1995.

(1317) Sarmiento, J.L., The Carbon Cycle and the Role of the Ocean in Climate, in *Ecological and Social Dimensions of Global Change*, edited by D.D. Caron, F.S. Chapin III, J. Donoghue, M. Firestone, J. Harte, L.E. Wells, and R. Stewardson, Institute of International Studies, University of California, Berkeley, CA, pp.-4-41, 1994.

(1318) Shaffer, G., and J.L. Sarmiento, Biogeochemical Cycling in the Global Ocean, I. A New, Analytical Model with Continuous Vertical Resolution and High Latitude Dynamics, *Journal of Geophysical Research*, 100(C2), 2659-2672, 1995.

(1319) Joos, F., and J.L. Sarmiento, Der Anstieg des Atmospharischen Kohlendioxds, *Physikalische Blatter*, 51(5), 405-411, 1995.

(1320) Sarmiento, J.L., R. Murnane, and C. LeQuéré, Air-Sea CO₂ Transfer and the Carbon Budget of the North Atlantic, *Philosophical Transactions of the Royal Society of London*, B348, 211-219, 1995.

(1321) Anderson, J.L., A Simulation of Atmospheric Blocking with a Forced Barotropic Model, *Journal of the Atmospheric Sciences*, 52(15), 2593-2608, 1995.

* (1322) Lawrence, M.G., W.L. Chameides, P.S. Kasibhatla, H. Levy II, and W.J. Moxim, Lightning and Atmospheric Chemistry: The Rate of Atmospheric NO Production, in *Handbook of Atmospheric Electrodynamics*, edited by Hans Volland, CRC Press, pp. 189-202, 1995.

(1323) Lau, N.-C., The Antarctic Ozone Hole Story, in *United Bulletin*, United College, Chinese University of Hong Kong, pp. 49-53, 1992-93.

* (1324) Chen, C.-T., and V. Ramaswamy, Parameterization of the Solar Radiative Characteristics of Low Clouds and Studies with a General Circulation Model, *Journal of Geophysical Research*, 100(D6), 11,611-11,622, 1995.

* (1325) Liu, Z., and S.G.H. Philander, How Different Wind Stress Patterns Affect the Tropical-Subtropical Circulations of the Upper Ocean, *Journal of Physical Oceanography*, 25(4), 449-462, 1995.

*In collaboration with other organizations

- * (1326) Sun, D.-Z., and A.H. Oort, Humidity-Temperature Relationships in the Tropical Troposphere, *Journal of Climate*, 8(8), 1974-1987, 1995.
- * (1327) Ezer, T., G.L. Mellor, and R.J. Greatbatch, On the Interpentadal Variability of the North Atlantic Ocean: Modeling Changes in Transport, Meridional Heat Flux and Coastal Sea Level Between 1955-1959 and 1970-1974, *Journal of Geophysical Research*, 100(C6), 10,559-10,566, 1995.
- * (1328) Chylek, P., and J. Li, Light Scattering by Small Particles in an Intermediate Region, in *Optics Communications*, 117, 389-394, 1995.
- (1329) Kurihara, Y., M.A. Bender, R.E. Tuleya, and R.J. Ross, Improvements in the GFDL Hurricane Prediction System, *Monthly Weather Review*, 123(9), 2791-2801, 1995.
- (1330) Knutson, T.R., and S. Manabe, Time-mean Response over the Tropical Pacific to Increased CO₂ in a Coupled Ocean-Atmosphere Model, *Journal of Climate*, 8(9), 2183-2199, 1995.
- (1331) Freidenreich, S.M., and V. Ramaswamy, Stratospheric Temperature Response to Improved Solar CO₂ and H₂O Parameterizations, *Journal of Geophysical Research*, 100(D8), 16,721-16,725, 1995.
- (1332) Hamilton, K., Simulation of Vertically-Propagating Waves in Comprehensive General Circulation Models: Opportunities for Comparison with Observations, *Proceedings of the Workshop on Wind Observations in the Middle Atmosphere*, Centre National d'Etudes Spatiales, Paris, France, 15-18 November 1994, pp. 4.3-4.15, 1994.
- (1333) Hamilton, K., Comprehensive Simulation of the Middle Atmospheric Climate: Some Recent Results, *Climate Dynamics*, 11, 223-241, 1995.
- * (1334) Ramaswamy, V., R.J. Charlson, J.A. Coakley, J.L. Gras, Harshvardhan, G. Kukla, M.P. McCormick, D. Moeller, E. Roeckner, L.L. Stowe, and J. Taylor, What are the Observed and Anticipated Meteorological and Climatic Responses to Aerosol Forcing?, Dahlen Workshop Report, in *Aerosol Forcing of Climate*, edited by R.J. Charlson and J. Heintzenberg, Wiley Interscience, pp. 386-399, 1995.
- * (1335) Galloway, J.N., W.H. Schlesinger, H. Levy II, A. Michaels, and J.L. Schnoor, Nitrogen Fixation: Anthropogenic Enhancement-Environmental Response, *Global Biogeochemical Cycles*, 9(2), 235-252, 1995.

*In collaboration with other organizations

MANUSCRIPTS SUBMITTED FOR PUBLICATION

(tg) Oort, A.H., Angular Momentum Cycle in Planet Earth, Contribution to *The Encyclopedia of Planetary Sciences*, February 1993.

* (wa) Pinardi, N., A. Rosati, and R.C. Pacanowski, The Sea Surface Pressure Formulation of Rigid Lid Models, Implications for Altimetric Data Assimilation Studies, *Journal of Marine Systems*, January 1994.

(wh) Wyman, B.L., A Step-Mountain Coordinate General Circulation Model: Description and Validation of Medium Range Forecasts, *Monthly Weather Review*, April 1994.

(wj) Seman, C.J., A Method for Generating an Initial State for Numerical Studies of Nonhydrostatic Conditional Symmetric Instability, *Monthly Weather Review*, May 1994.

(wl) Kurihara, Y., M.A. Bender, R.E. Tuleya, and R.J. Ross, Improvements in the GFDL Hurricane Prediction System, *Monthly Weather Review*, May 1994.

* (wm) Griffies, S.M., and E. Tziperman, A Linear Thermohaline Oscillator Driven by Stochastic Atmospheric Forcing, *Journal of Climate*, May 1994.

(wn) Miyakoda, K., A. Rosati, and R. Gudgel, ENSO Forecasting with a Coupled Model, Part I. The System, *Monthly Weather Review*, May 1994.

* (wu) Larichev, V.D., and I.M. Held, Eddy Amplitudes and Fluxes in a Homogeneous Model of Fully Developed Baroclinic Instability, *Journal of Physical Oceanography*, July 1994.

* (wv) Milly, P.C.D., Reply to Comment on "An Analytic Solution of the Stochastic Storage Problem Applicable to Soil Water", *Water Resources Research*, July 1994.

* (ww) Murnane, R.J., J.K. Cochran, K.O. Buesseler, and M.P. Bacon, Least Squares Estimates of Thorium, Particle, and Nutrient Cycling Rate Constants from the JGOFS North Atlantic Bloom Experiment, *Deep-Sea Research*, August 1994.

* (wy) Galloway, J.N., W.H. Schlesinger, H. Levy II, A. Michaels, and J.L. Schnoor, Nitrogen Fixation: Anthropogenic Enhancement-Environmental Response, *Global Biogeochemical Cycles*, August 1994.

(xc) Bender, M.A., A Numerical Study of the Asymmetric Structure of Tropical Cyclones, *Monthly Weather Review*, August 1994.

* (xf) Ezer, T., and G.L. Mellor, Data Assimilation in the Gulf Stream Region: How Useful are Satellite-Derived Surface Data for Nowcasting the Subsurface Fields?, *Journal of Atmospheric and Oceanic Technology*, August 1994.

* (xg) Chen, P., G.L. Mellor, and T. Ezer, The Optimization of Tidal Boundary Forcing for a U.S. East Coast Tidal Model, *Journal of Physical Oceanography*, August 1994.

* (xh) Overland, J.E., P. Turet, and A.H. Oort, Regional Variations of Moist Static Energy Flux into the Arctic, *Journal of Climate*, August 1994.

*In collaboration with other organizations

- (xi) Anderson, J.L., Selection of Initial Conditions for Ensemble Forecasts in a Simple Perfect Model Framework, *Journal of the Atmospheric Sciences*, August 1994.
- (xk) Orlanski, I., and J. Sheldon, Stages in the Energetics of Baroclinic Systems, *Tellus*, August 1994.
- (xr) Lanzante, J.R., Resistant, Robust and Nonparametric Techniques for the Analysis of Climate Data: Theory and Examples, Including Applications to Historical Radiosonde Station Data, *International Journal of Climatology*, October 1994.
- * (xs) Soden, B.J., and R. Fu, A Satellite Analysis of Deep Convection, Upper Tropospheric Humidity and the Greenhouse Effect, *Journal of Geophysical Research*, October 1994.
- (xt) Rosati, A., K. Miyakoda, and R. Gudgel, The Impact of Ocean Initial Conditions on ENSO Forecasting with a Coupled Model, *Monthly Weather Review*, October 1994.
- (xu) Dunne, K.A., and C.J. Willmott, Global Distribution of Soil Plant-Extractable Water Capacity, *International Journal of Climatology*, October 1994.
- (xv) Konikow, L.F., and P.C.D. Milly, Ground-Water Mining, Atmospheric Moistening, and Sea-Level Change, *Nature* (Scientific Correspondence), November 1994.
- * (ya) Hurt, G.C., and R.A. Armstrong, A Pelagic Ecosystem Model Calibrated with BATS Data, *Deep-Sea Research*, December 1994.
- (yb) Wetherald, R.T., Feedback Processes in the GFDL R30-14 Level General Circulation Model, *Proceedings of the NATO Advanced Research Workshop/FANG 10*, Paris, France, July 12, 1994, December 1994.
- * (yc) Li, J., and V. Ramaswamy, A General Study of Four-Stream Approximation for Solar Radiative Transfer. Part I: An Extension of δ -Eddington Approximation, *Journal of the Atmospheric Sciences*, January 1995.
- (yd) Anderson, J.L., and W.F. Stern, Evaluating the Predictive Utility of Ensemble Forecasts in a Perfect Model Setting, *Journal of Climate*, January 1995.
- (yf) Toggweiler, J.R., and S. Carson, What are Upwelling Systems Contributing to the Ocean's Carbon and Nutrient Budgets?, in *Upwelling in the Oceans: Modern Processes and Ancient Records*, Dahlem Konferenzen, Berlin.
- (yg) Wetherald, R.T., and S. Manabe, The Mechanisms of Summer Dryness Induced by Greenhouse Warming, *Journal of Climate*, January 1995.
- * (yh) Griffies, S.M., and K. Bryan, North Atlantic Thermohaline Circulation Predictability in a Coupled Ocean-Atmosphere Model, *Journal of Climate*, January 1995.
- * (yi) Tziperman, E., J.R. Toggweiler, Y. Feliks, K. Bryan, S.M. Griffies, and B. Samuels, Reply to Rahmstorf's Comment, *Journal of Physical Oceanography*, January 1995.

*In collaboration with other organizations

- * (yj) Lindberg, C., and A.J. Broccoli, Representation of Topography in Spectral Climate Models and Its Effect on Simulated Precipitation, *Journal of Climate*, January 1995.
- (yk) Manabe, S., and R.J. Stouffer, Low Frequency Variation of Surface Air Temperature in a 1,000 Year Integration of a Coupled Ocean-Atmosphere Model, *Journal of Climate*, January 1995.
- * (yl) Broccoli, A.J., S. Manabe, J.F.B. Mitchell, and L. Bengtsson, Comments on "Global Climate Change and Tropical Cyclones", *Bulletin of the American Meteorological Society*, February 1995.
- (ym) Delworth, T.L., S. Manabe, and R.J. Stouffer, Interannual to Interdecadal Variability in a Coupled Ocean-Atmosphere Model, *Proceedings of International Workshop on Numerical Prediction of Oceanic Conditions*, Tokyo, Japan, 7-11 March 1995, February 1995.
- (yn) Milly, P.C.D., Effects of Thermal Vapor Diffusion on Seasonal Dynamics of Water in the Unsaturated Zone, *Water Resources Research*, February 1995.
- (yp) Hamilton, K., Tides, in *Encyclopedia of Climate and Weather*, Oxford University Press, February 1995.
- * (yq) Oort, A.H., and J.J. Yienger, Observed Long-term Variability in the Hadley Circulation and Its Connection to ENSO, *Journal of Climate*, February 1995.
- * (yr) Jones, P.W., C.L. Kerr, and R.S. Hemler, A Scalable Version of the GFDL SKYHI General Circulation Model, *Parallel Computing*, March 1995.
- (ys) Delworth, T.L., North Atlantic Interannual Variability in a Coupled Ocean-Atmosphere Model, *Journal of Climate*, March 1995.
- (yt) Mahlman, J.D., Toward a Scientifically Centered Climate Monitoring System, *Climatic Change*, January 1995.
- * (yu) Pavan, V., and I.M. Held, The Diffusive Approximation for Eddy Fluxes in Baroclinically Unstable Jets, *Journal of the Atmospheric Sciences*, March 1995.
- * (yv) Kushnir, Y., and I.M. Held, On the Equilibrium Atmospheric Response to North Atlantic SST Anomalies, *Journal of Climate*, March 1995.
- * (yw) Held, I.M., and V.D. Lariehev, A Scaling Theory for Horizontally Homogeneous, Baroclinically Unstable Flow on a Beta-Plane, *Journal of the Atmospheric Sciences*, March 1995.
- * (yx) Sun, D.-Z., and I.M. Held, A Comparison of Modeled and Observed Relationships between Interannual Variations of Water Vapor and Temperature, *Journal of Climate*, March 1995.
- (yy) Anderson, J.L., A Method for Producing and Evaluating Probabilistic Forecasts from Ensemble Model Integrations, *Journal of Climate*, March 1995.

*In collaboration with other organizations

(yz) Miyakoda, K., J. Ploshay, and A. Rosati, Preliminary Study on SST Forecast Skill Associated with El Niño Process, using Coupled Model Data Assimilation, *Atmosphere and Ocean Dynamics, Canada*, March 1995.

* (za) Soden, B.J., and F.P. Bretherton, Interpretation of TOVS Water Vapor Radiances using a Random Strong Line Model, *Journal of Geophysical Research*, April 1995.

* (zb) Aikman, F., G.L. Mellor, T. Ezer, D. Sheinin, P. Chen, L. Breaker, K. Bosley, and D.B. Rao, Toward an Operational Nowcast/Forecast System for the U.S. East Coast, in *Modern Approaches to Data Assimilation in Ocean Modeling*, Elsevier Publishing, April 1995.

* (zc) Mellor, G.L., and T. Ezer, Sea Level Variations Induced by Heating and Cooling: An Evaluation of the Boussinesq Approximation in Ocean Models, *Journal of Geophysical Research*, April 1995.

* (zd) Kasibhatla, P.S., W.L. Chameides, H. Levy II, and A. Kloncki, Large-Scale Impact of Photochemical Pollution on Boundary-Layer Ozone over the North Atlantic Ocean during Summer, *Science*, March, 1995.

* (ze) Broccoli, A.J., and E.P. Marciniak, Comparing Simulated Glacial Climate and Paleodata: A Re-examination, *Paleoceanography*, April 1995.

* (zf) Hsieh, W.W., and K. Bryan, The Steric Component of Sea Level Rise Associated with Enhanced Greenhouse Warming: A Simple Model Study, *Climate Dynamics*, April 1995.

* (zg) Bryan, K., Sea Level Rise Associated with Enhanced Greenhouse Warming: A Model Study, *Climate Dynamics*, April 1995.

(zh) Soden, B.J., and J.R. Lanzante, Satellite and Radiosonde Climatologies of Upper Tropospheric Water Vapor, *Journal of Climate*, April 1995.

* (zi) Chen, C.-T., and V. Ramaswamy, Sensitivity of Simulated Global Climate to Perturbations in Low Cloud Microphysical Properties, Part I: Globally Uniform Perturbations, *Journal of Climate*, May 1995.

* (zj) Kasibhatla, P.S., H. Levy II, and A. Kloncki, A Three-dimensional View of the Large-Scale Tropospheric Ozone Distribution over the North Atlantic Ocean during the Summer, *Journal of Geophysical Research*, May 1995.

(zk) Manabe, S., and R.J. Stouffer, Impact of Fresh Water Infusion on the Thermohaline Circulation, *Nature*, May 1995.

* (zl) Donner, L.J., J. Warren, and J. Ström, Implementing Microphysics at Physically Appropriate Scales in GCMs, *Proceedings of the WCRP Workshop on Cloud Microphysics in GCMs*, June 1995.

(zm) Wilson, R.J., and K. Hamilton, Comprehensive Model Simulation of Thermal Tides in the Martian Atmosphere, *Journal of the Atmospheric Sciences*, June 1995.

* (zn) Ramaswamy, V., and C.-T. Chen, Climate Sensitivity to Greenhouse and Solar Radiative Perturbations, *Nature*, June 1995.

*In collaboration with other organizations

(zo) Ramaswamy, V., Longwave Radiation, in *Encyclopedia of Climate and Weather*, Oxford University Press, June 1995.

* (zp) Peixoto, J.P., and A.H. Oort, On the Climatology of Relative Humidity in the Atmosphere, *Journal of Climate*, June 1995.

* (zq) Armstrong, R.A., Structurally and Parametrically Congruent Tree-by-Tree and Landscape-Level Simulators of Forest Growth, *Ecology*, June 1995.

* (zr) Levy II, H., W.J. Moxim, and P.S. Kasibhatla, A Global Three-Dimensional Time-dependent Lightning Source of Tropospheric NO₂, *Journal of Geophysical Research*, June 1995.

(zs) Stern, W.F., Tropical Intraseasonal Variability in the GFDL/DERF GCM during AMIP, *Proceedings of AMIP Scientific Conference*, Monterey, CA, June 1995.

* (zt) Shine, K.P., B.P. Briegleb, A.S. Grossman, D. Hauglustaine, H. Mao, V. Ramaswamy, M.D. Schwarzkopf, R. Van Dorland, and W.-C. Wang, Radiative Forcing Due to Changes in Ozone: A Comparison of Different Codes, in *Atmospheric Ozone as a Climate Gas*, edited by W.-C. Wang and I.S.A. Isaksen, NATO ARW Series, Springer-Verlag, 1995.

* (zu) Beegle, C.J., K.W. Dixon, and R.H. Gammon, The Chlorofluorocarbon Transient in the North Pacific: A Model-Observation Comparison, *Journal of Physical Oceanography*, July 1995.

(zv) Lanzante, J.R., Lag Relationships Involving Tropical Sea Surface Temperatures, *Journal of Climate*, July 1995.

* (zw) Moxim, W.J., H. Levy II, and P.S. Kasibhatla, Simulated Global Tropospheric PAN: Its Transport and Impact on NO_x, *Journal of Geophysical Research*, July 1995.

(zx) Lau, N.-C., Variability of the Midlatitude Atmospheric Circulation in Relation to Tropical and Extratropical Sea Surface Temperature Anomalies, *Monograph in Celebration of the 80th Birthday of Professor T.C. Yeh*, July 1995.

(zy) Lau, N.-C., and M.J. Nath, The Role of the "Atmospheric Bridge" in Linking Tropical Pacific ENSO Events to Extratropical SST Anomalies, *Journal of Climate (Stan Hayes Special Issue)*, July 1995.

* (zz) Goswami, B.N., Internally Generated and Externally Forced Interannual Variations of Indian Summer Monsoon, *Journal of Climate*, August 1995.

* (aa) Frey, R.A., S.A. Ackerman, and B.J. Soden, Climate Parameters from Satellite Spectral Measurements, Part I: Collocated AVHRR and HIRS/2 Observations of Spectral Greenhouse Parameter, *Journal of Climate*, August 1995.

* (ab) Chen, C.-T., E. Roeckner, and B.J. Soden, A Comparison of Satellite Observations and Model Simulations of Column Integrated Moisture and Upper Tropospheric Humidity, *Journal of Climate*, August 1995.

(ac) Anderson, L., and J.L. Sarmiento, Global Ocean Phosphate and Oxygen Simulations, *Global Biogeochemical Cycles*, August 1995.

*In collaboration with other organizations

(ad) Figueroa, H.A., and J.L. Sarmiento, Thermocline Ventilation in a North Atlantic General Circulation Model, *Journal of Geophysical Research*, August 1995.

* (ae) Wacongne, S., and R.C. Pacanowski, Seasonal Heat Transport in a Primitive Equation Model of the Tropical Indian Ocean, *Journal of Physical Oceanography*, August 1995.

* (af) Li, X., P. Chang, and R.C. Pacanowski, A Wave-Induced Mixing Mechanism in the Mid-depth Equatorial Ocean, *Journal of Marine Research*, August 1995.

(ag) Hamilton, K., and R.A. Vincent, High Vertical Resolution Radiosonde Wind and Temperature Data: New Prospects for Widespread Availability and Some Important Research Applications, *EOS, Transactions*, American Geophysical Union, August 1995.

* (ah) Ramaswamy, V., M.D. Schwarzkopf, and W.J. Randel, An Unanticipated Climate Change in the Lower Stratosphere Due to Ozone Depletion, *Nature*, August 1995.

* (ai) Balasubramanian, G., and S.T. Garner, The Role of Momentum Fluxes in Shaping the Lifecycle of a Baroclinic Wave, *Journal of the Atmospheric Sciences*, August 1995.

(aj) Li, T., S.G.H. Philander, On the Annual Cycle of the Eastern Equatorial Pacific, *Journal of Climate*, August 1995.

* (ak) Philander, S.G.H., D. Gu, D. Halpern, G. Lambert, N.-C. Lau, T. Li, R.C. Pacanowski, Why the ITCZ is Mostly North of the Equator, *Journal of Climate*, August 1995.

* (al) Vinnikov, K. Ya., A. Robock, R.J. Stouffer, and S. Manabe, Vertical Patterns of Free and Forced Climate Variations, *Nature*, August 1995.

* (am) Wu, C.-C. and Y. Kurihara, A Numerical Study of the Feedback Mechanisms on Hurricane-Environment Interaction on Hurricane Movement from the Potential Vorticity Perspective, *Journal of the Atmospheric Sciences*, September 1995.

* (an) Ezer, T., and G.L. Mellor, Simulations of Seasonal, Interannual, and Interdecadal Variabilities Induced by Variations in the Wind Stress Over the Atlantic Ocean, *Journal of Geophysical Research*, September 1995.

* (ao) Ramaswamy, V., and J. Li, A High-Spectral Resolution Investigation of Solar Radiative Effects in Vertically Inhomogeneous Low Clouds, *Quarterly Journal of the Royal Meteorological Society*, September 1995.

* (ap) Joos, F., M. Bruno, R. Fink, U. Siegenthaler, T.F. Stocker, C. LeQuere and J.L. Sarmiento, An Efficient and Accurate Representation of Complex Oceanic and Biospheric Models of Anthropogenic Carbon Uptake, *Tellus*, September 1995.

* (aq) Lee, S., and J.L. Anderson, A Simulation of Atmospheric Storm Tracks with a Forced Barotropic Model, *Journal of the Atmospheric Sciences*, September 1995.

(ar) Toggweiler, J.R., E. Tziperman, Y. Feliks, K. Bryan, S.M. Griffies, and B. Samuels, Reply to Comment by S. Rahmstorf, *Journal of Physical Oceanography*, September, 1995.

*In collaboration with other organizations

- (as) Gross, B.D., The Effect of Compressibility on Barotropic and Baroclinic Instability, *Journal of the Atmospheric Sciences*, September 1995.
- * (at) Santer, B.D., K.E. Taylor, T.M.L. Wigley, P.D. Jones, D.J. Karoly, J.F.B. Mitchell, A.H. Oort, J.E. Penner, V. Ramaswamy, M.D. Schwarzkopf, R.J. Stouffer, and S. Tett, A Search for Human Influences on the Thermal Structure of the Atmosphere, *Nature*, September 1995.
- * (au) Burpee, R.W., J.L. Franklin, S.J. Lord, R.E. Tuleya, and S.D. Aberson, The Impact of Omega Dropwindsondes on Operational Hurricane Track Forecast Models, *Bulletin of the American Meteorological Society*, September 1995.
- * (av) Chen, C.-T., and V. Ramaswamy, Sensitivity of Simulated Global Climate to Perturbations in Low Cloud Microphysical Properties, Part II: Spatially Localized Perturbations, *Journal of Climate*, September 1995.

*In collaboration with other organizations

BIBLIOGRAPHY
1991-1995
CROSS REFERENCE BY AUTHOR

ACKERMAN, S.A. (1263),(aa),
AIKMAN, F. (zb),
ALLAART, M.A.F. (1081),
ALMEIDA, de Mario (1037),
ANDERSON, J.L. (1149),(1216),(1321),(xi),(yd),(yy),(aq),
ANDERSON, L.A. (1117),(1223),(1235),(ac),
ARANGO, H.G. (1291),
ARMSTRONG, R.A. (1170),(1253),(1294),(ya),(zq),
ARNOLD, M. (1024),
ARPE, K. (1059),
BACON, M.P. (ww),
BAKER, D.J. (1043),
BARD, E. (1024),
BALASUBRAMANIAN, G. (ai),
BATTISTI, D. (1241),
BEEGLE, C.J. (zu),
BENDER, Morris (1139),(1147),(1148),(1191),(1198),(1295),(1298),
(1329),(wl),(xc),
BENDER, Michael (1236),
BENGTSSON, L. (yl),
BERGER, A. (1181),
BLACKMON, J. (1043),
BLACKMON, M.L. (1043),
BLAIN, C.A. (1068),
BLANCHET, J.P. (1271),
BOER, G. (1059),(1233),(1302),

BONNEL, B.	(1032),
BOSLEY, K.	(zb),
BOWEN, M.M.	(1260),
BOYLE, E.A.	(1132),(1181),
BRANSTATOR, G.	(1277),
BREAKER, L.	(zb),
BRETHERTON, F.P.	(za),
BRIEGLEB, B.P.	(zt),
BROCCOLI, A.J.	(1099),(1123),(1246),(1258),(1266),(yj),(yl),(ze),
BRUNO, M.	(ap),
BRYAN, K.	(1023),(1042),(1055),(1074),(1080),(1091),(1108), (1126),(1185),(1202),(1228),(1241),(yh),(yi),(zf),(zg), (ar),
BUESSELER, K.O.	(ww),
BURPEE, R.W.	(1283),(au),
CANE, M.A.	(1081),
CARSON, S.	(yf),
CESS, R.D.	(1271),
CHALITA, S.	(1271),
CHAMEIDES, W.L.	(1051),(1245),(1322),(zd),
CHANG, E.K.M.	(1114),(1116),(1125),(1154),(1310),
CHANG, P.	(af),
CHAO, Y.	(1208),
CHARLSON, R.J.	(1334),
CHEN, C.-T.	(1171),(1187),(1324),(zi),(zn),(ab),(av),
CHEN, P.	(1105),(xg),(zb),
CHYLEK, P.	(1328),
CLEMENS, S.C.	(1132),(1181),
COAKLEY, J.A.	(1334),

COCHRAN, J.K. (1206),(ww),
COHEN, J.A. (1270),
COLMAN, R. (1233),(1240),(1271),(1302),
COOK, K.H. (1054),(1066),
CRANE, M.W. (1309),
CROWLEY, M.F. (1291),
CUBASCH, U. (1081),
DAZLICH, D.A. (1271),
DeLGENIO, A.D. (1271),
DELWORTH, T.L. (1112),(1145),(1182),(1196),(1312),(ym),(ys),
DEQUE, M. (1059),
DIX, M. (1233),(1302),
DIXON, K.W. (1057),(zu),
DONNER, L.J. (1133),(1218),(1234),(1247),(1297),(zl),
DUCKLOW, H.W. (1155),(1166),
DUFFY, A. (1132),(1181),
DUNNE, K.A. (1227),(xu),
DUPLESSY, J.C. (1024),
ELLINGSON, R.G. (1033),
ELLIS, J. (1033),
EMANUEL, K.A. (1284),(1285),
EVANS, G.T. (1155),
EZER, T. (1044),(1092),(1093),(1104),(1105),(1160),(1248),
(1249),(1250),(1251),(1291),(1327),(xf),(xg),(zb),
(zc),(an),
FASHAM, M.J.R. (1155),(1166),(1175),
FEELY, R.A. (1135),
FEIGELSON, E.M. (1035),
FELIKS, Y. (1228),(yi),(ar),

FELS, S.B.	(1033),(1034),(1038),
FERRARE, R.A.	(1263),
FIGUEROA, H.	(ad),
FINK, R.	(ap),
FOMIN, B.A.	(1035),
FOUQUART, Y.	(1032),(1303),
FRANKLIN, J.L.	(1283),(au),
FREIDENREICH, S.M.	(1031),(1095),(1136),(1331),
FREY, R.A.	(aa),
FU, R.	(xs),
GALIN, V.	(1233),(1302),
GALLOWAY, J.N.	(1243),(1335),(wy),
GAMMON, R.H.	(zu),
GARNER, S.T.	(1025),(1083),(1109),(1278),(1279),(ai),
GATES, W.L.	(1059),(1081),
GENT, P.R.	(1081),
GERDES, R.	(1163),(1164),
GHIL, M.	(1081),
GINIS, I.	(1198),(1305),
GLECKLER, P.J.	(1302),
GLENN, S.M.	(1291),
GNANADESIKAN, A.	(1054),
GODDARD, L.	(1311),
GOLDER, D.G.	(1118),(1272),(1299),
GORCHAKOVA, I.A.	(1035),
GORDON, A.L.	(1074),
GORDON, C.	(1081),
GORDON, C.T.	(1097),

GOSWAMI, B.N.	(zz),
GRAS, J.L.	(1334),
GRAUSTEIN, W.C.	(1130),
GRAVES, D.S.	(1039),
GREATBATCH, R.J.	(1327),
GRIFFIES, S.M.	(wm),(yh),(yi),(ar),
GROSS, B.D.	(1200),(1232),(as),
GROSSMAN, A.S.	(zt),
GU, D.	(1293),(ak),
GUDGEL, R.	(1308),(wn),(xt),
HAKKINEN, S.	(1141),(1161),
HALPERN, D.	(ak),
HAMILTON, K.	(1056),(1115),(1120),(1153),(1168),(1172),(1178), (1197),(1220),(1226),(1262),(1274),(1275),(1276), (1287),(1301),(1332),(1333),(yp),(zm),(ag),
HANAWA, K.	(1184),
HANSEN, F.C.	(1202),
HARSHVARDHAN	(1334),
HART, T.L.	(1059),
HAUGLUSTAINE, D.	(zt),
HAYASHI, Y.	(1118),(1272),(1299),
HELD, I.M.	(1026),(1029),(1066),(1107),(1109),(1131),(1138), (1144),(1176),(1183),(1195),(1231),(1269),(1277), (1279),(1290),(wu),(yu),(yv),(yw),(yx),
HELPAND, M.	(1233),(1302),
HEMLER, R.S.	(1052),(1064),(1103),(1183),(yr),
HERBERT, T.D.	(1089),
HOLLOWAY, L.	(1094),
HOWARD, W.R.	(1132),(1181),
HSIEH, W.W.	(zf),

HURTT, G.C.	(ya),
IMBRIE, J.	(1132),(1181),
JONES, P.D.	(at),
JONES, P.W.	(yr)
JOOS, F.	(1047),(1050),(1319),(ap),
KANTHA, L.H.	(1141),
KAROLY, D.J.	(1039),(1270),(at),
KASAHARA, A.	(1234),
KASIBHATLA, P.S.	(1051),(1137),(1151),(1167),(1243),(1245),(1322), (zd),(zj),(zr),(zw),
KATZFEY, J.J.	(1053),(1060),
KERR, C.L.	(yr),
KEUP, E.	(1271),
KIEHL, J.T.	(1038),(1233),(1302),
KITOH, A.	(1233),(1302),
KLONECKI, A.	(zd),(zj),
KNUTSON, T.R.	(1213),(1268),(1330),
KO, D.-S.	(1093),(1104),(1160),
KOBERLE, C.	(1252),
KONIKOW, L.F.	(xv),
KUBOKAWA, A.	(1184),
KUKLA, G.	(1132),(1181),(1334),
KURIHARA, Y.	(1101),(1139),(1140),(1147),(1148),(1152),(1190), (1191),(1198),(1281),(1295), (1329),(wl),(am),
KUSHNIR, Y.	(1078),(yv),
KUTZBACH, J.	(1132),(1181),
LABITZKE, K.	(1304),
LACIS, A.A.	(1038),(1271),
LAI, C.-C.A.	(1291),

LAMBERT, G. (ak),
LANZANTE, J. (1128),(1289),(1316),(xr),(zh),(zv),
LARICHEV, V.D. (wu),(yw),
LATIF, M. (1081),
LAU, K.-H. (1019),(1111),(1203),
LAU, N.-C. (1063),(1075),(1076),(1077),(1078),(1081),(1082),
(1111),(1127),(1169),(1203),(1221),(1222),(1256),
(1309),(1323),(zx),(zy),(ak),
LAU, W. (1233),(1302),
LAWRENCE, M.G. (1322),
LEE, S. (1029),(1040),(1144),(aq),
LEINEN, M.W. (1135),
LEQUERE, C. (1288),(ap),
LeTREUT, H. (1059),(1271),
LEVY II, H. (1051),(1102),(1130),(1137),(1151),(1243),(1244),
(1245),(1292),(1307),(1322),(1335),(wy),(zd),(zj),
(zr),(zw),
LI, J. (1328),(yc),(ao),
LI, T. (aj),(ak),
LI, X. (af),
LIANG, X.-Z. (1233),(1271),(1302),
LINDBERG, C. (yj)
LIPPS, F.B. (1052),(1064),(1103),
LIU, H. (1124),
LIU, S.C. (1030),
LIU, Z. (1215),(1217),(1280),(1325),
LOFGREN, B. (1113),
LORD, S.J. (1283),(au),
LYKOSsov, V. (1233),(1302),
McAVANEY, B. (1233),(1240),(1271),(1302),

McCORMICK, M.P. (1334),

McINTYRE, A. (1132),(1181),

MAHFOUT, J.F. (1271),

MAHLMAN, J.D. (1043),(1058),(1079),(1100),(1110),(1134),(1186),
(1193),(1224),(1225),(1274),(yt),

MALANOTTE-RIZZOLI, P. (1291),

MANABE, S. (1027),(1036),(1041),(1042),(1067),(1099),(1112),
(1121),(1123),(1145),(1146),(1182),(1192),(1194),
(1201),(1213),(1246),(1268),(1286),(1330),(yg),(yk),
(yl),(ym),(zk),(al),

MANZINI, E. (1062),(1153),

MAO, H. (zt),

MARCINIAK, E.P. (ze),

MARINO, M. (1060),

MARTINSON, D.G. (1132),(1181),

MATANO, R.P. (1158),(1159),(1229),

MAURICE, P. (1024),

MECHOSO, C.R. (1081),

MEEHL, G.A. (1081),(1270),

MEHTA, V.M. (1312),

MELESHKO, V.P. (1041),(1271),

MELFI, S.H. (1263),

MELLOR, G.L. (1044),(1045),(1092),(1093),(1104),(1105),(1141),
(1160),(1161),(1179),(1249),(1250),(1251),(1291),
(1306),(1327),(xf),(xg),(zb),(zc),(an),

MENENDEZ, C. (1060),

MERRILL, J.T. (1130),(1292),

MICHAELS, A. (1335),(wy),

MILLY, P.C.D. (1022),(1046),(1068),(1070),(1073),(1129),(1180),
(1227),(1242),(1254),(1259),(wv),(xv),(yn),

MITCHELL, J.F.B. (1041),(1270),(yl),(at),

MIX, A.C. (1132),(1181),
MIYAKODA, K. (1106),(1119),(1233),(1255),(1300),(1302),(1308),
(wn),(xt),(yz),
MIZZI, A.P. (1234),
MOELLER, D. (1334),
MOLFINO, B. (1132),(1181),
MOLINARI, R.L. (1241),
MOODY, J.L. (1292),
MORCRETTE, J.-J. (1271),
MORLEY, J.J. (1132),(1181),
MOXIM, W.J. (1051),(1137),(1151),(1322),(zr),(zw),
MURNANE, R.J. (1206),(1207),(1320),(ww),
MURRAY, J.W. (1135),
NAJJAR, R.G. (1069),(1214),
NAKAMURA, H. (1188),(1189),(1257),
NAKAMURA, N. (1109),(1162),
NATH, M.J. (1063),(1076),(1077),(1256),(zy),
NAVARRA, A. (1255),
NEELIN, J.D. (1081),
NORRIS, P.M. (1271),
NUTTLE, W.K. (1049),
OBERHUBER, J.M. (1081),
O'BRIEN, E. (1107),
OEY, L.-Y. (1105),(1251),
OHFUCHI, W. (1238),
OLTMANS, S.J. (1102),(1130),(1244),(1292),
OORT, A.H. (1037),(1065),(1124),(1209),(1210),(1223),(1230),
(1270),(1326),(tg),(xh),(yq),(zp),(at),
ORLANSKI, I. (1053),(1060),(1061),(1116),(1125),(1177),(1200),
(1237),(1310),(xk),

ORR, J.C. (1084),(1087),(1090),(1143),
OVERLAND, J.E. (xh),
PACALA, S.W. (1288),
PACANOWSKI, R.C. (1077),(wa),(ae),(af),(ak),
PAVAN, V. (1205),(yu),
PEIXOTO, J.P. (1037),(1065),(1209),(1210),(1223),(zp),
PENNER, J.E. (at),
PETERSON, L.C. (1132),(1181),
PHILANDER,S.G.H. (1076),(1077),(1081),(1159),(1208),(1229),(1252),
(1264),(1293),(1325),(aj),(ak),
PHILLIPPS, P.J. (1138),(1231),
PIERREHUMBERT, R.T. (1279),(1290),
PINARDI, N. (wa),
PINTO, J.P. (1193),
PISIAS, N.G. (1132),(1181),
PLANTON, S. (1233),(1302),
PLOSHAY, J. (1096),(1106),(1119),(yz),
POTTER, G.L. (1271),
PRELL, W.L. (1132),(1181),
PROSPERO, J.M. (1130),
RAMASWAMY, V. (1027),(1030),(1031),(1032),(1058),(1071),(1095),
(1122),(1136),(1171),(1183),(1212),(1230),(1260),
(1303),(1304),(1324),(1331),(1334),(yc),(zi),(zn),
(zo),(zt),(ah),(ao),(at),(av),
RANDALL, D.A. (1271),(1302),
RANDEL, W.J. (1026),(ah),
RAO, D.B. (zb),
RAVAL, A. (1230),
RAYMO, M.E. (1132),(1181),
RIKUS, L. (1271),

ROBINSON, A.R. (1291),
ROBOCK, A. (al),
ROECKNER, E. (1059),(1271),(1334),(ab),
ROSATI, A. (1308),(wa),(wn),(xt),(yz),
ROSS, B.B. (1064),
ROSS, R.J. (1101),(1139),(1140),(1147),(1148),(1191),(1281),
(1329),(wl),
ROYER, J.F. (1271),
ROZANOV, E.V. (1035),
SAMUELS, B. (1156),(1157),(1313),(1315),(yi),(ar),
SANTER, B.D. (at),
SARMIENTO, J.L. (1047),(1048),(1049),(1050),(1069),(1084),(1085),
(1086),(1087),(1088),(1089),(1090),(1142),(1143),
(1155),(1165),(1166),(1173),(1174),(1175),(1206),
(1235),(1236),(1288),(1294),(1317),(1318),(1319),
(1320),(ac),(ad),(ap),
SAVOIE, D.L. (1130),
SCANLON, B.R. (1254),
SCHLESE, U. (1271),
SCHLESINGER, W.H. (1335),(wy),
SCHOPF, P.S. (1081),
SCHNOOR, J.L. (1335),(wy),
SCHWARZKOPF, M.D. (1030),(1034),(1035),(1038),(1071),(1122),(zt),(ah),
(at),
SEMAN, C.J. (1239),(wj),
SHACKLETON, N.J. (1132),(1181),
SHAFFER, G. (1318),
SHEININ, D.A. (1059),(1271),(zb),
SHELDON, J. (1177),(xk),
SHINE, K.P. (1071),(1303),(1304),(zt),
SHUKLA, J. (1043),

SIEGENTHALER, U.	(1047),(1050),(1084),(1085),(1173),(ap),
SIMMONDS, I.	(1059),
SIMON, P.	(1304),
SIRKES, Z.	(1160),
SLATER, R.D.	(1155),(1166),(1175),(1294),
SMITH, R.N.B.	(1059),
SODEN, B.J.	(1247),(1263),(xs),(za),(zh),(aa),(ab),
SOKOLOV, A.P.	(1271),
SOLOMON, S.	(1303),(1304),
SPELMAN, M.J.	(1042),(1067),(1194),(1286),
SPERBER, K.R.	(1081),
SRINIVASAN, J.	(1303),
STARR, D.O'C.	(1263),
STEPHENSON, D.B.	(1108),(1176),
STERL, A.	(1081),
STERN, W.F.	(1096),(1106),(1119),(1255),(1300),(1302),(yd),(zs),
STOCKER, T.F.	(ap),
STOUFFER, R.J.	(1023),(1042),(1067),(1112),(1121),(1146),(1182), (1192),(1194),(1201),(1219),(1270),(1286),(yk),(ym), (zk),(al),(at),
STOWE, L.L.	(1334),
STRAHAN, S.E.	(1224),(1225),
STRÖM, J.	(zl),
SUAREZ, M.J.	(1269),
SUN, D.-Z.	(1211),(1326),(yx),
SUNDQUIST, E.	(1086),
SUTYRIN, G.	(1305),
SWANSON, K.L.	(1279),(1290),
TAYLOR, J.	(1334),

TAYLOR, K.E.	(1271),(at),
TETT, S.	(at),
THACKER, W.C.	(1080),
THORPE, A.J.	(1083),
TIMOFEYEV, Yu. M.	(1035),
TING, M.-F.	(1169),
TOGGWEILER, J.R.	(1024),(1057),(1069),(1072),(1132),(1135),(1155), (1156),(1157),(1181),(1214),(1228),(1267),(1273), (1313),(1314),(1315),(yf),(yi),(ar),
TOKIOKA, T.	(1041),(1059),(1081),
TOME, A.	(1037),
TRIBBIA, J.	(1081),
TROTSENKO, A.N.	(1035),
TULEYA, R.E.	(1028),(1139),(1148),(1191),(1199),(1283),(1295), (1329),(wl),(au),
TUREKIAN, K.K.	(1130),
TURET, P.	(xh),
TZIPERMAN, E.	(1080),(1185),(1228),(wm),(yi),(ar),
UMSCHEID, L.J.	(1193),(1274),
VAHLENKAMP, H.	(1197),
van den DOOL, H.M.	(1216),
VAN DORLAND, R.	(zt),
VERMA, R.K.	(1098),
VINNIKOV, K.Ya.	(1201),(al),
WACONGNE, S.	(ae),
WALLACE, J.M.	(1043),(1189),
WALSH, J.	(1241),
WANG, W.-C.	(1304),(zt),
WANNINKHOF, R.	(1135),
WARREN, J.	(zl),

WETHERALD, R.T. (1027),(1059),(1240),(1270),(1271),(yb),(yg),
WIGLEY, T.M.L. (at),
WILLEMS, R.C. (1291),
WILLIAMS, R.B. (1166),
WILLIAMSON, D. (1059),
WILLMOTT, C.J. (xu),
WILSON, R.J. (1197),(1274),(zm),
WROBLEWSKI, J.S. (1049),
WU, C.-C. (1284),(1285),(am),
WU, G. (1082),
WYMAN, B. (wh),
XIE, S.-P. (1184),(1204),(1261),(1264),(1265),(1280),(1282),
XUE, H.-J. (1021),(1179),
YAGAI, I. (1271),
YIENGER, J.J. (1245),(1307),(yq),
YOUNG, R.E. (1291),
YUAN, L. (1115),(1150),(1276),
ZAVATARELLI, M. (1306),
ZEBIAK, S.E. (1074),(1081),
ZHANG, J. (1296),
ZHANG, M.-H. (1271),
ZHU, X. (1020),

APPENDIX C

Seminars Given at GFDL

During Fiscal Year 1995



5 October 1994 Modelling the CFC Transient in the North Pacific: Comparison with Observations and Model Dynamics, by Ms. C.J. Beegle, School of Oceanography, University of Washington, Seattle, WA

6 October 1994 Circulation of the Baltic, by Dr. Wolfgang Fennel, Institute of Oceanography, Warnemuende, Germany

11 October 1994 Soil Moisture Simulations with a Bucket and SSIB Compared to Russian Observations, by Dr. Alan Robock, Atmospheric and Oceanic Sciences Program, Princeton University, Princeton, NJ

13 October 1994 New Operational Long-lead Seasonal Climate Forecasts Out to One Year, by Prof. H.M. van den Dool, Climate Analysis Center, National Weather Center, Washington, DC

17 October 1994 Cyclogenesis in the Atmosphere and Gulf Stream Ring Formation in the Ocean, by Dr. Andrew Bush, University of Toronto, Toronto, Canada

17 October 1994 A Fast, Mass-conserving, Multi-dimensional Flux Form, Semi-Lagrangian, Monotonic Advection Scheme for Geophysical Flows, by Dr. Shian-Jiann Lin, Data Assimilation Office, NASA/Goddard Space Center, Greenbelt, MD

21 October 1994 The Cloud-Radiation Consistency Method and its Application to the Asian Monsoon Region, by Dr. Pui-King Chan, Department of Meteorology, Pennsylvania State University, University Park, PA

25 October 1994 Volcanos and Climate, by Dr. Alan Robock, Atmospheric and Oceanic Sciences Program, Princeton University, Princeton, NJ

26 October 1994 The Behaviour of Dry Hurricane-like Vortices in Vertical Shear, by Dr. Sarah Jones, University of Munich, Munich, Germany

27 October 1994 The Sensitivity of Upper Tropospheric Clouds to Aerosol Size Distribution and Composition, by Dr. Eric Jensen, NASA Ames Research Center, Moffett Field, CA

1 November 1994 Potential Vorticity Diagnostics of Hurricane-Environment Interaction and its Feedback on Hurricane Movement, by Dr. Chun-Chieh Wu, Atmospheric and Oceanic Sciences Program, Princeton University, Princeton, NJ

8 November 1994 The Solubility Pump of Carbon in the Subtropical Gyres, by Mick Follows, Massachusetts Institute of Technology, Cambridge, MA

9 November 1994 Nonmodal Growth of Tropical IndoPacific Sea Surface Temperatures, by Dr. Cecile Penland, CIRES, University of Colorado, Boulder, CO

15 November 1994 Thermohaline Circulation Predictability: Some Ensemble Results, by Dr. Steven Griffies, Atmospheric and Oceanic Sciences Program, Princeton University, Princeton, NJ

22 November 1994 Bottom Water Circulation and the Antarctic Circumpolar Current, by Dr. John R. Toggweiler and Bonnie Samuels, Geophysical Fluid Dynamics Laboratory, Princeton, NJ

1 December 1994 Recent Development in Semi-Lagrangian Global Atmospheric Modeling at NASA, by Dr. John R. Bates, Laboratory for Atmospheres, NASA/Goddard Space Flight Center, Greenbelt, MD

6 December 1994 A Numerical Model for Bottom-Arrested Gravity Currents: Applications to Outflows and Overflows, by Dr. Johann Jungclaus, Atmospheric and Oceanic Sciences Program, Princeton University, Princeton, NJ

8 December 1994 Lagrangian-Mean Structure of the Stratospheric Polar Vortex in the GFDL SKYHI Model, by Dr. Noboru Nakamura, University of Chicago, Chicago, IL

12 December 1994 Dependence of the Thermohaline Circulation in the Non Eddy-Resolving CME Model of the North Atlantic, by Dr. Ralf Doscher, Institut fur Meereskunde, der University Kiel, Kiel, Germany

13 December 1994 The Climatological Version of the Bjerknes Hypothesis, by Prof. J. David Neelin, Department of Atmospheric Science, University of California, Los Angeles, CA

14 December 1994 Buoyancy Driven Circulation in an Ocean Basin with Isopycnals Intersecting the Sloping Boundary, by Dr. Robert Hallberg, University of Washington, Seattle, WA

15 December 1994 Assimilation of Geosat Altimeter Data into an Eddy-Resolving Primitive Equation Model of the North Atlantic Ocean, by Dr. Andreas Oschlies, Institut fur Meereskunde, der University Kiel, Kiel, Germany

20 December 1994 A Satellite Analysis of Deep Convection, Upper Tropospheric Humidity, and the Greenhouse Effect, by Dr. Brian Soden, Geophysical Fluid Dynamics Laboratory, Princeton, NJ

22 December 1994 Roles of ENSO and Internal Dynamics in Interannual Variations of Indian Summer Monsoon, by Dr. B.N. Goswami, Atmospheric and Oceanic Sciences Program, Princeton University, Princeton, NJ

4 January 1995 Large-Scale Variability in Marine Stratocumulus, by Dr. Steven Klein, Department of Atmospheric Science, University of Washington, Seattle, WA

11 January 1995 Is Recent Warming Man-Made? Result of an Optimal Fingerprint Method, by Dr. Gabriele Hegerl, Max Planck Institute for Meteorology, Hamburg, Germany

13 January 1995 Clouds, Radiation and Climate from EOS, by Dr. Michael King, NASA/Goddard Space Flight Center, Greenbelt, MD

17 January 1995 Phenomenology of Low Frequency Variability in a Double-Gyre Model, by Dr. John D. McCalpin, University of Delaware, Newark, DE

18 January 1995 Laboratory Model of Tropical Cyclones, by Vladimir S. Shandin, Moscow State University of Geodesy, Cartography, and Physics, Moscow, Russia

20 January 1995 GFDL: Present and Future, by Dr. Jerry D. Mahlman, Geophysical Fluid Dynamics Laboratory, Princeton, NJ

23 January 1995 Wave-Activity Conservation Laws and Stability Theorems for Semi-Geostrophic Dynamics, by Dr. Paul Kushner, University of Toronto, Toronto, Canada

24 January 1995 Internal Decadal Variability in Ocean General Circulation Models, by Dr. Michael Winton, JISAO, University of Washington, Seattle, WA

26 January 1995 Some Highlights from the Upper Atmosphere Research Satellite, by Dr. Mark Schoeberl, Atmospheric Chemistry & Dynamics Branch, NASA/Goddard Space Flight Center, Greenbelt, MD

27 January 1995 How Quickly is the Oceanic Surface Layer Mixed? Models and Observations of Langmuir Circulation, by Dr. Anand Gnanadesikan, Woods Hole Oceanographic Institution, Woods Hole, MA

31 January 1995 Overview of MOM-2 Development, by Ron Pacanowski, Charles Goldberg, Keith Dixon, and Tony Rosati, Geophysical Fluid Dynamics Laboratory, Princeton, NJ

2 February 1995 Applications of Large-Eddy Simulation to Boundary Layer Turbulence and Clouds, by Dr. Chin-Hoh Moeng, National Center for Atmospheric Research, Boulder, CO

3 February 1995 Modeling the Coupled Ice-Ocean System, by Dr. Ching-Chau "Abe" Cheng, Svedrup Technology, Inc., Stennis Space Center, MS

7 February 1995 Radiative Transfer in Cloud with Internal Inhomogeneity, by J. Li, Atmospheric and Oceanic Sciences Program, Princeton University, Princeton, NJ

9 February 1995 Recent Climate Research at the Hadley Center, by Dr. David A. Bennetts, Hadley Centre for Climate Prediction & Research, Meteorological Office, Bracknell, United Kingdom

10 February 1995 The World Ocean Historical Database: Status and Scientific Results, by Mr. Sydney Levitus, National Ocean Data Center, Washington, DC

13 February 1995 Numerical Ocean Modeling using Different Formulation of the Advection Scheme, by Dr. Julia Pietrzak, Danish Meteorological Institute, Copenhagen, Denmark

14 February 1995 Observed Interannual Variations in the Hadley Circulation and Connections with ENSO, by Dr. Abraham Oort and Jim Yienger, Geophysical Fluid Dynamics Laboratory, Princeton, NJ

21 February 1995 IPCC (1994): Radiative Forcing of Climate Change, by Dr. V. Ramaswamy, Geophysical Fluid Dynamics Laboratory, Princeton, NJ

24 February 1995 Prediction of Cloud Cover in the Marine Boundary Layer, by Dr. Christopher Bretherton, Center for Meteorology & Physical Oceanography, Massachusetts Institute of Technology, Cambridge, MA

28 February 1995 Ensemble Forecasts and Predictability, by Dr. Jeffrey Anderson, Geophysical Fluid Dynamics Laboratory, Princeton, NJ

7 March 1995 Baroclinic Instability and Transport of the Antarctic Circumpolar Current, by Dr. Anne-Marie Treguier, Atmospheric and Oceanic Sciences Program, Princeton University, Princeton, NJ

10 March 1995 Do Synoptic Eddies Damp Stationary Planetary Waves?, by Mr. Kyle Swanson, University of Chicago, Chicago, IL

14 March 1995 Selection of Initial Conditions for Ensemble Forecasts, by Dr. Jeffrey Anderson, Geophysical Fluid Dynamics Laboratory, Princeton, NJ

21 March 1995 Vorticity Production in Hydraulic Jumps, by Dr. Richard Rotunno, National Center for Atmospheric Research, Boulder, CO

28 March 1995 Middle Atmospheric O₃ Response to Solar UV Variations over Solar Rotations, by Dr. Chen Li, Princeton University, Princeton, NJ

30 March 1995 Interactions of Radiation and Convection in Simulated Tropical Cloud Clusters, by Dr. Steven K. Krueger, University of Utah, Salt Lake City, UT

11 April 1995 Atmospheric Model Parameterizations for Air-Sea Coupled Forecasts of ENSO, by Dr. K. Miyakoda, Geophysical Fluid Dynamics Laboratory, Princeton, NJ

13 April 1995 Implementation of a Data Pre-processor in the BMRC Limited Area Model (TAPS), by Dr. Harry Weber, Meteorological Institute of the University of Munich, Munich, Germany

18 April 1995 Middle Atmospheric Ozone Response to Solar UV Variations Over Solar Rotations, by Chen Li, Department of Chemistry, Princeton University, Princeton, NJ

20 April 1995 Evaluation of Multi-year Biosphere and Bucket Model Simulations for a Typical Midlatitude Grassland Catchment, by Dr. C. Adam Schlosser, University of Maryland, College Park, MD

25 April 1995 Modeling the Mediterranean Out Flow and the Exchange Flow Through the Straits of Gibraltar, by Dr. Johann Jungclaus, Atmosphere and Oceanic Sciences Program, Princeton University, Princeton, NJ

27 April 1995 The Coupling of Fronts and the Boundary Layer, by Dr. Chris Snyder, National Center for Atmospheric Research, Boulder, CO

8 May 1995 Stratospheric Ozone and Temperature Changes Due to Mount Pinatubo, by Dr. William Randel, National Center for Atmospheric Research, Boulder, CO

9 May 1995 Some Results Pertaining to Clouds and Radiation Obtained from Multi-year GCM Integrations, by Dr. Tony Gordon, Geophysical Fluid Dynamics Laboratory, Princeton, NJ

9 May 1995 Stratospheric QBO and Tracer Transport, by Dr. William Randel, National Center for Atmospheric Research, Boulder, CO

10 May 1995 Mid-latitude Response to Zonally Symmetric Tropical Heating, by Dr. Edmund Chang, Massachusetts Institute of Technology, Cambridge, MA

11 May 1995 Transient Eddy-Stationary Wave Feedbacks in a Simple Model, by Dr. Jeffrey S. Whitaker, University of Colorado, Boulder, CO

12 May 1995 Long and Short Time Scale Dynamics in the Climate Inferred from Ice Core Paleoclimatic Records, Dr. Peter Ditlevsen, Niels Bohr Institute, Copenhagen, Denmark

15 May 1995 Regulation of Tropical Sea Surface Temperature, by Dr. Ray Pierrehumbert, University of Chicago, Chicago, IL

16 May 1995 Impact of Dropwindsondes on Hurricane Forecasts, by Robert Tuleya, Geophysical Fluid Dynamics Laboratory, Princeton, NJ

18 May 1995 Simulation of Recent Global Temperature Trends, by Dr. Nick Graham, Scripps Institute of Oceanography, La Jolla, CA

19 May 1995 On the Evolution-dynamics of Tropical Ocean-Atmosphere Annual-cycle Variability, by Dr. Suman Nigam, University of Maryland, College Park, MD

23 May 1995 Dynamics and Energy Balance of Hadley Circulation and ITCZ, by A. Numaguti, Atmospheric and Oceanic Sciences Program, Princeton University, Princeton, NJ

25 May 1995 Dense Water Formation on Continental Shelves: Idealized Process Studies, by Dr. Glen Gawarkiewicz, Woods Hole Oceanographic Institute, Woods Hole, MA

26 May 1995 Aerosol Climate Interactions, by Dr. Joyce E. Penner, Global Climate Research Division, Lawrence Livermore National Laboratory, Livermore, CA

30 May 1995 A Unified Mechanism for the Generation of Low- and High-Frequency Tropical Waves, by Dr. Yoshikazu Hayashi and Mr. Donald G. Golder, Geophysical Fluid Dynamics Laboratory, Princeton, NJ

30 May 1995 Sensitivity of the Global Climate System to Change in the Northern Hemisphere Ice Sheets using NCAR CCM1, by Dr. Benjamin Felzer, Department of Geological Sciences, Brown University, Providence, RI

1 June 1995 Non-linear Equilibration of Baroclinic Systems: Effect of Asymmetric Dissipation, by Dr. Patrice Klein, Laboratoire de Physique des Oceans, Brest, France

6 June 1995 NOAA and GFDL Budget Stuff, by Dr. Jerry D. Mahlman and Dr. Bruce Ross, Geophysical Fluid Dynamics Laboratory, Princeton, NJ

8 June 1995 The Future of Ocean Modeling, by Dr. Dale Haidvogel, Institute of Marine & Coastal Sciences, Rutgers State University, New Brunswick, NJ

12 June 1995 Circumventing Storage Requirements in Data Assimilation Studies, by Dr. Juan Restrepo, Argonne National Laboratory, Argonne, IL

13 June 1995 Eastward Propagation of Southern Oscillation Signals, by Mr. Joseph Sirutis, et al., Geophysical Fluid Dynamics Laboratory, Princeton, NJ

14 June 1995 Characterizing the Variability of Snow Cover over the Central United States: 1910 to Present, by Dr. Marilyn Hughes, Department of Geography, Rutgers University, New Brunswick, NJ

8 August 1995 The Vertical Structure Equation for Planetary Scale Flows, by Dr. E.V. Chelam, World Meteorological Organization, United Nations (retired), now residing at Matawan, NJ

15 August 1995 Role of Momentum Fluxes in Organizing Deep Convection Along an Idealized Dryline, by Dr. Charles Seman, Geophysical Fluid Dynamics Laboratory, Princeton, NJ

22 August 1995 Quasi-stationary Zonal Flow/Eddy Relationship and its Dynamics, by Dr. Peitao Peng, Atmospheric and Oceanic Sciences Program, Princeton University, Princeton, NJ

24 August 1995 Lidar Studies of the Middle Atmosphere, by Prof. Robert Sica, Department of Physics, University of Western Ontario, Ontario, Canada

7 September 1995 Global Acoustic Mapping of Ocean Temperatures, by Dr. John Speisberger, Department of Meteorology, Pennsylvania State University, State College, PA

13 September 1995 Sensitivity Studies and Singular Vector Instabilities in the ECMWF Model, by Dr. Ron Gelaro, NRL/European Center for Medium Range Forecasts, Shinfield Park, Reading, UK

19 September 1995 Wave Action, Downstream Development, and Nonlinear Baroclinic Wave Packets, by Dr. Kyle Swanson, Atmospheric and Oceanic Sciences Program, Princeton University, Princeton, NJ

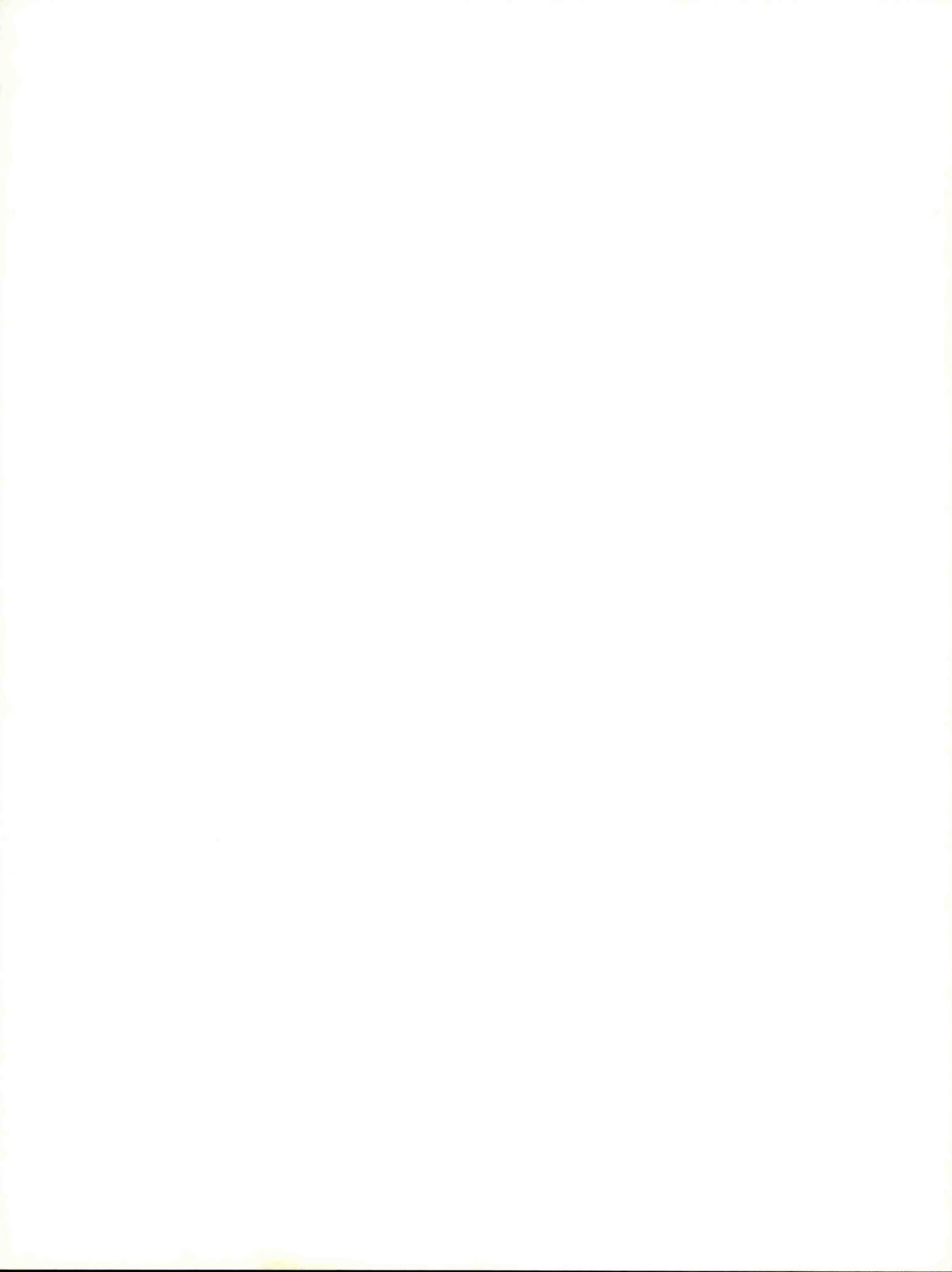
21 September 1995 Decadal-Scale Trends in Mechanisms Controlling Meridional Sea Surface Temperature Gradients in the Tropical Atlantic, by Dr. Richard Wagner, University of Wisconsin-Madison, Madison, WI

29 September 1995 Assessing the Budget for the Absorption of Short Wave Radiation in the Atmosphere, by Dr. Thomas Charlock, NASA Langley Research Center, Hampton, VA

APPENDIX D

Talks, Seminars, and Papers Presented Outside GFDL

During Fiscal Year 1995



4 October 1994

Dr. Syukuro Manabe

"Modeling Global Climate Change: Capability and Limitations of Climate Models", International Petroleum Industry Environmental Conservation Association, Workshop on Critical Issues in the Science of Global Climate Change, Woods Hole Oceanographic Institution, Woods Hole, MA

5 October 1994

Dr. Kikuro Miyakoda

"Data Assimilation for Air-Sea Coupled System", Andrè Robert Memorial Symposium, Montreal, Canada

5 October 1994

Dr. Isidoro Orlanski

"Wavelet Analysis for Detection of Baroclinic Packets in Storm Tracks", Andrè Robert Memorial Symposium, Montreal Canada

5 October 1994

Mr. Anthony J. Rosati

1. "Decadal Ocean Analysis", 2. "Ocean Data Assimilation and ENSO Forecasting", BMRC Modeling Workshop on Data Assimilation in Meteorology and Oceanography, Melbourne, Victoria, Australia

5 October 1994

Dr. Isaac M. Held

1. "The Fluid Dynamics of Global Warming", 2. "Baroclinic Instability and Geostrophic Turbulence", University of Miami, Miami, FL

11 October 1994

Dr. Thomas L. Delworth

"North Atlantic Variability in the GFDL Coupled Model", Workshop on Global Coupled General Circulation Models, Scripps Institution of Oceanography, La Jolla, CA

12 October 1994

Mr. Ronald J. Stouffer

1. "Response of a Coupled Model to Various Rates of Increase in Atmospheric CO₂", 2. "The Effects of Oceans on Interdecadal Variability", Scripps Institution of Oceanography, La Jolla, CA

12 October 1994

Dr. John Lanzante

"Resistant, Robust and Non-parametric Techniques for the Analysis of Climate Data: Theory and Examples, Including Applications to Historical Radiosonde Station Data", Air Resources Laboratory, Silver Spring, MD

25 October 1994

Dr. Abraham H. Oort

"The Climatology of Relative Humidity in the Atmosphere", American Geophysical Union Conference, Jekyll Island, GA

26 October 1994

Dr. Brian J. Soden

"Climatologies of Upper Tropospheric Moisture", American Geophysical Union Conference, Jekyll Island, GA

31 October 1994 Dr. Hiram Levy II
"Natural vs. Pollutant Control of Tropospheric Ozone", New York State Department of Public Health, Wadsworth Center, Albany, NY

1 November 1994 Dr. Leo J. Donner
"Parameterization of Cirrus Clouds in GCM's", European Centre for Medium Range Weather Forecasts/Global Energy and Water Experiment Workshop, Reading, England

1 November 1994 Mr. Anthony J. Rosati
"Intercomparison of ENSO Forecasts for 1990-94", TOGA-NEG Meeting, Scripps Institution of Oceanography, La Jolla, CA

3 November 1994 Dr. Kevin P. Hamilton
"Resolved and Parameterized Gravity Waves in Atmospheric GCMs", Canadian Middle Atmosphere Modeling Project Workshop on Gravity Wave Parameterization, Toronto, Canada

4 November 1994 Mr. Anthony J. Broccoli
"The Greenhouse Effect: The Science Base", Metropolitan New York in the Greenhouse: Infrastructure Planning for an Uncertain Future, New York, NY

7 November 1994 Dr. John R. Toggweiler
"Antarctic Bottom Water Formation in Ocean GCMs", Conference on Antarctic Bottom Water Formation, Lamont-Doherty Geological Observatory, Palisades, NY

9 November 1994 Dr. Thomas L. Delworth
"North Atlantic Variability in the GFDL Coupled Model", McGill University, Montreal, Canada

9 November 1994 Dr. Leo J. Donner
"Clouds as a Problem in Scale Interactions for Large-Scale Atmospheric Models", New York University, Courant Institute, New York, NY

10 November 1994 Dr. Bruce B. Ross
"Activities of HPCC Computing Panel", NOAA/HPCC Council Meeting, Silver Spring, MD

14 November 1994 Dr. John R. Lanzante
"Analysis of Climate Data Using Resistant, Robust, and Non-Parametric Techniques: Some Examples and Some Applications to the Historical Radiosonde Record", 19th Climate Diagnostics Workshop, College Park, MD

14 November 1994	Dr. Abraham H. Oort "Observed Long-Term Variability in the Hadley Circulation", 19th Climate Diagnostics Workshop, College Park, MD
15 November 1994	Dr. Jeffrey L. Anderson "A Method of Evaluating the Potential Predictability in Ensemble Forecasts", 19th Climate Diagnostics Workshop, College Park, MD
15 November 1994	Mr. William F. Stern "Interannual Variability and Reproducibility from Multiple GCM Simulations", 19th Climate Diagnostics Workshop, College Park, MD
16 November 1994	Dr. Kikuro Miyakoda "Atmospheric Model Parameterizations for Air-Sea Coupled ENSO and Monsoon Forecasts", Instituto per lo Studio Delle Meteorology, Geofisiche Ambientali, Modena, Italy
16 November 1994	Dr. Kevin P. Hamilton "Simulation of Tides, Planetary Waves and Gravity Waves in Comprehensive Models: Opportunities for Comparison with Observations", Workshop on Wind Observations in the Middle Atmosphere, CNES, Paris, France
16 November 1994	Dr. Jerry D. Mahlman "Greenhouse Warming: Sorting Out the Real Truth", Global Climate Coalition Meeting, Washington, DC
22 November 1994	Dr. Lori M. Perliski "Stratospheric Photochemical Modeling using GFDL's SKYHI GCM", York University, Toronto, Ontario, Canada
5 December 1994	Dr. Hiram Levy II 1. "The Impact of Anthropogenic and Natural NO _x Sources on the Global Distribution", 2. "Tropospheric Reactive Nitrogen and the Net Chemical Production of Ozone", 3. "Tropospheric Ozone over the Western North Atlantic", American Geophysical Union Fall Meeting, San Francisco, CA
7 December 1994	Dr. Thomas L. Delworth "The Atlantic Thermohaline Circulation and Climate", American Geophysical Union Fall Meeting, San Francisco, CA
7 December 1994	Mr. Anthony J. Broccoli "Comparing Simulated Glacial Climate and Paleodata: A Re-examination", American Geophysical Union Fall Meeting, San Francisco, CA

24 April 1995	Mr. Morris A. Bender "A Numerical Study of the Asymmetric Structure in the Interior of Tropical Cyclones", American Meteorological Society Conference on Hurricanes & Tropical Meteorology, Miami, FL
25 April 1995	Mr. Robert E. Tuleya "Impact of Dropwindsonde Data on Hurricane Prediction Using the GFDL Model", American Meteorological Society Conference on Hurricanes & Tropical Meteorology, Miami, FL
26 April 1995	Dr. Jerry D. Mahlman 1. "Greenhouse Warming: A Challenge for Future Generations", 2. "High Resolution Modeling of the Lower Stratosphere: What Can We Learn in the Real World?", 1995 Colorado State University Honor Alumnus Award Ceremony, Colorado State University, Fort Collins, CO
28 April 1995	Dr. John R. Toggweiler "A Mechanical View of the Ocean's Large-Scale Overturning", University of Chicago, Chicago, IL
2 May 1995	Dr. Thomas L. Delworth "North Atlantic Interannual Variability in a Coupled Ocean-Atmosphere Model", ACCP Principal Investigator's Meeting, Miami, FL
5 May 1995	Dr. Jerry D. Mahlman "Greenhouse Warming: On the State of the Science", State House Briefing at Congress on the Berlin Climate Convention Meeting, Washington, DC
9 May 1995	Dr. John R. Toggweiler "Nutrient Balance for the Equatorial Pacific", JGOFS Scientific Symposium, Villefranche-sur-Mer, France
9 May 1995	Mr. Richard G. Gudgel "The Assimilation of TOPEX Altimetry Data in a Global Ocean GCM", IMGA-CNR, Bologna, Italy
9 May 1995	Mr. Anthony J. Rosati 1. "An Overview of Seasonal/Interannual Prediction at GFDL", 2. "The Data Assimilation of TOPEX Altimetry Data in an Ocean GCM", IMGA-CNR, Bologna, Italy
15 May 1995	Mr. William F. Stern 1. "Tropical Intraseasonal Variability in the GFDL/DERF GCM During AMIP", 2. "Activities Involving the GFDL/DERF GCM and the GISST Dataset", AMIP Scientific Conference, Monterey, CA

15 May 1995	Mr. Richard T. Wetherald "Simulation of Temperature and Moisture from the GFDL AMIP Experiment", AMIP Scientific Conference, Monterey, CA
15 May 1995	Dr. Jeffrey L. Anderson "Evaluating Potential Predictability and Skill in Ensemble Forecasts", European Centre for Medium Range Weather Forecasts, Reading, England
16 May 1995	Dr. Lori M. Perliski "Simulation of Stratospheric Photochemistry in the NOAA SKYHI GCM", International Conference on Ozone in the Lower Stratosphere, Halkidiki, Greece
16 May 1995	Dr. Brian J. Soden "Recent Studies of Upper Tropospheric Water Vapor", Space Science and Engineering Center, University of Wisconsin, Madison, WI
17 May 1995	Dr. Charles T. Gordon "Some Preliminary Results from a 40-year GCM Integration of Equatorial Temporal Variability over the Interannual to Interdecadal Range", AMIP Science Conference, Monterey, CA
18 May 1995	Dr. Kikuro Miyakoda "Numerical Prediction of ENSO", Tokyo University, Tokyo, Japan
18 May 1995	Dr. Syukuro Manabe "Role of Oceans in Climate", Tokyo University, Tokyo, Japan
22 May 1995	Dr. Jerry D. Mahlman "Greenhouse Warming: IPCC 1995 Conclusions and Assessment of Climate Models", Second International Conference on Climate Change, Washington, DC
23 May 1995	Dr. John R. Toggweiler "A Mechanical View of the Ocean's Overturning Circulation", National Center for Atmospheric Research, Boulder, CO
24 May 1995	Dr. Leo J. Donner "Implementing Microphysics at Physically Appropriate Scales in GCMs", Cloud Microphysics in GCMs Workshop, Kananaskis, Alberta, Canada
25 May 1995	Mr. M. Daniel Schwarzkopf "GFDL LBL Results", ICRCCM Workshop, College Park, MD
25 May 1995	Dr. V. Ramaswamy "On Solar Radiative Transfer Modeling", ICRCCM Workshop, College Park, MD

30 May 1995 Dr. Leo J. Donner
"Current and Planned Research for FIRE", FIRE Science Team Meeting, Baltimore, MD

31 May 1995 Dr. Jerry D. Mahlman
"Global Warming: What are the Facts?", Bermuda Insurance Symposium II, Tuckers, Bermuda

1 June 1995 Mr. Anthony J. Broccoli
"Climate Model Simulation of Tropical Temperatures at the Last Glacial Maximum", American Geophysical Union Spring Meeting, Baltimore, MD

1 June 1995 Dr. Lori M. Perliski
"Stratospheric Ozone Development", 1995 NOAA Colloquium on Operational Environmental Prediction, Baltimore, MD

3 June 1995 Dr. V. Ramaswamy
"Solar Radiative Transfer Modeling", National Meteorological Center, Camp Springs, MD

6 June 1995 Dr. Yoshikazu Hayashi
"The Generation Mechanism of Tropical Transient Waves: Control Experiments and a Unified Theory of Moist Convection Adjustment", Tenth Conference on Atmospheric and Oceanic Waves and Stability, Big Sky, MT

6 June 1995 Dr. Isaac M. Held
"On Eddy Amplitudes and Length Scales in Baroclinically Unstable Flows", Tenth Conference on Atmospheric and Oceanic Waves and Stability, Big Sky, MT

6 June 1995 Dr. Hiram Levy II
"Global Lightning NO_x Source: Impact on Tropospheric Chemistry", Lightning Imaging Sensor Science Team Meeting, Huntsville, AL

7 June 1995 Dr. Syukuro Manabe
"On the Role of Oceans in Natural Variability and Anthropogenic Change of Climate", 18th Pacific Science Congress, Beijing, China

9 June 1995 Dr. Bruce B. Ross
"Status Report on Computing Panel Activities", HPCC/NII Council Meeting, Silver Spring, MD

9 June 1995 Mr. Anthony J. Broccoli
"Greenhouse Warming", 1995 NOAA Colloquium on Operational Environmental Prediction, Camp Springs, MD

12 June 1995 Dr. John R. Toggweiler
"Role of Denitrification in the Nutrient Budget of the Equatorial Pacific Upwelling System", Gordon Conference on Chemical Oceanography, Henniker, NH

13 June 1995 Dr. Kevin P. Hamilton
"Issues Concerning General Circulation Modeling of Stratosphere-Troposphere Exchange", SPARC Workshop on Stratospheric Processes and Their Role in the Climate Program, Pointe-du-Lac, Quebec, Canada

16 June 1995 Dr. Kevin P. Hamilton
"Simulation of Tides in Planetary Atmospheres", Department of Atmospheric and Oceanic Sciences, McGill University, Montreal, Quebec, Canada

19 June 1995 Dr. Hiram Levy II
"Regional Impact of Elevated Ozone", NASA Workshop on Assessing the Vulnerability of Agriculture to Variations in Climate and Air Quality, New York, NY

20 June 1995 Dr. Steven R. Carson
"Effects of Interannual Variability in Forcing on the Behavior of the GFDL/Princeton Physical-Ecosystem Model of the Equatorial Pacific", NATO Advanced Research Workshop on Carbon Cycle of the Equatorial Pacific Ocean, Noumea, New Caledonia

26 June 1995 Dr. Jeffrey Anderson
"Selection of Initial Conditions for Ensemble Forecasts", National Center for Environmental Prediction, Camp Springs, MD

27 June 1995 Dr. Kevin P. Hamilton
"Possible Contributions to Upper Atmospheric Physics from Comprehensive Meteorological Simulation Models", Coupling of Energetic and Dynamic Atmospheric Regions (CEDAR) Annual Meeting, Boulder, CO

27 June 1995 Mr. Anthony J. Rosati
"Assimilation of TOPEX Altimetry Data in the GFDL Ocean Model", National Center for Environmental Prediction, Camp Springs, MD

3 July 1995 Dr. Leo J. Donner
"Cirrus Clouds in a General Circulation Model: Radiative Transfer and Re-vaporization", International Association of Meteorology and Atmospheric Sciences Meeting, Boulder, CO

3 July 1995

Dr. Syukuro Manabe

"The Role of Thermohaline Circulation in Climate: Modeling Study", International Union of Geodesy and Geophysics (IUGG) General Assembly, Boulder, CO

3 July 1995

Dr. Lori M. Perliski

"Simulation of Stratospheric Photochemistry in the NOAA SKYHI GCM", XXI IUGG General Assembly, Boulder, CO

5 July 1995

Dr. Kevin P. Hamilton

1. "Gravity Wave Processes and Parameterization", 2. "Middle Atmospheric Climatology as Simulated by General Circulation Models", 3. "The Problem of Simulating a Realistic Stratospheric QBO in General Circulation Models", International Union of Geodesy and Geophysics (IUGG) General Assembly, Boulder, CO

5 July 1995

Dr. Isidoro Orlanski

"Stages in the Energetics of Baroclinic Systems", International Union of Geodesy and Geophysics (IUGG) General Assembly, Boulder, CO

5 July 1995

Dr. Leo J. Donner

"Applications of a Three-Dimensional Cloud-System-Resolving Model to Cumulus Parameterization", National Center for Atmospheric Research, Boulder, CO

7 July 1995

Dr. Ngar-Cheung Lau

"A Modeling Study of the Relative Roles of Tropical and Extratropical SST Anomalies in the Variability of the Global Atmosphere-Ocean System", International Union of Geodesy and Geophysics (IUGG) General Assembly, Boulder, CO

7 July 1995

Dr. Isaac M. Held

"Thinking About Storm Tracks", Meeting of NOAA-Universities Consortium, Boulder, CO

7 July 1995

Dr. V. Ramaswamy

"Stratospheric Ozone and Climate Change", Middle Atmosphere Symposium, International Union of Geodesy and Geophysics (IUGG) General Assembly, Boulder, CO

7 July 1995

Mr. M. Daniel Schwarzkopf

"Sensitivity of the Middle Atmosphere Climate Simulated in a GCM to Radiative Effects of Methane, Nitrous Oxide CFC's", International Union of Geodesy and Geophysics (IUGG) General Assembly, Boulder, CO

12 July 1995 Dr. V. Ramaswamy
"Stratospheric Temperature Trends Assessment: A SPARC Project",
Middle Atmosphere Symposium, International Union of Geodesy and
Geophysics (IUGG) General Assembly, Boulder, CO

12 July 1995 Dr. Brian Soden
"Climatological Analysis of the Spectral and Broadband Radiative
Energy Budget", International Union of Geodesy and Geophysics
(IUGG) General Assembly, Boulder, CO

12 July 1995 Dr. Jerry D. Mahlman
"Model Predictions of Greenhouse Warming", Meeting of the American
Bankers' Association/American Insurance Association, Washington, DC

17 July 1995 Mr. Anthony J. Broccoli
"Representation of Topography in Spectral Climate Models and its Effect
on Simulated Precipitation", American Meteorological Society,
Conference on Mountain Meteorology, Breckenridge, CO

3 August 1995 Dr. Isaac M. Held
"Geostrophic Turbulence and Baroclinic Instability", National Center for
Atmospheric Research, Boulder, CO

4 August 1995 Mr. Anthony J. Broccoli
"Climate Model Simulation of Atmospheric Forcing Over the Glacial
North Atlantic", XIV International Congress of International Union for
Quaternary Research, Berlin, Germany

13 September 1995 Mr. Anthony J. Rosati
"Assimilation of Topex Altimetry in an Ocean GCM", GCOSS/World
Meteorological Organization, TAO Implementation Panel Meeting,
Fortaleza, Brazil

27 September 1995 Dr. Syukuro Manabe
"Natural Variability of Climate and the Detection of the Global Warming",
First GAIM Science Conference sponsored by the International
Geosphere-Biosphere Program, Garmisch-Partenkirchen, Germany

APPENDIX E

ACRONYMS

ACRONYMS

AASE	Arctic Airborne Stratospheric Experiment
ABLE	Atmospheric Boundary Layer Experiment
AEROCE	Air Ocean Chemistry Experiment
AGCM	Atmospheric General Circulation Model
AMEX	Australian Monsoon Experiment
AMIP	Atmospheric Model Intercomparison Project
AOML	Atlantic Oceanographic and Meteorological Laboratory/NOAA
AOU	Apparent Oxygen Utilization
ARL	Atmospheric Research Laboratory/NOAA
A94/P95	GFDL Activities FY94, Plans FY95
CCN	Cloud Condensation Nuclei
CEM	Cumulus Ensemble Model
CFC	Chlorofluorocarbon
CHAMMP	Computer Hardware, Advanced Mathematics and Model Physics project
CIRA	COSPAR International Reference Atmosphere
CLIPER	A simple model combining CLImatology and PERsistence used in hurricane prediction.
CMC	Carbon Modeling Consortium
CMDL	Climate Monitoring and Diagnostics Laboratory/NOAA
COADS	Comprehensive Ocean-Atmosphere Data Set
COARE	Coupled Ocean-Atmosphere Response Experiment

COSPAR	Congress for Space Research
CRAY	Cray Research, Inc.
CSIRO	Commonwealth Scientific & Industrial Research Organization
DAMEE	Data Assimilation and Model Evaluation Experiments
DJF	December, January, February (winter)
E	A physical parametrization package in use at GFDL. E physics includes a high-order closure scheme for subgrid turbulence.
ECMWF	European Centre for Medium-Range Weather Forecasts
E“n”	Horizontal model resolution corresponding to “n” points between a pole and the equator on the E-grid.
ENSO	El Niño - Southern Oscillation
EOF	Empirical Orthogonal Function
EPOCS	Equatorial Pacific Ocean Climate Studies
ERBE	Earth Radiation Budget Experiment
FDDI	Fiber Distributed Data Interface
FDH	Fixed Dynamic Heating model
FIRE	First ISCCP Regional Experiment
FY“yy”	Fiscal Year “yy” where “yy” are the last two digits of the year.
GARP	Global Atmospheric Research Program
GATE	GARP Atlantic Tropical Experiment
GCM	General Circulation Model
GCTM	Global Chemical Transport Model
GEOSAT	Geodetic Satellite

GFD	Geophysical Fluid Dynamics
GFDL	Geophysical Fluid Dynamics Laboratory/NOAA
GMT	Greenwich Mean Time
GOES	Geostationary Operational Environmental Satellite
GTE	Global Tropospheric Experiment
HIBU	Federal Hydrological Institute and Belgrade University
HPCC	High Performance Computing and Communications
HRD	Hurricane Research Division/AOML
ICRCCM	InterComparison of Radiation Codes in Climate Models
IGBP/PAGES	International Geosphere-Biosphere Project/ Past Global Changes
I/O	Input/Output
IPCC	Intergovernmental Panel on Climate Change
ISCCP	International Satellite Cloud Climatology Project
IT	Information Technology
ITCZ	Intertropical Convergence Zone
JGOFS	Joint Global Ocean Flux Study
JJA	June, July, August (summer)
JPL	Jet Propulsion Laboratory
KFA	Forschungszentrum Julich
LAHM	Limited Area HIBU Model
LAN	Limited Area Nonhydrostatic
LBL	Line By Line

LIMS	Limb Infrared Monitor of the Stratosphere
L“n”	Vertical model resolution of “n” levels.
LWP	Liquid Water Path
MLS	Microwave Limb Sounder
MMM	Multiply-nested Movable Mesh
MOM	Modular Ocean Model
MOM2	Modular Ocean Model, Version 2
MOODS	Master Oceanographic Observations Data Set
MPP	Massively Parallel Processor
NABE	North Atlantic Bloom Experiment
NADW	North Atlantic Deep Water
NARE	North Atlantic Regional Experiment
NASA	National Aeronautics and Space Administration
NCAR	National Center for Atmospheric Research
NCDC	National Climate Data Center/NOAA
NH	Northern Hemisphere
NMC	National Meteorological Center/NOAA
NOAA	National Oceanic and Atmospheric Administration
NODC	National Oceanographic Data Center/NOAA
ODA	Ocean Data Assimilation
OLR	Outgoing Longwave Radiation
OTL	Ocean Tracers Laboratory/Princeton University

PCMDI	Program for Climate Model Diagnosis and Intercomparison
PFC	Perfluorocarbon
PILPS	Project for Intercomparison of Land-Surface Parameterization Schemes
PMEL	Pacific Marine Environmental Laboratory
PMIP	Paleoclimate Model Intercomparison Project
PNA	Pacific-North American
POM	Princeton Ocean Model
QBO	Quasi-Biennial Oscillation
QG	Quasi-Geostrophic
RAS	Relaxed Arakawa-Schubert
RFP	Request for Proposal
R“n”	Horizontal resolution of spectral model with rhomboidal truncation at wavenumber “n”.
SAGE	Stratospheric Aerosol and Gases Experiment
SAMS	Stratospheric Aerosol Measurement System
SAVE	South Atlantic Ventilation Experiment
SBUV	Solar Backscatter Ultraviolet (satellite)
SGI	Silicon Graphics, Inc.
SH	Southern Hemisphere
SiB	Simple Biosphere
SKYHI	The GFDL Troposphere-Stratosphere-Mesosphere GCM
SME	Solar Mesosphere Explorer

SOI	Southern Oscillation Index
SPCZ	South Pacific Convergence Zone
SPECTRE	Spectral Radiation Experiment
SST	Sea Surface Temperature
SUN	Sun Microsystems, Inc.
THC	Thermohaline Circulation
TIO	Tropical Intraseasonal Oscillations
T“n”	Horizontal resolution of spectral model with triangular truncation at wavenumber “n”.
TOGA	Tropical Ocean and Global Atmosphere project
TOGA/TAO	Tropical Ocean Global Atmosphere/Tropical Atmosphere Ocean
TOMS	Total Ozone Mapping Spectrometer
TOPEX	Topographic Experiment
TOVS	Tiros Operational Vertical Sounder
TTO	Transient Tracers in the Oceans
UARS	Upper Atmosphere Research Satellite
WGNE	Working Group on Numerical Experimentation
WMO	World Meteorological Organization
WOCE/HP	World Ocean Circulation Experiment/Hydrographic Program
XBT	Expendable Bathythermograph
ZODIAC	Gridpoint Climate Model